Sequential reprogramming of *Medicago truncatula* root cells during the accommodation of symbiotic arbuscular mycorrhizal fungi

Von der Naturwissenschaftlichen Fakultät
der Gottfried Wilhelm Leibniz Universität Hannover
zur Erlangung des Grades
Doktorin der Naturwissenschaften
Dr. rer. nat.
genehmigte Dissertation

von

Diplom-Biologin Claudia Hogekamp
geboren am 01.06.1982 in Emmerich

2013

Referent: Prof. Dr. Helge Küster
Korreferent: Prof. Dr. Jutta Papenbrock
Tag der Promotion: 16.01.2013

ZUSAMMENFASSUNG

Die arbuskuläre Mykorrhiza (AM) Symbiose, die zwischen Landpflanzen und Glomeromycota Pilzen ausgebildet wird, ist weltweit eine der am weitesten verbreiteten Symbiosen, da ungefähr 80% der heutigen Landpflanzen von dieser mutualistischen Verbindung zur Verbesserung ihrer Nährstoffversorgung abhängig sind. In den letzten Jahren wurden viele der molekularen Mechanismen aufgeklärt, welche die Besiedlung von Pflanzenwurzeln mit AM Pilzen steuern. Untersuchungen von Genexpressionsmustern in definierten Stadien der Symbiose gestalten sich aufgrund der asynchronen Entwicklung jedoch schwierig, was eine Vorhersage von Genfunktionen erschwert. In dieser Arbeit wurden anhand der Modelleguminose *Medicago truncatula* die Expressionsmuster während der wichtigsten Entwicklungsstadien von AM-Symbiosen untersucht. Um diese Transkriptomanalysen zu ermöglichen, wurden spezifische Zelltypen mit definierten Entwicklungsstadien der Symbiose mittels Laser Mikrodissektion aus mykorrhizierten Wurzeln isoliert. Zunächst wurde die Expression von 62 ausgewählten Genen mittels *real-time* RT-PCR in arbuskelhaltigen Zellen und den benachbarten Kortexzellen, die von intraradikalen Hyphen besiedelt waren, analysiert. Dabei konnte gezeigt werden, dass die mikrodissektierten Zellen eine spezifische Unterscheidung der Genaktivität in direkt benachbarten Zellen erlauben. Neben Genen, welche die Besiedlung des gesamten Kortex steuern, konnten 25 Gene mit einer arbuskelspezifischen Expression identifiziert werden. Im Anschluss wurde die Analyse auf eine genomweite Untersuchung von Expressionsprofilen der vier Hauptentwicklungsstadien der AM Symbiose ausgedehnt. Hierzu wurden die Transkriptionsprofile von insgesamt fünf verschiedenen Zelltypen mittels Hybridisierung von Affymetrix® *Medicago* GeneChips analysiert. Neben arbuskelhaltigen und kortikalen Zellen mit Pilzhyphen wurden Epidermiszellen aus mykorrhizierten Wurzeln untersucht, vor allem aber Zellen, die frühe Infektionsstadien des Pilzes enthielten. Durch einen Vergleich mit Expressionsprofilen aus Zellen, die kein Anzeichen für eine Pilzbesiedlung aufwiesen, ergab sich ein umfassender Überblick über die zelluläre Umprogrammierung während der prä-Kontakt-Phase, der frühen Infektion, der intraradikalen Verbreitung von Pilzhyphen und der Ausbildung von Arbuskeln. Dabei konnten unterschiedliche Gengruppen identifiziert werden, die während der aufeinanderfolgenden Schritte der Wurzelbesiedlung aktiviert werden. Neben schon bekannten AM Markergenen konnten einige Gene zum ersten Mal mit der intrazellulären Infektion durch den Pilz in Verbindung gebracht werden. Eine relativ große Gruppe von Genen durchläuft im Zuge der fortschreitenden Wurzelbesiedlung durch den Pilz offenbar eine Verschiebung ihres Aktivitätsmusters hin zu arbuskelhaltigen Zellen und erfüllt dort spezifische Funktionen. Hier sind auch die 125 Gene zu nennen, für die eine ausschließliche Aktivierung während der Ausbildung von Arbuskeln nachgewiesen werden konnte. Zudem kommt es während der frühen Infektion und während der Ausbildung von Arbuskeln zu zwei Wellen der transkriptionellen Herunterregulierung von Genen, die zumindest teilweise mit der Unterdrückung von Abwehrreaktionen der Pflanze beim Kontakt mit wachstumsfördernden Mikroben korreliert sein könnten. Die zellulären Transkriptionsprofile wurden durch eine funktionelle Analyse mittels *RNA-interference* (RNAi) ergänzt. Dabei wurden ausgewählte Gene untersucht, die während unterschiedlicher Symbiose-Stadien aktiviert werden. Phänotypische Analysen von transgenen Wurzeln ergaben Hinweise auf die Beteiligung des Annexin-Gens *MtAnn2* und des *Myb*-Transkriptionsfaktorgens *MtMyb1* an der Entwicklung von Arbuskeln. Für *MtMyb1*-RNAi-Wurzeln konnte zudem eine erschwerte Besiedlung des Kortex nachgewiesen werden. Zusammen liefern diese Ergebnisse einen Beitrag, um die schrittweise Umprogrammierung von Pflanzenwurzeln im Zuge der Besiedlung mit AM-Pilzen zu verstehen.

Schlagworte: arbuskuläre Mykorrhiza-Symbiose, zelluläre Expressionsanalysen, Laser Mikrodissektion, *RNA-interference*, schrittweise Umprogrammierung

ABSTRACT

The arbuscular mycorrhizal (AM) symbiosis established between terrestrial plants and Glomeromycota fungi is one of the most widespread symbioses on Earth, with around 80% of today's land plants depending on this mutualistic interaction to improve their nutrient supply. In the last years, many molecular mechanisms governing plant root colonization by AM fungi have been revealed. However, analyses of gene expression during distinct developmental stages were hampered by the asynchronous development of the AM symbiosis, making predictions of gene functions difficult. In this work, expression profiling of the main AM stages was conducted in the model legume *Medicago truncatula*, utilizing laser microdissection to obtain specific cell types that represent defined developmental AM stages. In a first step, expression of 62 AM-related genes was monitored via real-time RT-PCR in arbusculated and the surrounding cortical cells colonized by fungal hyphae. The experiment confirmed that the cell pools obtained via laser-microdissection allow a reliable differentation between gene expression in neighbouring root cells, revealing arbuscule-specific expression of 25 genes in addition to identifying general regulators of root colonization. Subsequently, this approach was extended to cover the four main developmental stages of AM symbioses on a genome-wide scale. Gene expression patterns were identified for five different cell-types via Affymetrix® *Medicago* GeneChip experiments, including not only arbusculated and cortical cells colonized by intraradical hyphae, but in addition epidermal cells and, most importantly, cells harbouring early fungal infection sites. In comparison to cells obtained from root areas with no sign of fungal penetration, the data provided a comprehensive overview of cellular reprogramming during the pre-contact stage, the initial infection, the intraradical growth of fungal hyphae, and the formation of arbuscules. Distinct sets of genes activated during the sequential steps of root colonization were identified, including known AM marker genes, but also novel genes related to intracellular infection and a large group of genes obviously undergoing a shift of expression towards arbusculated cells, in addition to 125 genes displaying a specific activation during arbuscule-formation. The analysis also revealed two waves of transcriptional downregulation during infection and arbuscule formation, e.g. shedding light on the suppression of plant defence responses during the interaction with beneficial microbes. The cellular transcriptome profiling was complemented via a functional analysis of selected genes, activated at different stages of the AM symbiosis. To this end, an RNA-interference (RNAi) approach was used. Here, phenotypical investigations of transgenic roots displaying a knockdown of the annexin gene *MtAnn2* and the Myb-transcription factor gene *MtMyb1* revealed an involvement of both genes in arbuscule-formation, whereas *MtMyb1* was shown to be involved in propagation of the infected area. Together, the results presented in this work contribute to an understanding of the sequential reprogramming of host roots towards an accomodation of AM-microsymbionts.

Keywords: arbuscular mycorrhizal symbiosis, cellular expression profiling, laser microdissection, RNA-interference, sequential reprogramming

CONTENTS

GENERAL INTRODUCTION

Symbiotic interactions – Distribution and biological importance

The term symbiosis describes an association between individuals of two or more different species, which live in close contact and influence each other (de Bary 1879). Although it initially referred to all kinds of associations, ranging from parasitism, where one species lives at the expense of the other, to mutualism, where both species benefit from the interaction, it is mostly used for mutualistic relationships nowadays (Czihak *et al.* 1990). Symbiotic associations can be found between a wide range of species from all ecosystems and are extremely diverse in terms of physical closeness and impact on the biological fitness of the partners involved. These two factors are correlated with each other, since facultative relationships, which are only established under specific circumstances, are often characterized by a loose contact between the partners. In contrast, obligate interactions, where the species involved depend on each other to survive and complete their life-cycle, are characterized by a close physical contact, which is often kept up throughout the whole lifespan of the individuals (Czihak *et al.* 1990).

In the life-cycle of many higher plants, two main aspects of survival and reproduction are influenced by symbiotic interactions. On the one hand, many plants depend on other species, like insects, birds or small mammals for pollination, while in return they represent important food sources for these species (Bayrhuber and Kull 1989). On the other hand, as sessile organisms plants often have to cope with limited nutrient resources in their habitat. During evolution, plants have established associations with soil-borne microorganisms, which can improve their nutrition-supply and are of special importance for the colonization of nutrient-deprived habitats (Nultsch 2001). Some plants interact with bacteria which are capable of fixing atmospheric nitrogen in the so called root nodule symbiosis (Markmann and Parniske 2009). The second and more common association is established with mycorrhizal fungi, which mainly improve the phosphate supply of the host plants (Strack *et al.* 2001). In both cases, the microsymbiont is supplied with photoassimilates of the host in return (Nultsch 2001).

The mycorrhizal symbiosis

The association of terrestric plants with mycorrhizal fungi is one of the most widespread symbioses on Earth (Smith and Read 2008). The term mycorrhiza was deduced from the Greek words *mykes* (fungus) and *rhiza* (root), describing the colonization of plant roots by soil-borne fungi (Franck 1885). Two different kinds of mycorrhizal interactions can be distinguished (Figure 1A). In ectomycorrhizal associations, fungal hyphae form a tight network around the root, the so called "Hartig net", but furthermore only colonize the intercellular space of the outer root cell layers. In contrast, endomycorrhiza are characterized by a much more intimate contact of the two partners with fungal hyphae actually invading plant cells of the inner root cortex (Bonfante and Genre 2010).

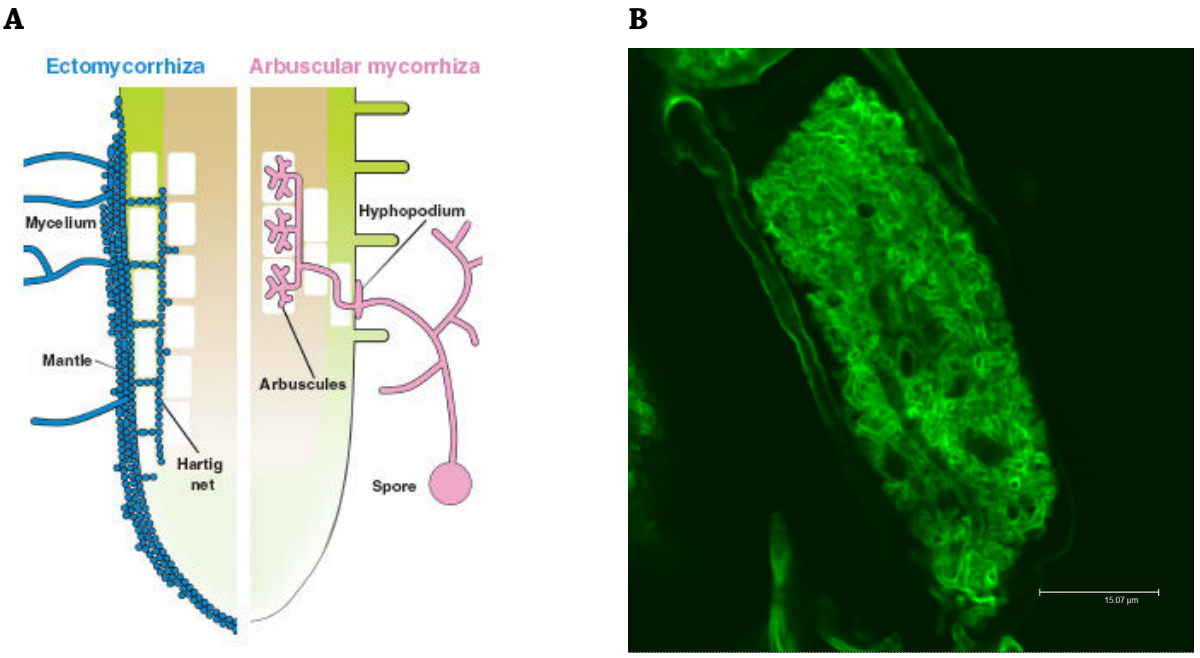

Figure 1: Differences between ecto- and endomycorrhizal associatons.
A: Left side: Schematic overview of fungal structures in the an ectomycorrhizal symbiosis. The fungal mycelium forms a tight mantle around the host root. Fungal hyphae also enter the root, but are restricted to the intercellular space of epidermal and outer cortical cells forming the "Hartig net". Right side: Schematic overview of fungal structures in an endomycorrhizal symbiosis – in this case the arbuscular mycorrhizal symbiosis. Fungal hyphae infect the root via an hyphopodium or appressorium and form tree-shaped structures called arbuscules in the inner cortical cells. (Adapted by permission from Macmillan Publishers Ltd: Nat Commun, Bonfante and Genre 2010, copyright 2010). **B:** Confocal image of a single arbuscule. In the vicinity fungal hyphae are visible. The densely packed arbuscule fills the complete cell lumen. The fungus was stained with Alexa488®-WGA. The scale bar represents 15 µm.

Since they are formed between fungi belonging to the Basidomycetes or Asomycetes and trees from the families Pinaceae, Fagaceae, Dipterocarpaceae and Caesalpinoidaceae, ectomycorrhizal associations are predominantly found in forest ecosystems (Smith and Read 2008). The fungi involved in these associations are facultative symbionts.

Endomycorrhizal associations on the other hand are found in three main forms: orchid and ericoid mycorrhiza and the large group of arbuscular mycorrhizal (AM) interactions. AM interactions are established between fungi of the phylum Glomeromycota and a wide range of host species, covering approximately 80% of today's land plants. Only the families Brassicaceae, Chenopodiaceae and Proteaceae are completely devoid of mycorrhizal symbioses (Smith and Read 2008). The term AM was deduced owing to the small tree-shaped structures built by highly ramificated fungal hyphae in the inner cortex (Figure 1B). The strongly enlarged surface of these structures renders them optimal sites for efficient nutrient exchange between the two partners (Paszkowski 2006).

From an evolutionary point of view, the AM symbiosis represents a very old association, with fossil records dating back 400 million years into the early Devonian (Taylor *et al.* 1995), where they coincide with the appearance of first land plants. Structures resembling arbuscules were found in fossil plants representing a link between bryophytes and vascular plants, although they had not yet evolved true roots at that time and the fungi were hosted in shoot tissue or rhizomes instead (Redecker *et al.* 2000). Humphreys *et al.* (2010) showed that arbuscular mycorrhiza in a recent thalloid liverwort promotes photosynthetic rates, growth and asexual reproduction of this ancient plant. Therefore it seems feasible that AM fungi may have been a crucial factor for the successful colonization of terrestrial ecosystems by plants and coevolution has rendered them obligate symbionts since (Pirozinski and Malloch 1975).

The infection of host plants by AM fungi (Figure 2) begins with the germination of fungal spores in the soil. Strigolactones produced by the host plant promote branching of the fungal hyphae and an increased respiration in the fungal mitochondria (Buee *et al.* 2000, Tamasloukht *et al.* 2003, Akiyama *et al.* 2005). Strigolactones are used as a signal for the presence of potential host plants also by other plant-colonizing species and were originally identified as promoting the growth of parasitic weeds (Matusova *et al.* 2005). Simultaneously, the plant is influenced by Myc-factors, diffusible molecules produced by the fungus, which trigger specific reactions in the root cells of the host plant (Kosuta *et al.* 2003). After reaching the root epidermis the growing hyphae forms an appressorium or hyphopodium (Figure 2). The formation of this structure is triggered exclusively by epidermal cells of host plants (Nagahashi and Douds, 1997). The plant cell underneath the appressorium undergoes severe rearrangements of the cytoskeleton, facilitating the entry of the fungus. The nucleus migrates to the place of appressorium formation, and then moves ahead of the invading hyphae. A tubular

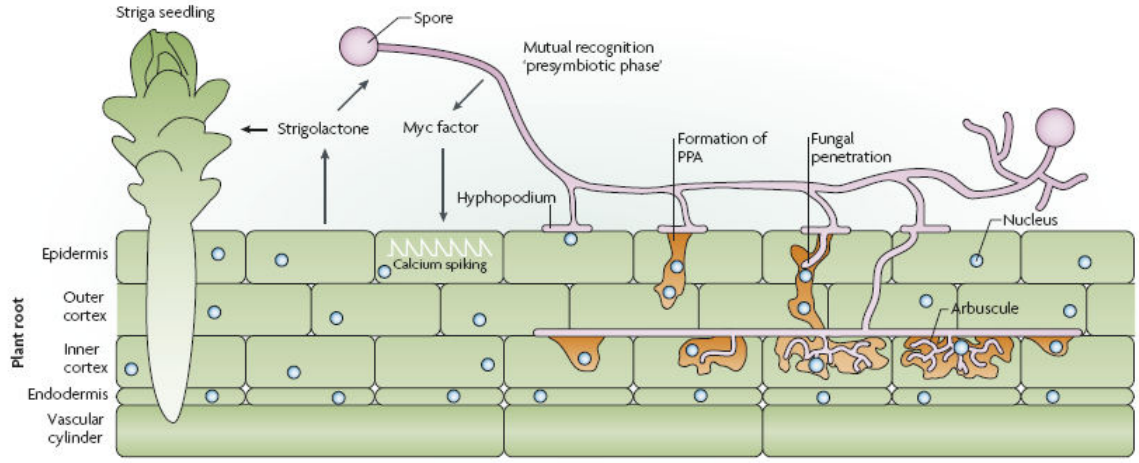

Figure 2: Development of an AM symbiosis.
Fungal spores are activated by strigolactones exudated by the host plants. These plant exudates also promote germination of parasitic weeds, like *Striga* plants. In turn, diffusible factors of the fungus induce first reactions in the plant including calcium spiking in the root cells. The spores germinate and fungal hyphae grow towards the root epidermis where they form an hyphopodium or appressorium. The plant reacts with the formation of the prepenetration apparatus (PPA) guiding fungal hyphae through the cells. In the inner cortex the fungus forms arbuscules, which improve nutrient exchange between the partners. (Adapted by permission from Macmillan Publishers Ltd: Nat Rev Microbiol, Parniske 2008, copyright 2008).

structure surrounded by cytoskeletal components is formed, which leads the hyphae during growth throughout the cell and which is called pre-penetration apparatus (PPA) (Genre *et al.* 2005).

Subsequently, the hyphae enter the inner cell layers of the root cortex, where side-branches of the hyphae, each leading into a single cortical cell, differentiate into arbuscules. The arbuscule is enclosed by a membrane of plant origin, the so called peri-arbuscular membrane (PAM) (Strack *et al.* 2001). It contains specific P_i-transporters which deliver the phosphate supplied by the fungus into the plant cells (Harrison *et al.* 2002, Javot *et al.* 2007). Recently, a fungal hexose transporter was identified, which seems to account for the major part of carbon allocation to the microsymbiont and is localized in arbuscules as well as intercellular hyphae of the fungus (Helber *et al.* 2011). Hexoses are procured by the plant via the activity of sucrose-cleaving enzymes like sucrose-synthase (Hohnjec *et al.* 2003) and invertases (Saarschmidt and Hause 2008).

Whereas the expression of the symbiotic P_i-transporter is upregulated in mycorrhizal roots (Rausch *et al.* 2001, Harrison *et al.* 2002, Paszkowski *et al.* 2002), the expression of the P_i-transporters localized in the root epidermis of the plant, which serve for phosphate uptake under non-symbiotic conditions, is downregulated (Liu *et al.* 1998, Chiou *et al.* 2001, Smith *et al.* 2003). The fine and wide-stretched network of fungal hyphae strongly enhances the exploitation zone of mycorrhized

plants in the soil and takes over large parts of the host's phosphate supply (Hijikata *et al.* 2010). Similarly, the fungus enhances access to nitrogen, water and micronutrients, which are taken up by the extraradical hyphae of the fungus and are translocated into the roots of the host plant (Clark and Zeto 2000). An aspect that is only partly understood is the interconnection of plants in certain habitats via the hyphae of their microsymbionts, allowing the transfer of nutrients and signal molecules between them (Bonfante and Genre 2010).

The root nodule symbiosis

In contrast to mycorrhizal symbioses, associations with nitrogen-fixing bacteria are more seldom in the plant kingdom. Plants belonging to the Fagales, Cucurbitales and Rosales can establish an actinorhiza symbiosis with *Frankia* bacteria, but interactions with rhizobial bacteria are restricted to legume plants (Fabaceae), which evolved 60 million years ago, and the genus *Parasponia* belonging to the Canabaceae (Geurts *et al.* 2012). The scattered distribution of the ability to undergo root nodule symbioses (RNS) within the phylogenetic tree of the rosid clade suggests that it has evolved independently several times (Markmann and Parniske 2009).

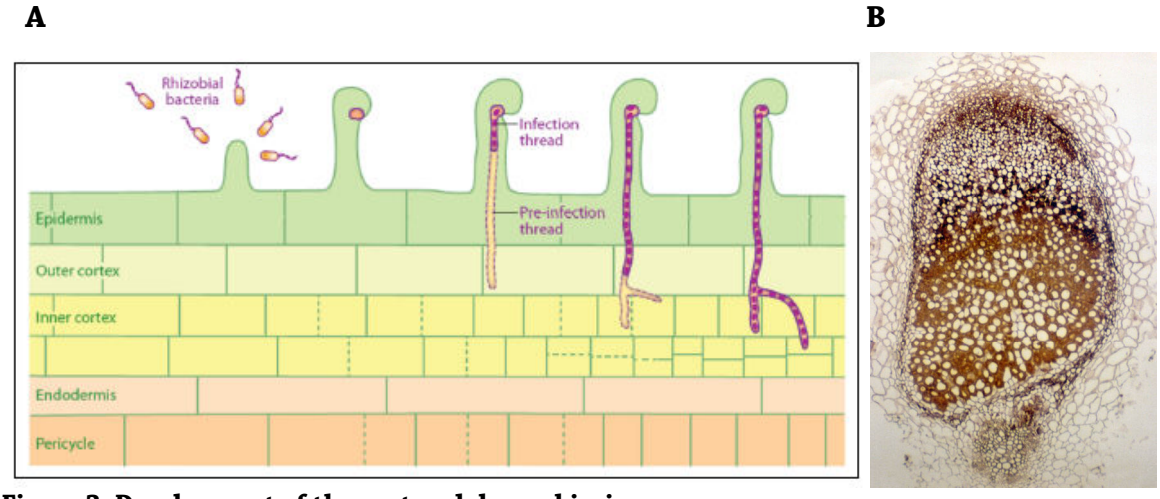

Figure 3: Development of the root nodule symbiosis.
A: Infection process. Rhizobial bacteria are attracted by flavonoids exudated by the host. They attach to root hairs which start to curl and enclose the bacteria in the so-called shepherds crook. An infection thread is formed, guiding the bacteria through the root hair and the outer cortex. In the inner cortex, cells are activated and form a meristem which generates the root nodule. (Republished with permission of Annual Reviews, from Oldroyd *et al.* 2011, copyright 2011). **B**: Thin section of a fully developed nodule (Dieter Kapp, Universität Bielefeld).

Like the mycorrhizal symbiosis, the establishment of a RNS between legumes and rhizobial bacteria starts with a molecular crosstalk in the soil (Figure 3). The production of root exudates - mainly flavonoids - attracts free-living rhizobial bacteria and stimulates them to produce special signal

molecules, called Nod-factors (Dénarié *et al*. 1996, Oldroyd *et al*. 2005). Similar to Myc-factors, they mediate specific recognition of the microsymbiont by the host plant. Subsequently, the bacteria attach to root hairs, which start to swell and curl, thereby enclosing the bacteria in the so-called shepherds crook (Murray 2011). An infection thread is formed allowing the bacteria to enter the root via the root hair (Fournier *et al*. 2008). Simultaneously, cells in the inner cortex are activated and start to divide, ultimately forming a new root organ - the root nodule (Figure 3B) - which is colonized by the bacteria (Oldroyd and Downie 2008). Inside the nodule cells, bacteria are released from the infection threads by membrane budding. They differentiate into nitrogen-fixing bacteroids and divide many times, so that in infected cells the whole cytoplasm is densely packed. Each bacteroid stays surrounded by a membrane of plant origin, called the peri-bacteroid-membrane (PBM) (Verma and Hong 1996). By producing specific leghemoglobins, the plant provides an ideal microaerobic surrounding for the activity of the rhizobial nitrogenase, securing the supply of ammonium to the plant (Cullimore and Bennet 1992).

Common features of root endosymbioses

Apart from the improvement of nutrient supply for their host plants, the AM symbiosis and the RNS share additional common features, especially with regard to the infection processes involved. Both microsymbionts communicate their presence to the host plant via specific signal molecules – the Nod- and Myc-factors - which are highly similar lipo-chitooligosaccharides (LCOs) (Dénarié *et al*. 1996, Maillet *et al*. 2011). While AM fungi are known to produce only two different variants of the signal molecule – either sulphated or non-sulphated (Maillet *et al*. 2011) - rhizobial Nod-factors are more diverse with regard to their substitutional groups, which mediate the host-specificity between certain rhizobial species and their respective plant (Lerouge *et al*. 1990, D`Haeze and Holsters 2002). These signal molecules trigger plant responses before physical contact is established, including transient cytosolic calcium elevation and oscillations in the proximity of the nucleus (Navazio *et al*. 2007, Kosuta *et al*. 2008, Maillet *et al*. 2011, Gough and Cullimore 2011), as well as expression of symbiosis-related genes (Kosuta *et al*. 2003, Weidmann *et al*. 2004, Czaja *et al*. 2012) via a common symbiotic (SYM) signalling pathway. In Figure 4, this SYM pathway is shown for the gene products identified in *Medicago truncatula*.

The diffusible signal molecules are recognized by membrane-bound receptor-kinases. While for Nod-factor perception, the two LysM receptor-kinases MtNFP and MtLYK3 are required, only MtNFP is

essential for Myc-factor signalling, but other yet unidentified receptors may exist (Gough and Cullimore 2011). In addition, the leucine-rich repeat receptor-like kinase MtDMI2 is essential for the establishment of root nodule and mycorrhizal symbioses, although it has so far not been shown to interact with the signal molecules or the other receptor kinases (Stracke *et al.* 2002). The next step in the signalling cascade is the activation of the potassium channel MtDMI1 located in the nuclear membrane, leading to a flow of potassium into the intermembrane space, which in turn triggers the release of internal calcium stores (Venkateshwaran *et al.* 2012). This is evident by a typical calcium spiking which can be measured in the cytoplasm and the nucleus of activated root cells (Kosuta *et al.* 2008). The calcium signal is decoded by the calcium/calmodulin dependent kinase MtDMI3

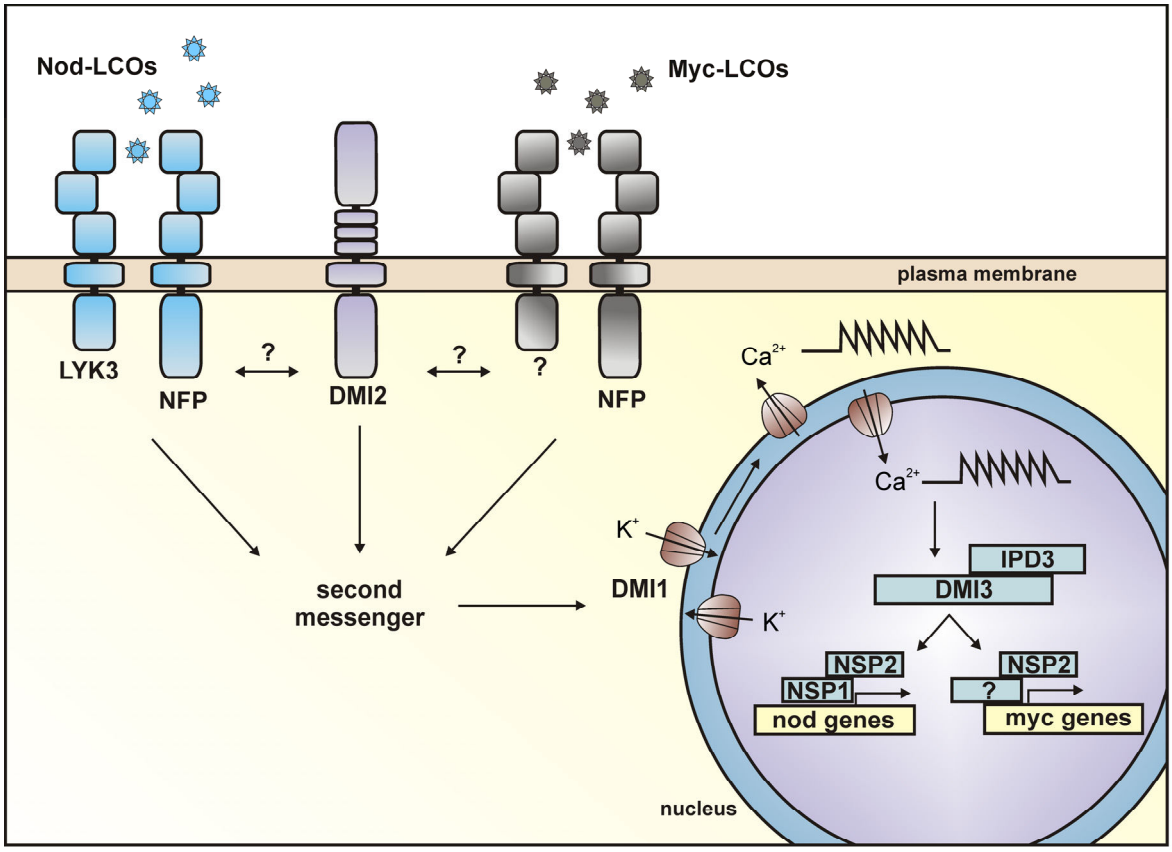

Figure 4: Common SYM pathway.
Diffusible signal molecules from rhizobial bacteria (Nod-factors) and mycorrhizal fungi (Myc-factors) are perceived via membrane-bound receptor-kinases. Via unknown second messengers the signal is transduced to the potassium channel DMI1 located in the nuclear membrane. Upon its activation, potassium flows into the intermembrane space, which in turn activates calcium channels. Calcium is released from the intermembrane space, which leads to the typical calcium spiking in the nucleus and the cytoplasm. The calcium signal is decoded by the calcium/calmodulin dependent kinase DMI3, which interacts with IPD3 to activate the transcription factors NSP1 and NSP2. A complex of NSP1 and NSP2 was shown to activate genes involved in RNS. NSP2 probably activates genes involved in mycorrhizal symbioses via interaction with another GRAS transcription factor. Abbreviations and gene names: LCO: lipo-chitooligosaccharides, NFP: Nod-factor perception, LYK3: LysM domain containing receptor-like kinase 3, DMI: doesn't make infection, IPD3: interacting protein of DMI3, NSP: nod-signalling pathway. (Illustration of the pathway adapted from Parniske 2008).

located in the nucleus (Levy *et al.* 2004), which interacts with the protein MtIPD3 to activate specific transcription factors controlling the symbiotic program (Horváth *et al.* 2011). Here, the pathway leading to rhizobial or mycorrhizal symbiosis apparently splits up. In RNS the two GRAS transcription factors - MtNSP1 and MtNSP2 - are required and form a complex (Hirsch *et al.* 2009), while MtNSP2 and an unknown GRAS transcription factor are involved in Myc-factor signalling (Maillet *et al.* 2011). In addition, three ethylene-responsive transcription factors were shown to be involved in gene regulation during RNS (Adriankaja *et al.* 2007).

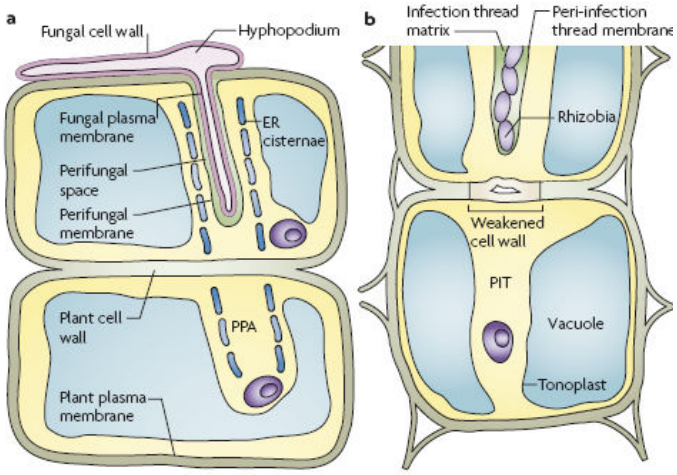

Figure 5: Similarities in the infection process of AM (a) and rhizobial (b) symbiosis.
Both in mycorrhizal (a) and rhizobial (b) infection processes the plant prepares the way for the invading microsymbionts by the formation of the pre-penetration-apparatus (PPA) or pre-infection-thread (PIT). When fungal hyphae or rhizobial bacteria transverse epidermal and cortical cells they are surrounded by a membrane of plant origin, which also stays in place at the symbiotic interface of arbuscules or bacteroids in nitrogen-fixing cells of root nodules. (Adapted by permission from Macmillan Publishers Ltd: Nat Rev Microbiol, Parniske 2008, copyright 2008).

More parallels can be found between the colonization processes of the two symbioses (Figure 5). Cell passage of both microsymbionts is guided by very similar structures - the PPA on the AM side and the PIT (pre-infection thread) during root nodule development (Timmers *et al.* 1999, Genre *et al.* 2005, Parniske *et al.* 2008). In addition, evidence could be provided that there are common genetic programs activated by different fungal species as well as by rhizobia during nodule formation (Manthey *et al.* 2004). A widely accepted hypothesis states that the younger root nodule symbiosis recruited signalling pathways and infection mechanisms already established for the mycorrhizal symbiosis (Parniske *et al.* 2008). The question remains, how the plant differentiates between fungal and bacterial symbionts. Evidence exists, that the calcium signals provoked by the two microsymbionts show different patterns (Kosuta *et al.* 2008) and signalling complemental to the common SYM pathway is involved in the AM symbiosis (Gutjahr *et al.* 2009, Bonfante and Requena 2011). Still, more detailed investigations are required to understand the commonalities and

differences of the two root endosymbioses, which might also deliver new insights into recognition of pathogenic fungi and bacteria.

Functional genomics in the model legume *Medicago truncatula* and its microsymbionts

Due to the fact that legume plants are the only clade able to establish symbiotic interactions with mycorrhizal fungi as well as rhizobial bacteria, they are ideal candidates to study the molecular mechanisms underlying these associations. The standard model plant for genetic studies, *Arabidopsis thaliana*, is not suited here, since it belongs to one of the few plant families unable to enter an AM symbiosis. Apart from this, legumes have been of special interest in plant science, since many of them are important crops.

In the last years, *Medicago truncatula* (Figure 6) has become one of the major model organisms in this area (Cook 1999). The species is closely related to crop legumes like *Medicago sativa* and *Pisum sativum*, but offers the advantage of a small diploid genome (< 500 Mbp), combined with autogamous fertilization and a short generation cycle (Ané *et al*. 2008). The genome sequencing project currently covers ~94% of the *Medicago truncatula* genes (Young *et al*. 2011) and a wide range of standard genetic tools are available. Tools for transcriptome approaches are reviewed in the introduction of Results - Chapter I. For functional analyses, several mutant collections (Sagan *et al*. 1995, Penmetsa *et al*. 1997, Tadege *et al*. 2008) and a database of ready-to-use RNA-interference (RNAi) constructs (http://projects. genomecommunity.org/mtrnai/) were established. RNAi constructs mediate a sequence-dependent knock-down of the target transcript and have been extensively used in plants over the last years (Fusaro *et al*. 2006). The target organism is transformed with a construct leading to the expression of a hairpin RNA (hpRNA), which is homologous to the gene of interest. Due to its secondary structure containing double-stranded regions, the hpRNA is degraded by Dicer-like (DCL) enzymes into small interfering RNAs (siRNAs). These siRNAs form an endonuclease complex which subsequently also degrades the endogenous mRNA (Hammond *et al*. 2001, Hannon *et al*. 2002). Different suppression levels can be obtained with this method, sometimes even comparable to the use of complete knockout-mutants (Wesley *et al*. 2001). Functional analyses of *Medicago truncatula* genes via RNAi are reviewed in the introduction of Results - Chapter III.

The rhizobial species interacting with *Medicago truncatula*, *Sinorhizobium meliloti*, has also been a subject of extensive genetic research. Sequencing of the genome was already completed in 2001

Figure 6: The model legume *Medicago truncatula*.
The photos show the plant like it appears in its natural habitat, a seedling like it is usually used for experiments and several plant organs, including seeds, seed vessels, flowers and the typical trifoliate leaves. Sources: www1.montpellier.inra.fr, www.jic.ac.uk, http://mips.helmholtz-muenchen.de/plant/medi/

(Galibert *et al.* 2001) and genes necessary for the colonization of the host plant, especially those involved in Nod-factor production have been characterized (Baev *et al.* 1992, Demont *et al.* 1993, Atkinson *et al.* 1994, Cren *et al.* 1995, Roche *et al.* 1996). In contrast, genetic analyses of AM fungi have been a hard task for scientists so far, since Glomeromycota are heterocaryotic organisms with many nuclei present in a single spore, have no separated cells and cannot be cultured without their host (Sanders and Croll 2010). Meanwhile, the sequencing project of *Glomus intraradices* provided access to first genomic sequences as well as an EST index (Martin *et al.* 2008, Tisserant *et al.* 2011), and AM fungi have been genetically transformed to express exogenous fluorescence proteins (Helber and Requena 2008).

Transcriptional analyses of AM roots have identified hundred of genes, which are specifically activated in host plants during AM interactions (for an overview of these studies see introduction to Results - Chapters I and II), but were hampered by the asynchronous development of the fungus in the root. The symbiosis is characterized by recurrent infection of the host root by fungal hyphae and their advancement through the layers of the root cortex, culminating in the iterant formation and break-down of arbuscules in the inner cortex, which leads to the concomitant presence of different developmental stages in the host root. This prevents the harvest of distinct stages and an identification of their specific gene expression patterns. With the invention of laser microdissection, a possibility for the targeted harvest of cell types representing different developmental stages of the symbiotic interaction is now at hand.

Gene expression studies of specific cell-types harvested by laser microdissection

Laser-assisted microdissection (LAM) is a microscopy-based method developed to cut and separate material at the microscale. It offers the possibility to obtain single cells from thin sections of complex biological tissues, allowing downstream-analyses of the cell-specific transcriptome, proteome or even metabolome. Originally developed and widely used for cancer research (Gillespie *et al*. 2001, Fend *et al*. 2002), the method has been adapted for plant material in the last years, which has proven to be highly amenable to this technique (Nelson *et al*., 2006, Day *et al*. 2007). Several variants exist with regard to how separation and harvest of cells are performed, which can be sub-divided into two main methods: laser capture microdissection (LCM) and laser excision microdissection (LEM) (Day *et al*. 2005). LCM-systems rely on an IR-Laser, which melts a thermoplastic membrane attached to a collection cap onto the area of a sample designated for harvest. Once the cap is removed, the desired area is torn out of the surrounding tissue (Emmert-Buck *et al*. 1996). In contrast, LEM-systems employ an UV-laser that excises the desired cells via ablation (Day *et al*. 2005). The cells are either transferred into a collection tube beneath the sample via gravity or catapulted into a cap above the sample by a defocused laser pulse. The latter method of laser microdissection and pressure catapulting (LMPC, Schütze *et al*. 2003) was used for the experiments presented in this work. It can be combined with the use of membrane-coated slides, with the membrane acting as a support for the sample during harvest, which provides the possibility to collect larger areas that remain intact during sampling (Day *et al*. 2005). Nevertheless, mounting of thin sections on normal glass slides, which have been heat-treated to remove RNAses, is also possible and was applied in this work. Since the desired areas are collected via multiple laser-pulses in this case, it might even be preferable for plant tissues, because the disruption of the material is supposed to facilitate subsequent extraction of macro-molecules.

The preparation of thin sections, which involves processing of the biological sample, is an inevitable prerequisite for the application of laser microdissection and a critical step, since it influences the histological preservation of the sample, as well as the integrity of cellular macro-molecules. Although in most cases, samples are either cryo-sectioned or embedded in paraffin, a wide range of different protocols for both methods exists and has to be optimized for each sample type individually to obtain optimal results (Day *et al*. 2007). This is especially the case, if the harvested cells are dedicated for transcriptome-analyses, since RNA is easily degraded. In addition, the RNA amounts obtained from the samples range in the area of several hundred picograms to several nanograms, depending on

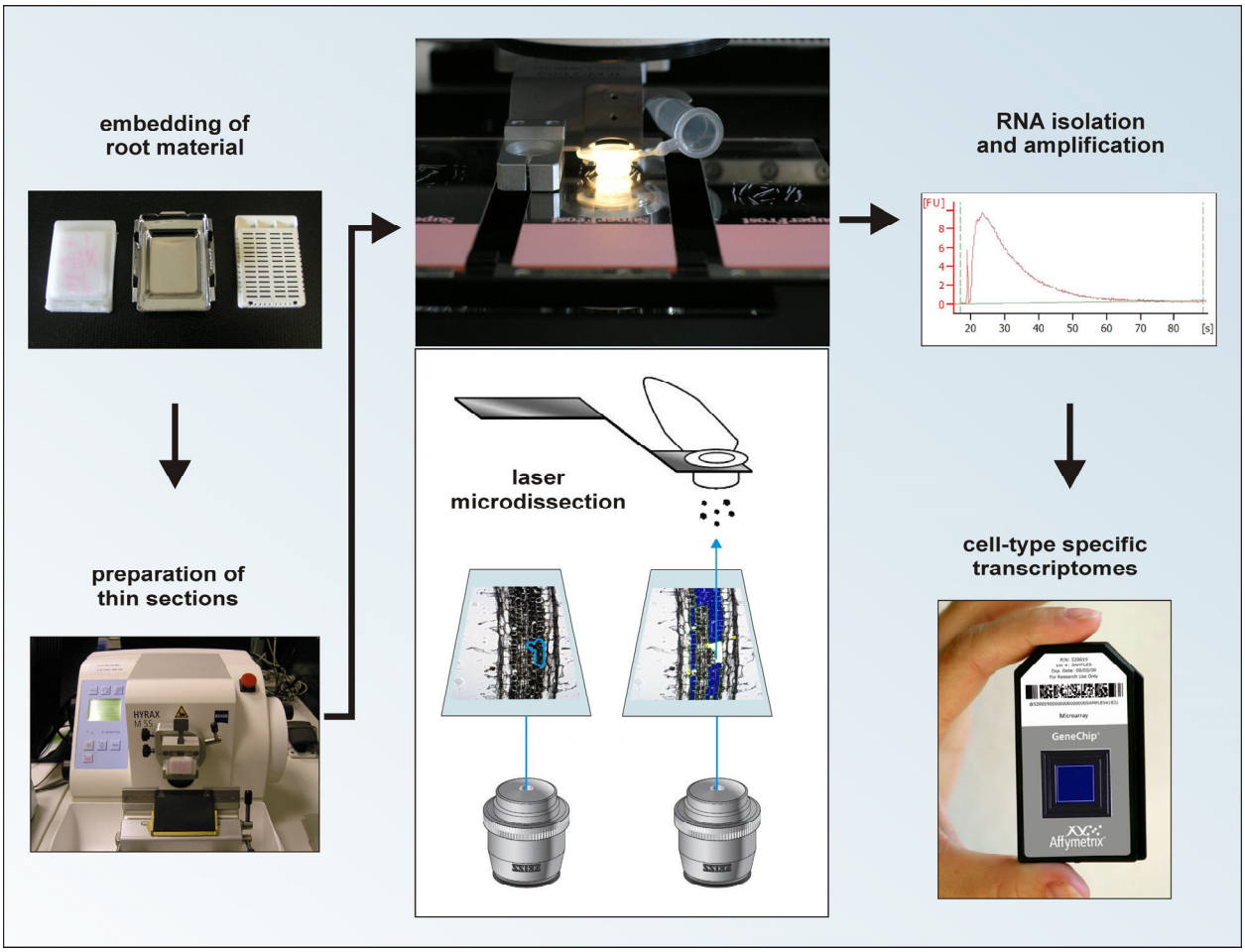

Figure 7: Workflow of laser microdissection experiments performed in this work.
In the first step, root samples are embedded in wax. The first photograph shows the embedding mould (middle), the embedding cassette (right side) and a wax block attached to the cassette (left side) containing root fragments (visible in pink due to eosin staining). Subsequently, thin sections of the roots are prepared using a microtome (photograph 2). The third photograph shows slides with thin sections and a collection cap positioned above them to perform the cell harvest via laser microdissection. Below, the process of laser microdissection and pressure catapulting (LMPC) is shown schematically. The area dedicated for cell harvest is first separated from the surrounding tissue and subsequently, cell flakes are transported into the cap via laser pressure catapulting. After cell harvest, RNA isolation and amplification is performed. The picture here shows a typical electropherogram produced during a bioanalyzer run of amplified mRNA. The RNA can then be used for the analysis of cell-type specific transcriptomes using Affymetrix GeneChips. Parts of the picture showing the schematic overview of LMPC were taken from www.zeiss.de/mikroskopie. The picture of the Affymetrix GeneChip was taken from www.affymetrix.com.

the cell type and number. Therefore, an additional amplification of mRNA is necessary for downstream applications like GeneChip experiments. In most of the investigations carried out with plant material, in vitro transcription (IVT) has been the method of choice for RNA amplification, coupled to the use of an oligodT-primer for cDNA-synthesis (Day *et al.* 2007), which may enhance 3' biases already caused by RNA degradation (Day *et al.* 2005).

In general, paraffin-embedding, which comprises fixation, dehydration and paraffin-infiltration of the tissue often leads to more severe RNA degradation, but on the other hand preserves the

morphology of the samples, while the use of cryo-sections results in a better quality of the isolated RNA, but may destroy the cell integrity (Nelson *et al*. 2006). Plant tissues which contain large vacuoles are particularly affected, since the presence of large water-filled compartments promotes the formation of ice crystals (Day *et al*. 2005).

Nevertheless, both methods have been used successfully for transcriptional analyses in plant tissues. The application of laser microdissection was first reported for the collection of phloem cells from rice leaves (Asano *et al*. 2002) and has since then be extended to the analysis of many different cell types from flowers (Ivashikina *et al*. 2003), seeds and embryos (Casson *et al*. 2005, Tauris *et al*. 2009), roots (Nakazono *et al*. 2003, Jiang *et al*. 2006), and fruit (Matas *et al*. 2010). Also the interaction of plants with parasitic root nematodes (Ramsay *et al*. 2004, Portillo *et al*. 2009, Klink *et al*. 2010, Ithal and Mitchum 2011) and pathogenic fungi (Tang *et al*. 2006, Chandran *et al*. 2009, Hacquard *et al*. 2010) has been investigated using laser microdissection.

With regard to AM interactions, only one report of laser microdissection, used to investigate differential expression of P_i-transporters in arbusculated and surrounding cortical cells of tomato roots (Balestrini *et al*. 2007), was available at the start of this PhD-work. Subsequently, similar experiments were published for subsets of genes identified during high-throughput expression profiling of AM roots in tomato (Fiorilli *et al*. 2009), *Lotus japonicus* (Guether *et al*. 2009) and *Medicago truncatula* (Gomez *et al*. 2009), in the last case restricted to arbusculated cells. In addition, the method was used to analyze abundance of fungal transcripts in arbuscules and extraradical mycelium (González-Chávez *et al*. 2009). The aim of the work presented here was to extend the utilization of laser-microdissection to harvest cell types of *Medicago truncatula* roots, representing all main developmental steps of AM symbioses, from the pre-infection stage to appressorium formation, intraradical growth of fungal hyphae and finally arbuscule formation. In addition, a functional analysis of four *Medicago trunctula* genes activated at the different developmental stages of the symbiosis should be performed to elucidate their influence on mycorrhizal colonization.

Aims of this work

I. Establishing methods for the harvest of cell types that represent distinct stages of AM development via laser microdissection, and subsequent validation of their suitability via real-time RT-PCR based analysis of cell type specific transcription of candidate genes, selected from expression data obtained from whole root samples.
II. Application of *Medicago* GeneChips for genome-wide monitoring of gene expression patterns in cell types representing the main developmental stages of AM symbioses.
III. Functional analysis of selected *Medicago truncatula* genes activated at the different stages of AM development via RNA-interference (RNAi) in transgenic roots.

Chapter I:
Laser-microdissection unravels cell-type specific transcription in arbuscular mycorrhizal roots, including CAAT-box TF gene expression correlating with fungal contact and spread*

Abstract

Arbuscular mycorrhizae (AM) are the most widespread symbioses on Earth, promoting nutrient supply of most terrestrial plant species. To unravel gene expression in defined stages of *Medicago truncatula* root colonization by AM fungi, we here combined genome-wide transcriptome profiling based on whole mycorrhizal roots with real-time RT-PCR experiments that relied on characteristic cell-types obtained via laser-microdissection. Our genome-wide approach delivered a core set of 512 genes significantly activated by the two mycorrhizal fungi *Glomus intraradices* and *Glomus mossae*. Focussing on 62 of these genes being related to membrane transport, signalling, and transcriptional regulation, we distinguished whether they are activated in arbuscule-containing or the neighbouring cortical cells harbouring fungal hyphae. In addition, cortical cells from non-mycorrhizal roots served as a reference for gene expression under non-colonized conditions. Our analysis identified 25 novel arbuscule-specific genes and 37 genes expressed both in the arbuscule-containing and the adjacent cortical cells colonized by fungal hyphae. Amongst the AM-induced genes specifying transcriptional regulators were two members encoding CAAT-box binding transcription factors (CBF), designated *MtCbf1* and *MtCbf2*. Promoter analyses demonstrated that both genes were already activated by the first physical contact between the symbionts. Subsequently, and corresponding to our cell-type expression patterns, they were progressively up-regulated in those cortical areas colonized by fungal hyphae, including the arbuscule-containing cells. The encoded CBFs thus represent excellent candidates for regulators that mediate a sequential reprogramming of root tissues during the establishment of an AM symbiosis.

INTRODUCTION

Ecto- and endomycorrhizal symbioses between higher plants and soil fungi are the most widespread beneficial plant-microbe interactions on Earth. Mycorrhizae are characterized by the transfer of limiting nutrients, in particular phosphorus and nitrogen, from fungal hyphae to the plant. In return, plants deliver hexoses to the fungi (Nehls *et al.* 2007), leading to a strongly increased photosynthate allocation to mycorrhizal roots. Apart from direct advantageous effects resulting from improved nutrition, indirect benefits of mycorrhizal interactions are enhanced resistences against abiotic and biotic stress conditions (Smith and Read 2008).

Some 80% of all terrestrial plants enter an arbuscular mycorrhiza (AM) symbiosis with *Glomeromycota* fungi (Schüssler *et al.* 2001). During AM, extraradical hyphae emerging from germinating spores penetrate the rhizodermis via hyphopodia, pass through outer cortical cells and proliferate in the inner cortex (Parniske 2008). In Arum-type AM, these intraradical hyphae form highly branched intracellular structures termed arbuscules (Harrison 1999). It has been shown that arbuscules are transient structures that only operate for a couple of days, indicating a tight control of their development and function (Harrison 2005). Transfer of phosphorus and other minerals from fungal hyphae to the plant cytoplasm occurs at the periarbuscular interface that comprehends the fungal arbuscular membrane, the periarbuscular matrix, and the plant periarbuscular membrane (Parniske 2000, 2008). The uptake of phosphorus is energy-dependent and requires plant and fungal H^+-ATPases (Requena *et al*. 2003) for an acidification of the periarbuscular space. Based on the localization of reporter proteins, Pumplin and Harrison (2009) demonstrated that different proteins are apparently targeted to specific domains of the periarbuscular membrane, indicating the presence of functional compartments at the symbiotic interface. In addition to AM-specific phosphate transporters essential for symbiotic P_i transfer (Harrison *et al*. 2002, Bucher 2007, Javot *et al.* 2007), two half-ABC transporters have recently been shown to be required for a functional AM symbiosis (Zhang *et al.* 2010).

An important benefit of legumes as AM models derives from the fact that this genus is able to enter a second beneficial plant-microbe interaction that leads to the development of nitrogen-fixing root nodules (Brewin *et al.* 1991). To initiate nodulation, secreted flavonoids first induce rhizobial genes required for the synthesis of lipochitooligosaccharide (LCO) nodulation (Nod)-factors. These Nod-factors, after perception by plant LysM-domain receptor kinases (Arrighi *et al.* 2006), activate downstream responses; that way inducing the formation of nodule primordia and mediating bacterial

infection (Oldroyd and Downie 2008). During AM, a similar molecular dialogue is initiated by the host plant via strigolactones that promote the branching of fungal hyphae and activate fungal metabolism (Akiyama *et al.* 2005, Besserer *et al.* 2006). Subsequent recognition of AM fungi by the host involves the perception of diffusible Myc-signals (Kosuta *et al.* 2003) including LCOs structurally related to rhizobial Nod-factors (Maillet *et al.* 2011). Together, the diffusible Myc-signals prepare root infection by communicating the symbiotic nature of mycorrhizal fungi (Oldroyd *et al.* 2005, Ercolin and Reinhardt 2011). Following their entry via hyphopodia, fungal hyphae grow along a pre-penetration apparatus (PPA), a cytoplasmic channel formed after the establishment of hyphopodia (Genre *et al.* 2005, 2008). This coordinated cytological response of epidermal cells indicates that in addition to diffusible Myc-signals acting at a distance (Kuhn *et al.* 2010), there are others that require fungal contact (Kosuta *et al.* 2003, Kloppholz *et al*. 2011). It has to be pointed out that signalling also takes place in later stages of the symbiosis; where genes specifically expressed in arbuscule-containing cells have to be activated (Harrison 2005). One such late signal triggering the induction of a phosphate transporter gene was identified as lyso-phosphatidylcholine (Drissner *et al.* 2007).

Targeted molecular research on AM suffers from two obstacles: an asynchronous development of the symbiosis leading to the concomitant presence of different stages, and an obligate biotrophy of AM fungi. In the last couple of years, untargeted high-throughput expression profiling was pursued to generate an inventory of AM-induced genes (Liu *et al*. 2003, Wulf *et al.* 2003, Frenzel *et al*. 2005, Hohnjec *et al*. 2005, Hohnjec *et al*. 2006, Küster *et al*. 2007b). These approaches benefited from the identification of two legumes that proved to be excellent AM models: *Medicago truncatula* (Barker *et al*. 1990, Rose 2008) and *Lotus japonicus* (Handberg and Stougaard 1992). In case of *M. truncatula*, current research relies on an advanced genome project (Cannon *et al.* 2009, Young and Udvardi 2009), more than 250.000 ESTs in the DFCI *Medicago* Gene Index (Quackenbush *et al*. 2001), and different microarray as well as GeneChip tools (Küster *et al*. 2004, Küster *et al.* 2007a, Hohnjec *et al*. 2005, Lohar *et al*. 2006, Benedito *et al*. 2008). Publicly available expression profiles based on EST, microarray, and GeneChip data can be queried using the DFCI *Medicago* Gene Index (Quackenbush *et al*. 2001), the Truncatulix (Henckel *et al.* 2009) and MediPlEx (Henckel *et al.* 2010) data warehouses as well as the *Medicago truncatula* Gene Expression Atlas, the latter exclusively integrating expression profiles generated via GeneChips (Benedito *et al.* 2008).

Although the transcriptome studies performed so far resulted in an identification of hundreds of AM-related genes (Balestrini and Lanfranco 2006, Hohnjec *et al.* 2006), there is limited information on the signalling components activated during the formation of arbuscules and in particular on the transcriptional regulators involved in the reprogramming of root cortical cells towards an accomodation of symbiotic fungi. One obvious reason for this can be seen in the fact that most AM-related expression profiles were based on pooled tissue samples containing a mixture of different cell-types and stages of arbuscule development. To overcome this problem, Balestrini *et al.* (2007) pioneered the use of laser-microdissection for the identification of arbuscule-specific phosphate transporter genes in AM roots of tomato via RT-PCR. A similar approach was later used in the studies of Gomez *et al.* (2009) and Guether *et al.* (2009) to track genes up-regulated in arbuscule-containing cells of *M. truncatula* and *L. japonicus*, respectively. On the level of individual genes, detailed *in situ* expression analyses were performed for selected genes (Küster *et al.* 2007b), including amongst others the phosphate transporter gene *MtPt4* (Liu *et al.* 2003), the *MtBcp1* gene encoding a blue-copper-binding protein (Hohnjec *et al.* 2005), and members of the AM-induced lectin gene family (Frenzel *et al.* 2005). Nevertheless, to our knowledge no promoter of a transcription factor gene specifically activated in AM roots was investigated so far.

In this study, we intended to sharpen our view on AM-related gene expression by a two-step approach. First, we performed a global transcriptome analysis of *M. truncatula* roots inoculated with the two widely studied AM fungi *Glomus intraradices* and *Glomus mosseae*. By using these two different microsymbionts, we were able to make use of the overlap of gene activation in both AM interactions, that way minimizing strain- or inoculum-related effects. To achieve a genome-wide identification of AM-activated genes, we relied on *Medicago* GeneChips; reported to cover more than 80% of the gene space in the model legume *M. truncatula* (Benedito *et al.* 2008). This marked extension of gene-specific probes significantly advanced earlier microarray-based AM transcriptome studies (Liu *et al.* 2003, Manthey *et al.* 2004, Hohnjec *et al.* 2005), leading to the identification of a core set of 512 *M. truncatula* genes involved in both AM interactions. In a second step, we intended to shed light on the spatial expression of a subset of AM-related genes. To achieve this goal, we performed cellular expression studies via real-time RT-PCR, using RNA isolated from distinct pools of laser-microdissected cells. In our study, gene expression in *M. truncatula* arbuscule-containing cells was for the first time directly compared with transcription in the adjacent cortical cells colonized by fungal hyphae. As a control, cortical cells from non-mycorrhized roots were used to gain information

on gene expression in the absence of a symbiotic interaction. With an emphasis on genes encoding membrane transporters, signalling-related proteins, and transcriptional regulators, this approach identified novel components of the cell-specific programme orchestrating AM symbiosis. In total, we identified 25 arbuscule-specific genes, while 37 genes were activated both in arbuscule-containing and in the neighbouring cells. Together, these results highlight general mechanisms underlying fungal colonization up to the formation of arbuscules. Among the transcriptional regulators, we identified two highly similar genes encoding CAAT-box binding transcription factors (CBF), which we analyzed in more detail via the expression of promotor-GUS fusions in transgenic roots. Remarkably, both genes are already activated by the initial physical contact between fungal hyphae and the plant epidermis and are expressed concomitantly with fungal colonization of the root cortex up to the formation of arbuscules, making the encoded CBFs excellent candidates for regulators mediating the sequential reprogramming of root tissues during the establishment of an AM symbiosis.

MATERIAL AND METHODS

Plant growth, AM fungal inoculation, and visualisation of AM fungal structures

Medicago truncatula Gaertn cv Jemalong genotype A17 seeds were surface-sterilized and scarified as reported by Hohnjec *et al.* (2003). Plants were grown in the climate chamber (humidity: 70 %; photosynthetic photon flux: 150 µmol m^{-2} s^{-1}) at a 16 h light (23 °C) and 8 h dark (18 °C) regime. For subsequent *Medicago* GeneChip hybridizations using whole roots, plants were mycorrhized with AM fungi under conditions of phosphate limitation (20 µM phosphate). In addition, nonmycorrhizal roots grown at 20 µM phosphate as well as nonmycorrhizal roots grown at 2 mM phosphate were generated as described previously (Hohnjec *et al.* 2005). Two different AM fungal inocula were used: *Glomus mosseae* granular AMF inoculum BEG 12 (Biorize R&D, Dijon, France), and *Glomus intraradices* Schenck and Smith DAOM197198 inoculum (Premier Tech Biotechnologies, Rivière-de-Loup, Québec, Canada), the latter having recently been reassigned to *Rhizophagus irregularis* (Błaszk., Wubet, Renker, and Buscot) C. Walker & A. Schüßler comb. nov. (Stockinger *et al*. 2009). At 28 days post inoculation (dpi) with AM fungi or at 28 days growth under nonmycorrhizal conditions, roots were harvested and frozen in liquid nitrogen. Randomly selected areas of mycorrhizal roots were stained for fungal colonization using the gridline intersection method according to McGonigle *et al*. (1990). Here, the percentage of root length colonization (RLC; scoring hyphae, spores, vesicles, or arbuscules) ranged from 60% to 80%, while the relative arbuscule frequency in colonized fragments varied between 60% and 75%.

To obtain mycorrhizal roots for embedding in Steedman's wax, two-weeks old seedlings were mycorrhized by adding 15% (v/v) inoculum *Glomus intraradices* isolate 49 (Maier *et al*. 1995) produced in leek cultures (*Allium porrum* cv. Elefant) to the substrate. Mycorrhizal and non-mycorrhizal plants were fertilized with half-strength Hoagland`s solution containing 20 µM phosphate and an additional 2mM NH_4NO_3. RLC was checked regularly via ink-staining according to the protocol of Vierheilig *et al*. (1998) and gridline intersection counting according to McGonigle *et al*. (1990). 70-80% RLC turned out to be most convenient for the selection of arbuscule-containing and adjacent cortical cells. This level of colonization was usually reached at 21 dpi.

Tissue embedding, tissue sectioning, and laser-microdissection

Roots were embedded using the Steedman's wax protocol (Gomez *et al.* 2009) with the following modifications: Eosin was already added in the first step of the ethanol series (75% (v/v) ethanol with

0,1% (v/v) Eosin y), the overnight fixation step in Farmer`s fixative and the overnight incubation step in 1:1 ethanol:wax were extended from 12 to 14 h, and root pieces were embedded in TurbOflow®II molds as well as cassettes (McCormick Scientific, Richmond, USA). Blocks were stored in vacuum-sealed plastic bags containing desiccant bags at 4°C.

Longitudinal root sections of 12 µm were obtained using a Hyrax M55 rotary microtome (Zeiss, München, Germany). Ribbons were spread on heat-sterilized glass slides and were stretched with DEPC-treated autoclaved water. Slides were dried for one hour in a hybridization oven at 32°C. Slides with sections were used on the same or the following two days and stored in vaccum-sealed plastic bags with desiccation bags at 4°C if necessary. Sections were de-waxed immediately before cell harvest by washing the slides with absolute ethanol several times at 40°C on a heating plate, until the wax was not visible anymore. Subsequently, slides were dried on the heating plate.

The P.A.L.M. Microbeam system with a Capmover (Zeiss, München, Germany) was used for laser-microdissection and pressure catapulting (LMPC). To collect cells, the "CloseCut and Auto-LPC" function was used according to the manufacturer's instructions. Cells were collected into 500 µl adhesive caps (Zeiss, München, Germany) and stored directly at -80°C after the harvest was completed.

For each cell-type, four biological replicates were produced, based on distinct rounds of plant cultivation and root embedding. Biological replicates consisted of three technical replicates of approximately 1000 cells each, which were pooled after RNA isolation and amplification.

RNA isolation and amplification

Whole-root mycorrhizal samples were taken from frozen stocks, pooled, and ground using lysing matrix D tubes (MP Biomedicals, Illkirch, France) in a FastPrep (MP Biomedicals, Illkirch, France) prior to RNA extractions. Total RNA isolation and DNase I on-column digestion was performed via RNeasy kits (Qiagen, Hilden, Germany) according to the manufacturer's instructions. RNA preparations were quality-checked both via spectrophotometry (NanoDrop ND-1000, Peqlab, Erlangen, Germany) and via capillary electrophoresis in RNA Nano chips (Agilent Bioanalyzer, Agilent, Böblingen, Germany), as recommended by the manufacturers.

Total RNA was isolated from laser-microdissected cells using the RNeasy Micro kit (Qiagen, Hilden, Germany). 350 µl RLT buffer containing ß-mercaptoethanol were added to each sample followed by a 30 min incubation at room temperature. The lysate was spun down for 5 min at 13.400 g, mixed

1:1 with ethanol absolute and transferred to the clean-up column. On-column DNAse I digestion was peformed according to the manufacturer`s instructions. RNA from laser-microdissected cells was amplified using the TargetAmp 2-round aRNA amplification kit (Epicentre Biotechnologies, Madison, USA), as specified by the manufacturer. Quantity and quality of total RNA as well as T7-amplified aRNA was checked via capillary electrophoresis in RNA Pico and Nano Chips, respectively, using an Agilent 2100 Bioanalyzer (Agilent, Böblingen, Germany).

Medicago GeneChip hybridizations

RNA was processed for use on Affymetrix (Santa Clara, CA, USA) GeneChip *Medicago* Genome Arrays, according to the manufacturer's GeneChip 3' IVT Express kit user manual. Briefly, 100 ng of total RNA with by a RIN number (Agilent 2100 Bioanalyzer, Agilent, Böblingen, Germany) of at least 8.5 containing spiked-in poly-A^+ RNA controls was used in a reverse transcription reaction (GeneChip 3' IVT Express Kit; Affymetrix, Santa Clara, CA, USA) to generate first-strand cDNA. After second-strand synthesis, double-stranded cDNA was used in a 16 h *in vitro* transcription (IVT) reaction to generate aRNA (GeneChip 3' IVT Express Kit; Affymetrix, Santa Clara, CA, USA). Size distribution of *in vitro* transcribed aRNA and fragmented aRNA, respectively, was assessed via an Agilent 2100 Bioanalyzer (Agilent, Böblingen, Germany), using an RNA 6000 Nano Assay. 10 µg of fragmented aRNA was added to a 300-µl hybridization cocktail also containing hybridization controls. 200 µl of the mixture was hybridized on GeneChips for 16 h at 45°C. Standard post hybridization wash and double-stain protocols (FS450_0001; GeneChip HWS kit; Affymetrix, Santa Clara, CA, USA) were used on an Affymetrix GeneChip Fluidics Station 450. GeneChips were scanned on an Affymetrix GeneChip scanner 3000 7G.

Evaluation of data from *Medicago* GeneChip hybridizations

Cel files obtained from *Medicago* GeneChip hybridizations were analysed using the Robin software (http://mapman.gabipd.org/web/guest/robin). Normalization was performed across all GeneChips using the Robust Multichip Average (RMA) algorithm. Intensity values calculated for each probe set were log2-transformed and averaged across all three biological replicates. Log2 differences between the conditions studied were evaluated statistically by applying a false discovery rate (FDR) correction for p-values implemented in Robin. Original annotations of probes from *Medicago* GeneChips were replaced by automated annotations as well as functional classifications generated via SAMS (Bekel *et*

al. 2009) and Gene Ontology (GO) classifications (http://www.medicago.org/GeneChip). To visualize gene expression profiles, MapMan (Usadel *et al.* 2005) was used. Data from *Medicago* GeneChip hybridizations were related to *in silico* expression profiles using MediPlEx (Henckel *et al.* 2010), applying the "arbuscular mycorrhizal root libraries" preselection. Since *Medicago* GeneChips are based on gene models from EST and genomic sequences, the number of probe sets exceeds the number of genes represented to a certain extent. Nevertheless, we refer to genes instead of probe sets in this work for reasons of simplicity.

real-time RT-PCR

Primers were designed using the Primer3 web interface (Rozen and Skaletsky, 2000) according to the following criteria: product size range 100-150 bp; primer size min: 18 bp, opt: 21 bp, max: 24 bp; primer Tm min: 52°C, opt: 53°C, max: 55°C. If the position of the coding region was known, the amplicon was preferentially positioned in the 3' region of the gene or the 3' UTR. The primer pairs suggested by the primer3 program were blasted against the DFCI Medicago Gene Index (Quackenbush *et al.* 2001) to check for mispriming in known *M. truncatula* transcript sequences. The number of matching base pairs in off-target genes and especially matches at the 3' end of the primer were taken into account and the most suitable primer pair according to these parameters was chosen. All primer pairs were tested for performance and specifity with RNA from whole root tissue prior to using them for RNA from laser-microdissected samples. For some of the genes, primer pairs published by Gomez *et al*. (2009) were used. These are indicated in Supplemental Table S5, where all primer pairs are listed.

For the laser-microdissected samples, 50 ng of T7-amplified RNA (aRNA) were used for real-time RT-PCR, using the SensiMix™ SYBR one-Step kit (Bioline, Luckenwalde, Germany). RT-PCR conditions (Realplex cycler, Eppendorf, Germany) were as follows: 10 min 42°C, 10 min 95°C, 50 cycles (15 sec 95°C, 30 sec 55 °C, 30 sec 72°C), 15 sec 95°C, melting curve from 40-95°C. In addition to a melting curve analysis, all real-time PCR-products were separated on 2 %(w/v) agarose gels to check both for specificity and a correct amplification size. Resequencing of selected PCR-products was used to additionally confirm the specific amplification of the target gene. Expression results were averaged over 3 biological replicates. In case one replicate delivered a significantly deviant result from the other two, the measurement was repeated. If the difference persisted, the fourth replicate was included into the analysis and replaced the replicate in question, if this resulted

in a more consistent expression pattern. The constitutive translation elongation factor gene *MtTefα* (TC178258 in the DFCI *Medicago* Gene Index) was used for normalization across different conditions. *MtTefα* expression was analyzed in 4 technical replicates, and the average value was used to calculate relative gene expression levels using the $2^{-\Delta CT}$ value with $\Delta CT=CT_{gene}-CT_{MtTef\alpha}$. Expression differences were analyzed for significance using the Student's t-test incorporated in MS® Excel® 2007 (Microsoft® Corp., Seattle, USA).

For the whole root samples, 50 ng of total RNA were used for real-time RT-PCR, using the SensiMix™ SYBR one-Step kit (Bioline, Luckenwalde, Germany) according to the manufacturer's instructions. The constitutive translation elongation factor gene *MtTefα* (TC178258 in the DFCI *Medicago* Gene Index) was used for normalization across different conditions. All expression results were averaged over 3 biological replicates. Relative gene expression levels were calculated as described above.

Construction and Histological Analysis of Transgenic Hairy Roots

The promoters of two CAAT-box transcription factor genes represented by probe sets Mtr.51511.1.S1_at (referred to as *MtCbf1*) and Mtr.16863.1.S1_at (referred to as *MtCbf2*) were PCR-amplified with Phusion Hot Start DNA polymerase (Finnzymes, Biozym, Hessisch Oldendorf, Germany) from *Medicago truncatula* Gaertn cv Jemalong genotype A17 genomic DNA, using gene-specific primers containing appropriate restriction sites. The amplified products covered the -1513/-3 region for *MtCbf1* and the -1484/-6 region for *MtCbf2* relative to the start codon. The promoter regions were cloned in front of the *gus*Aint gene of pGUSint (Hohnjec *et al*. 2003) using *Sph*I/*Sma*I restriction sites for *MtCbf1* and *Sph*I/*EcoR*I restriction sites for *MtCbf2*. Whereas the promoter-GUS-fusion of *MtCbf1* was excised using *Spe*I, the promoter-GUS-fusion of *MtCbf2* was excised using *Sal*I/*Stu*I. Both fragments were filled in with Klenow Polymerase, and cloned into the *Sma*I site of the binary plasmid pRedRoot (Limpens *et al*. 2004). The plasmids obtained were electroporated into *Agrobacterium rhizogenes* ARqua1, and the resulting strains were used to generate hairy roots on *M. truncatula* cv Jemalong A17 according to Vieweg *et al*. (2004). Transgenic roots were identified using dsRed fluorescence (Leica MZ 10F, Leica Microsytems, Wetzlar, Germany) and were mycorrhized by adding 15% (v/v) inoculum *Glomus intraradices* isolate 49 (Maier *et al*. 1995) produced in leek cultures (*Allium porrum* cv. Elefant) to the substrate. GUS assays were performed as described by Hohnjec *et al*. (2003), without preheating of the samples. To obtain thin

sections, GUS-stained roots were embedded in 5% agarose and cut using a Leica VT1000S vibratome (Leica, Wetzlar, Germany). Counterstaining of fungal structures was performed with Alexa Fluor® 488 WGA conjugate (Invitrogen, Darmstadt, Germany). Roots were bleached for 3 min in 10% KOH at 95°C, washed three times with water and stained in PBS-buffer containing 20 µg/ml Alexa Fluor® 488 WGA conjugate overnight. For staining of fungal structures in thin sections and staining of extraradical hyphae on the root surface, samples were directly transferred into PBS-buffer containing 20 µg/ml Alexa Fluor® 488 WGA conjugate and stained overnight. Photo documentation was performed with a Leica MZ 10F stereomicroscope (Leica Microsytems, Wetzlar, Germany), equipped with an Olympus XC50 camera (Olympus, Hamburg, Germany) and with a Zeiss Axio Observer Z1 microscope equipped with an AxioCam ICc1 (Zeiss, München, Germany).

RESULTS AND DISCUSSION

Genome-wide transcriptome profiling identifies a core set of 512 *Medicago truncatula* genes related to root colonization by AM fungi

M. truncatula roots colonized with either *G. intraradices* or *G. mosseae* under conditions of phosphate limitation (20 µM phosphate) were stained for fungal structures 28 days post inoculation (McGonigle *et al.* 1990). To minimize dilution by non-colonized regions, we selected roots with a similarly high root length colonization (60 to 80%) and high arbuscule frequencies (60 to 75%) for the isolation of total RNA. Samples were checked for AM (*MtPt4*) and nodule marker (*MtEnod18*) gene expression via RT-PCR, as described by Hohnjec *et al.* (2005). Since some AM-induced genes can be activated by phosphate, we incorporated a study of gene expression in nonmycorrhizal roots grown for 28 days in the presence of a high (2 mM) phosphate concentration. As a common control, nonmycorrhizal roots grown for 28 days under phosphate limitation (20 µM phosphate) were harvested.

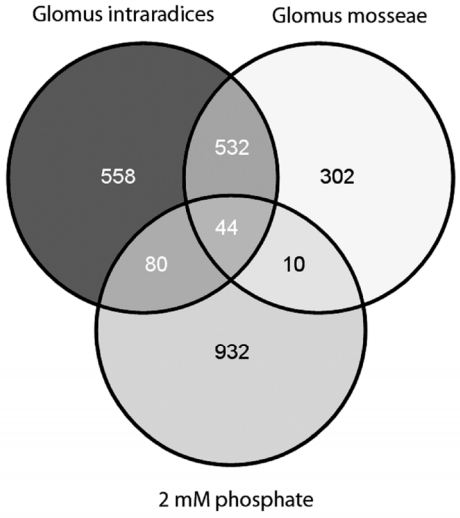

Figure I_1: Transcriptional response of *M. truncatula* roots to a colonization with different AM fungi and to a treatment with 2 mM phosphate.
M. truncatula roots were inoculated with *G. intraradices* and *G. mosseae* for 28 days under conditions of phosphate limitation (20 µM phosphate). Alternatively, roots were grown for 28 days in the presence of 2 mM phosphate. Genes significantly upregulated 2-fold at an FDR-corrected p-value of $p<0.05$ in relation to control roots grown under conditions of phosphate limitation were compared to identify co-regulation of expression. Numbers indicate genes activated in different conditions. Diagrams were drawn using Venny: (http://bioinfogp .cnb.csic.es/ tools/venny/index.html).

Total RNA isolated from three biological replicates of mycorrhizal and nonmycorrhizal roots was used for GeneChip hybridizations. In our study, each biological replicate is defined as a pool comprising five root systems. The complete dataset is available from the Gene Expression Omnibus (accession number GSE32208) and is also included as Supplemental Table S_I_1. Applying a two-fold induction at a false discovery rate (FDR)-corrected p-value of $p<0.05$ as cutoff, we found that 1214 and 888 genes were up-regulated in *G. intraradices*- and *G. mosseae*-colonized roots, respectively, whereas 576 genes were co-

activated in both AM interactions (Figure I_1, Supplemental Table S_I_2).

Of the 576 AM-induced genes, 44 were also activated at the cutoffs mentioned above in roots treated with 2 mM phosphate, leaving a core set of 532 genes significantly induced by two different AM fungi but not via elevated phosphate levels (Figure I_1, Supplemental Table S_I_2). The low overlap between phosphate-induced gene expression and transcriptional activation by AM fungal colonization is in line with reports of Liu et al. (2003) and Hohnjec et al. (2005), illustrating that phosphate supply is unable to mimic AM-induced gene expression.

Our core set of 532 AM-related genes is supported by a search in the MediPlEx database (Henckel *et al.* 2010), combining *in silico* gene expression in AM EST collections from the DFCI *Medicago* Gene Index (libraries #ARE, #ARB, T1682, #GFS, 5520, #9CR) with the GeneChip hybridizations detailed above. This search returned 91 genes of the core set as AM-induced with an R-value larger than 2 (Stekel *et al*. 2000, Supplemental Table S_I_2). Moreover, our core set contained 51 genes reported as co-induced in the same two AM interactions when relying on oligonucleotide microarrays (Hohnjec *et al*. 2005, Supplemental Table S_I_2), whereas it

Table I_1: *M. truncatula* AM marker genes activated in roots colonized with *G. intraradices* and *G. mosseae*.

Probe IDs of *Medicago* GeneChips are referenced to the corresponding DFCI *Medicago truncatula* Gene Index IDs (release 10) and to *M. truncatula* gene names from the literature. Log2 ratios of gene expression for *G. intraradices*-colonized (Gi-Myc), *G. mosseae*-colonized (Gm-Myc), and 2 mM phosphate-treated (2 mM-P) roots, all measured against roots grown at 20 µM phosphate, are given. Whereas all 15 AM marker genes are significantly upregulated in the AM roots used for expression profiling, none of them is activated in roots treated with 2 mM phosphate. FDR-corrected p-values (FDR-p) are indicated. References for the AM-induced genes identified are as follows: *MtPt4* (Javot *et al*. 2007), *MtMyb1* (Liu *et al.* 2003), *MtTi1* (Grunwald *et al.* 2004), *MtLec7* (Frenzel *et al*. 2005), *MtGst1* (Wulf *et al*. 2003), *MtBcp1* (Hohnjec *et al*. 2005), *MtLec5* (Frenzel *et al.* 2005), *MtGlp1* (Doll *et al*. 2003), *MtHa1* (Krajinski *et al.* 2002), *MtScp1* (Liu *et al.* 2003), *MtVapyrin* (Pumplin *et al.* 2009), *MtSbtM1* (Takeda *et al.* 2011), *MtZip7* (Burleigh *et al.* 2003), *MtAnn2* (Manthey *et al*. 2004), and *MtDxs2* (Floss *et al.* 2008b).

GeneChip Probe ID	DFCI 10 ID	Gene	Gi-Myc	FDR-p	Gm-Myc	FDR-p	2 mM-P	FDR-p
Mtr.43062.1.S1_at	TC142142	MtPt4	10.02	2.7E-10	8.65	1.0E-09	-0.38	5.1E-01
Mtr.8863.1.S1_at	TC146022	MtMyb1	9.90	6.7E-10	8.99	2.3E-09	0.21	8.1E-01
Mtr.16454.1.S1_at	TC152603	MtTi1	9.71	5.0E-11	8.41	1.7E-10	-0.04	9.6E-01
Mtr.45648.1.S1_at	TC143767	MtLec7	9.02	2.7E-10	8.30	8.7E-10	0.40	4.3E-01
Mtr.15957.1.S1_at	TC166174	MtGst1	8.98	1.7E-09	8.13	6.6E-09	-0.14	8.9E-01
Mtr.15627.1.S1_at	TC159695	MtBcp1	8.15	5.1E-09	6.63	6.8E-08	-0.19	8.5E-01
Mtr.15653.1.S1_at	TC143161	MtLec5	8.01	8.9E-10	7.64	2.0E-09	-0.08	9.3E-01
Mtr.12500.1.S1_at	TC153539	MtGlp1	7.94	5.1E-10	7.80	8.8E-10	-0.39	4.2E-01
Mtr.43470.1.S1_at	TC141883	MtHa1	7.80	8.3E-09	6.80	5.7E-08	0.11	9.2E-01
Mtr.40285.1.S1_at	TC143816	MtScp1	5.35	6.7E-08	5.16	1.9E-07	-3.51	7.7E-06
Mtr.39050.1.S1_at	TC149084	MtVapyrin	4.89	1.4E-06	3.77	3.2E-05	-0.59	4.2E-01
Mtr.32129.1.S1_at	AW584611	MtSbtM1	4.80	2.2E-06	3.61	6.1E-05	0.38	6.7E-01
Mtr.40995.1.S1_at	TC145398	MtZip7	2.62	4.2E-06	2.29	2.7E-05	0.38	3.6E-01
Mtr.20364.1.S1_at	TC153713	MtAnn2	2.42	1.9E-02	1.53	3.2E-02	0.46	7.3E-01
Mtr.43585.1.S1_at	TC141952	MtDxs2	1.57	4.7E-04	1.87	2.1E-04	-4.26	2.8E-07

encompassed 346 genes reported as activated at least twofold by *G. intraradices* under different experimental conditions on the basis of *Medicago* GeneChips (Gomez *et al.* 2009, Supplemental Table S_I_2).

Among the core set of AM-related genes, 15 well-known AM expression markers (Hohnjec et al. 2006, Küster et al. 2007b) were identified as strongly induced in our conditions (Table I_1). As an example, the *MtPt4* gene encoding a phosphate transporter known to be required for an efficient AM symbiosis (Javot *et al.* 2007) was activated more than 1000 (log_2=10.02)- and 400 (log_2=8.65)-fold in *G. intraradices*- and *G. mosseae*-colonized roots, respectively. This very strong induction of AM-related marker genes (Table I_1) indicates that our approach should allow an identification also of those genes expressed either transiently or activated less strongly during arbuscule development.

Via comparisons of Medicago GeneChip probes to currently available *Glomus intraradices* sequences (Tisserant *et al.* 2011), 20 Glomus genes were identified amongst the set of 532 genes co-induced in both AM interactions (Supplemental Table S_I_2). The remaining 512 AM-related *M. truncatula* genes were grouped into functional categories, based on automated annotations of the encoded gene products via the SAMS software (Bekel *et al.* 2009) and Gene Ontology classifications (http://www.medicago.org). In addition, MapMan (Usadel *et al.* 2005) was used to visualize gene expression profiles and to identify functional categories expressed most significantly different from others.

In Figure I_2, the distribution of AM-coinduced genes into functional categories is shown. Typical AM-related gene families of unknown biological function encoding annexins (e.g. *MtAnn2*, Manthey *et al.* 2004), blue-copper proteins (e.g. *MtBcp1*, Hohnjec *et al.* 2005), germin-like proteins (e.g. *MtGlp1*, Doll *et al.* 2003), and lectins (e.g. *MtLec5* and *MtLec7*, Frenzel *et al.* 2005) are classified seperately. For all these gene families except the one encoding annexins, comparisons to the *Medicago truncatula* Gene Expression Atlas (He *et al.* 2009) revealed that their members were expressed either specifically or were almost exclusively activated in AM roots in comparison to all other tissues analysed (data not shown), that way widening our knowledge on previously unknown AM-related family members.

In addition to these gene families, the following functional categories were most prominent (Figure I_2, Supplemental Table S_I_2): (1) cell wall biosynthesis and modification, including several enzymes related to a remodeling of the extracellular matrix; (2) chitin degradation,

including several chitinases that might be involved in the disassembly of fungal structures; (3) protein degradation, including a range of different proteinases and peptidases that can be connected to the dynamic turnover of mycorrhizal structures; (4) hormone metabolism, including several genes involved in gibberellin biosynthesis; and (5) secondary metabolism, including a high number of cytochromes, components of the carotenoid metabolism, and UDP-sugar transferases. The activation of these functions is in line with previous reports on gene expression in AM roots (Liu *et al.* 2003, Wulf *et al.* 2003, Hohnjec *et al.* 2006, Küster *et al.* 2007b, Guether *et al.* 2009). Interestingly, the categories "membrane transporters", "signalling" and "transcription factors" were not only prominent but their members were also expressed most significantly different from others in AM roots (data not shown), based on statistical analyses implemented in MapMan (Usadel *et al.* 2005). In addition, many of these candidate genes either displayed a mycorrhiza-specific or mycorrhiza-enhanced expression in AM roots according to the *Medicago* Gene

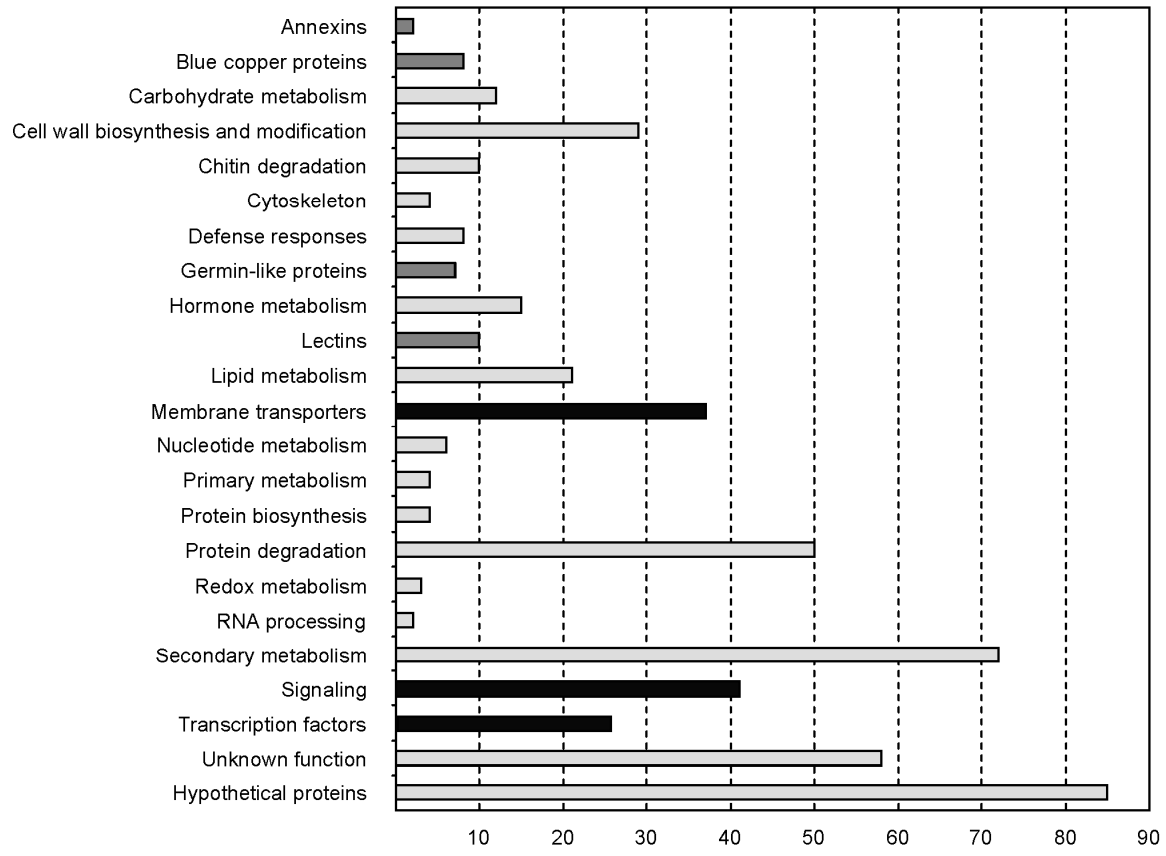

Figure I_2: Cellular functions of *M. truncatula* genes activated in mycorrhizal roots.
All 512 *M. truncatula genes* co-induced at least two-fold at an FDR-corrected p-value of $p<0.05$ in response to the AM fungi *G. intraradices* and *G. mosseae* that were not induced by a treatment with 2 mM phosphate (Supplemental Table S_I_2) were grouped into functional categories. The number of genes allocated to each functional category is indicated. The bars are coloured as follows: black, functional categories studied by laser-microdissection; dark grey, AM-related gene families; light grey, other functional categories.

Expression Atlas (He *et al*. 2009), suggesting a relevance for AM interactions. Remarkably, these analyses also returned six TF genes co-induced in our conditions as being specifically expressed in AM tissues (Supplemental Figure S_I_1). Since the three cellular functions mentioned are particularly relevant for coordinating the reprogramming of root cortical cells towards an accomodation of fungal structures, we investigated the cellular expression patterns of 71 candidate genes selected from these categories via laser-microdissection.

Longitudinal sections allow an accurate separation of specific cell-types from AM roots via laser-microdissection

We used laser-microdissection to obtain specific pools of three different cell-types in four biological replicates: cortical cells from non-colonized control roots (CCR), cortical cells from mycorrhizal roots (CMR), and cortical cells containing arbuscules (ARB) (Figure I_3). We found that embedding of roots in Steedman`s wax (Gomez *et al*. 2009) preserves root morphology, allowing an identification of vascular tissues, cortical cells and the epidermal cell layer including root hairs (Figure I_3 A-C). In contrast to transverse sections (Balestrini *et al*. 2007, Gomez *et al*. 2009), our longitudinal sections offered the possibility to evaluate the colonization status of whole root regions. Chains of arbuscules in different developmental stages and fungal hyphae growing in the extracellular space of adjacent cortical cells were clearly visible (Figure I_3 E-H). This facilitated cell harvest and allowed us to focus not only on mature arbuscules filling the complete cell lumen (ARB-samples; Figure I_3 D,G,H), but also on cortical cells interspersed with fungal hyphae in the immediate neighbourhood of arbuscule-containing cells (CMR-samples; Figure I_3 E,F). Since each cell pool from the CMR cell-type differs in the density and growth of fungal hyphae, the CMR samples are expected to display the strongest variation of transcriptional changes.

To assess the suitability of the collected samples and to check in particular for cross-contamination between CMR and ARB samples, the expression of the six AM marker genes *MtPt4*, *MtBcp1*, *MtScp1*, *MtLec5*, *MtGlp1* and *MtHa1* (Harrison *et al*. 2002, Hohnjec *et al*. 2005, Liu *et al*. 2003, Frenzel *et al*. 2005, Doll *et al*. 2003, Krajinski *et al*. 2002) was measured in all four biological replicates. Whereas transcripts of the *MtTef*α gene used as a constitutive control were amplified from all three cell-types (Figure I_4 A), transcripts of the six AM-specific genes tested were not detected in CCR samples, as could be expected (data not shown). The

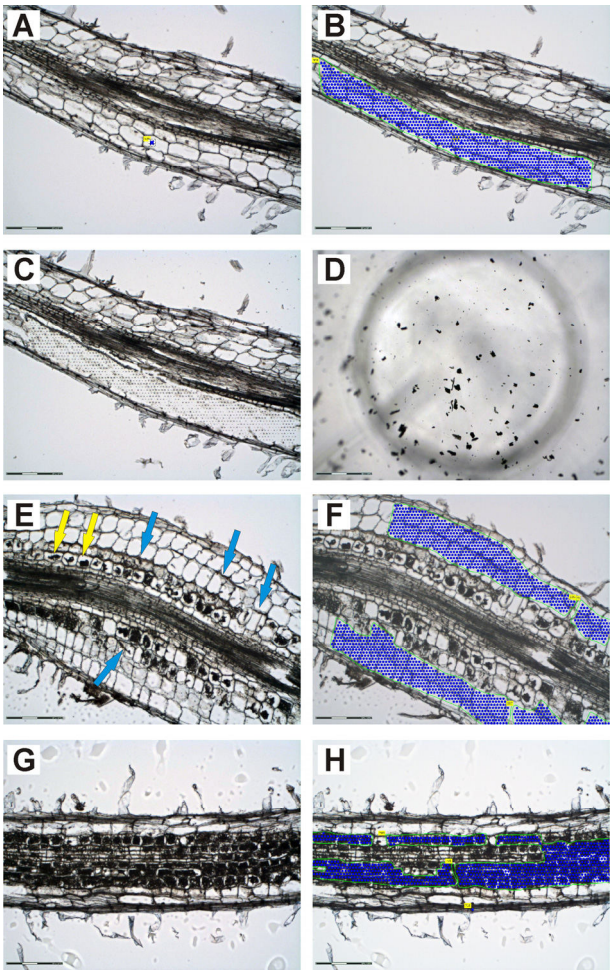

Figure I_3: Laser-microdissection of three specific cell-types from *M. trunctula* roots. Root areas designated for cell harvest are marked with a green line and blue dots. Along the line the laser dissects the cells from the surrounding tissue, while dots represent single catapulting events. **A to C**: Longitudinal section of a non-mycorrhized root used for the collection of cortical cells from control roots (CCR). **A and B**: Section before and after selection of CCR for laser-microdissection. **C**: Section after laser-microdissection of CCR. **D**: View into the collection-tube showing typical flakes of harvested cells (in this case arbuscule-containing cells). **E to H**: Longitudinal sections of mycorrhized roots displaying chains of arbuscules at different developmental stages and fungal hyphae growing in the apoplast of outer cortical cells. **E and F**: Section before and after selection of cortical cells from mycorrhized roots (CMR). The harvested area was extended to inner cortical cells in case no arbuscules were visible in these cells. Fungal hyphae are present in the apoplast (blue arrows). **G and H**: Section before and after selection of arbuscule-containing cells (ARB). Only cells harbouring mature arbuscules filling up the whole lumen were harvested. These cells could be easily distinguished from those containing young or severly degraded arbuscules (yellow arrows in E). Scale bars represent 300 µm for D and 150 µm for all other panels.

phosphate transporter gene *MtPt4* was used as an expression marker for cross-contamination between the CMR and ARB samples, since this gene is exclusively transcribed in cells containing arbuscules (Harrison *et al.* 2002). The detection of *MtPt4* transcripts in all ARB in contrast to their absence in all CMR samples (Figure I_4 B) indicates that no significant cross-contamination of CMR-samples with material from arbuscule-containing cells occured. In contrast to *MtPt4*, transcripts of the other five genes tested could be amplified both in CMR and ARB samples (Figure I_4 B). Of these, the serine carboxypeptidase gene *MtScp1* was the only one expressed at similar levels in both cell-types, whereas the *MtBcp1* gene encoding a blue copper protein, the lectin gene *MtLec5*, the *MtGlp1* gene specifying a germin-like protein, and the H^+-ATPase gene *MtHa1* displayed an up to 160-fold induction in ARB-cells (Figure I_4 C). While the results obtained for *MtScp1* and *MtBcp1* are in accordance with promoter studies indicating expression outside of arbuscule-containing cells (Liu *et al.* 2003, Hohnjec *et al.* 2005), *MtLec5*, *MtGlp1* and

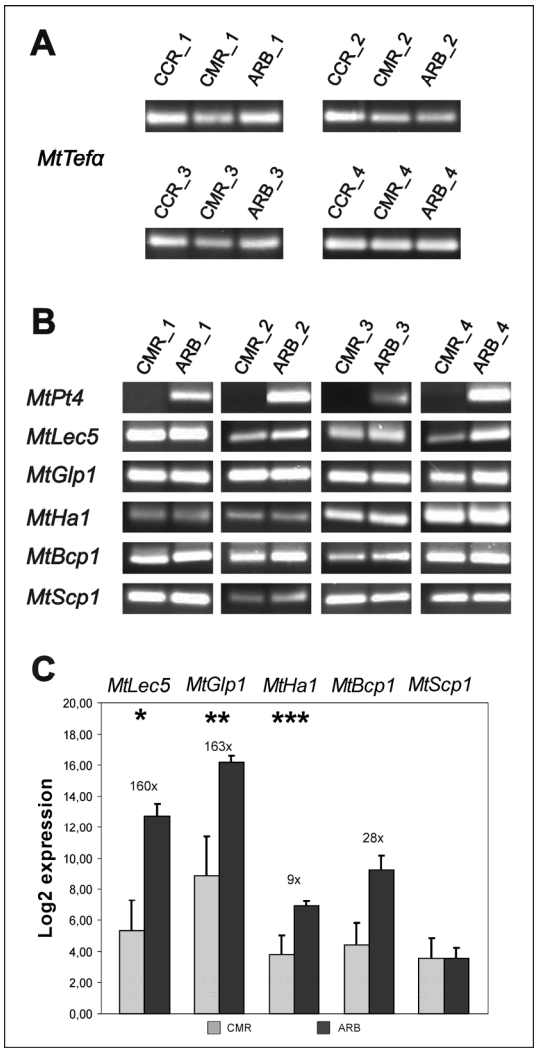

Figure I_4: Detection of AM marker gene transcripts in laser-microdissected cell-types. Marker gene expression was measured by real-time RT-PCR in four biological replicates of three different cell-types: cortical cells from non-mycorrhizal control roots (CCR), cortical cells from mycorrhizal roots containing fungal hyphae (CMR), and arbuscule-containing cells (ARB). **A and B**: Gel-electrophoresis of the final real-time RT-PCR amplification products representing the control gene *MtTefα* and six AM marker genes. All amplified fragments had the correct sizes. Note that *MtPt4* transcripts were not detected in CMR. **C**: Real-time RT-PCR measurement of five AM marker genes induced in ARB in comparison to CMR. Expression values are displayed as log2 mean values of all four biological replicates. Numbers and bars represent fold-induction and standard errors, respectively. Asterisks indicate significance levels of a Student`s t-test on the expression values in the two different cell-types: *=p<0,1; **=p<0,05; ***=p<0,005. Abbreviations: CCR, cortical cells from non-mycorrhized control roots; CMR, cortical cells from mycorrhized roots; ARB, arbuscule-containing cells; *MtTefα*, transcriptional elongation factor α; *MtPT4*, phosphate transporter 4; *MtBcp1*, blue copper protein 1, *MtScp1*; serine carboxypeptidase 1; *MtLec5*, lectin 5, *MtGlp1*: germin-like protein 1; *MtHa1*, H+-ATPase 1.

MtHa1 have so far been reported to be arbuscule-specific (Frenzel *et al*. 2005, Doll *et al*. 2003, Krajinski *et al*. 2002,). This deviance might be due to a higher sensitivity of our PCR-based method in comparison to the *in situ* expression methods used in the cited studies.

Together, our results demonstrate that the total RNA prepared from all three cell-types was suitable for identifying arbuscule-specific as well as arbuscule-enhanced expression patterns, even if the harvested cell-types were collected in close proximity.

Laser-microdissection identifies novel arbuscule-specific genes and genes being generally expressed in cortical cells colonized by AM fungi

Expression of 71 candidate genes was measured by one-step real time RT-PCR in at least three biological replicates. In these experiments, nine genes could not be amplified reproducibly from any cell-type and were not considered further. Figure I_5 gives an overview of the remaining 62

genes and their expression patterns in the laser-microdissected samples. Except of three genes encoding an ABC-transporter (Mtr.44070.1.S1_at), a calcium-binding protein (Mtr.4781.1.S1_at), and an AP2/ERF transcription factor (Mtr.11570.1.S1_at), none of these genes could be amplified reproducibly from CCR cells (data not shown), suggesting that they are either truly mycorrhiza-specific or are expressed in other cell-types than the ones investigated here, e.g. the vasular tissue.

Amongst the 62 genes analysed for cell-specific expression, a total of 21 displayed a specific activation in the arbuscule-containing cells, including six membrane transporter genes, seven signalling-related genes, six genes encoding transcription factors, and two fungal genes (Figure I_5, Supplemental Figure S_I_2). In addition, four genes were detected in all ARB, but in only one out of three CMR samples, indicating that they are expressed at a very low level in the latter cell-type. Six genes specifically expressed in arbuscule-containing cells were described to be activated in these cells before (Gomez *et al*. 2009), but none of them was so far known to be restricted to this cell-type within mycorrhizal roots.

Interestingly, the majority of the genes investigated was found to be expressed both in arbuscule-containing cells (ARB) and in the adjacent cortical cells being colonized by fungal hyphae at different levels (CMR). Here, transcripts of 37 genes, including 14 membrane transporter genes, 8 signalling-related genes, 12 transcription factor genes, and three fungal genes were detected. Of these 37 genes, 28 were expressed at comparable levels in both cell-types, whereas 9 were significantly induced in either CMR or ARB (Figure I_6). So far, only four genes of this group were known to be expressed in arbuscule-containing cells (Gomez *et al*. 2009), but no information was available on their activity in the adjacent cells being connected to hyphal growth.

In total, cell-specific expression patterns were identified for 62 AM-related genes. In the following, our results are discussed in detail with respect to the functional classification of the genes.

Glomus intraradices genes

Seven AM-related genes of fungal origin were selected for cell-specific transcriptome analysis. These genes encoded five membrane transporters, one signalling-related calcium-binding protein, and two transcription factors (Figure I_5). Interestingly, our analysis of the expression patterns in the specific cell pools revealed that four genes seemed to be specifically expressed in arbuscules,

A: AM marker genes

Probe set ID	Annotation	Expression profile		p-value
		log2 ratio	CMR ARB	
Mtr.43062.1.S1_at	Phosphate transporter MtPt4	10,02		-
Mtr.15653.1.S1_at	Bark lectin precursor MtLec5	8,01		0,080
Mtr.12500.1.S1_at	Germin-like protein MtGlp1	7,94		0,014
Mtr.15627.1.S1_at	Blue copper protein MtBcp1	8,15		0,123
Mtr.43470.1.S1_at	H+ATPase MtHa1	7,80		0,003
Mtr.40285.1.S1_at	Serine carboxypeptidase MtScp1	5,35		0,989

B: Membrane transporters

Probe set ID	Annotation	Expression profile		p-value
		log2 ratio	CMR ARB	
Mtr.52071.1.S1_at	ABC transporter	4,34		-
Mtr.37525.1.S1_at	Aquaporin MtNip1	5,10		-
Mtr.45021.1.S1_at	Carbohydrate transporter	2,33		- (2)
Mtr.37110.1.S1_at	Copper transporter	7,32		-
Mtr.35854.1.S1_at	Defensin	7,60		- (1)
Mtr.7741.1.S1_at	Oligopeptide transporter	3,98		- (1)
Mtr.4863.1.S1_at	Oligopeptide transporter	4,39		- (4)
Mtr.31214.1.S1_s_at	Defensin	7,19		0,007
Mtr.7210.1.S1_at	Defensin	9,32		0,029
Mtr.36985.1.S1_at	Oligopeptide transporter	7,89		0,018
Mtr.1103.1.S1_at	ABC transporter	5,49		0,455
Mtr.44070.1.S1_at	ABC transporter	6,17		0,789
Mtr.46524.1.S1_at	ABC transporter	6,69		0,266
Mtr.7596.1.S1_at	Aquaporin	7,09		0,255
Mtr.25178.1.S1_at	Carbohydrate transporter	1,55		0,893
Mtr.40995.1.S1_at	Manganese transporter MtZip7	2,62		0,302
Mtr.17764.1.S1_at	Oligopeptide transporter	5,52		0,434
Mtr.37112.1.S1_at	Oligopeptide transporter	3,64		0,490
Mtr.47098.1.S1_at	Oligopeptide transporter	3,24		0,192
Msa.2748.1.S1_at	Zinc transporter	1,88		0,291
Mtr.46057.1.S1_at	Oligopeptide transporter	4,55		0,025 (1)

C: Signaling components

Probe set ID	Annotation	Expression profile		p-value
		log2 ratio	CMR ARB	
Mtr.49716.1.S1_at	Chitinase	8,11		- (1)
Mtr.11892.1.S1_at	Chitinase	7,40		- (4)
Mtr.23004.1.S1_at	Clathrin assembly protein	1,41		-
Mtr.17352.1.S1_at	Inositol triphosphate phosphatase	3,98		-
Mtr.19870.1.S1_at	Receptor protein kinase MtLyr1	1,81		-
Mtr.17343.1.S1_at	Serine/threonine protein kinase	5,00		-
Mtr.17467.1.S1_at	Serine/threonine protein kinase	6,94		-
Mtr.1591.1.S1_at	SNF1-related protein kinase	4,33		- (2)
Mtr.39153.1.S1_at	Serine/threonine protein kinase	4,32		0,004
Mtr.31873.1.S1_at	Syntaxin	2,00		0,018
Mtr.4781.1.S1_at	Calmodulin	7,69		0,230
Mtr.36018.1.S1_at	Chitinase	7,52		0,211 (3)
Mtr.45869.1.S1_at	G-protein	5,13		0,324
Mtr.45646.1.S1_at	Lectin	2,56		0,655
Mtr.35414.1.S1_at	LRR receptor kinase	3,10		0,490
Mtr.16214.1.S1_at	Serine/threonine protein kinase	2,97		0,880

D: Transcriptional regulators

Probe set ID	Annotation	Expression profile		p-value
		log2 ratio	CMR ARB	
Mtr.31671.1.S1_at	AP2/ERF transcription factor	1,51		-
Mtr.46362.1.S1_at	AP2/ERF transcription factor	5,08		-
Mtr.25270.1.S1_at	C2H2 zinc finger transcription factor	5,13		-
Mtr.1484.1.S1_at	GRAS family transcription factor	1,61		-
Mtr.36004.1.S1_at	GRAS family transcription factor	6,69		-
Mtr.24642.1.S1_at	GRAS family transcription factor	5,26		-
Mtr.7264.1.S1_at	GRAS family transcription factor	5,38		0,068 (1)
Mtr.8863.1.S1_at	Myb transcription factor MtMyb1	9,90		0,002
Mtr.21492.1.S1_at	AP2/ERF transcription factor	3,52		0,147
Mtr.15867.1.S1_at	AP2/ERF transcription factor	2,80		0,122
Mtr.43947.1.S1_at	AP2/ERF transcription factor MtErn2	2,55		0,384
Mtr.28153.1.S1_at	C2H2 zinc finger transcription factor	3,26		0,158 (3)
Mtr.51511.1.S1_at	CAAT-box binding transcription factor	7,34		0,389
Mtr.16863.1.S1_at	CAAT-box binding transcription factor	2,36		0,394
Mtr.4282.1.S1_at	CAAT-box binding transcription factor	3,29		0,211
Mtr.31955.1.S1_at	GRAS family transcription factor	3,88		0,308 (2)
Mtr.47463.1.S1_at	GRAS family transcription factor	3,06		0,721 (3)
Mtr.11570.1.S1_at	AP2/ERF transcription factor	-1,02		0,071

E: *Glomus intraradices* genes

Probe set ID	Annotation	Expression profile		p-value
		log2 ratio	CMR ARB	
Mtr.31910.1.S1_at	G.i. ATPase	6,33		- (1)
Mtr.31826.1.S1_at	G.i. Phospholipid-transporting ATPase	3,98		- (4)
Mtr.31993.1.S1_at	G.i. RNA-binding protein	7,45		- (4)
Mtr.31879.1.S1_at	G.i. C2H2 zinc finger transcription factor	5,37		-
Mtr.31878.1.S1_at	G.i. ATPase	6,13		0,370 (3)
Mtr.42508.1.S1_at	G.i. Calcium-binding protein	6,19		0,733
Mtr.38858.1.S1_at	G.i. Voltage dependent channel	6,95		0,240

Cell-type specific expression:
No significant difference ≥ 5 fold > 10 fold > 50 fold arb.-specific

Figure I_5: Cell-type specific expression of genes activated in mycorrhizal roots.
Real-time RT-PCR measurement of gene expression in three biological replicates of the laser-microdissected cell-types CMR (cortical cells from mycorrhized roots) and ARB (arbuscule-containing cells). Differences in transcription are indicated by different shades of grey (legend see below). p-values represent significance levels of a Student`s t-test on the expression values in the two different cell-types. In addition, the log2 expression ratios of gene expression in roots mycorrhized with *Glomus intraradices* vs. non-mycorrhizal roots (Supplemental Table S1) are shown. Footnotes: (1): One of the three biological replicates was replaced by replicate four, to obtain three gene-specific PCR-products of the correct size or a consistent expression pattern. (2): A gene-specific PCR product could only be obtained for two out of three biological replicates of ARB. (3): A gene-specific PCR product could only be obtained for two out of three biological replicates of CMR. (4): A gene-specific PCR product was obtained for only one out of three biological replicates of CMR.

indicating that the distribution of fungal transcripts can be restricted to these structures, irrespective of the coenocytic nature of the microsymbiont.

The genes investigated included three members specifying ATPases, two of which represented cytoplasmatic ATPases probably associated with proteasomes and thus being involved in protein degradation, whereas the third one was predicted to be membrane-localized and involved in the transport of phospholipids or cations (Figure I_5). While two of the ATPase genes showed a specific expression in arbuscules, one was induced at comparable levels in both CMR and ARB samples. In addition, a gene specifying a voltage dependent channel protein was also activated in both cell-types, similar to a signalling-related gene encoding a calcium-binding protein (Figure I_5).

Interestingly, the two fungal genes related to transcriptional regulation, encoding a zinc finger and an RNA-binding protein, showed specific expression in ARB (Figure I_5). These genes might therefore control the transcription of fungal genes specifically required during arbuscule formation or function.

Medicago truncatula genes encoding membrane transporters

A functional AM symbiosis is characterized by the exchange of nutrients between the micro- and macrosymbionts. It is thus not surprising that 37 *M. truncatula* genes encoding membrane transporters were co-activated in the two AM-interactions studied (Supplemental Table S_I_3), including 13 genes that Benedito *et al.* (2010) identified previously on the basis of expression data reported by Gomez *et al.* (2009). Apart from the AM marker genes *MtPt4* and *MtHa1* already discussed above as well as the mycorrhiza-induced aquaporin gene *MtNip1* (Uehlein *et al.*, 2007), cellular expression patterns were determined for 20 genes of this functional category (Figure I_5).

The largest group comprised genes encoding oligopeptide transporters of the H^+/oligopeptide symporter type. Eleven members of this class were coinduced in both AM interactions and seven of them were examined in the laser-microdissected cell pools (Figure I_5). Proton-dependent oligopeptide transporters (POTs) are reported to be involved in the uptake of small peptides into eukaryotic cells (Paulsen and Skurray 1994). Possible functions are thus connected to an intake of degraded fungal proteins subsequent to the action of AM-activated proteases (Supplemental Table SI_2), alternatively the uptake of fungal effector peptides, such as the recently reported SP7

protein (Kloppholz *et al*. 2011, Plett *et al*. 2011), is an intriguing possibility. The wide range of possible POT functions is mirrored by cellular expression patterns, since we found two arbuscule-specific POT genes, three POT genes equally expressed in CMR and ARB cells, and one POT gene being induced in each cell-type (Figures I_5, I_6).

A second prominent group of AM-related genes encoded five ABC-transporters and three aquaporins. From this collection, we identified one ABC-transporter gene as ARB-specific and three more as being expressed with no significant difference between CMR and ARB (Figure I_5). With *MtStr* and *MtStr2*, two *M. truncatula* ABC transporter genes were recently reported to be important for AM function (Zhang *et al.* 2010). Both genes belong to the G subfamily of ABC-transporters and are specifically expressed in arbuscule-containing cells (Zhang *et al*. 2010). The ABC-transporter identified as arbuscule-specific in our study belongs to the same subfamily, suggesting a similar function. Zhang *et al*. (2010) speculated, that strigolactones might be a substrate for these transporters, inducing the strong ramification of fungal hyphae that leads to arbuscule formation, which would explain the cell-specific expression. In contrast, the three ABC-transporter genes we found to be expressed in arbuscule-containing and adjacent cortical cells specify PGP MDR (P-glycoprotein multidrug resistance) transporters of the ABCB subfamily. Since several members of this group are known to transport auxins (Geisler and Murphy, 2006), a role for these might be the fine-tuning of auxin distribution in colonized root cells.

In the group of aquaporins, we investigated the expression pattern of two Nodulin 26-like intrinsic protein (NIP) genes including *MtNip1,* which was first described as AM-induced by Uehlein *et al.* (2007) and was also strongly AM-induced in our experiment. Due to the fact that this gene is also slightly induced by phosphate, it was not included in our core set of 512 AM-related genes. In line with the results of Gomez *et al*. (2009), we found *MtNip1* to be activated in ARB cells. In addition, we could show here that this gene is expressed exclusively in this cell-type, whereas the second NIP gene was expressed in the surrounding, hyphae-containing cortical cells as well (Figure I_5). Interestingly, MtNip1 and other NIPs did not facilitate water uptake in heterologous expression systems, but acted as low-affinity transport system for ammonium (Uehlein *et al*. 2007), which is the main form in which nitrogen is supplied to the plant by AM fungi (Govindarajulu *et al*. 2005). These observations support the idea that nitrogen is provided by the microsymbiont via arbuscules as well as fungal hyphae growing in the apoplast of cortical cells, and the two NIPs might be involved in uptake of these nutrients into host cells.

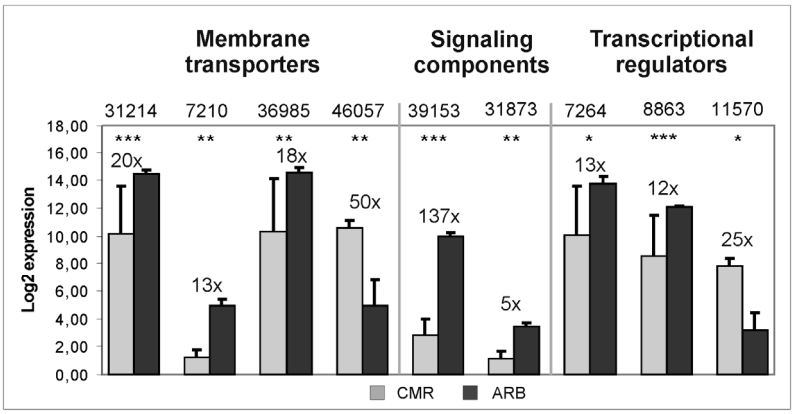

Figure I_6: Genes differentially expressed in cortical and arbuscule-containing cells.
Real-time RT-PCR measurement of the expression of selected genes classified as CMR- or ARB-induced in Figure I_5. Gene expression is displayed as the log2 mean value of three biological replicates. Numbers and bars represent fold-induction and standard errors, respectively. Different genes are labeled with abbreviated GeneChip probe IDs (compare Figure I_5). Asterisks indicate significance levels of a Student`s t-test on expression values in the two different cell-types: *=p<0,1; **=p<0,05; ***=p<0,005. Abbreviations: CMR: cortical cells from mycorrhizal roots; ARB: arbuscule-containing cells.

Strikingly, the most strongly induced transporter genes in our experiment encoded three defensins. These seem to be of special importance for arbuscule-containing cells, since one defensin gene was exclusively expressed and the other two were significantly upregulated in ARB (Figures I_5, I_6). Many members of the defensin gene family are activated in plants during defense reactions in response to diverse pathogens (Thomma *et al.* 2002), including harmful fungi. Although the activation of plant defence responses has been reported for the initial stages of mycorrhizal colonization, they seem to be effectively controlled and downregulated when the symbiosis is completely established (Harrison and Dixon 1993). Therefore, defensins specifically activated during a mature mycorrhiza must play a different role and may represent a specialized system of the plant to avoid unrestricted spread of the microsymbionts. Interestingly, some defensins are known to reduce the elongation of fungal hyphae and to cause strong hyphal branching (Broekaert *et al.* 1995), a function that could be related to arbuscule-formation.

The remaining membrane transporter genes we found to be upregulated during AM are mainly involved in the transfer of micro-nutrients, macro-nutrients such as nitrate, or carbohydrates. Concerning ion transporters of the MtZIP family (Burleigh *et al.* 2003), we identified a gene encoding the manganese transporter MtZip7 (López-Millán *et al.* 2004). We found the *MtZip7* gene and a zinc transporter gene to be expressed in CMR and ARB cells alike, whereas a copper transporter gene was found to be ARB-specific (Figure I_5). Since AM fungi probably improve micro-nutrient supply of host plants (Clark and Zeto 2000, Parniske 2008), the three transporter

genes might be activated by the plant to enhance uptake of these elements from the microsymbiont. The fact that we found two of the transporter genes mentioned to be expressed in both arbuscule-containing and surrounding, hyphae-containing cortical cells supports the assumption that an exchange of nutrients by the symbiotic partners or at least an uptake by the plant is not restricted to arbuscules.

With respect to sugar allocation in AM roots, we analyzed the expression patterns of two carbohydrate transporters. Due to the fact that hexoses derived from the plant metabolism are supplied to mycorrhizal fungi, AM roots represent strong carbon sinks. Whereas hexoses generated from sucrose via the activity of apoplastic invertases are directly available to the fungus (Schaarschmidt *et al.* 2007), hexoses provided by cytoplasmic invertases or sucrose synthases (Hohnjec *et al.* 1999) first have to be exported to the extracellular space (Baier *et al.* 2010). Up to now, little is known about the carbohydrate transporters involved in the translocation of symplastic hexoses to the apoplastic interface. The two genes investigated here are candidates for this function, but showed no consistent expression. Since only one was ARB-specific (Figure I_5), sucrose transfer is probably not limited to arbuscules, which is consistent with the expression of genes encoding the cytoplasmatic sucrose-cleaving enzyme MtSucS1 (Hohnjec *et al.* 2003) and the hexose transporter Mtst1 (Harrison 1996).

Medicago truncatula genes related to signalling

In Supplemental Table S_I_4, the expression characteristics of 41 genes encoding signalling-related components induced in both AM interactions are summarized. A large group consists of genes probably involved in intracellular signal transduction, including 13 genes encoding protein kinases, a phosphatase and a protein phosphatase inhibitor. Furthermore, genes specifying two inositol polyphosphate phosphatases, a phosphatidylinositol transfer protein, a calmodulin-binding protein, two Rop guanine nucleotide exchange factors, and a G-protein deserve attention. Together, they might represent those members of large gene families that mediate calcium, phosphoinosite, or G-protein signalling in AM roots. Seven genes from this group and an additional calmodulin gene only induced by *G. intraradices* were investigated for their cellular expression pattern (Figure I_5). Interestingly, we found genes encoding three protein kinases (two serine/threonine kinases and a SNF1-related kinase) and one inositol triphosphate phosphatase to be exclusively expressed in ARB (Figure I_5). To our knowledge, these are the

first genes reported to be involved in internal signalling processes that are specifically up-regulated in arbuscule-containing in comparison to the neighbouring cells. Another serine/threonine protein kinase gene was strongly induced in ARB (Figure I_6), whereas a calmodulin gene, a G-protein gene and one additional serine/threonine protein kinase gene were expressed at equal levels in ARB and CMR (Figure I_5), hinting that they are involved in signal processes occuring in cortical cells of colonized root areas in general.

A second group of AM-activated, signalling-related genes encodes components associated with vesicle-mediated transport, including a syntaxin, a clathrin assembly protein, a GTP-binding protein, and a basic secretory protein. It is tempting to speculate that these proteins are involved in the membrane biogenesis associated with an intracellular accomodation of fungal structures. The expression pattern of the two genes we analyzed in the specific cell pools is in line with the assumption that in particular the arbuscule-containing cells are places of intensive membrane build-up and turnover, since a gene encoding a clathrin assembly protein was exclusively detected in ARB and a syntaxin gene was found to be ARB-induced (Figures I_5, I_6).

Three chitinase genes strongly induced in both AM interactions were included in the analysis of signalling-related genes (Figure I_5). Chitinases hydrolyze ß-1,4-glycosidic bonds (Salzer *et al.* 2000) and are mostly regarded as part of plant defence mechanisms (Arlorio *et al.* 1992). Although several chitinase genes are up-regulated during early phases of nodulation and mycorrhization, this activation is transient and they are in general not regarded to play a role during later stages. Nevertheless, several members of the class III chitinase gene family are activated specifically during AM (Salzer *et al.* 2000), and for one of these genes an arbuscule-specific localization was found by *in situ* hybridization (Bonanomi *et al.* 2001). In this study, we investigated three members of the chitinase gene family and found two of them only in ARB, whereas the third one was active in CMR and ARB (Figure I_5). The predominant ARB-localization of chitinase transcripts might thus allow the formation of functional symbiotic interfaces by reducing the amount of chitinous elicitors.

The largest group of signalling-related genes encompassed 15 genes encoding receptor kinases with a predicted membrane localization that presumably perceive extracellular AM-related signals. From this group, we investigated genes encoding a leucin-rich repeat (LRR) receptor kinase and the LysM receptor kinase MtLyr1. In addition, a gene encoding a membrane-bound lectin with predicted kinase activity was analyzed (Figure I_5). Whereas the lectin gene and the LRR receptor

kinase gene were equally expressed in both cell-types studied, *MtLyr1* was specifically expressed in ARB cells (Figure I_5). In *Medicago truncatula*, the two LysM receptor kinases MtNfp, representing the Lyr-type, and MtLyk3, representing the Lyk-type of this family, were identified as Nod-factor receptors (Gough and Cullimore 2011). MtNfp also plays a role during early AM interactions, since it is essential for the perception of the recently characterized Myc-LCO signals (Maillet *et al*. 2011). Since *MtNfp* is not essential for the establishment of an AM (Amor *et al*. 2003), Maillet *et al*. (2011) speculated that another receptor active at higher Myc-LCO concentrations must exist. These could be achieved during arbuscule formation, as a result of a tighter contact between the two symbiotic partners during infection of cortical cells. Interestingly, it was shown recently that in the non-legume *Parasponia*, an orthologue of *MtNfp* named *PaNfp* is essential for the symbioses with nitrogen-fixing bacteria as well as AM fungi (Op den Camp *et al*. 2011). In contrast to legume plants, the *Parasponia* genome only contains a single Lyr-type receptor kinase gene, whereas legume plants contain two copies (Op den Camp *et al*. 2011). It was speculated, that during evolution of legume plants and their ability to form nodules, duplication of the initial Lyr-gene occurred and one copy became the receptor for rhizobial LCOs, whereas the other one is targeted by Myc-LCOs. The closest relative of *MtNfp* is *MtLyr1*, which could thus represent a potential receptor for Myc-LCOs (Op den Camp *et al*. 2011). We could show here that *MtLyr1* is exclusively expressed in ARB and not in the surrounding cortical cells from mycorrhized roots. This fits well to the phenotype of RNAi-knockdowns of the more ancient *PaNfp* gene, since here the AM symbiosis is aborted at the point of arbuscule formation. Our finding that *MtLyr1* is exclusively expressed in arbuscule-containing cells supports the fact that the encoded receptor is needed for this step, possibly to perceive Myc-LCOs secreted during later stages of AM.

Medicago truncatula genes encoding transcriptional regulators

In total, 25 genes encoding transcription factors (TFs) were identified as co-induced in AM roots (Table 2), comprising the families AP2/ERF, Z-C2H2, CAAT-box binding, GRAS, MYB, WRKY, and NAC. Of these, only five GRAS-TF genes and one gene encoding a Myb-TF (designated *MtMyb1* in Table I_1) were previously reported to be specifically activated in roots colonized with *Glomus* spec. (Liu *et al.* 2003, Gomez *et al*. 2009), while a few members of other gene families were reported to be of relevance in the root nodule symbiosis.

Table I_2: Overview of 25 *M. truncatula* AM-induced genes encoding transcriptional regulators.
Probe IDs of Medicago GeneChips are referenced to *M. truncatula* gene names, where applicable. Log2 ratios of gene expression for *G. intraradices*-colonized (Gi-Myc), *G. mosseae-colonized* (Gm-Myc), and 2 mM phosphate-treated (2 mM-P) roots, all measured against roots grown at 20 µM phosphate, are given. FDR-corrected p-values (FDR-p) are indicated. References for the AM-induced transcription factor genes identified are as follows: *MtErn1* (Middleton *et al*. 2007), *MtErn2* (Adriankaja *et al*. 2007), *MtMyb1* (Liu *et al*. 2003), *MtCbf1* (this work), and *MtCbf2* (this work).

GeneChip Probe ID	Gene	Annotation	Gi-Myc	FDR-p	Gm-Myc	FDR-p	2 mM-P	FDR-p
Mtr.46362.1.S1_at		AP2/ERF transcription factor	5.08	2.4E-05	4.07	3.3E-04	0.05	9.8E-01
Mtr.21492.1.S1_at		AP2/ERF transcription factor	3.52	1.2E-06	3.49	2.6E-06	-4.05	9.0E-07
Mtr.15867.1.S1_at		AP2/ERF transcription factor	2.80	3.6E-04	2.39	2.4E-03	0.61	4.3E-01
Mtr.31671.1.S1_s_at		AP2/ERF transcription factor	2.77	1.2E-04	2.31	1.1E-03	0.65	2.9E-01
Mtr.43947.1.S1_at	*MtErn2*	AP2/ERF transcription factor	2.55	4.3E-05	2.32	1.9E-04	-1.38	4.4E-03
Mtr.7556.1.S1_at	*MtErn1*	AP2/ERF transcription factor	1.61	5.0E-03	1.27	3.1E-02	-0.04	9.7E-01
Mtr.25270.1.S1_at		C2H2 zinc finger transcription factor	5.13	5.9E-06	3.99	1.1E-04	0.01	9.9E-01
Mtr.28153.1.S1_at		C2H2 zinc finger transcription factor	3.26	3.2E-06	2.18	2.4E-04	-0.78	8.3E-02
Mtr.41957.1.S1_at		C2H2 zinc finger transcription factor	1.06	1.5E-03	1.12	2.0E-03	0.78	1.0E-02
Mtr.51511.1.S1_at	*MtCbf1*	CAAT-box transcription factor	7.34	1.8E-09	6.15	1.5E-08	-0.67	1.5E-01
Mtr.51511.1.S1_s_at	*MtCbf1*	CAAT-box transcription factor	6.45	1.0E-08	5.58	7.7E-08	-0.82	9.2E-02
Mtr.4282.1.S1_at		CAAT-box transcription factor	3.29	4.8E-07	3.32	8.1E-07	-0.45	2.7E-01
Mtr.16863.1.S1_at	*MtCbf2*	CAAT-box transcription factor	2.36	1.8E-04	1.56	7.3E-03	-0.34	6.1E-01
Mtr.36004.1.S1_at		GRAS transcription factor	6.69	1.4E-08	6.08	6.9E-08	-0.78	1.5E-01
Mtr.7264.1.S1_at		GRAS transcription factor	5.38	1.9E-08	3.05	9.3E-06	-0.66	1.4E-01
Mtr.31954.1.S1_at		GRAS transcription factor	4.05	1.9E-05	3.14	3.5E-04	-1.18	7.9E-02
Mtr.31955.1.S1_at		GRAS transcription factor	3.88	2.2E-06	3.05	4.1E-05	-2.39	1.8E-04
Mtr.47463.1.S1_at		GRAS transcription factor	3.06	7.8E-06	2.85	2.8E-05	-1.33	5.6E-03
Mtr.1484.1.S1_at		GRAS transcription factor	1.61	1.6E-03	1.21	1.7E-02	0.04	9.7E-01
Mtr.8863.1.S1_at	*MtMyb1*	Myb transcription factor	9.90	6.7E-10	8.99	2.3E-09	0.21	8.1E-01
Mtr.10894.1.S1_at		Myb transcription factor	2.59	6.2E-04	1.47	3.8E-02	1.01	1.2E-01
Mtr.33210.1.S1_at		Myb transcription factor	1.60	3.1E-02	1.71	3.2E-02	1.06	1.6E-01
Mtr.49044.1.S1_at		NAC-domain transcription factor	5.42	1.7E-07	2.72	2.2E-04	-0.23	8.0E-01
Mtr.51555.1.S1_at		WRKY transcription factor	1.63	2.2E-02	1.82	1.8E-02	0.06	9.7E-01
Mtr.23616.1.S1_at		WRKY transcription factor	1.59	4.2E-02	1.96	2.1E-02	-1.54	4.2E-02

With six members each, genes encoding GRAS and AP2/ERF transcriptional regulators were most prominent amongst the TFs identified. This is particularly interesting, since analogous proteins are involved in early signalling in the root nodule symbiosis. Here, the GRAS-TFs MtNsp1 and MtNsp2 (Smit *et al*. 2005, Kalo *et al*. 2005) as well as the AP2/ERF-TF MtErn1 (Middleton *et al*. 2007) are essential for the activation of symbiosis-related genes via Nod-factor signalling. Detailed studies on these transcription factors led to the identification of two further AP2/ERFs (MtErn2, MtErn3) and revealed that GRAS and AP2/ERF proteins interact with promoter sequences of early nodulin genes (Andriankaja *et al*. 2007, Hirsch *et al.* 2009). Since the TF proteins mentioned obviously represent an important control system in the regulation of symbiosis-specific genes, it is interesting that with *MtErn1* and *MtErn2*, two of these were found to be induced in AM roots in our study.

Additional prominent TF genes induced in AM roots specified CAAT-box binding factors (Cbf) of the HAP3 and HAP5 type, C2H2 zinc finger proteins, and Myb proteins, with three members

each (Table I_2). In the root nodule symbiosis, the MtHap2-1 CAAT-box binding factor was identified as a key developmental regulator by Combier *et al.* (2006), whereas the zinc-finger protein Mszpt2-1 was shown to be essential for the differentiation of the nitrogen-fixing zone of root nodules (Frugier *et al.* 2000). So far, both gene families were not reported to be related to *Glomus*-colonized roots.

Since we regarded transcriptional regulators as particularly interesting for our study, we investigated the cellular expression pattern of a large subset of 17 TF genes, including members of the five most prominent families. Additionally, an AP2/ERF induced by diffusible factors from AM fungi (N. Hohnjec, Leibniz Universität Hannover, Germany, unpublished data) was included in the analysis (Figure I_5).
Interestingly, we found arbuscule-specific or ARB-induced genes in four of the families investigated. Whereas a C2H2 zinc finger, two AP2/ERF, and three GRAS TF genes were ARB-specific, *MtMyb1* and a further GRAS gene were significantly activated in ARB cells (Figures I_5, I_6). The encoced TFs thus represent candidates for regulators that control the expression of genes required for proper arbuscule development and function. On the other hand, all gene families containing ARB-specific members also included genes expressed at equal levels in CMR and ARB (Figure I_5), indicating that different members of a gene family control different steps of the symbiosis.

In contrast to the TF genes mentioned so far, all three *Cbf* genes were expressed at equal levels in CMR and ARB (Figure I_5), indicating a more general role in the coordination of fungal colonization. Cbf proteins are known to regulate the expression of genes containing CCAAT motifs in their promoter sequences by forming heterotrimeric complexes that bind to the CAAT-box (Combier *et al.* 2008). Since CCAAT motifs are present in about 30% of eukaryotic promotors (Mantovani *et al.* 1998), Cbf proteins represent global regulators of gene expression that probably gain specificity via interactions with other transcription factors (Maity and Crombrugghe 1998). That way, Cbf activation during an AM symbiosis can mediate an expression of whole sets of AM-related genes via the recognition of their promoter regions and a subsequent interaction with other transcriptional regulators. We therefore analysed the two genes

Mtr.51511.1.S1_at (designated *MtCbf1*) and Mtr.16863.1.S1_at, (designated *MtCbf2*), both encoding CAAT-box binding TFs of the HAP5-type, in more detail.

Expression of the *MtCbf1* and *MtCbf2* genes encoding CAAT-box binding transcription factors correlates with fungal contact and spread

The two genes *MtCbf1* and *MtCbf2* are highly similar (96.3% identity on the level of nucleic acids, Supplemental Figure S_I_3), indicating that they might be derived from a duplication event. They are located in close proximity on *M. truncatula* chromosome 2 (http://www.medicagohapmap.org/, BAC clone AC136138), being separated by two different *M. truncatula* genes. Both *MtCbf* promoter sequences display no marked similarities, except of the region immediately upstream of the start codons (Supplemental Figure S_I_4). To obtain a comprehensive insight into the up-regulation of the *MtCbf1* and *MtCbf2* genes during successive stages of fungal colonization, their activity was analyzed both via real-time RT-PCR and via the expression of promoter-GUS-fusions in transgenic roots, using a four week time-course of mycorrhization. The results obtained confirmed the expression patterns of *MtCbf1* and *MtCbf2* detected in ARB and CMR cell-pools, and in addition revealed a striking activation of these genes already during very early stages of the AM interaction.

The analysis of reporter gene expression in transgenic roots showed that both promoters displayed no activity in roots grown in the absence of mycorrhizal fungi (data not shown). In mycorrhizal transgenic roots, first spots of blue staining in epidermal cell layers were observed as early as 5 dpi for *MtCbf1* and *MtCbf2* in those places where fungal hyphae just attached to the plant epidermis, but had not yet entered the host cells (Figures I_7 A-C; I_8 A,D,B,E). This activation was always dependent on direct physical contact between the two symbiotic partners and is therefore most probably not induced by diffusible signals from AM fungi. Once the fungus had entered the root cortex, promotor activity expanded to cortical and arbuscule-containing cells, always related to the progression of fungal hyphae (Figures I_7 D,G,E,H; I_8 C,F). Whereas epidermal staining became even more pronounced for *MtCbf1* during these stages and was so intense that staining of underlying cell layers could hardly be distinguished (Figure I_7 F,I), epidermal staining for *MtCbf2* remained at a lower level, and the activity of this promoter appeared stronger in the cortex (Figure I_8 G,H). During later AM stages, when fungal progress is mostly achieved by an intraradical spread of the hyphae, no activity in epidermal cells was observed any more for both

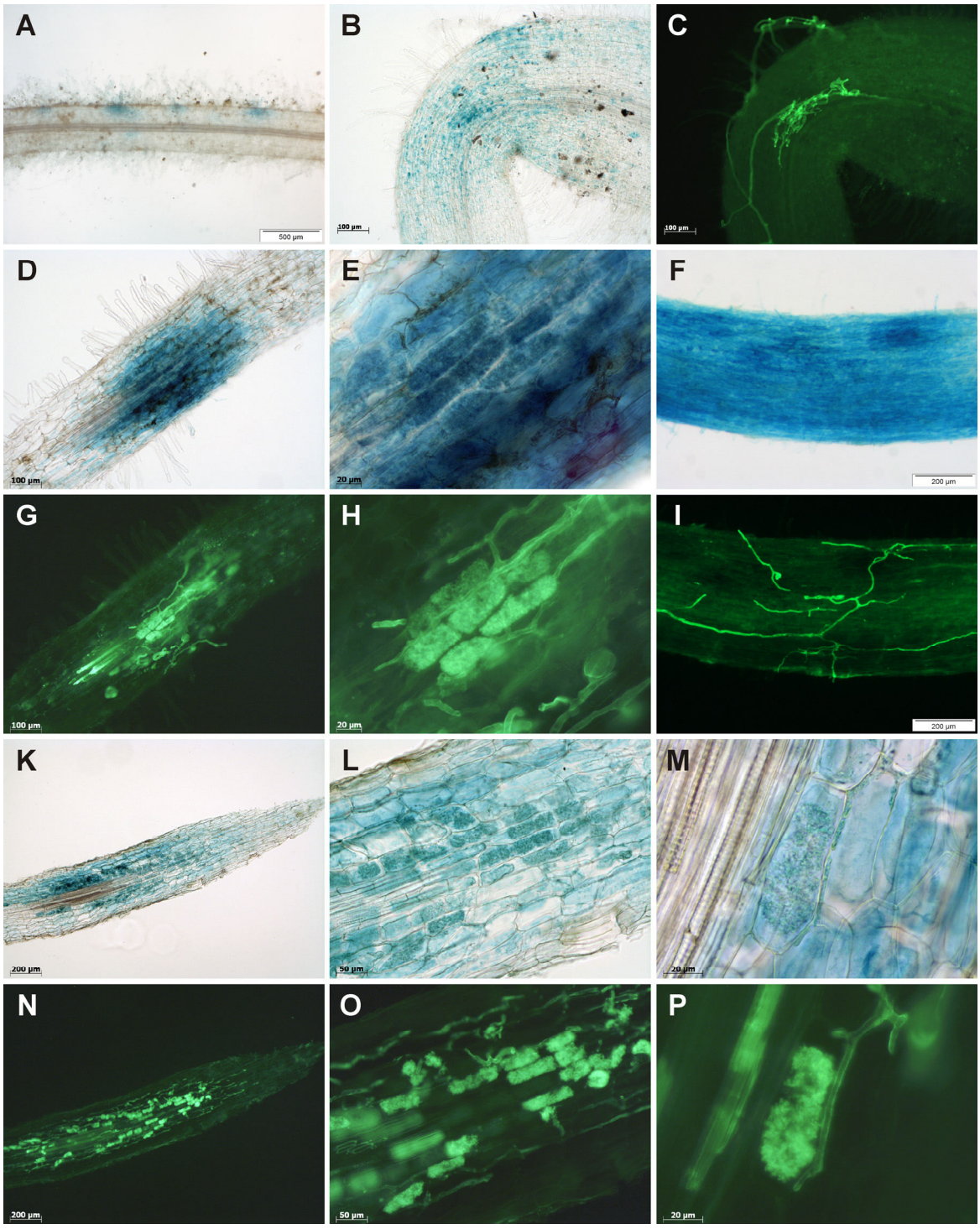

Figure I_7: Activity of the *MtCbf1* promoter in *M. truncatula* mycorrhizal roots.
A, B, D, E, F, K, L, and M: Light micrographs of *M. truncatula* mycorrhizal roots expressing the gusAint gene under the control of the *MtCbf1* promoter. **C, G, H, I, N, O, P**: Corresponding fluorescence micrographs showing counterstaining of fungal structures with Alexa Fluor® 488 WGA conjugate at exactly the same root position. In **A**, **B**, **C**, **F**, and **I**, whole roots are shown; whereas **D**, **E**, **G**, **H**, and **K** to **P** show 60 µm thin sections. **E**, **H**, **L**, and **O** represent enlarged regions of the roots shown in **D**, **G**, **K**, and **N**, respectively. **A to C**: Promoter activity during early AM stages, with fungal hyphae being just attached to the root epidermis. **D, E, G, and H**: Promoter activity in a young infection unit. **F and I**: Strong epidermal promoter activity in a region with an expanding infection unit. **K, L, N, and O**: Promoter activity in a densely colonized root. **M and P**: Enlargement of a single arbuscule. Scale bars represent 500 µm for A; 200 µm for F,I , K and N; 100 µm for B, C, D and G; 50 µm for L and O; 20 µm for E, H, M and P.

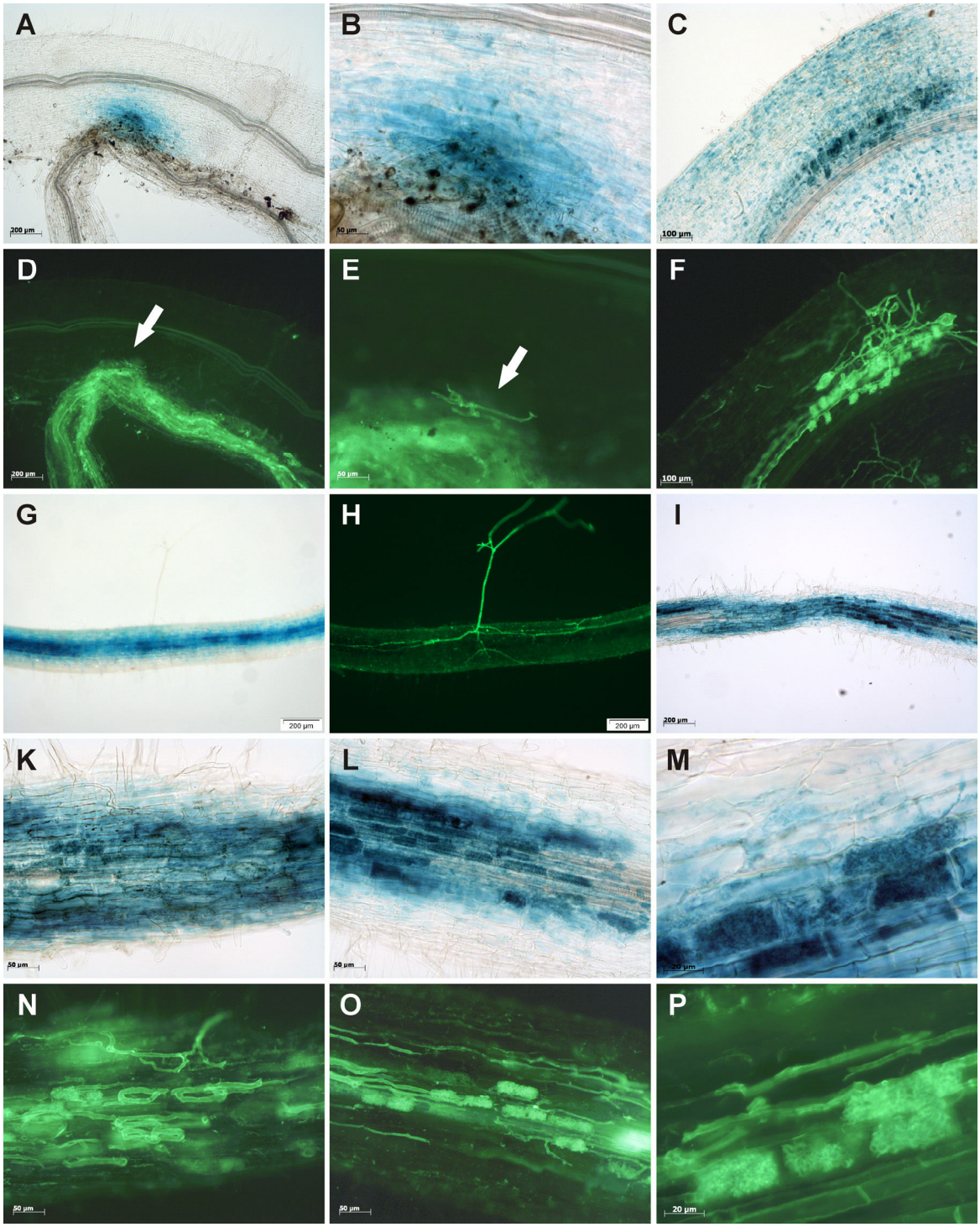

Figure I_8: Activity of the *MtCbf2* promoter in *M. truncatula* mycorrhizal roots.
A, B, C, G, I, K, L and M: Light micrographs of *M. truncatula* mycorrhizal roots expressing the *gusA*int gene under the control of the *MtCbf2* promoter. **D, E, F, H, N, O, and P**: Corresponding fluorescence micrographs showing counterstaining of fungal structures with Alexa Fluor® 488 WGA conjugate at exactly the same root position. In **A** to **H**, whole roots are shown, whereas **I** to **P** show 60 µm thin sections. **B** and **E** represent enlarged regions of the root shown in **A** and **D**. **K**, **L**, **N** and **O** represent enlarged regions of the root shown in **I**. **A, B, D and E**: Promoter activity during early stages, with fungal hyphae being just attached to the root epidermis. In this case, the hyphae in contact to the root surface (indicated by arrows) emerged from a highly mycorrhized leek root attached to the *M. truncatula* root. **C and F**: Promoter activity in a young infection unit. **G and H**: Promoter activity in a region with an expanding infection unit. In contrast to *MtCbf1*, no strong *MtCbf2* activity can be observed in epidermal cell layers in this stage, hence the strong GUS-staining in the cortex is visible from the outside. **I, K, L, N and O**: Promoter activity in a densely colonized root. **M and P**: Enlargement of a group of arbuscules. Scale bars represent 200 µm for A, D, G, H, and I; 100 µm for C and F; 50 µm for B, E, K, L, N, and O; 20 µm for M and P.

promoters, and reporter gene activity became restricted to those cortical cells that were either in contact with fungal hyphae or that contained arbuscules (Figures I_7 K-P; I_8 I-P). No GUS-staining was observed in root regions which did not contain fungal infection units (data not shown).

In our laser-microdissection experiments, both genes were identified as expressed with no significant difference between CMR and ARB (Figure I_9 A,B), although *MtCbf1* tended to be more strongly expressed in CMR (3,5-fold induction) and MtCbf2 appeared activated in ARB (3,8-fold induction). This tendency is also mirrored in the reporter gene expression patterns driven by the two promoters, since GUS-staining mediated by the *MtCbf2* promoter seemed to be more intense in arbuscule-containing cells (Figure I_8_M), whereas GUS-staining mediated by the promoter of *MtCbf1* was equal in arbuscule-containing and the surrounding cortical cells

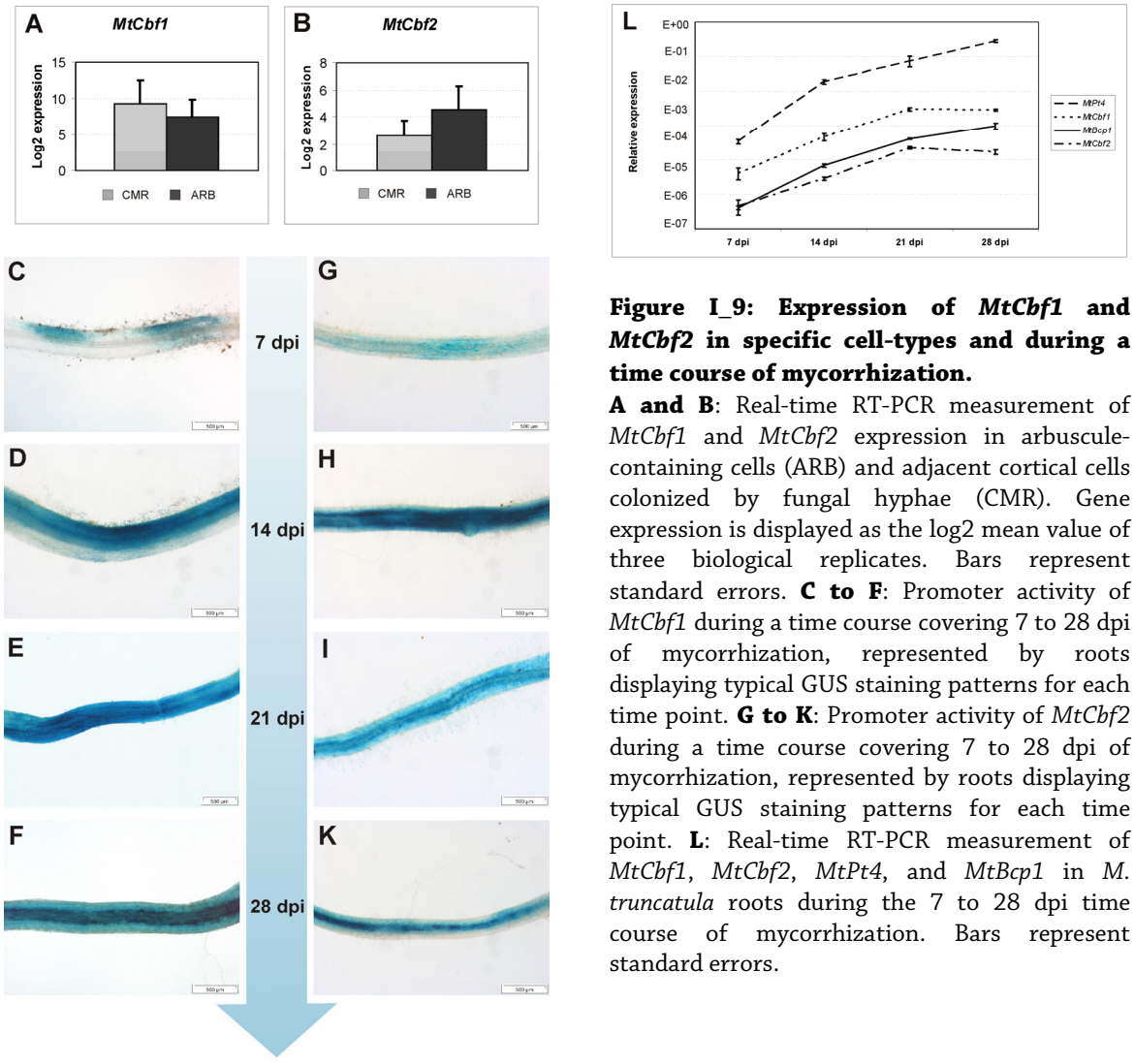

Figure I_9: Expression of *MtCbf1* and *MtCbf2* in specific cell-types and during a time course of mycorrhization.

A and B: Real-time RT-PCR measurement of *MtCbf1* and *MtCbf2* expression in arbuscule-containing cells (ARB) and adjacent cortical cells colonized by fungal hyphae (CMR). Gene expression is displayed as the log2 mean value of three biological replicates. Bars represent standard errors. **C to F**: Promoter activity of *MtCbf1* during a time course covering 7 to 28 dpi of mycorrhization, represented by roots displaying typical GUS staining patterns for each time point. **G to K**: Promoter activity of *MtCbf2* during a time course covering 7 to 28 dpi of mycorrhization, represented by roots displaying typical GUS staining patterns for each time point. **L**: Real-time RT-PCR measurement of *MtCbf1*, *MtCbf2*, *MtPt4*, and *MtBcp1* in *M. truncatula* roots during the 7 to 28 dpi time course of mycorrhization. Bars represent standard errors.

interspersed with fungal hyphae (Figure I_7_M): Taking into account, that GUS-staining usually appears more intense in the densly filled cells containing arbuscules, these reporer gene expression patterns largely confirm our results obtained via laser-microdissection.

During the mycorrhizal time course performed from 7 to 28 dpi, the *MtCbf1* and *MtCbf2* promoters displayed a constantly rising activity, visualized by representative GUS staining patterns from different timepoints (Figure I_9 C-K). This increase closely correlated to the expression of the AM marker genes *MtPt4*, representing an arbuscule-specific gene, and *MtBcp1,* representing a gene expressed in arbuscule-containing as well as in the surrounding, hyphae-containing cortical cells (Figure I_9 L). In our time course, *MtPt4* and *MtBcp1* from 7 dpi to 28 dpi showed a constantly increased transcription, leading to an up-regulation of 836-fold and 341-fold, respectively, at 28 dpi in comparison to 7 dpi. Interestingly, the expression of both *MtCbf1* and *MtCbf2* was strongest already at 21 dpi, where 70-fold and 37-fold inductions in comparison to 7dpi was reached. At 28 dpi, the activity of both transcription factor genes already declined, probably due to a reduced number of epidermal infection events at this timepoint. Together with our promoter studies (Figure I_9 F,K), this observation underlines the importance of both genes already for early infection stages.

It can be concluded that *MtCbf1* and *MtCbf2* seem to be relevant during all stages of the AM symbiosis being characterized by a direct physical contact between the two partners. Therefore, the encoded CAAT-box transcription factors represent excellent candidates for novel regulators not only during later AM stages, but especially for the first steps of the interaction, where knowledge both on regulators mediating infection as well as infection-related expression markers is scarce. Interestingly, after the first activation in the epidermal cell layer, activity of both promoters seemed to precede the actual fungal colonization, since GUS staining did not only spread into the surrounding epidermal cells, but was several cells ahead of the proceeding fungal hyphae in the cortex. It is tempting to speculate that this gene expression pattern is promoted by a short-distance signal that prepares cells for an arrival of the microsymbiont, possibly faciliating fungal entry in the proximity of the first infection site or the hyphal spread in the cortex. In this context, the ability of CBFs to interact with a large range of promoters becomes particularly interesting, since they might thus be able to activate large parts of the symbiotic programme in colonized root cortical cells, ultimately leading to the reprogramming of host cells towards an accomodation of symbiotic fungi.

Conclusion

An attribution of gene activity to defined developmental stages is an important step towards the understanding of complex biological processes. That way, our identification of specific cellular expression patterns for a large subset of AM-related genes in mycorrhizal roots allows an association of these genes with the different developmental stages of an AM symbiosis, as shown in Figure I_10. The colonization of plant roots by AM fungi is characterized by at least four distinct steps. While the first step is characterized by an exchange of diffusible signals between the two partners, causing the activation of signal cascades in epidermal and cortical cells, the second step involves direct physical contact, leading to hyphopodium formation by the fungus and PPA formation on the plant side, followed by penetration of rhizodermal cells by fungal hyphae. In the third step, fungal hyphae spread in the apoplast, resulting in the fourth and most intimate step, the formation of arbuscules. It has to be noted that step two, three, and four are achieved in a short time period, where AM development is characterized by a spread of infection units from initial entry points, being accompanied by a sequential build-up and decay of arbuscules.

Due to the fact that our AM expression profiles were recorded on the basis of pooled tissue samples of strongly mycorrhized roots, it is likely that processes occuring during later, functional stages of AM (step three and four) were preferentially identified, and these are also represented by our specific cell pools derived by laser-microdissection. We propose that the genes we identified to be active in cortical cells colonized by fungal hyphae and arbuscule-containing cells are related to the general progression of fungal hyphae in the root cortex, whereas genes only active in arbuscule-containing cells account for specific functions of this highly specialized symbiotic interface. Our identification of transporters, signalling-related genes and transcription factors with distinct expression patterns provide insight into the genetic processes accompanying and allowing progression towards a functional symbiosis (Figure I_10). Interestingly, only two genes with enhanced expression in cortical cells colonized by fungal hyphae in comparison to arbuscule-containing cells were identified, suggesting that processes exclusively related to the growth of fungal hyphae in the cortex, which are not needed for arbuscule formation and function, are rare. It remains unclear, wether the mechanisms allowing fungal penetration of roots also guide intraradical growth of fungal hyphae. Regarding the fact that the primary infection is guided intracellularly via the PPA, whereas the growth of fungal hyphae in the cortex is mostly apoplastic and keeping in mind that fungal hyphae in contact to cortical cells may also be involved in

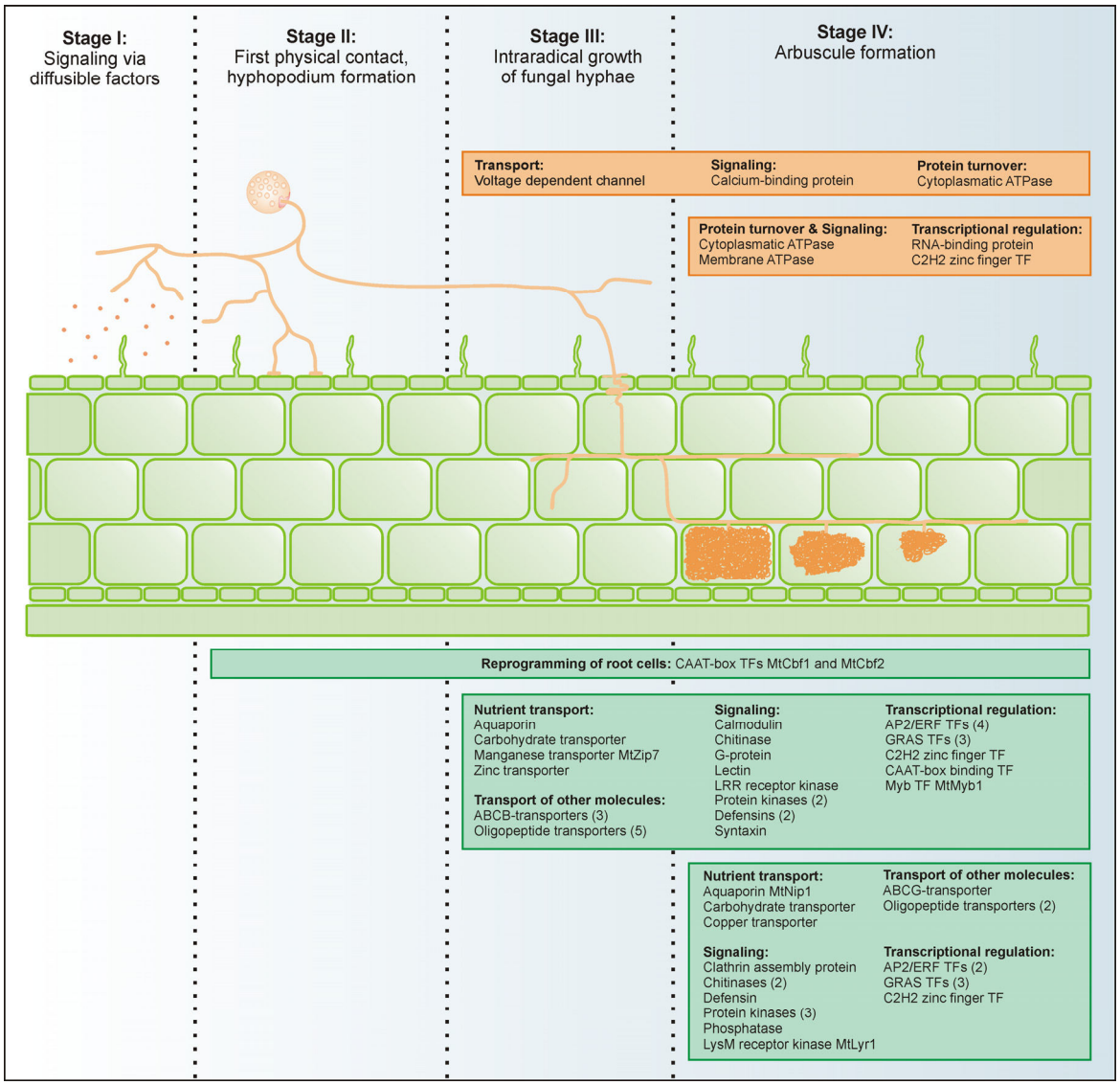

Figure I_10: Schematic summary of fungal and plant gene expression patterns during four different stages of the AM symbiosis.
Proteins encoded by the genes identified are grouped according to functional categories. Fungal gene products are listed in orange, plant gene products in green boxes. The total number of genes with identical annotations is indicated in brackets. Note that it remains to be elucidated to what extent genes identified as expressed in arbuscule-containing as well as in the adjacent cortical cells colonized by fungal hyphae are already active during stages I and II.

nutrient transfer to the plant, there are differences between these two steps. It therefore seems feasible that there will be a set of genes whose activity is required during all stages, like the two CAAT-box transcription factor genes identified in this study (Figure I_10). In addition, some genes specifically needed for the initial infection likely exist, analogous to the arbsucule-specific genes we identified here. Both steps are tightly controled by the plant, mirrored in two types of mutants identified for the AM symbiosis (Harrison 2005). These either mediate no entry of

fungal hyphae at all, or allow entry and spread but no arbsucule-formation, suggesting the existence of specific fungal signal molecules and transduction pathways required in these stages.

The identification of two CBF genes specifically activated during all stages of an AM infection delivers two candidates mediating a high-level control of gene expression during the colonization of roots by AM fungi. It will be interesting to see, wether other CAAT-box TF genes identified as AM-induced show a similar expression pattern and how many genes active during apoplastic growth of fungal hyphae are already activated during earlier stages. These questions can only be solved via an analysis of cell-types from early stages of AM interaction such as epidermal regions challenged with AM fungal signals or cortical regions harbouring PPAs.

Chapter II:
A roadmap of gene expression during different stages of arbuscular mycorrhizal symbioses

Abstract

About 80% of today's land plants establish an arbuscular mycorrhizal symbiosis with *Glomeromycota* fungi to improve their access to nutrients and water in the soil. On the molecular level, this process is only partly understood. Although many genes specifically activated during fungal colonization of the host root have been identified, information on the exact place and timepoint of activation is only available for a small subset of genes, due to the asynchronous development of the microsymbiont in the host root. In this study, we relied on a combination of laser microdissection and the use of *Medicago* GeneChips to perform a genome-wide analysis of gene expression patterns in defined cell-types of *Medicago truncatula* roots mycorrhized with *Glomus intraradices*. We compared gene expression in arbusculated cells, cortical cells colonized by intraradical hyphae, and epidermal cells of mature mycorrhizal roots, in addition to appressorial areas and non-appressorial areas from roots containing first infection units. These cell-types covered the main developmental stages of an AM symbiosis, allowing the identification of subsets of genes governing the sequential reprogramming of host roots towards the accomodation of microsymbionts. Taken together, cellular expression patterns for 18014 genes were revealed. For a subset of 1645 genes, these expression patterns were shown to be influenced by mycorrhizal colonization, providing information on the activity of genes already known from transcriptome studies based on pooled tissues, but also on the differential expression of new genes, revealing an adjustments of transcript accumulation within the root tissue in response to fungal colonization.

INTRODUCTION

The arbuscular mycorrhiza (AM) symbiosis represents one of the most ancient and widespread symbioses known. Around 80% of all land plants establish this interaction with fungi of the phylum *Glomeromycota* (Schüssler *et al.* 2001). Fossil records date back over 450 million years and coincide with the appearance of the first land plants, indicating that the symbiosis may have been an important factor during the colonization of terrestrial ecosystems by plants (Redecker *et al.* 2000). During the symbiosis the plant roots get colonized by fungal hyphae, originating from spores in the soil, which form specialized structures in the inner cortical cells of the plant. These are termed arbuscules, due to their highly branched tree-like anatomy, facilitating nutrient exchange between the two partners (Parniske 2008). While the fungus is supplied with photoassimilates from the host (Douds *et al.* 2000), the plant benefits from the wide-stretched network of fungal hyphae in the soil, providing access to phosphate, nitrate and water (Davies *et al.* 1993, George *et al.* 1995). The establishment of such an intimate interaction, allowing the fungus to grow intracellularly in the host cells, demands for recognition of the fungus as a symbiotic partner by the plant and a tight regulation of processes leading to the accommodation of the fungus in the root. On the molecular level, this process is only partly understood and the exact place and timepoint of activation, as well as the precise function of most genes known to be upregulated during fungal colonization of the host plant remain elusive. To some extent, this is due to the way mycorrhizal fungi proliferate in the host roots. During the symbiotic interaction, different developmental stages can be distinguished, ranging from the pre-contact phase followed by appressorium formation on the root epidermis and initial infection to spread of fungal hyphae in the outer cortex and finally arbuscule formation in the inner cortex (Parniske *et al.* 2008). While all of these stages are present at the infection site within hours of the first contact between the two symbiotic partners, the further progress of the symbiosis is characterized by permanent arbuscule build-up and break-down, while colonization of new root parts occurs in parallel via intraradical hyphae, as well as extraradical hyphae and appressorium formation. This asynchronous development leads to the concomitant presence of all developmental stages at the timepoint root colonization has reached sufficient levels for molecular analyses, making it extremely difficult to relate gene activity to distinct stages of the AM symbiosis.

In the recent years, several attempts have been undertaken to enrich mycorrhizal roots for early symbiotic stages, in order to investigate the underlying transcriptional changes. Suppressive subtractive hybridization (SSH) expression profiling and EST sequencing as well as proteome

analyses of *Medicago truncatula* roots colonized with mycorrhizal fungi for five to ten days (Brechenmacher *et al*. 2004, Weidmann *et al*. 2004, Amiour *et al*. 2006) resulted in the identification of several plant genes potentially related to appressorium formation.

One of the first reactions of root cells to the presence of mycorrhizal fungi is the occurrence of a characteristic calcium-spiking in the cytoplasm and the nucleus, which is decoded by the calcium-dependent protein kinase DMI3 (Lévy *et al*. 2004). The usage of *dmi3*-mutant plants allowed a first classification of the identified genes with regard to their activation upstream or downstream of the calcium-spiking initiated upon recognition of the microsymbiont (Weidmann *et al*. 2004, Amiour *et al*. 2006).

Another indication of forthcoming infection is the formation of an intracellular prepenetration apparatus (PPA) consisting of a membrane tunnel surrounded by cytoskeletal components which guides the invading hyphae through the cell (Genre *et al*. 2005). Siciliano *et al*. (2007) used PPA formation as a marker for beginning infection and selected such root parts where PPAs were visible for the construction of a SSH library, thereby circumventing the dilution effects which hampered the earlier investigations.

Nevertheless, an important draw-back of all these approaches was that presence of arbuscules was not excluded and identified genes might well be related to later stages of the symbiosis. Such commingling can be avoided by analyses restricted to defined cell-types obtained via laser-microdissection. First applications of this method revealed differential expression patterns between arbusculated and surrounding cortical cells for subsets of genes identified in high-throughput transcriptome analyses of AM roots from tomato (Balestrini *et al*. 2007, Fiorilli *et al*. 2009) and *Lotus japonicus* (Guether *et al*. 2009). In *Medicago truncatula* laser microdissection revealed the presence of transcripts from 27 genes in arbusculated cells (Gomez *et al*. 2009) and differential expression of 62 genes between arbusculated and surrounding cortical cells (Hogekamp *et al*. 2011). Gaude *et al*. (2012) combined laser-microdissection with a genome-wide transcriptome analysis using *Medicago* GeneChips, relying on cryo-sectioning for the preparation of thin sections for laser microdissection in contrast to the paraffin-embedding used in the earlier approaches.

Here, we report the use of laser-microdissection in paraffin-embedded roots for a comprehensive inventory of gene expression during several developmental stages of the AM symbiosis in roots of *Medicago truncatula* colonized with *Glomus intraradices*. Gene expression was monitored in five different cell-types comprising arbusculated cells, surrounding cortical cells colonized by fungal

hyphae and epidermal cells from mature mycorrhizal roots, as well as appressorial areas and non-appressorial areas from roots with first infection units. Taken together, cellular expression patterns for 18014 genes were revealed. For a subset of 1645 genes, these expression patterns were shown to be influenced by mycorrhizal colonization, revealing their activation at distinct stages of the symbiotic interaction. Four substes of genes were shown to be activated during the pre-contact phase, the initial infection, the spread of intraradical hyphae and arbuscule formation, including many known AM marker genes. In addition, two subsets of genes, which were either downregulated during infection or arbuscule formation were identified, as well as a large group of genes which displayed a shift of their expression pattern within the root during mycorrhization, including mainly genes, which were not known so far to be involved in processes related to mycorrhizal symbioses.

MATERIAL AND METHODS

Plant growth and inoculation with mycorrhizal fungi

Medicago truncatula Gaertn 'Jemalong' genotype A17 seeds were surface sterilized and scarified as reported by Hohnjec *et al*. (2003). Plants were grown in the climate chamber (humidity: 70%; photosynthetic photon flux: 150 µmol m^{-2} s^{-1}) at a 16-h light (23°C) and 8-h dark (18°C) regime. Plants were fertilized with half-strength Hoagland solution containing 20 µM phosphate and an additional 2mM NH_4NO_3. Mycorrhizal roots used for the collection of cortical cells containing arbuscules (ARB), cortical cells from mycorrhizal roots (CMR) and epidermal cells from mycorrhizal roots (EPI) were mycorrhized after 2 weeks and harvested at around 21 dpi as described in Hogekamp *et al*. (2011). In contrast, mycorrhizal roots used for the collection of APP (appressorial areas) and the corresponding non-appressorial controls (NAP) were mycorrhized after 3 weeks and harvested at 5-6 dpi. This resulted in a larger root system at the time of mycorrhization and an enhanced number of infection units per root system. Since no infection sites were visible at 4 dpi, appressorial areas had a maximum age of 48h.

Tissue embedding, tissue sectioning and laser microdissection

Roots were embedded using the Steedman`s wax protocol (Gomez *et al*. 2009) with the modifications reported in Hogekamp *et al*. (2011). For the collection of ARB, CMR and EPI cell pools, the whole root system of mycorrhizal plants was cut into approximately 1 cm pieces and embedded. For the collection of APP and NAP cell pools, an additional screening step was included into the protocol. The root system of the mycorrhizal plant was submerged in ink staining solution (Vierheilig *et al*. 1998) prepared with RNAse free water and 8% glacial acetic acid for 5-10 min on ice. Roots were then transferred into 0,8 % acetic acid solution prepared with glacial acetic acid and RNAse free water and screened for extraradical hyphae using a stereo microscope. Root segments with extraradical hyphae were embedded for the APP samples, while distant root segments with no visible fungal structures were embedded for the NAP samples.

Longitudinal sections of 12 µm on glass slides were obtained as described in Hogekamp *et al*. (2011). Also, the P.A.L.M. microbeam system with a Capmover (Zeiss, München) was used for laser microdissection and pressure catapulting as described before (Hogekamp *et al*. 2011).

For each cell-type, three biological replicates were produced, based on distinct rounds of plant cultivation and root embedding. For CMR, ARB and EPI cells, each biological replicate consisted of

three technical replicates with approximately 1,000 cells, which were pooled after RNA isolation and amplification. For NAP and APP cells, biological replicates consisted of one technical replicate of approximately 100 appressorial areas or control areas. These areas on average comprised 10 cells, leading to a final number of 1,000 cells in each sample.

RNA isolation and amplification

Total RNA was isolated from laser-microdissected cells using the RNeasy Micro kit (Qiagen, Hilden, Germany). 350 µl of RLT buffer containing β-mercaptoethanol were added to each sample followed by a 30-min incubation at room temperature. The lysate was spun down for 5 min at 13400 g, mixed 1:1 with ethanol absolute, and transferred to the clean-up column. On-column DNAse I digestion was performed according to the manufacturer's instructions. RNA was amplified using the TargetAmp 2-round Biotin aRNA amplification kit (Epicentre Biotechnologies, Madison), as specified by the manufacturer. The optional RiboGuard RNase Inhibitor was not used, since this led to poor results in pilot experiments (data not shown). For each sample, several rounds of amplification were carried out and pooled subsequently. Quantity and quality of total RNA as well as T7-amplified biotinylated aRNA was checked via capillary electrophoresis in RNA 6000 pico and nano assays, respectively, using an Agilent 2100 bioanalyzer (Agilent Technologies, Böblingen, Germany). Additionally, the pooled samples of T7-amplified biotinylated aRNA were checked via real-time RT-PCR for the presence or absence of marker genes. Primer design and real-time RT-PCR conditions were already described in Hogekamp *et al.* (2011).

Medicago GeneChip hybridizations

The whole amount of biotinylated aRNA obtained for each sample was fragmented. Size distribution of fragmented aRNA was assessed via an Agilent bioanalyzer (Agilent Technologies, Böblingen, Germany) using an RNA 6000 assay. The fragmented aRNA was added to a 300 µl hybridization cocktail also containing hybridization controls. 200 µl of the mixture was hybridized on GeneChips for 16 h at 45°C. Standard post-hybridization wash and double-stain protocols (FS450_0001; GeneChip HWS hit; Affymetrix) were used on an Affymetrix GeneChip fluidics station 450. GeneChips were scanned on an Affymetrix GeneChip scanner 3000 7G.

Evaluation of Data from *Medicago* GeneChip Hybridization

Cel files obtained from *Medicago* GeneChip hybridizations were analysed using the Robin software (http://mapman.gabipd.org/web/guest/robin). Normalization was performed via the Robust Multichip Average (RMA) algorithm. The two datasets referring to mature mycorrhizal stages (ARB, CMR, EPI) and early infection events (APP, NAP) were normalized separately. Intensity values calculated for each probe set were log2-transformed and averaged across all three biological replicates. Log2 differences between the either three or two cell-types investigated were evaluated statistically via p-values generated in Robin. Original annotations of probes from *Medicago* GeneChips were replaced by automated annotations as well as functional classifications generated via SAMS (Bekel *et al*. 2009) and Gene Ontology (GO) classifications (http://www.medicago.org/GeneChip). Since *Medicago* GeneChips are based on gene models from EST and genomic sequences, the number of probe sets exceeds the number of genes represented to a certain extent. Nevertheless, we refer to genes instead of probe sets in this work for reasons of simplicity. The functional classification of genes was primarily based on KOG categories or on their annotation, in case no automated KOG classification was available. The complete dataset is available from the Gene Expression Omnibus (accession number GSE42748).

RESULTS AND DISCUSSION

Obtaining RNA from five specific cell-types of mycorrhizal roots via laser microdissection

Medicago truncatula roots mycorrhized with *Glomus intraradices* were used to obtain RNA from pools of five specific cell-types via laser microdissection. Cortical cells from mycorrhizal roots containing fungal hyphae (CMR) and cortical cells containing arbuscules (ARB) were collected around 21 dpi as described in Hogekamp *et al.* (2011). Additionally, epidermal cells from mycorrhized roots (EPI) were collected. Care was taken to harvest epidermal cells only from areas of the root which clearly contained fungal structures (Figure II_1 A-C).

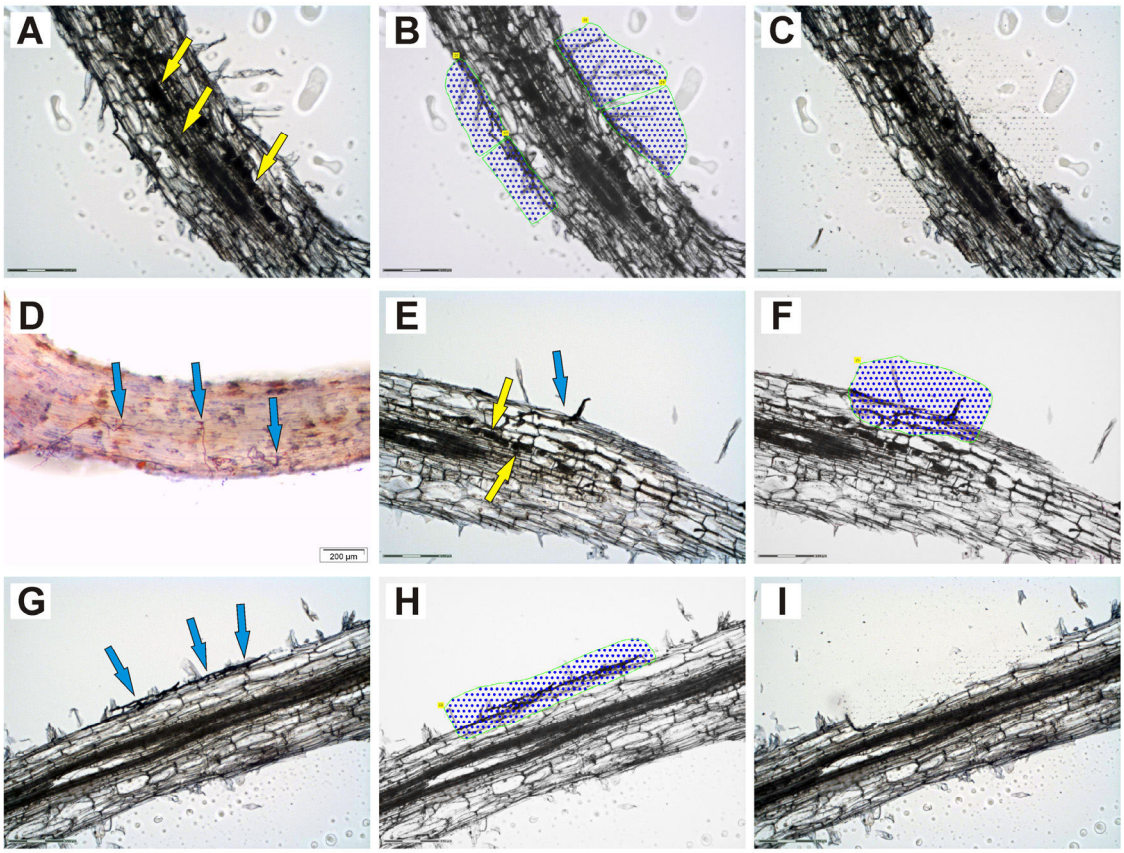

Figure II_1: Laser microdissection of epidermal cells from mycorrhized roots (EPI), (A-C) and root areas containing fungal appressoria (APP), (D-I).
Collected areas are marked with blue dots framed in green. Arbuscules and appressoria are marked with yellow and blue arrows, respectively. EPI samples were collected from areas of the root containing mature mycorrhizal structures. For the harvest of APP samples, roots were subjected to a short ink staining and screened for early infection units prior to embedding (**D**). During laser microdissection, epidermal areas where fungal hyphae were penetrating the root and the cortical cells beneath were harvested for the APP samples. In cases where arbuscules had already developed in the inner cortical cells (**E+F**), those cells were not included. Scale bars represent 200 µm for D and 150 µm for all other panels.

By using an additional screening step, we were also able to collect root cells containing appressoria (APP). In this case, roots were harvested already at 5-6 dpi and regions where extraradical hyphae had attached to the surface were identified after a short ink staining (Figure II_1 D). Regions with no sign of fungal colonization from the same root systems were used for the harvest of non-appressorial areas (NAP).

In 12 µm thin sections of the wax embedded roots, appressoria were still clearly visible (Figure II_1 E,G). During laser microdissection, a small root area was collected, comprising the epidermal cells in contact with the penetrating fungal hyphae and the colonized outer cortical cells beneath it (Figure II_1 F,H,I). Although the roots were harvested at the earliest possible time point showing any fungal structures on the root surface, in some cases the infection units had already proceeded to the development of arbuscules (Figure I_1 E). These appressorial areas were also collected, but care was taken to include no inner cortical cells containing arbuscules (Figure I_1 F), to avoid contamination with transcripts from later mycorrhizal stages. For the NAP samples, corresponding areas of epidermal and cortical cells were harvested (data not shown).

Two-round amplified biotinylated aRNA from three biological replicates of each cell-type was used for *Medicago* GeneChip (Benedito *et al*. 2008) hybridizations. The complete datasets are included in Supplemental Tables S_II_1a (ARB, CMR, EPI) and S_II_1b (APP, NAP). For our analysis and classification of genes according to their expression pattern in the five cell-types investigated, the two datasets referring either to mature mycorrhizal roots (ARB, CMR, EPI) or early infection events (APP, NAP) were first analyzed separately. The strategy for the identification of cellular expression patterns was based on two main aspects presented in the following two sections.

Expression of 18014 genes was detected in five cell-types from mycorrhizal roots

In the first step, we analyzed whether genes were expressed in the different cell-types at all. We already showed that transcripts of the arbuscule-specific phosphate transporter *MtPt4* can only be detected by RT-PCR in ARB samples, but not in CMR samples (Hogekamp *et al*. 2011). In our GeneChip experiments, *MtPt4* again showed high mean signal intensities only in the ARB samples (10,77). In comparison, mean signal intensities of *MtPt4* were extremely low in CMR and EPI samples (2,58). We used this biological threshold for a first classification of genes in mature

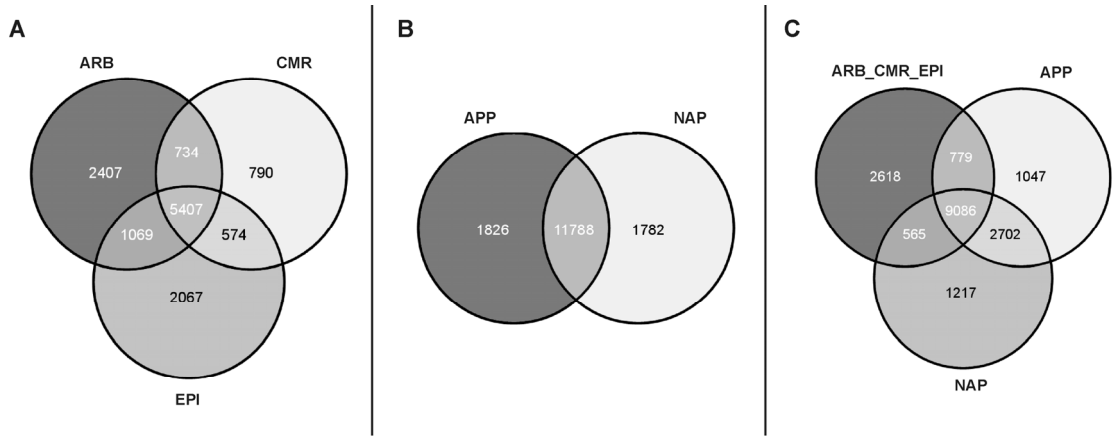

Figure II_2: Gene expression in the five cell-types investigated.
A: Overview for ARB, CMR and EPI. Genes were classified as expressed in a cell-type, if the corresponding mean signal intensity was >2,58 (higher as the mean signal intensity of *MtPt4* in CMR and EPI). **B**: Overview for APP and NAP. Genes were classified as expressed in a cell-type, if the corresponding mean signal intensity was > 2,95 (higher as the mean signal intensity of *MtPt4* in APP and NAP). **C**: Overlap of genes expressed in the two datasets. Abbreviations: ARB: cortical cells containing arbuscules, CMR: cortical cells from mycorrhizal roots, EPI: epidermal cells from mycorrhized roots, ARB_CMR_EPI: non-redundant sum of ARB, CMR and EPI, APP: appressorial areas, NAP: non-appressorial areas. Venn diagrams were drawn using the VENNY software (Oliveros 2007).

mycorrhizal roots. Those with a mean signal intensity above 2,58 were regarded as expressed (exp) in the respective cell-type, those with a lower value as not expressed (ne).

The validity of this classification is underlined by the fact that 14 of the 25 genes we identified as ARB-specific in our RT-PCR-analysis (Hogekamp *et al.* 2011) are again only expressed in this cell-type in our GeneChip dataset. Transcripts of one gene were now also detected in the EPI cell pool, which was not included in the previous analysis. Four genes were detected as additionally expressed in other cell-types, but the genes were still strongly ARB-induced (log_2FC between 6 and 8,5), thus showing the same tendency. The remaining six genes showed differing results, with two expressed in ARB and CMR with no significant difference, one being only expressed in EPI and three being not expressed in any cell-type. The detection of genes in single cell-types by RT-PCR but not on the GeneChip is probably due to a higher sensitivity of the first method. Nevertheless, the strong general congruency shows that the *MtPt4*-treshold leads to correct classification of other ARB-expressed genes as well, and should allow a reliable identification of gene transcription in general. Since both cell pools prepared from young mycorrhizal roots contained no arbuscules, the mean signal intensity of *MtPt4* was also low in APP and NAP (2,95), allowing to apply the same method for the classification of genes in this dataset.

In the dataset referring to mature mycorrhizal roots, we identified 13048 genes as expressed in either one, two or all three cell-types investigated (Supplemental Table S_II_2, mean signal intensity above the threshold in a cell-type is marked in blue). The distribution of genes in the three cell-types is shown in Figure II_2 A. The largest group of genes was expressed in all three cell-types (5407). Also prominent were genes only expressed in ARB (2407) or EPI (2067) or both cell-types (1069). Smaller but still considerable groups of genes were transcribed only in CMR (790), CMR and ARB (734) or CMR and EPI (574).

The distribution of expressed genes in the dataset referring to early infection events is shown in Figure II_2 B. 1826 genes were only expressed in APP, 1782 only in NAP and 11788 genes were transcribed in both cell pools, resulting in a total number of 15396 genes identified as expressed in this dataset (Supplemental Table S_II_3, mean signal intensity above the threshold in a cell-type is marked in blue). Figure II_2 C shows a comparison between both datasets. As expected, there is a considerable overlap between the two, since the APP and NAP cell pools also consist of cortical and epidermal cells. Taken together, 18014 genes were classified as expressed in at least one of the five investigated cell-types.

To obtain an estimate how many genes can be expected to be expressed in mycorrhizal root tissue in general, a comparative analysis was performed with gene expression in whole mycorrhizal roots (Hogekamp *et al*. 2011). In this experiment, transcript levels in *M. truncatula* roots colonized either with *Glomus intraradices* or *Glomus mossae* had been compared to transcript levels in non-mycorrhizal roots under low (20 µM) and high (2 mM) phosphate supply. Again, the mean signal intensity of *MtPt4* (3,38) in three biological replicates of non-mycorrhizal roots under low phosphate supply was used as a threshold for gene expression. The analysis resulted in a total of 31337 genes, which were expressed in mycorrhizal roots according to this classification. The 18014 genes we detected as expressed in our cell-type specific samples contained 16023 of these, ~ 51% of the genes expressed in this tissue in general. Two main reasons can be found for the absence of transcripts from the remaining genes in the cell-type specific samples. On the one hand, RNA degradation, which cannot be completely avoided during the preparation of root material for laser microdissection, may lead to a loss of less abundant transcripts resulting in poor signal intensities on GeneChips. In addition, probe sets on the GeneChip are not evenly distributed across the transcript in some cases and a 5' bias of probe sets may lead to similar effects, since RNA degradation starts at the 5' end of the

mRNA. On the other hand, genes may also be expressed in tissues and cell-types which were not included in the current analysis, for example vascular tissues or meristematic regions such as root tips and areas of lateral root formation. Since several hundred genes of fungal origin are represented on *Medicago* GeneChips (Gomez *et al*. 2009), this explanation can also be extended to fungal tissues, e.g. spores, extraradical hyphae and vesicles. Interestingly, 1991 genes were detected as expressed in our cell-type specific samples, but not on the level of whole mycorrhizal roots. In these cases, the focus on single cell-types probably leads to the detection of low abundance transcripts which are otherwise lost due to dilution effects. This is supported by the observation that the portion of these genes was particularly high for those expressed in epidermal cells, which can be expected to be underrepresented in whole root tissues.

Classification of genes according to their cell-specific expression patterns

In a second step, we classified genes according to significant expression differences between the cell-types investigated. For the dataset referring to mature mycorrhizal stages, we applied a log_2FC-threshold of >2,32 (5-fold expression difference) at a p-value of ≤ 0,01 for genes expressed in up to two cell-types, whereas for genes which were expressed in all three cell-types, a lower log_2FC-threshold of >1,32 (2,5-fold expression difference) was used.

Based on these conditions, we identified 1648 genes with differential expression in ARB, CMR and EPI and 4599 which were equally expressed. All 6247 genes were grouped into seven categories (Table II_1 A). The first three categories showed induction in a single cell-type (ARB, CMR or EPI). The following three categories contain genes which were induced in two cell-types in comparison to the third (ARB+CMR, CMR+EPI, or ARB+EPI). In each of these categories, genes were further classified according to whether they had been identified as expressed based on the *MtPt4*-threshold in the three cell-types, to select for cell-type specific expression (Table II_1 A). For example, in the first category of 865 ARB-ind genes, 348 were classified as ARB-specific, meaning that they were not expressed in CMR and EPI while they displayed a significant induction in ARB in comparison to at least one of the other cell-types (Table II_1 A). In addition, 63 and 47 genes were only expressed in ARB+CMR or ARB+EPI, respectively. Finally, 407 of the ARB-induced genes were transcribed in all three cell-types, but displayed two different expression patterns. Whereas, 335 of these were strongly induced in ARB with no significant difference between CMR and EPI (ARB>CMR=EPI), 72 genes displayed a pattern with decreasing expression levels from ARB to CMR to EPI (ARB>CMR>EPI).

While the following five categories were sub-divided accordingly, the last category consists of the 4599 genes equally expressed in all three cell-types (Table II_1 A).

For the dataset referring to early infection events, we applied a log_2FC-threshold of >2,32 (5-fold expression difference) at a p-value of ≤ 0,05 to identify significant expression differences between APP and NAP (Figure II_3 B). The lower p-value was applied, since these samples consisted of cortical and epidermal cells instead of one specific cell-type and were therefore expected to have a

Table II_1: Classification of genes according to their specific expression patterns in the five cell-types investigated.

A: Genes expressed in ARB, CMR and EPI were classified into seven categories. **B**: Genes expressed in APP and NAP were classified into three categories. While categories were defined on the basis of significant expression differences, subcategories were based on detectable expression only. Coloured boxes represent different levels of expression in the respective cell-types from white (no expression) to black (strong expression) Abbreviations: ARB: cortical cells containing arbuscules, CMR: cortical cells from mycorrhizal roots, EPI: epidermal cells from mycorrhized roots, APP: appressorial areas, NAP: non-appressorial areas, equ.: equally, ind: induced, logFC: log2 fold-change, p: p-value.

A

category	subcategory	signal mean			logFC ratio (p ≤ 0,01)			number of genes
		ARB	CMR	EPI	ARBvsCMR	EPIvsARB	EPIvsCMR	
1 ARB-induced	ARB-specific*				>2,32	<-2,32		348
	ARB+CMR-specific				>2,32	<-2,32		63
	ARB+EPI-specific				>2,32	<-2,32		47
	all celltypes (ARB>CMR=EPI)°				>1,32	<-1,32		335
	all celltypes (ARB>CMR>EPI)°				>1,32	<-1,32	<-1,32	72
								865
2 CMR-induced	CMR-specific*				<-2,32		<-2,32	3
	ARB+CMR-specific				<-2,32		<-2,32	3
	CMR+EPI-specific				<-2,32		<-2,32	0
	all celltypes°				<-1,32		<-1,32	26
								32
3 EPI-induced	EPI-specific*					>2,32	>2,32	113
	CMR+EPI-specific					>2,32	>2,32	23
	ARB+EPI-specific					>2,32	>2,32	19
	all celltypes°					>1,32	>1,32	95
								250
4 ARB+CMR-induced	ARB+CMR-specific*					<-2,32	<-2,32	78
	all celltypes°					<-1,32	<-1,32	87
								165
5 CMR+EPI-induced	CMR+EPI-specific*				<-2,32	>2,32		32
	all celltypes°				<-1,32	>1,32		46
								78
6 ARB+EPI-induced	ARB+EPI-specific*				>2,32		>2,32	111
	all celltypes°				>1,32		>1,32	147
								258
7 equ. expressed	all celltypes							**4599**
								6247

* genes were also considered as specific for the respective cell-type(s) if only one logFC ratio was above the thresholds
° genes were also grouped into this subcategory if only one of the logFC ratios was significant

B

category	subcategory	signal mean		logFC ratio (p ≤ 0,05)	number of genes
		APP	NAP	APPvsNAP	
1 APP-induced	APP-specific			>2,32	235
	NAP+APP			>2,32	93
					328
2 NAP-induced	NAP-specific			<-2,32	53
	NAP+APP			<-2,32	155
					208
3 equ.expressed	NAP+APP				**11540**
					12076

higher range of biological variation. 328 genes were found to be significantly induced in APP, whereas 208 genes were induced in NAP. Together with the 11540 genes equally expressed in both cell pools, 12076 genes showed a clear expression pattern.

We decided to focus our analysis mainly on the 6247 and 12076 genes from the two datasets displayed in Table II_1, since the remaining were only expressed in a maximum of two cell-types for ARB, CMR and EPI or one cell-type for APP and NAP, but with no significant differences, due to their weak overall signal intensities.

Cell-specific expression of key marker genes for AM symbioses

In a next step we wanted to investigate, whether we had been successful in identifying cellular expression patterns of genes known to be up-regulated during AM symbioses in the host root. To this end, a comparison with the AM core set (Hogekamp *et al.* 2011) consisting of 532 genes significantly induced at least 2-fold (FDR-corrected p-value ≤ 0,05) in roots colonized with *Glomus intraradices* and roots colonized with *Glomus mossae*, but not in roots treated with additional phosphate, was performed. The comparison was done separately for genes listed in the seven categories from mature mycorrhizal roots and genes grouped in the three categories from early infection events. The results of this comparison are shown in Figure II_3, including a diagram illustrating the predicted expression pattern in mycorrhizal roots (Figure II_3 A) and a table with detailed results for 16 AM marker genes (Figure II_3 B). Whereas 237 genes from the AM core set were part of one of the seven categories from mature mycorrhizal stages, 158 were part of the three categories from early infection events. Since there were also overlaps between the two datasets, cellular expression patterns could be identified for 293 individual genes of the AM core set. Of the remaining 239 genes, 103 had been detected as expressed in at least one of the five investigated cell-types, but were neither equally expressed in all cell-types nor had significant expression differences between those they were transcribed in. Finally, transcripts of 136 genes had not been detected in any of the five cell-types. Possible reasons for this were already discussed above.

Most of the genes, for which a cellular expression pattern was identified, belonged to the category of ARB-induced genes (181) (Figure II_3 A). With regard to the subcategories, most of them were ARB-specific (87), including several AM marker genes known to be specifically expressed or highly upregulated in this cell-type such as *MtPt4* (Harrison *et al.* 2002, Hogekamp *et al.* 2011), *MtTi1* (Grunwald *et al.* 2004), the two lectin genes *MtLec5* and *MtLec7* (Frenzel *et al.* 2005, Hogekamp *et*

A

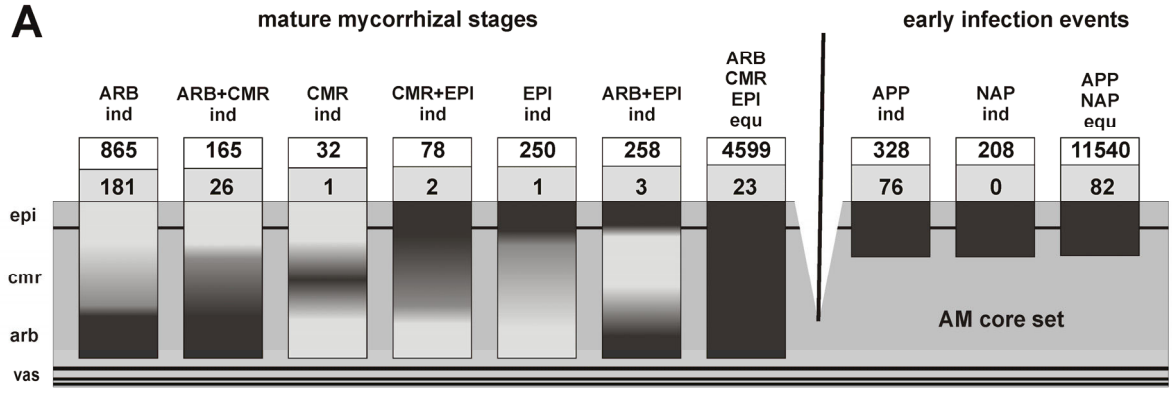

B

Expression category	Identifier	Gene	ARB Mean	CMR Mean	EPI Mean	logFC ARB_vs_CMR	p ARB_vs_CMR	logFC EPI_vs_ARB	p EPI_vs_ARB	logFC EPI_vs_CMR	p EPI_vs_CMR
ARB-ind											
ARB-specific	Mtr.43062.1.S1_at	MtPt4	10,77	2,58	2,58	8,20	0,000	-8,20	0,000	0,00	0,997
	Mtr.16454.1.S1_at	MtTi1	7,52	1,96	2,23	5,56	0,000	-5,29	0,000	0,27	0,742
	Mtr.45648.1.S1_at	MtLcc7	4,10	2,21	1,75	1,90	0,021	-2,35	0,008	-0,46	0,502
	Mtr.15653.1.S1_at	MtLec5	10,21	2,27	2,43	7,94	0,000	-7,78	0,000	0,16	0,677
	Mtr.20364.1.S1_at	MtAnn2	7,59	2,05	2,12	5,54	0,000	-5,47	0,000	0,07	0,858
ARB+CMR-specific	Mtr.15957.1.S1_at	MtGst1	9,90	3,06	2,49	6,83	0,000	-7,41	0,000	-0,58	0,404
all cell types	Mtr.8863.1.S1_at	MtMyb1	12,12	3,86	4,38	8,26	0,002	-7,74	0,003	0,52	0,778
ARB>CMR=EPI	Mtr.12500.1.S1_at	MtGlp1	10,16	3,05	3,11	7,11	0,000	-7,05	0,000	0,06	0,904
	Mtr.43585.1.S1_at	MtDxs2	5,27	2,95	2,99	2,32	0,001	-2,28	0,001	0,04	0,931
all cell types	Mtr.43470.1.S1_at	MtHa1	11,68	6,36	3,80	5,31	0,002	-7,87	0,000	-2,56	0,054
ARB>CMR>EPI	Mtr.15627.1.S1_s_at	MtBcp1	11,82	8,08	5,96	3,74	0,001	-5,86	0,000	-2,13	0,013
	Mtr.42828.1.S1_at	MtVapyrin	9,54	6,65	4,52	2,89	0,006	-5,02	0,000	-2,13	0,024
ARB+CMR-ind											
all cell types	Mtr.40285.1.S1_at	MtScp1	11,72	10,70	5,41	1,02	0,000	-6,30	0,000	-5,29	0,000
	Mtr.42072.1.S1_at	MtFlot4	7,05	6,00	3,60	1,05	0,009	-3,45	0,000	-2,40	0,000
	Mtr.16863.1.S1_at	MtCbf2	8,92	9,82	6,44	-0,90	0,189	-2,48	0,005	-3,38	0,001
equ. expressed											
ARB=CMR=EPI	Mtr.51511.1.S1_at	MtCbf1	8,89	9,97	5,16	-1,08	0,477	-3,73	0,035	-4,81	0,012

Expression category	Identifier	Gene	NAP Mean	APP Mean	logFC APPvsNAP	p APPvsNAP
APP-ind						
APP-specific	Mtr.43470.1.S1_at	MtHa1	1,91	7,57	5,65	0,020
APP+NAP	Mtr.15627.1.S1_s_at	MtBcp1	3,64	10,61	6,97	0,003
	Mtr.42828.1.S1_at	MtVapyrin	5,54	9,37	3,82	0,032
	Mtr.40285.1.S1_at	MtScp1	3,02	9,71	6,69	0,000
	Mtr.42072.1.S1_at	MtFlot4	5,52	8,08	2,56	0,006
	Mtr.51511.1.S1_at	MtCbf1	5,04	10,87	5,82	0,032
	Mtr.16863.1.S1_at	MtCbf2	6,66	11,47	4,81	0,027
equ. expressed						
APP=NAP	Mtr.43585.1.S1_at	MtDxs2	6,02	6,82	0,80	0,586
	Mtr.15653.1.S1_at	MtLec5	3,31	4,09	0,77	0,274

Figure II_3: Genes with a clear expression pattern in mature mycorrhizal stages or early infection events in comparison to genes from the AM core set.

A: Diagram showing the overlap and predicted gene expression pattern in mycorrhizal roots for the seven expression categories referring to mature mycorrhizal stages and the three categories referring to early infection events. Numbers in white boxes represent the total number of genes in an expression category, numbers in grey boxes the overlap in this category with the 532 genes from the AM core set (Hogekamp *et al*. 2011). Note: the overlap between gene expression in mature mycorrhizal stages and early infection events is not shown in this diagram for reasons of simplicity. In total, cellular expression patterns were identified for 293 of the 532 genes from the AM core set. **B**: Detailed results for 16 well-characterized AM marker genes, including mean signal intensities in the cell-types investigated (signal intensities above the *MtPt4* threshold are marked in blue) and expression differences between the cell-types (red/dark green: significant expression differences (logFC≥2,32; p≤0,01) for genes expressed in only one of the cell-types compared, orange/green: significant expression differences (logFC≥2,32; p≤0,01) for genes expressed in both of the cell-types compared). Abbreviations: ARB: cortical cells containing arbuscules, CMR: cortical cells from mycorrhizal roots, EPI: epidermal cells from mycorrhized roots, APP: appressorial areas, NAP: non-appressorial areas, vas: vascular tissue, ind: induced, equ.: equally expressed, logFC: log2 fold-change, p: p-value.

al. 2011) and *MtAnn2* (Manthey *et al*. 2004) (Figure II_3 B). The glutathione-S-transferase gene *MtGst1* was found to be ARB-induced, but also expressed in the surrounding cortical cells (Figure II_3 B), which is in line with the results of Wulf *et al*. (2003). The transcription factor gene *MtMyb1*

(Liu *et al*. 2003), the *MtGlp1* gene encoding a germin-like protein (Doll *et al*. 2003) and the 1-deoxy-D-xylulose-5-phosphate synthase gene *MtDxs2* (Floss *et al*. 2008b) were found to be expressed in all cell-types with a strong induction in ARB in comparison to CMR and EPI, whereas the ATPase gene *MtHa1* (Krajinski *et al*. 2002), the *MtBcp1* gene encoding a blue copper protein (Hohnjec *et al*. 2005) and the *MtVapyrin* gene (Pumplin *et al*. 2010) were found in the subcategory of genes with an expression gradient from ARB to EPI (Figure II_3 B). Another part of the AM core set consists of genes induced in ARB+CMR alike (26) (Figure II_3 A), including the serine carboxypeptidase *MtScp1*, which was first identified and shown to be related to fungal spread in the cortex by Liu *et al*. (2003) and the flotillin gene *MtFlot4* (Figure II_3 B) known to be involved in infection of root nodules (Haney and Long 2010). The two CAAT-box transcription factor genes *MtCbf1* and *MtCbf2*, recently shown to be active during all stages of mycorrhizal colonization (Hogekamp *et al*. 2011), were also expressed in all three cell-types (Figure II_3 B). While *MtCbf2* was significantly induced in ARB and CMR in comparison to EPI, this expression difference was not significant for *MtCbf1*, which was therefore grouped into the category of equally expressed genes. This effect mirrors the slightly higher activity of *MtCbf1* in epidermal cells, which was already detected via promotor-GUS-studies (Hogekamp *et al*. 2011). Besides *MtCbf1*, 22 other genes of the AM core set were also equally expressed in all three cell-types from mature mycorrhizal roots (Figure II_3 A). Only one gene of the core set, coding for a germin-like protein, was CMR-induced, one was EPI-induced and two induced in both cell-types (Figure II_3 A). The overlap to the category of genes induced in ARB+EPI was also very small, consisting of three genes encoding a chlathrin assembly protein we had previously identified as ARB-specific (Hogekamp *et al*. 2011) and two chitinases genes (Figure II_3 A and Supplemental Table S_II_5).

While no genes were found to be NAP-induced, a higher overlap existed to genes which were either APP-induced (76) or equally expressed in APP and NAP (82) (Figure II_3 A). Some of the AM marker genes were also found in these two categories. As expected from their activation by the first physical contact between plant and fungus (Hogekamp *et al*. 2011) *MtCbf1* and *MtCbf2* were found to be APP-induced (Figure II_3 B). Additionally, *MtHa1*, *MtBcp1*, *MtVapyrin*, *MtScp1*, and *MtFlot4* were already activated at this early stage of the interaction, while *MtLec5* and *MtDxs2* were equally expressed in APP and NAP (Figure II_3 B).

Taken together, our investigation delivered clear information on the cellular expression pattern of 293 genes from the AM core set and gave first hints with regard to the remaining genes, since 103 of them were at least detected as expressed in one or several of the investigated cell-types. For the 136 genes which were not detected at all in our approach, it can be assumed that at least some of them are expressed in those root tissues which were not analyzed here.

Appressorial cell pools are enriched for fungal genes

Since APP cell pools were harvested from regions of the root already colonized by the AM fungus, whereas NAP cell pools contained no fungal material, we expected to find *Glomus intraradices* genes among those induced in APP. Therefore, a comprehensive search for fungal genes was performed. For all APP-induced probe sets, the corresponding gene sequences from the *Medicago truncatula* GeneExpressionAtlas (GEA) (Benedito *et al*. 2008) were blasted against the Glomus EST collection, the Glomus genome and sequences from Glomus Nimble Arrays (http://mycor.nancy.inra.fr/IMGC/GlomusGenome). Hits with an e-value ≤ 0,001 in at least one of these were considered further. If those had no match in *Medicago* coding sequences (http://www.medicagohapmap.org/genome), they were classified as fungal genes. Strikingly, this resulted in a number of 202 fungal sequences among the APP-induced genes, which was roughly two third of all genes induced in this cell pool. As can be expected, most of these genes had been specifically "induced" only by *Glomus intraradices* but not by *Glomus mossae* on the level of whole roots (Hogekamp *et al*. 2011). Even in case they had been detected as induced in both interactions, which probably occurred for highly conserved genes with similar sequences in different AM fungi, the induction in roots colonized by *Glomus mossae* was very low. Therefore, we also had a closer look at genes from other categories, which showed a *Glomus intraradices* specific induction on the level of whole roots. This resulted in the identification of another 10 fungal genes in addition to five fungal genes that had already been identified earlier (Hogekamp *et al*. 2011), leading to a total number of 217 fungal genes. The complete set is listed in Supplemental Table S_II_4. Only 20 of these are part of the AM core set, since it exclusively consists of genes coinduced by colonization with *Glomus intraradices* and *Glomus mossae* (Hogekamp *et al*. 2011).

In Figure II_4, the classification of fungal genes into functional categories is shown. Most of the genes were of unknown function (100). Among the rest, the three most prominent functional classes

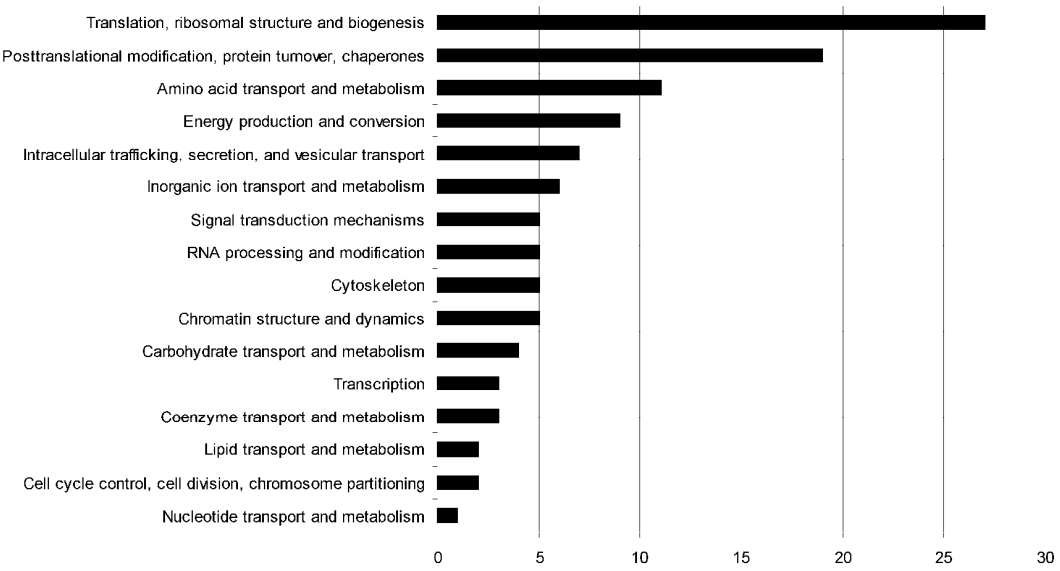

Figure II_4:Functional classification of fungal genes.
The 217 fungal genes were grouped into functional classes according to their KOG classification or their annotation in case no automated classification was available. Note: The 100 fungal genes grouped into the class "Unknown function" are not included in this diagram.

were translation (28), posttranslational modification of proteins (19) and amino acid transport and metabolism (11). Whereas the first two classes probably contain a high number of fungal housekeeping genes, the third represents an important part of the nutrient exchange network between AM fungi and plants, since nitrogen is transported within the fungal mycelium after incorporation into amino acids (Govindarajulu *et al.* 2005).

Apart from being APP-induced, most of the fungal genes showed either no clear expression pattern or were not expressed in cell-types from mature mycorrhizal roots (82 and 34 genes, respectively). Since the APP cell pools also contained considerable parts of extraradical hyphae, the 34 genes not expressed in mature mycorrhizal stages are probably expressed in the extraradical mycelium (ERM). The remaining genes were either ARB-induced (57), ARB+CMR-induced (29) or equally expressed in all three cell-types (15) (Supplemental Table S_II_4). To get an impression how fungal material was generally distributed in these cell-types, we had a look at a fungal housekeeping gene coding for the translation elongation factor GiTefα (Mtr.4378). As expected, the corresponding transcripts were specifically detected in APP and not in NAP (Supplemental Table S_II_4). The identified expression pattern in cell-types from mature mycorrhizal roots validates the presence of fungal structures in all three cell-types, but suggests that fungal material was not equally distributed between them, since the gene was grouped into the category of ARB-induced genes with an expression gradient (ARB>CMR>EPI). This is plausible, since arbusculated cells contain a high amount of fungal

material due to the highly ramificated intracellular hyphae, whereas in the other cortical cells, fungal hyphae mainly grow in the extracellular space and the epidermal cell pool will at the most contain single hyphae growing on the surface of the root. Due to this, fungal genes which were classified as ARB-induced, at least those with an expression gradient similar to *GiTefα*, have to be treated with caution, since they might be equally expressed within the fungal part of the symbiotic tissue instead. In contrast, the 29 fungal genes which were specifically detected in ARB probably show a true differential expression pattern.

Genes expressed constitutively in root tissue

A large fraction of those genes, for which we identified a cellular expression pattern can be expected to be constitutively expressed in root tissues, irrespective of colonization with AM fungi. Although some exceptions exist, which are discussed below, most of the 4250 genes we found to be expressed at equal levels in ARB, CMR and EPI and in addition in APP and NAP (Table II_2 B) can be considered as consistently expressed in both root cortex and epidermis under our experimental conditions. As an example the gene encoding the translation elongation factor α (Tefα) of *M. truncatula*, which is considered a housekeeping gene and often used for normalization of RT-PCR-data (Wulf *et al*. 2003, Lee *et al*. 2010), indeed displayed an equal expression across all investigated cell-types in both datasets (Supplemental Table S_II_5).

Furthermore, in addition to genes with an equal expression across all cell-types, candidates with a tissue-specific yet constitutive expression either in the root epidermis or the cortex, which is not influenced by AM symbiosis, can be found in the categories of EPI-induced and ARB+CMR-induced genes. This is in particular the case for the 250 EPI-induced genes (Table II_1 A), which is illustrated by the following aspects. An analysis of gene expression profiles of EPI-induced genes in the GeneExpressionAtlas (GEA) revealed, that many of these genes were also expressed in all other plant organs besides roots (data not shown), therefore it seems probable that they contribute to the basic protein equipment of epidermal cells. Nearly no overlap was found to genes induced by fungal colonization on the level of whole roots (6 genes, Table II_2 C) and none of the EPI-induced genes were APP-induced as well (Table II_2 B). Surprisingly, a considerable part of EPI-induced genes displayed no clear expression pattern in APP and NAP samples (38 genes, Table II_2 B) or was not expressed in these cell-types (35 genes, Table II_2 B). The respective genes were likely candidates for genes preferentially activated in epidermal cells during later stages of the symbiosis, which were not

identified on the level of whole roots due to dilution effects. Nevertheless, when gene function is regarded, this does not seem to be the case, since those genes are mainly annotated as coding for ribosomal proteins or parts of the respiratory chain, indicating enhanced metabolic rates and energy demand in these cells (Supplemental Table S_II_3). The specific detection of the respective transcripts in epidermal cells from mature mycorrhizal roots may therefore be either due to slight age differences of the plants used in the two approaches, or the dilution of epidermal cells with cortical cells in the APP and NAP samples already leads to a loss of transcripts from epidermal cells in those samples. Notably, nearly all of these genes were EPI-specific, making a decrease in signal intensity below the threshold in combined cell pools more likely.

Cellular expression patterns provide insights into differential gene activity during developmental stages of the AM symbiosis

To draw a comprehensive picture of gene activity and possible gene functions during AM symbioses, results obtained on cellular expression patterns during early infection events and mature mycorrhizal roots were combined. In Table II_2, results are shown for all 52796 *Medicago* probe sets on the GeneChip. The picture was completed by comparisons to gene expression patterns in whole mycorrhizal roots (Hogekamp *et al*. 2011) or in roots exposed to diffusible signal molecules of the fungus (Czaja *et al*. 2012). Based on these results, genes were divided into four main groups representing the four stages of AM symbioses, defined in Hogekamp *et al*. (2011). Three additional groups were defined for genes either repressed during initial infection or during arbuscule formation, and for genes which obviously experience a shift of their expression and become preferentially active in arbusculated cells during fungal colonization. In the following these seven groups (A-G) will be discussed with regard to their relevance during the four stages of AM development (for an overview see also Figure II_11 in the conclusion and Supplemental Table S_II_6).

Stage I: Signalling via diffusible factors

The establishment of an AM symbiosis is initiated by a cross-talk between the two partners based on diffusible signal molecules. Whereas strigolactones were identified on the plant side (Akiyama *et al*. 2005), mycorrhizal fungi exude lipochitoligosaccharides (LCOs), the so-called Myc-factors (Maillet *et al*. 2011) and probably other still undiscovered signal molecules (Kosuta *et al*. 2003), which activate the first steps of the symbiotic signalling cascade in the host plants. In our analysis, this

initial stage is represented by the APP and NAP samples. Although the majority of genes expressed at equal levels in APP and NAP (Table II_2 B) will be constitutively expressed in the root, both cell pools were derived from root systems containing first infection sites and both cell pools were subjected to potential diffusible signal molecules. Thus, systemic reactions triggered by the presence of the fungus, are likely to be detected in both cell-types.

This is in line with the observation, that a small fraction of 152 genes which displayed an equal expression in APP and NAP in our analysis are also induced upon inoculation of roots with Myc-LCOs (at least 1,5 fold induction in roots treated with sulphated LCOs, non-sulphated LCOs or a mixture of both, Czaja *et al*. 2012). The complete list of these genes (Group A) is included in Supplemental Table S_II_6.

Table II_2: Comparison of gene expression in cell-types from mature mycorrhizal stages (ARB, CMR and EPI) and early infection events (APP and NAP).

Results for all 52796 *Medicago* probe sets on the GeneChip are shown. The expression categories of the dataset referring to mature mycorrhizal stages (ARB, CMR, EPI) are shown in columns, those of the dataset referring to early infection events (APP, NAP) in rows. Additionally, genes that were detected as expressed (exp) according to the *MtPt4*-threshold, but did not show significant expression differences between the cell-types, as well as genes that were not expressed (ne) are listed for both datasets. The numbers of genes in each combination of categories is given. In the last column and the last row, results for each category are summed up. In **A** the 217 fungal genes that were identified are included, in **B** they were kept out, reducing the total number of genes to 52579. **C** shows, how many of the genes in each comparison were already known to be induced by mycorrhizal fungi (at least 2-fold induced with a FDR-corrected p-value ≤ 0,05 by colonization with *Glomus intraradices*, *Glomus mossae*, or both, but not induced by enhanced phosphate supply) based on gene expression in whole roots (Hogekamp *et al*. 2011). For example from the 36 ARB- and APP-induced *Medicago truncatula* genes, 35 were also identified as induced by fungal colonization on the level of whole roots and one gene was not. Abbreviations: ARB: cortical cells containing arbuscules, CMR: cortical cells from mycorrhizal roots, EPI: epidermal cells from mycorrhized roots, APP: appressorial areas, NAP: non-appressorial areas, ind: induced, ~: equally expressed, exp: expressed, ne: not expressed.

A Complete overview containing also fungal genes

	ARB-ind	CMR-ind	EPI-ind	ARB+CMR-ind	CMR+EPI-ind	ARB+EPI-ind	ARB~CMR~EPI	ARB/CMR/EPI-exp*	ne in ARB/CMR/EPI	total
APP-ind	87	1	0	43	0	1	34	117	45	**328**
APP~NAP	563	25	174	110	70	240	4252	3459	2647	**11540**
NAP-ind	4	2	3	0	1	3	39	86	70	**208**
APP/NAP-exp°	83	1	38	4	5	9	127	849	2204	**3320**
ne in APP/NAP	128	3	35	8	2	5	147	2290	34782	**37400**
total	**865**	**32**	**250**	**165**	**78**	**258**	**4599**	**6801**	**39748**	**52796**

B Complete overview without fungal genes

	ARB-ind	CMR-ind	EPI-ind	ARB+CMR-ind	CMR+EPI-ind	ARB+EPI-ind	ARB~CMR~EPI	ARB/CMR/EPI-exp*	ne in ARB/CMR/EPI	total
APP-ind	36	1	0	14	0	1	23	37	14	**126**
APP~NAP	562	25	174	110	70	240	4250	3459	2647	**11537**
NAP-ind	4	2	3	0	1	3	39	86	70	**208**
APP/NAP-exp°	81	1	38	4	5	9	126	849	2204	**3317**
ne in APP/NAP	125	3	35	8	2	5	146	2288	34779	**37391**
total	**808**	**32**	**250**	**136**	**78**	**258**	**4584**	**6719**	**39714**	**52579**

C Overlap to genes induced by colonization with *Glomus intraradices*, *Glomus mossae*, or both on the level of whole roots, without fungal genes

	ARB-ind	CMR-ind	EPI-ind	ARB+CMR-ind	CMR+EPI-ind	ARB+EPI-ind	ARB~CMR~EPI	ARB/CMR/EPI-exp*	ne in ARB/CMR/EPI	total
APP-ind	35/1	1/0	0	11/3	0	0/1	7/16	17/20	5/9	**76/50**
APP~NAP	40/522	1/24	3/171	11/99	4/66	3/237	27/4223	67/3392	41/2606	**197/11340**
NAP-ind	2/2	0/2	0/3	0	0/1	0/3	0/39	1/85	1/69	**4/204**
APP/NAP-exp°	44/37	0/1	0/38	3/1	0/5	3/6	2/124	42/807	63/2141	**157/3160**
ne in APP/NAP	95/30	0/3	3/32	4/4	0/2	1/4	3/143	120/2168	528/34251	**754/36637**
total	**216/592**	**2/30**	**6/244**	**29/107**	**4/74**	**7/251**	**39/4545**	**247/6472**	**638/39076**	**1188/51391**

*genes were expressed in one or two of the three cell-types, but with no significant induction in comparison to the others
°genes were expressed in one of the two cell-types, but with no significant induction in comparison to the other

With regard to functional categories (Figure II_5), genes related to secondary metabolism were most prominent among those 152 genes induced by Myc-LCOs and equally expressed in APP and NAP, which may reflect the production of internal and external signal components during this stage. Only one of these genes, *MtDxs2*, has been analyzed in detail so far. It codes for a 1-deoxy-D-xylulose-5-phosphate synthase involved in the synthesis of isoprenoid-precursors via the methylerythritol phosphate (MEP) pathway (Walter *et al*. 2002). The gene was shown to be specifically expressed in arbusculated cells and involved in maintenance of arbuscule function (Floss *et al*. 2008b), which is in line with the ARB-specific expression pattern we identified in cell-types from mature mycorrhizal roots (Figure II_3). Nevertheless, the fact that a knock-down of *MtDxs2* also leads to strongly reduced expression of many other AM-related genes already hinted that the protein might be a general regulator of AM-specific gene expression (Floss *et al*. 2008b), which would demand for an early induction and continuing expression during later stages.

Besides *MtDxs2*, another 57 of the 152 genes showed a characteristic expression pattern in cell-types from mature mycorrhizal roots (Supplemental Table S_II_6). Taken together, eleven genes were found to be preferentially expressed in ARB during later mycorrhizal stages, while expression of six

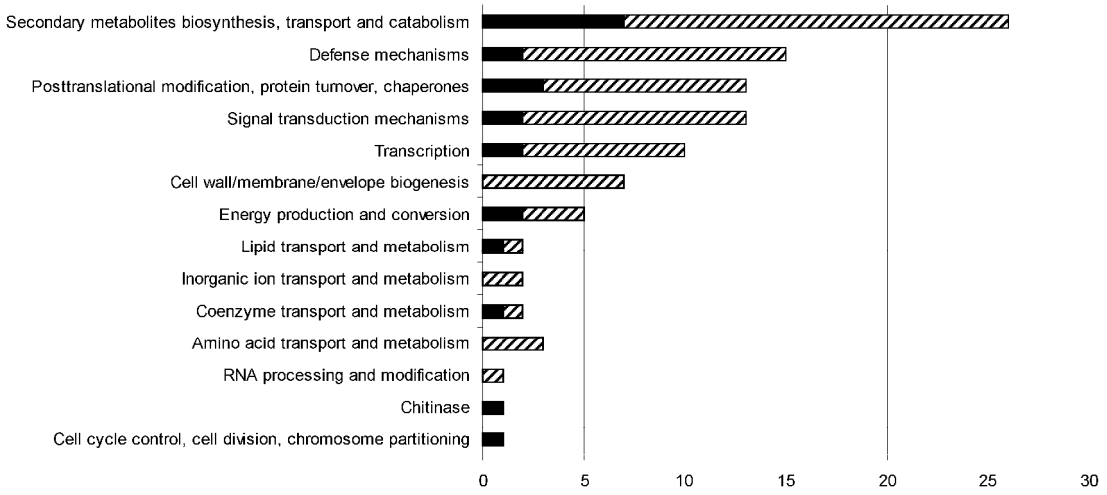

Figure II_5: Functional classification of genes equally expressed in APP and NAP and induced by Myc-LCOs.

Genes displayed no significant expression differences between APP and NAP and were induced at least 1.5 fold ($p \leq 0,05$) in roots treated with sulphated Myc-LCOs or non-sulphated Myc-LCOs, or a combination of both (Czaja *et al*. 2012). Black bars refer to genes which were also significantly induced (at least 2-fold induced with a FDR-corrected p-value ≤ 0,05 by colonization with *Glomus intraradices*, *Glomus mossae*, or both, but not induced by enhanced phosphate supply) on the level of whole roots (Hogekamp *et al*. 2011), striped bars to genes which were not induced under those conditions. The genes were grouped into functional classes according to their KOG classification or their annotation in case no automated classification was available. Note: The 51 genes grouped into the class "Unknown function" are not included in this diagram.

genes was retained to epidermal or cortical cells (Figure II_11). The majority of genes was either induced in ARB+CMR alike (5 genes) or equally expressed in ARB, CMR and EPI (36 genes), indicating that most of them code for proteins needed for fungal colonization in general rather than arbuscule formation.

The remaining 94 genes were expressed only transiently, especially those genes related to defense mechanisms and surprisingly also those genes related to cell wall and membrane biogenesis (Supplemental Table S_II_6, Figure II_5). We identified seven genes coding for enzymes which target different components of the plant cell wall like pectin, xyloglucan polymers and cellulose. Such proteins are often discussed to promote fungal colonization by rearrangements of the plant cell wall. Obviously, some of these processes are executed and completed already during the first contact of the two symbiotic partners.

Diffusible fungal factors are able to induce calcium spiking in roots of *Medicago truncatula* (Navazio *et al*. 2007) via the well-known signal transduction pathway common to AM and root nodule symbiosis. The only gene known so far, being able to decode the calcium spiking is *MtDmi3*, coding for a calcium-dependent protein kinase (Lévy *et al*. 2004). Interestingly, we found five genes coding for calcium-binding proteins among a group of 13 signalling-related genes, which might be involved in the interpretation of calcium signals. While one remained expressed in all cell-types investigated during later stages, three were only active during stage I. With regard to transcriptional regulators activated downstream of the calcium signalling, we identified 10 transcription factor (TF) genes (Supplemental Table S_II_7). Two of them encode CAAT-box binding transcription factors (Mtr.4282 = *MtCbf3*, Mtr.28326 = *MtCbf4*). This is of special interest, since the expression patterns identified here differ from those identified for two other CAAT-box binding transcription factors - *MtCbf1* and *MtCbf2* - which were recently shown to be activated during fungal infection (Hogekamp *et al*. 2011) and are consequently found in the group of APP-induced genes. *MtCbf3* was strongly induced by both sulphated and non-sulphated Myc-LCOs and in whole mycorrhizal roots, whereas *MtCbf4* was only slightly induced by non-sulphated Myc-LCOs and repressed in whole roots (Supplemental Table S_II_7). The activity pattern of *MtCbf3* during later mycorrhizal stages remains ambiguous. Whereas the gene was identified as equally expressed in ARB and CMR via RT-PCR (Hogekamp *et al*. 2011), the signal intensity was below the *MtPt4*-threshold for all cell-types from mature mycorrhizal roots on the GeneChip. This indicates that *MtCbf3* is predominantly

active in the pre-contact stage, whereas transcripts only accumulate at very low levels in CMR and ARB, being only detectable via more sensitive RT-PCR-analyses. *MtCbf4* is also active in the pre-contact stage, but does not seem to be involved during colonization of the root. Therefore, it can be speculated, that at least *MtCbf1*, *2* and *3* probably are activated in a temporal sequence and control different parts of the symbiotic program. It will be interesting to investigate whether all three gene products are essential for a successful colonization of *Medicago* roots by mycorrhizal fungi and if the three TFs act separately or as a complex.

Stage II: Initial physical contact

In the next step of root colonization, physical contact between the two symbiotic partners is established. Fungal hyphae form appressoria on the surface of the root epidermis, triggering the development of a so-called pre-penetration apparatus (PPA) inside plant cells, thought to guide the invading fungal hypha on its way through the epidermal and the first cortical cells (Genre *et al.* 2005). In our analysis, this stage is represented by genes either induced in APP (126) or in NAP (208), with those induced in APP representing genes which are activated during the initial infection (Figure II_11 Group B) and those induced in NAP representing genes which are repressed during this stage (Figure II_11 Group F).

Among the APP-induced genes, *MtVapyrin* together with 14 other genes was also induced in roots treated with Myc-LCOs. In contrast to those 152 genes equally expressed in APP and NAP which are activated by Myc-LCOs prior to physical contact, activation of these 15 genes seems to require a locally enhanced concentration of signal molecules, like it is created by the presence of appressoria. Besides they are probably activated in a defined area around the infection site, rather than systemically.

Most of the APP-induced genes also had a clear expression pattern in cell-types from mature mycorrhizal roots, with 36 induced in ARB, 23 equally expressed in all cell-types, 14 induced in ARB+CMR and one gene each induced in CMR and ARB+EPI (Table II_2 B, Supplemental Table S_II_3). Besides, many of these genes (76) were already known to be induced by fungal colonization from whole roots (Table II_2 C, Figure II_6, Supplemental Table S_II_3), including the marker genes *MtCbf1* and *MtCbf2* (Hogekamp *et al.* 2011), *MtHa1* (Krajinski *et al.* 2002), *MtBcp1* (Hohnjec *et al.* 2005) and *MtScp1* (Liu *et al.* 2003).

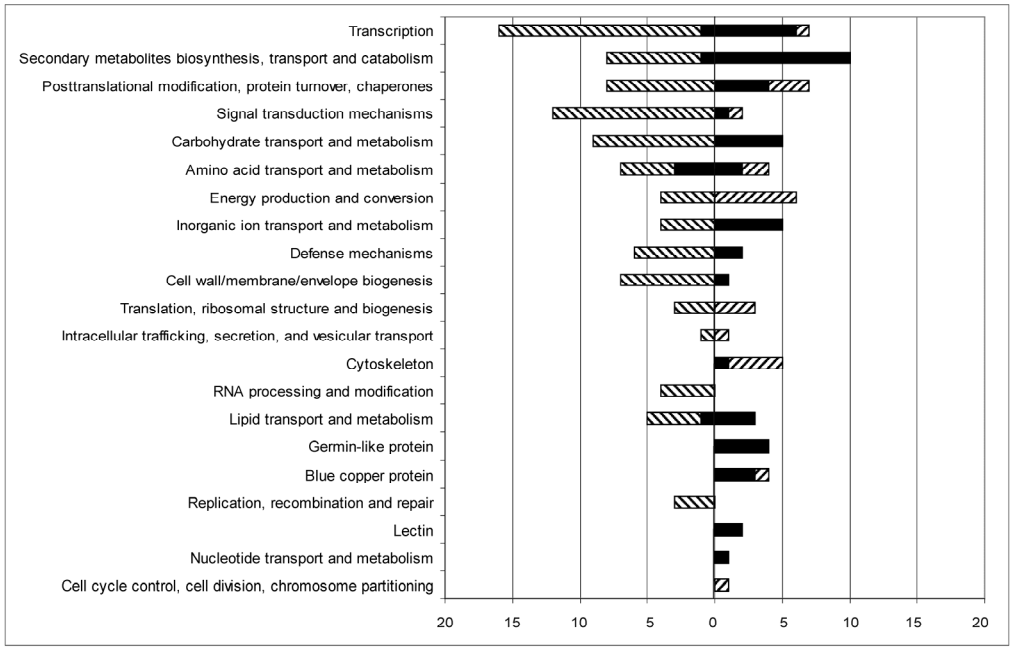

Figure II_6: Functional classification of genes induced in NAP *or* APP.
APP-induced genes are depicted on the right side, NAP-induced (or APP-repressed) genes on the left. Black bars refer to genes which showed the same expression tendencies on the level of whole roots (Hogekamp *et al*. 2011), being at least 2-fold induced with a FDR-corrected p-value ≤ 0,05 by colonization with *Glomus intraradices*, *Glomus mossae*, or both, but not induced by enhanced phosphate supply for APP-induced genes or being at least 2-fold repressed with a FDR-corrected p-value ≤ 0,05 under those conditions for NAP-induced genes. Striped bars refer to genes which did not show the same expression tendencies on the level of whole roots. The genes were grouped into functional classes according to their KOG classification or their annotation in case no automated classification was available. Members of AM-related gene families of unknown function (Annexins, Blue copper proteins, Germin-like proteins, Lectins) were grouped separately. Note: The genes grouped into the class "Unknown function" (111 NAP-induced and 53 APP-induced) are not included in this diagram.

As could be expected, the 208 NAP-induced genes displayed nearly no overlap to genes induced by fungal colonization (4 genes, Table II_2 C, Supplemental Table S_II_3) or Myc-LCO treatment (8 genes, data not shown) on the level of whole roots. This is in line with the fact, that most of the NAP-induced genes were either not expressed at all in cell-types from mature mycorrhizal roots (70 genes, Table II_2 B, Supplemental Table S_II_3) or detected as weakly expressed in one or two of the cell-types (86 genes, Table II_2 B, Supplemental Table S_II_3). Only 39 genes were equally expressed in all cell-types from mature mycorrhizal roots, while the overlap to other categories was neglectable (Table II_2 B), indicating that in most cases, transcript levels stay low during later stages of the interaction. Interestingly, many of the NAP-induced genes also displayed a slight repression on the level of whole mycorrhizal roots (Supplemental Table S_II_3), although only 17 genes were significantly repressed (at least 2-fold repressed with a FDR-corrected p-value ≤ 0,05 by colonization with *Glomus intraradices*, *Glomus mossae*, or both, but not by enhanced phosphate supply).

Together, this shows that many of the processes relevant during later stages of the symbiosis are already initiated by the first direct contact with the fungus. Whereas specific activation of the respective genes was in many cases already known from whole mycorrhizal roots, but not associated with early infection events, the down-regulation of genes obviously was too weak to be detected on the level of whole roots. In combination with the distribution of functional classes (Figure II_6), our results revealed two sets of genes either induced or repressed during this stage, consisting of genes coding for regulatory proteins as well as possible target genes. With regard to regulators, we identified 17 transcription factors (Supplemental Table S_II_7) and several protein kinases, as well as proteins involved in calcium-signalling. Possible targets are diverse, with genes related to synthesis of secondary metabolites represented most strongly, besides genes related to protein modification and turnover or primary metabolism. Among the genes related to secondary metabolism we identified a Gibberellin 2-beta-dioxygenase, which is in line with recent results of Ortu *et al.* (2012), who found genes involved in the synthesis of this plant hormone to be upregulated during appressorial stages.

Stage III: Intraradical growth of fungal hyphae

Beyond the initial infection site, where fungal hyphae have crossed the epidermis and often form thick coils in the underlying cortical cells, the typical appearance of fungal hyphae in the cortex changes and is now dominated by thin fungal hyphae growing in the apoplast, leading to expansion of the infected area. It can be expected that genes exclusively needed during the spread of fungal hyphae in the cortex will be preferentially found in the group of CMR-induced genes. Nevertheless, this group was very small (32 genes, Table II_2 B, Supplemental Table S_II_5) and gene expression profiles in whole roots led us to the assumption, that these are in fact ARB-repressed genes, which are therefore discussed with respect to arbuscule formation in the following section. Only three genes in this category seem to be specifically activated during AM, including the gene induced by Myc-LCOs (Figure II_11, Group A) and the gene induced in APP (Figure II_11 Group B), which together with the third gene was also found to be induced on the level of whole roots (Supplemental Table S_II_5) and might therefore be of special importance for apoplastic growth of fungal hyphae in the cortex. Based on our RT-PCR based results, we already speculated that genes exclusively related to spread of fungal hyphae are rare (Hogekamp *et al.* 2011), which is now validated by the genome-wide approach. Apparently, genes expressed during stage III and IV of the symbiotic interaction can only be separated into genes relevant for fungal colonization in general, which are

also active in arbusculated cells and additional genes exclusively needed during arbuscule-formation and thus preferentially expressed in ARB.

The former will be expressed at equal levels in the root cortex in arbusculated and the surrounding cortical cells and thus found in the category of ARB+CMR-induced genes or will be expressed at equal levels throughout all cell-types colonized by the fungus and thus found in the category of genes with an equal expression strength in ARB, CMR and EPI. Since both categories also contain - or even mainly consist of - genes with a constitutive expression in roots, which is not influenced by fungal colonization, a clear correlation of gene activity to the presence of fungal hyphae in the root only exists for those genes, which have also been identified as induced by fungal colonization on the level of whole roots (Table II_2 C). Some of these genes have already been discussed, since they are initially activated during stage I or II (compare Figure II_11, Group A and B), but a remaining 27 genes equally expressed in ARB, CMR and EPI, as well as 18 genes induced in ARB+CMR alike were neither induced by Myc-LCOs, nor in appressorial areas. In both categories, the majority of these genes were equally expressed in APP and NAP, indicating that these genes are also expressed in the root under non-symbiotic conditions and their activity is just enhanced during propagation of the infected area in the root.

Stage IV: Arbsucule formation

The formation of arbuscules represents the last and most intimate step of the AM symbiosis. Fungal hyphae penetrate cells of the inner cortex and proliferate to highly branched structures, providing an extremely enhanced surface. They remain surrounded by a membrane of plant origin, called the peri-arbuscular membrane (PAM), hosting specific transporters like the phosphate transporter *MtPt4* (Pumplin *et al*. 2009) or the recently identified ABC-transporters *MtStr* and *MtStr2* (Zhang *et al*. 2010). Since arbuscules are the functional units enabling the bidirectional transfer of nutrients between the symbiotic partners, many of the transcriptional changes observed in mycorrhizal roots relate to the formation of those structures. This is also mirrored in our data, since the majority of genes with a cell-type specific induction were 808 ARB-induced genes (Table II_1 A).

Our identification of ARB-induced genes is validated by a comparison to expression data recently published by Gaude *et al*. (2012), who compared gene expression in arbusculated and non-colonized cortical cells from mycorrhizal roots of *Medicago truncatula* to gene expression in cortical cells from non-mycorrhized roots. A calculation of the relative induction ratios between arbusculated and

cortical cells from mycorrhizal roots revealed that 81 of the 100 genes we detected to be most strongly induced or even specifically expressed in arbusculated cells, were also found to be induced by Gaude *et al*. (2012) (Supplemental Table S_II_8). These included the marker genes *MtPt4*, *MtBcp1*, *MtGlp1*, *MtLec5*, *MtNip1*, *MtMyb1* and *MtGst1*, although expression ratios between arbusculated and cortical cells described by Gaude *et al*. (2012) were considerably smaller than those reported here (for example logFC ARBvsCMR 2,39 for *MtPt4* compared to 8,20 in our approach, equivalent to a ~60-fold difference in expression induction), which might reflect contaminations between the cell-types which occurred during the cryo-sectioning-method employed by Gaude *et al*. (2012).

Of the 808 genes classified as ARB-induced in our analysis, 125 genes were not present in APP or NAP (Table II_2 B). With 97 genes, the majority of these were ARB-specific and in addition, most of the genes were detected as induced by fungal colonization on the level of whole roots (Table II_2 C). This group can therefore be regarded as specifically activated during stage IV of the symbiotic interaction with a typically exclusive expression in arbusculated cells, although some genes with

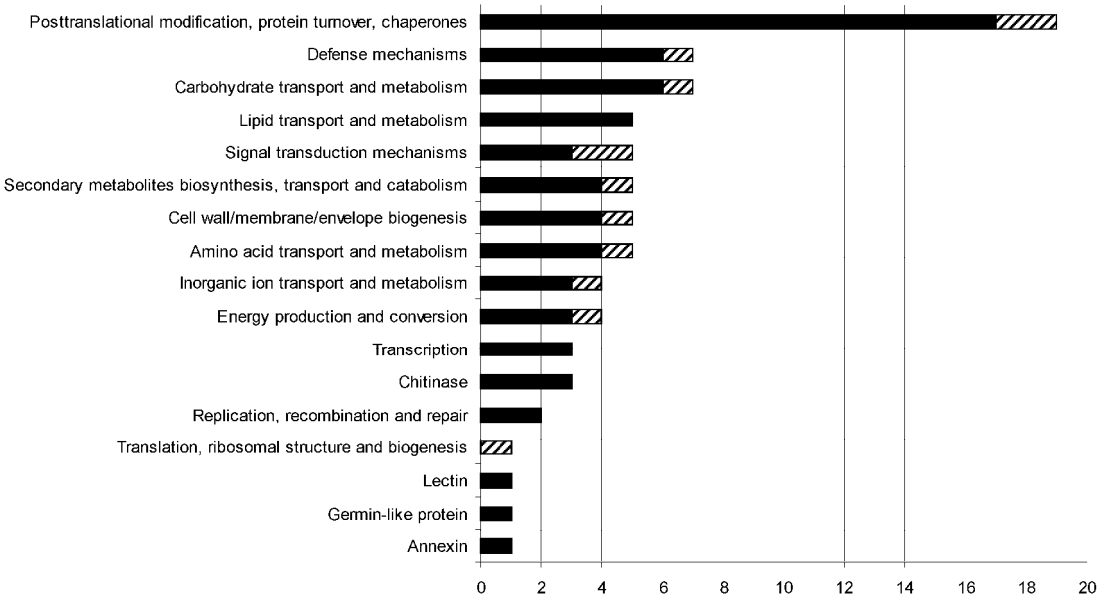

Figure II_7: Functional classification of genes induced in ARB and not expressed in APP and NAP.

Black bars refer to genes which were also significantly induced (at least 2-fold induced with a FDR-corrected p-value ≤ 0,05 by colonization with *Glomus intraradices*, *Glomus mossae*, or both, but not induced by enhanced phosphate supply) on the level of whole roots (Hogekamp *et al*. 2011). Striped bars refer to genes which were not induced under these conditions. The genes were grouped into functional classes according to their KOG classification or their annotation in case no automated classification was available. Members of AM-related gene families of unknown function (Annexins, Blue copper proteins, Germin-like proteins, Lectins) were grouped separately. Note: The 47 genes grouped into the class "Unknown function" are not included in this diagram.

additional expression in the surrounding cells were also found, e.g. the gene encoding the transcription factor *MtMyb1* (Liu *et al*. 2003). The functional classification of these 125 ARB-related genes revealed that they cover a broad spectrum of cellular processes (Figure II_7). As could be expected, genes involved in transport and metabolism are highly represented, including the phosphate transporter *MtPt4*. Besides, genes involved in arbuscule-specific signal transduction and transcriptional regulation were identified. Also, genes encoding proteins involved in cell wall rearrangement and members of gene families, known to be specifically induced in symbiotic tissues of *Medicago truncatula* were found in this group, e.g. the annexin gene *MtAnn2* (Manthey *et al*. 2004). The most prominent functional classes were posttranslational modification and protein turnover and defense mechanisms. We could already show that some defensin and chitinase genes are preferentially expressed in arbusculated cells (Hogekamp *et al*. 2011) and therefore seem to be related to arbuscule formation or control of arbuscule-lifespan, rather than representing typical defense responses in this context. Induction of genes related to posttranslational protein modification and protein turnover has often been reported for mycorrhizal roots (Liu *et al*. 2003, Hohnjec *et al*. 2005) and like the expression of defensin genes has been associated with the transient nature of single arbuscules. This demands for a tight control of fungal hyphae in these cells and break-down of fungal material, once the arbuscule loses its function. Such a function has for example been proposed for *MtTi1*, a gene encoding a trypsin inhibitor shown to be specifically expressed in arbusculated cells (Grunwald *et al*. 2004). Our data support this hypothesis for *MtTi1* and the 18 other genes from this functional class. Similarly, the 81 genes we found to be ARB-induced and only weakly expressed in APP or NAP (Table II_2B) are probably involved in processes related to arbuscule formation and function, although the results are less clear in these cases. Together with the 125 genes discussed above they form the large group of genes exclusively or predominantly active during stage IV of the symbiosis (Figure II_11, Group D). A third subset of genes included into Group D are those genes which displayed an induction in ARB as well as in EPI cells. This category is somehow the most artificial and hard to discuss. One possible explanation for the relatively large number of 258 genes in this category could have been the presence of appressoria in the EPI cells from mature mycorrhizal stages, leading to the induction of genes relevant for intracellular infection in both cell-types. In this case, those genes would have been APP-induced, too, but this is only the case for one of the genes. Besides, only seven genes in this category were already known to be induced by mycorrhizal fungi on the level of whole roots. A possible explanation would be that arbuscules as the

main interface between fungus and plant have functional similarities to epidermal cells which represent the interface with the environment under non-symbiotic conditions. Five of the genes from this category were also part of other groups (Figure II_11, Groups A, B and F), leaving a total number of 253 ARB+EPI-induced genes in Group D.

In addition to the specific upregulation of the genes discussed above, arbuscule formation will probably also require the cell-specific deactivation or downregulation of genes, which are otherwise expressed in the whole cortex. Such genes may be found in the category of CMR-induced genes, consisting of 32 genes with high transcript levels in CMR and significantly lower or non-detectable transcript levels in ARB and EPI (Tables II_1 A, II_2 B). Similarly, the 78 CMR+EPI-induced genes might represent ARB-repressed genes, which are otherwise expressed in the cortex and the epidermis. This is in line with the fact that nearly all genes from these two categories showed no significant expression differences between APP and NAP, indicating that they are also expressed under non-

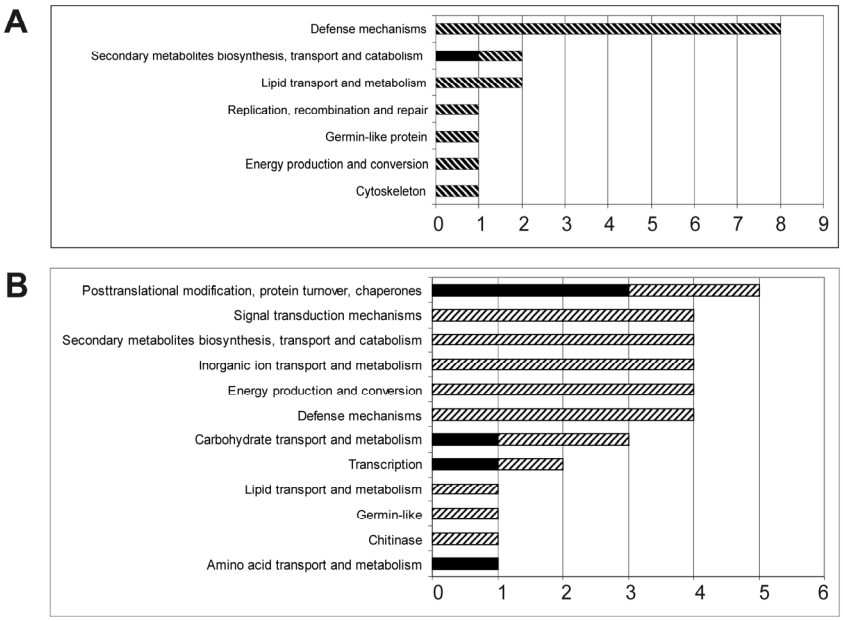

Figure II_8: Functional classification of genes induced in CMR (A) or CMR+EPI (B).
Black bars refer to genes which were also significantly induced (at least 2-fold induced with a FDR-corrected p-value ≤ 0,05 by colonization with *Glomus intraradices*, *Glomus mossae*, or both, but not induced by enhanced phosphate supply) on the level of whole roots (Hogekamp *et al*. 2011). Striped bars refer to genes which were not repressed under these conditions. The genes were grouped into functional classes according to their KOG classification or their annotation in case no automated classification was available. Members of AM-related gene families of unknown function (Annexins, Blue copper proteins, Germin-like proteins, Lectins) were grouped separately. Note: The genes grouped into the class "Unknown function" (16 CMR-induced and 44 CMR+EPI-induced) are not included in this diagram.

symbiotic conditions. Together they from the group of ARB-repressed genes (Figure II_11, Group G), except for those 4 genes which are part of other groups and were already discussed above.
Interestingly, beside genes of unknown function the most prominent functional class among the CMR-induced genes, which was also represented among those induced in CMR+EPI were genes related to defense mechanisms (Figure II_8). In contrast to the defensin genes induced in arbusculated cells that were discussed above, none of these genes were induced on the level of whole roots. Besides, many of the defensin genes induced in ARB code for gamma thionins which we proposed to play a role during the typical ramification of fungal hyphae in these cells (Hogekamp *et al*. 2011), whereas the ARB-repressed defense-related genes predominately encode peroxidases, representing a more general defense mechanism, which seems to be down-regulated when intracellular growth of fungal hyphae for arbuscule-formation is requested.
Interestingly, only two of the CMR-induced genes and eleven of the CMR+EPI-induced genes were downregulated by fungal colonization on the level of whole roots, although many showed a slight non-significant reduction as observed for the NAP-induced genes, indicating that the downregulation in arbusculated cells is a transient event that might be closely correlated to the life-span of arbuscules and can thus only be detected on a cellular level.

A considerable overlap of 36 genes between those induced in ARB and those induced in APP was identified (Table II_2 B; Figure II_11, Group B). A process relevant in both arbusculated cells and appressorial areas is the intracellular passage of fungal hyphae, whereas in the surrounding cortex the fungus mainly proceeds in the intercellular space. Genes activated in appressorial areas as well as arbusculated cells may therefore be of special importance to allow an intracellular accommodation of the fungus. This is validated by the fact that *MtVapyrin*, which is one of the AM marker genes found in this group, was shown to be relevant for the initial infection as well as for arbuscule formation (Pumplin *et al*. 2010). In addition, *MtVapyrin* is also essential for infection of root nodules by rhizobial bacteria, where an infection thread similar to the PPA is formed by the plant to guide symbiotic bacteria into the developing nodule (Murray *et al*. 2011). Further AM marker genes in this group were the H^+ATPase *MtHa1* and the blue copper protein *MtBcp1*. *MtHa1* was so far only reported to be expressed in arbusculated cells (Krajinsiki *et al*. 2002) and during nodulation (Manthey *et al*. 2004). *MtBcp1* encoding a protein of unknown function belongs to the gene families with strongly induced expression during AM. This were most strongly represented by three blue

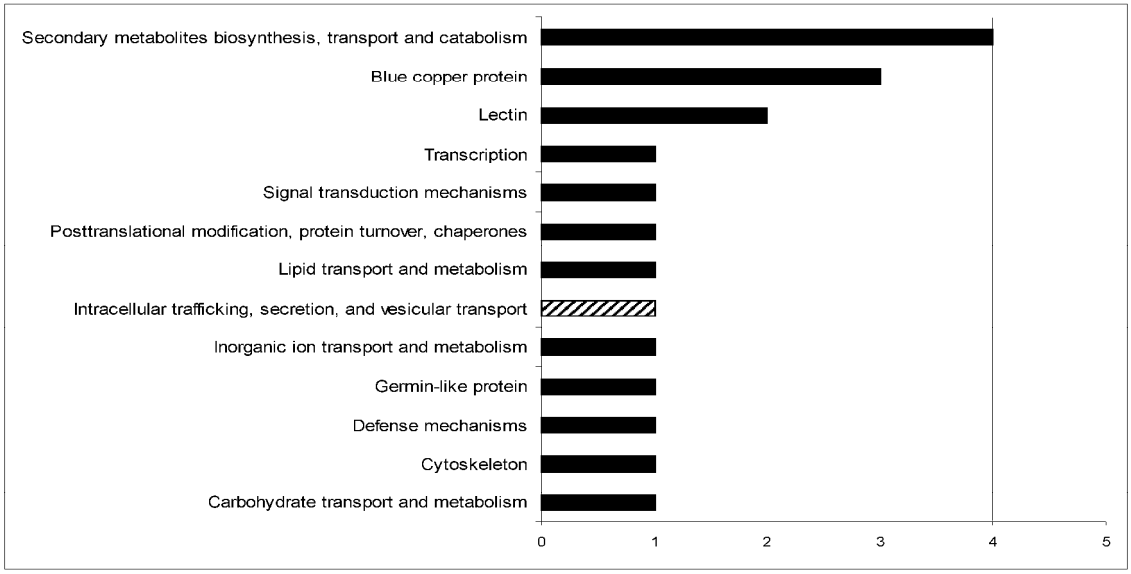

Figure II_9: Functional classification of genes induced in ARB and APP.
Black bars refer to genes which were also significantly induced (at least 2-fold induced with a FDR-corrected p-value ≤ 0,05 by colonization with *Glomus intraradices*, *Glomus mossae*, or both, but not induced by enhanced phosphate supply) on the level of whole roots (Hogekamp *et al*. 2011). Striped bars refer to genes which were not induced under these conditions. The genes were grouped into functional classes according to their KOG classification or their annotation in case no automated classification was available. Members of AM-related gene families of unknown function (Annexins, Blue copper proteins, Germin-like proteins, Lectins) were grouped separately. Note: The 17 genes grouped into the class "Unknown function" are not included in this diagram.

copper protein genes, two lectin genes and a gene encoding a germin-like protein (Figure II_9). This sheds a new light on the function of these proteins, which have so far only been related to arbuscule formation (Hohnjec *et al*. 2005, Frenzel *et al*. 2005, Doll *et al*. 2003) and not to early infection.

The majority of ARB-induced genes was equally expressed in APP and NAP (Table II_2 B), indicating that those genes are expressed in the outer cortex or even in epidermal cells already at the outset of the symbiotic interaction. Of these 562 genes, only 40 were induced by fungal colonization on the level of whole roots. This raises the question, whether the observed expression pattern in the remaining 522 genes is related to the presence of AM fungi in the root or influenced by other factors. If genes were specifically, but only weakly induced in the root by arbuscule formation, this will probably not be detected on the level of whole roots, where enhanced transcript levels in arbusculated cells are lost in the dilution with other cell-types. In this case, the induction in ARB should be rather weak and signal intensities of genes with an ARB-specific expression should be low on GeneChips hybridized with RNA from whole mycorrhizal roots. Nevertheless, most of the genes concerned display a strong induction in ARB and high signal intensities in the experiment using

whole roots. On the other hand, ARB-induced genes may simply be more active in inner cortical cells in comparison to the outer cortex, irrespective of fungal colonization. Because, although inner cortical cells were included in the CMR-samples if they didn't contain arbuscules, the ARB-samples were surely enriched for inner cortical cells. But even if this is the case for some genes, it does not seem feasible, that 562 genes are subjected to this expression regime. Also, this explanation is not in line with the observation, that 164 genes were identified as ARB-specific in mature mycorrhizal roots, but equally expressed in APP and NAP.

We therefore propose that the arbuscule formation induces a massive shift in gene expression patterns, leading to a preferential or even specific accumulation of transcripts in this new cell-type,

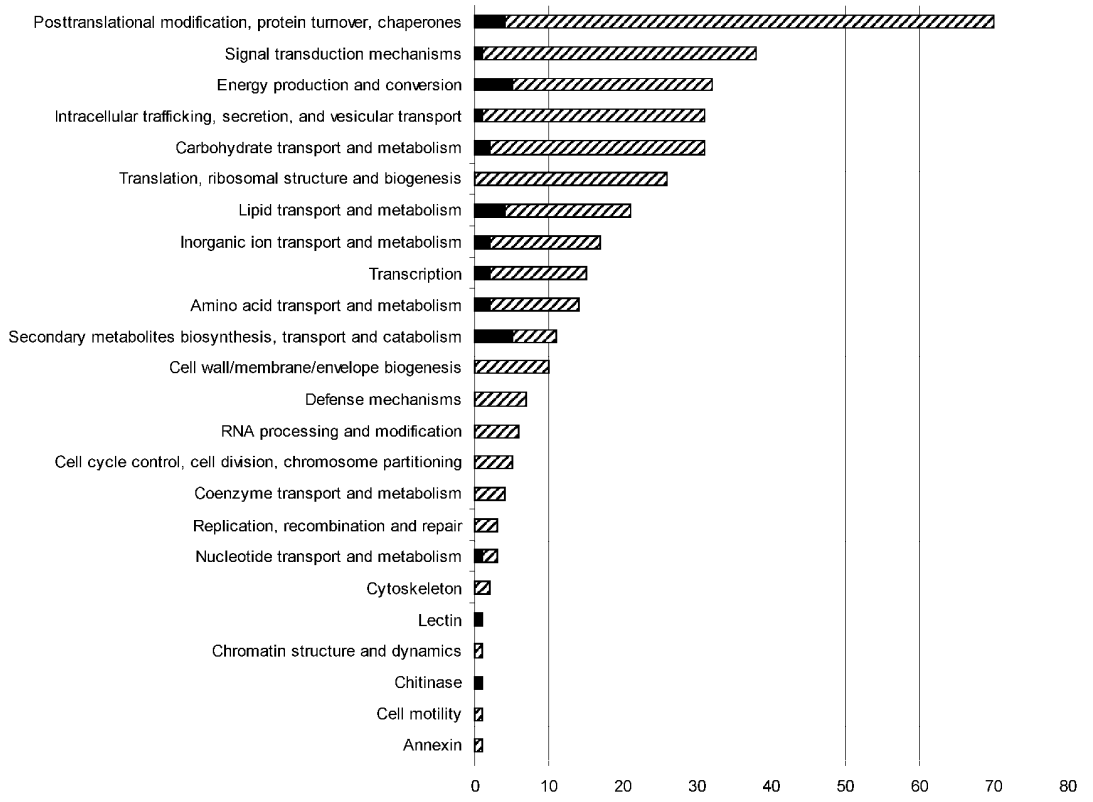

Figure II_10: Functional classification of genes induced in ARB and equally expressed in APP and NAP.

Black bars refer to genes which were also significantly induced (at least 2-fold induced with a FDR-corrected p-value ≤ 0,05 by colonization with *Glomus intraradices*, *Glomus mossae*, or both, but not induced by enhanced phosphate supply) on the level of whole roots (Hogekamp *et al*. 2011). Striped bars refer to genes which were not induced under these conditions. The genes were grouped into functional classes according to their KOG classification or their annotation in case no automated classification was available. Members of AM-related gene families of unknown function (Annexins, Blue copper proteins, Germin-like proteins, Lectins) were grouped separately. Note: The 211 genes grouped into the class "Unknown function" are not included in this diagram.

while gene activity on the whole root level remains the same (Figure II_11, Group E). An excellent example for this is the gene *MtSucS1*, encoding a sucrose synthase involved in providing hexoses for the symbiotic partner. The gene was shown to be expressed in arbusculated as well as the surrounding cortical cells, but with a strong induction in the former in promoter-GUS-studies (Hohnjec *et al*. 2003) and is essential for the establishment of an effective symbiosis, since a knock-down results in early arbuscule senescence and impaired nutrient flow between plant and fungus (Baier *et al*. 2010). Nevertheless, an induction of this gene was not detected on the level of whole roots (Supplemental Table S_II_3), since in non-mycorrhizal roots the gene displays a strong expression in the vascular tissue and a weak but even expression throughout the root cortex (Hohnjec *et al*. 2003). Due to this, genes with similar expression patterns will not be detected on the level of whole roots, but are covered by our cellular approach.

Exocytosis recently moved into the focus of interest with respect to intracellular accommodation of fungal and bacterial symbionts (Genre *et al*. 2011, Ivanov *et al*. 2012). It could be shown that the secretive system of root cells is activated and concentrated in the areas of fungal penetration (Genre *et al*. 2011). Two *M. truncatula* genes encoding v-SNARE proteins involved in the recognition and specific fusion of vesicles with target membranes were shown to be essential for arbuscule formation

---

Figure II_11: Overview of gene expression patterns for 1645 *Medicago truncatula* genes found to be influenced by colonization with the mycorrhizal fungus *Glomus intraradices* during four distinct stages of AM development.

Genes activated during one of the four developmental AM stages (Group A-E) are shown in pink, repressed genes (Group F and G) are shown in green. **Group A**: 152 genes displaying an equal expression in APP and NAP samples and found to be activated via Myc-LCOs (Czaja *et al*. 2012), thus probably activated before physical contact in stage I. Transcripts of 58 genes in this group were also detected in cell-types from mature mycorrhizal roots. **Group B**: 126 genes found to be induced in APP samples in comparison to NAP samples, thus activated during initial intracellular infection (stage II). 75 of these genes were still active during later stages of AM development. **Group C**: 45 genes with an equal expression in all three cell-types from mature mycorrhizal roots (ARB~CMR~EPI) or induced in ARB+CMR alike and also found to be induced on the level of whole mycorrhizal roots. These genes were not induced by Myc-LCOs or during appressorium formation, are therefore probably activated during intraradical spread of fungal hyphae (stage III) and needed for colonization of the root in general. **Group D**: Genes preferentially expressed in ARB. Transcripts of 125 genes were not found in APP or NAP samples, 81 genes were only weakly expressed in APP or NAP, indicating a specific activation during arbuscule formation (stage IV). 253 genes were induced in ARB+EPI. **Group E**: 552 genes which displayed an induction in ARB, but were not identified to be induced during mycorrhizal interactions on the level of whole roots, which indicates a shift of expression to arbusculated cells during the course of fungal colonization. **Group F**: 208 genes induced in NAP in comparison to APP, thus repressed upon fungal infection. **Group G**: 103 genes induced in CMR, or CMR+EPI, thus potentially repressed during arbusculae formation.

Abbreviations: LCOs: lipo-chitooligosaccharides, APP: appressorial areas, NAP: non-appressorial areas, ARB: cortical cells containing arbuscules, CMR: cortical cells from mycorrhizal roots, EPI: epidermal cells from mycorrhized roots.

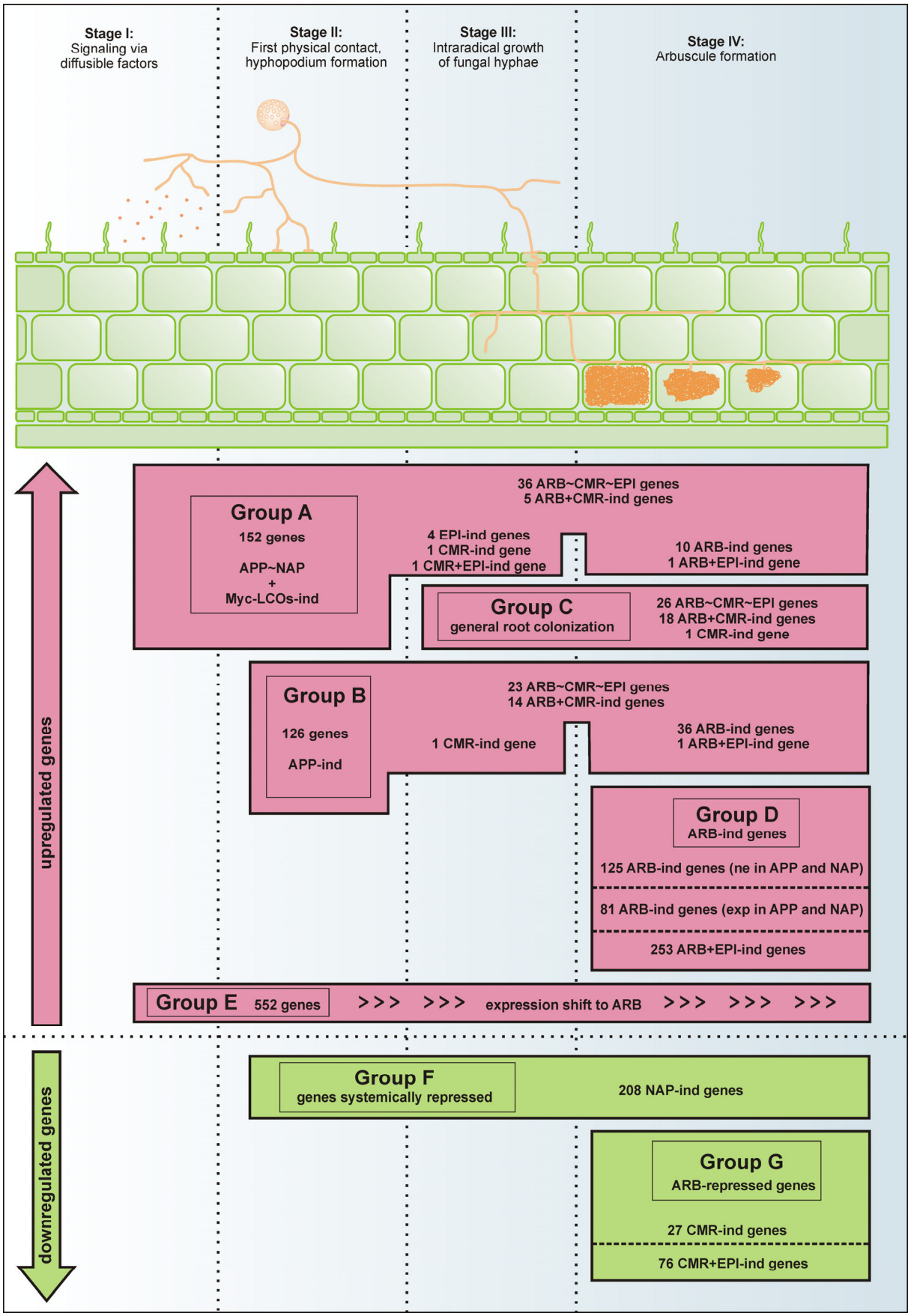
Stage I:
Signaling via
diffusible factors
Stage II:
First physical contact,
hyphopodium formation
Stage III:
Intraradical growth
of fungal hyphae
Stage IV:
Arbuscule formation
upregulated genes
Group A
152 genes
APP~NAP
+
Myc-LCOs-ind
36 ARB~CMR~EPI genes
5 ARB+CMR-ind genes
4 EPI-ind genes
1 CMR-ind gene
1 CMR+EPI-ind gene
10 ARB-ind genes
1 ARB+EPI-ind gene
Group C
general root colonization
26 ARB~CMR~EPI genes
18 ARB+CMR-ind genes
1 CMR-ind gene
Group B
126 genes
APP-ind
23 ARB~CMR~EPI genes
14 ARB+CMR-ind genes
1 CMR-ind gene
36 ARB-ind genes
1 ARB+EPI-ind gene
Group D
ARB-ind genes
125 ARB-ind genes (ne in APP and NAP)
81 ARB-ind genes (exp in APP and NAP)
253 ARB+EPI-ind genes
Group E 552 genes
>>> >>> expression shift to ARB >>> >>> >>>
downregulated genes
Group F
genes systemically repressed
208 NAP-ind genes
Group G
ARB-repressed genes
27 CMR-ind genes
76 CMR+EPI-ind genes

(Ivanov *et al*. 2012), indicating that exocytotic processes are involved in PAM formation. This is in line with a strong representation of genes related to intracellular trafficking, secretion and vesicular transport among this last group of ARB-induced genes. We identified 31 genes belonging to this functional class (Figure II_10), with only one of them induced on the level of whole roots. These genes represent interesting new candidates for further elucidation of the processes related to arbuscule formation.

CONCLUSION

With the dataset presented here, we intended to fill the gap existing between the identification of genes activated during mycorrhizal interactions in plant roots and the time-consuming analysis of expression patterns for single genes. Via a genome-wide analysis of gene expression in different cell-types representing distint stages of AM symbiosis development, we were able to provide a substantial spatial and temporal resolution that allowed the identification of subsets of genes governing the sequential reprogramming of host roots towards accomodation of microsymbionts. Our analysis provided not only information on the activity of genes already known from transcriptome studies based on pooled tissue, but moreover identified the differential expression of novel genes and revealed fine-tuned adjustments of transcript accumulation within the root tissue in response to fungal colonization. Together with other datasets on cell-specific gene expression in AM roots (Gaude *et al*. 2012, Gomez *et al*. 2009, Guether *et al*. 2009, Fiorilli *et al*. 2009), our dataset will provide a valuable tool to support and facilitate the search for genes involved in specific aspects of mycorrhizal symbioses.

Chapter III:

Application of RNA-interference for a functional analysis of four *Medicago truncatula* genes activated in arbuscular mycorrhizal roots

Abstract

RNA-interference (RNAi) in Agrobacterium-induced transgenic roots of *Medicago truncatula* offers an ideal tool for the functional analysis of plant genes activated during arbuscular mycorrhiza (AM) symbioses. We obtained RNAi-constructs from the *Medicago truncatula* RNAi-database of the University of Minnesota, directed against four genes of the model plant, encoding a GRAS-type (MtGRAS2) and a MYB-type transcription factor (MtMyb1), as well as an annexin (MtAnn2) and a blue copper protein (MtBcp1). A significant knock-down effect of transcript levels was achieved for *MtAnn2* and *MtMyb1*. Extensive phenotypical analyses of mature mycorrhizal structures and early infection events in RNAi roots revealed a role in arbuscule-formation for both genes, while an impaired fungal colonization was evident for *MtMyb1*-RNAi roots.

INTRODUCTION

The arbuscular mycorrhizal symbiosis represents one of the most important mutualistic interactions between different organisms, with nearly 80% of all land plants able to establish this relationship with fungi of the genus *Glomeromycota* (Schüssler *et al*. 2001). The existence of arbuscular mycorrhizae has a major impact on terrestric ecosystems, with an estimated 20% of carbon fixed by the host plants allocated to the fungal partner. In return, the fungus improves nutrient and water supply of the host plants via its extensive network of fungal hyphae, which also colonize the plant roots and enable intracellular nutrient exchange (Parniske 2008). In addition to nutritional benefits, colonized plants exhibit an improved resistance to abiotic and biotic stressors (Singh *et al*. 2011, van Wees *et al*. 2008). In the recent years, many efforts have been undertaken to understand the molecular mechanisms underlying this relationship. Whereas several hundred plant genes are known by now to be transcriptionally activated during fungal colonization of the host roots (Liu *et al*. 2003, Küster *et al*. 2004, Manthey *et al*. 2004, Hohnjec *et al*. 2005, Frenzel *et al*. 2005, Küster *et al*. 2007 a+b, Deguchi *et al*. 2007), with the latest transcriptome approaches already reaching cellular resolution (Guether *et al*. 2009, Gomez *et al*. 2009, Hogekamp *et al*. 2011, Gaude *et al*. 2012, Results – Chapter II), a detailed functional analysis has so far only been performed for a handful of them. Only few genes, whose knock-out completely abolishes the colonization of plant roots with symbiotic fungi have been identified by forward genetics. In the model legume *Medicago truncatula*, these are mainly the three *DMI* (doesn't make infection) genes with knock-out mutants unable to establish a symbiosis with both mycorrhizal fungi and nitrogen-fixing bacteria (Ané *et al*. 2002). Common to all three *DMI* gene products is their participation in the initial signaling cascade communicating the presence of microsymbionts to the plant and leading to their accommodation in the root; with *DMI1* encoding an ion channel in the nuclear membrane (Ané *et al*. 2004), *DMI2* encoding a receptor-kinase (Stracke *et al*. 2002) and *DMI3* encoding a calcium/calmodulin-dependent intracellular kinase (Lévy *et al*. 2004). An alternative way to specifically analyse the function of single genes, which have been identified in genome-wide transcriptional screens for mycorrhiza-induced genes beforehand, is the RNAi-mediated knock-down of the respective genes. In the model plant *Medicago truncatula*, this method can be combined with the induction of transgenic hairy roots via *Agrobacterium rhizogenes* infection, thus avoiding the time-consuming generation of completely transgenic plants (Boisson-Dernier *et al*. 2001, Limpens *et al*. 2004). The transgenic hairy roots are capable of normal symbiosis build-up (Mrosk *et al*. 2009) and offer an ideal tool for the

functional analyses of symbiosis-related genes. Several *Medicago truncatula* genes have been investigated using this method, revealing the participation of the encoded proteins in diverse processes related to mycorrhizal symbiosis. Specifically, the phosphate transporter MtPt4 (Javot *et al*. 2007) and the two ABC-transporters MtStr and MtStr2 (Zhang *et al*. 2010) were clearly related to arbuscule maintenance and function, since a knock-down of the respective genes resulted in impaired or abolished arbuscule growth, while root infection and colonization in general were not affected. Similar results were obtained for MtDxs2, a 1-deoxy-D-xylulose-5-phosphate synthase involved in the synthesis of isoprenoid-precursors (Floss *et al*. 2008b) and MtCCD1, a carotenoid cleavage deoxygenase (Floss *et al*. 2008a), with an enhanced percentage of decaying arbuscules in RNAi-roots, revealing the impact of secondary metabolite abundance on arbuscule formation. Interestingly, with *MtMSBP1* (Kuhn *et al*. 2010) and *MtVapyrin* (Pumplin *et al*. 2010) two genes were identified that are obviously required during initial infection and arbuscule formation, since RNAi-roots displayed hindered penetration of the epidermis by fungal appressoria, as well as blocked - or in case of *MtMSBP1* – impaired arbuscule formation, while intercellular growth of fungal hyphae was not affected.

Since 2008, agrobacteria carrying ready-to-use RNAi-constructs against *Medicago truncatula* genes can be obtained from the University of Minnesota (https://mtrnai.msi.umn.edu/), making the functional analysis of genes from this model plant more convenient. We selected four genes, including an annexin gene, a gene encoding a blue copper protein and two transcription factor genes encoding a MYB-type and a GRAS-type transcription factor based on their expression patterns with different time points of activation during mycorrhizal symbioses and the availability of RNAi-constructs. Whereas *MtGRAS2* is activated during the pre-contact-phase of an AM symbiosis, *MtBcp1* expression is correlated with intraradical growth of fungal hyphae and arbuscule formation. Similar, *MtMyb1* is expressed in arbusculated cells and the surrounding cortex, but its activation seems to be coupled to arbuscule formation. Finally, *MtAnn2* represents an arbuscule-specific gene. An RNAi-mediated knock-down could be achieved for *MtAnn2* and *MtMyb1*, and phenotypical analyses of mycorrhizal structures indicate a role in arbuscule-formation for both genes in addition to an impaired colonization in *MtMyb1*-RNAi roots.

MATERIAL & METHODS

Construction of RNAi-fusions

RNAi-fusions for the four *Medicago truncatula* genes *MtAnn2*, *MtBcp1*, *MtMyb1* and *MtGras2* used for the generation of transgenic roots were obtained from the RNAi database of the University of Minnesota (https://mtrnai.msi.umn.edu/). All RNAi-fusions were provided as ready-to-use constructs transformed in the *Agrobacterium rhizogenes* strain Arqua1 (Quandt *et al*. 1993), in the binary vector pHellsgate8 (pHG8). In pHG8, the inverted repeat of the gene-specific target sequence is separated by a spliceable intron thought to improve the formation of the hpRNA (hairpinRNA) in the target cells (Helliwell & Waterhouse, 2003). A list of all RNAi-constructs can be found in Supplemental Table S_III_1. A corresponding construct containing a target sequence against the human myosin gene, also obtained from the RNAi-database (pHG8::Myo-RNAi_c) and a construct containing an *E.coli* target sequence, were used for the transformation of control roots. All plasmids were sequenced using the primers p27-3 and p27-5 (Supplemental Tab. S_III_2A) to confirm that the correct target sequence was inserted. All constructs already contained a marker to select for expression in plant tissue, except for pHG8::1641. This marker consisted of the *dsRed*-gene under the control of an ubiquitin-promoter and a NOS terminator (Limpens *et al*. 2004). The *dsRed*-cassette of pHG8::Myo-RNAi_c was subcloned into pHG8::1641 using the flanking *Nhe*I restriction sites (Supplemental Figure S_III_2). The correct insertion into pHG8::1641-RNAi was verified via sequencing with the primers pHG8-ocs and pHG8-dsRed_ATG (Supplemental Tab. S_III_2A).

Plant growth, transformation and mycorrhization

All plants were grown in the climate chamber (humidity: 70%) at a 16-h light (23°C) and 8-h dark (18°C) regime and fertilized with half-strength Hoaglands solution (Arnon and Hoagland, 1940) containing 20 µM phosphate. *Medicago truncatula* Gaertn 'Jemalong' genotype A17 seeds were surface sterilized and scarified as reported by Hohnjec *et al*. (2003). After germination, seedlings were transformed with the *A. rhizogenes* strains using the protocol of Boisson-Dernier *et al*. (2001). To enhance transformation efficiency, the root of the seedling was sliced along the vascular tissue on a length of approximately 0,5 cm after removal of the root tip and before application of the agrobacteria. Seedlings were transferred to 120-mm-square slant agar plates (Doctor Lab, Jena, Germany) with 2,5% phytoagar (Duchefa Biochemie, Harlem, The Netherlands). To improve

humidity and adhesion of seedlings, they were covered with filter paper. After four weeks, when first transgenic roots had developed, plants were transferred into pots with seramis (Mars Plantcare GmbH, Mogendorf, Germany) and grown for two more weeks before screening of transgenic roots was performed using a fluorescence stereomicroscope (Leica, Wetzlar, Germany). Transgenic plants were mycorrhized with commercially available inoculum of *Glomus intraradices* (Biorize Sarl, Dijon, Frankreich) for five weeks before harvest. Each transgenic root was harvested separately and divided into two parts. The first part was used for RNA-isolation, the second part for phenotypic analyses. Care was taken to include older and younger parts of the root in both samples.

As an exception, seedlings used for the phenotyping of early infection units in *MtMyb*-RNAi roots were transformed via hypocotyl-wounding (Quandt *et al.* 1993) and directly potted into seramis fertilized with half-strength Hoagland`s solution containing 20 µM phosphate and an additional 2mM NH_4NO_3. They were screened and mycorrhized after 4 weeks using *Glomus intraradices* inoculum produced in leek cultures (*Allium porrum* cv. Elefant). Since no analysis of single roots could be done, due to the rare event of infection unit formation, the whole amount of transgenic roots from individual plants was taken as one sample.

RNA isolation and real-time RT-PCR-analysis

RNA was isolated from single root samples using the RNeasy Mini Plant Kit (Qiagen, Hilden, Germany) with on-column DNA digestion according to the manufacturer's instructions. RNA quantity and quality was assessed using a NanoDrop ND-1000 (Peqlab, Erlangen, Germany). 50 ng of total RNA was used for real-time RT-PCR, using the SensiMix™ SYBR One-Step kit (Bioline, Luckenwalde, Germany). The constitutive translation elongation factor gene *MtTefα* (TC178258 in the DFCI *Medicago* Gene Index) was used for normalization across different conditions. Primer pairs are listed in Supplemental Table S_III_2B. Expression differences were analyzed for significance using the Student's t-test incorporated in MS® Excel® 2007 (Microsoft® Corp., Seattle, USA).

Phenotypical analyses of RNAi-roots

For the morphological analysis of mature mycorrhizal stages RNAi-roots were stained with Alexa488-WGA-conjugate (WGA=wheat germ agglutinin). Roots were incubated for 10 min at 95°C in 10% KOH, rinsed 3 times with water and stained overnight with 20µg/ml Alexa488-WGA-

conjugate in PBS-buffer. For the analysis of the development of early infection units, *MtMyb*-RNAi roots were stained with ink according to the protocol of Vierheilig *et al*. (1998).

RESULTS

Sequence and expression properties of the gene products investigated by RNAi

In a first step, the annotation of the four genes *MtGRAS2*, *MtMyb1*, *MtBcp1* and *MtAnn2* was validated by a search for typical motifs in the deduced protein sequences. In addition, *in silico* expression profiles were obtained to derive information on gene activity in tissues of *Medicago truncatula* other than mycorrhizal roots.

GRAS transcription factors represent a family of plant specific transcriptional regulators with 36 members identified in *Medicago truncatula* so far (Libault *et al*. 2009). These TFs are characterized by several specific sequence motifs in their C-termini, whereas the sequence of the N-terminus is not conserved. Typically, a VHIID motif is flanked by two leucine-rich domains of around 100 amino acids (LHRI and LHRII), followed by the PFYRE and the SAW motif (Pysh *et al*. 1999). These motifs can also be found in the deduced amino acid sequence of the *MtGRAS2* gene (Figure III_1).

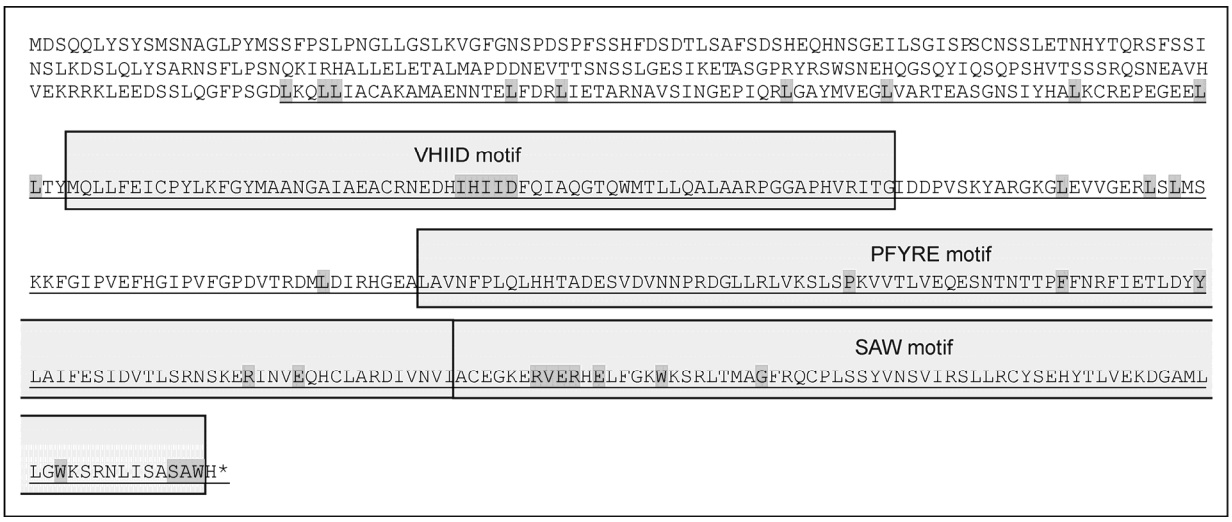

Figure III_1: Amino acid sequence of MtGRAS2.
The sequence contains a GRAS domain (predicted with Pfam, Punta *et al*. 2012). The conserved region (underlined) starts at position 209 and comprises the C-terminal region of the protein. The VHIID motif, the PFYRE motif and the SAW motif (light grey boxes) were identified according to the consensus sequence defined by Pysh *et al*. (1999). These are named after the typical conserved amino acids which are marked in dark grey here. The VHIID motif displays an aberrant sequence in MtGRAS2, with an isoleucin replacing the first valin, which is a conservative exchange occurring in several GRAS TFs (Pysh *et al*. 1999). The VHIID motif is flanked by two leucine-rich domains (LHRI and LHRII) of around 100 amino acids (leucines are marked in dark grey). Only two of the leucines in LHRII form one of the typical leucine heptads, which are found in some GRAS transcription factors. The LHRI motif of MtGRAS2 starts with the typical L(xx)LL motif. *: stop codon.

In silico expression profiles obtained from the *Medicago truncatula* GeneExpressionAtlas (Benedito *et al*. 2008) revealed that *MtGRAS2* is expressed in roots as well as all other plant tissues, including the shoot, leafs and reproductive organs (Supplemental Figure S_III_3).

In contrast to *MtGras2*, *MtMyb1* is exclusively expressed in mycorrhizal roots (Supplemental Figure S_III_4). MYB type transcription factors form a large family found in all eukaryotes, including 171 members in *Medicago truncatula* (Libault *et al*. 2009). They are characterized by the presence of one to four MYB domain repeats, located in the N-terminal region of the protein and consisting of three consecutive α-helices (Prouse and Campbell, 2011). In plants, most MYB transcription factors exhibit two of these repeats (Dubos *et al*. 2010), which is also the case for *MtMyb1* (Figure III_ 2).

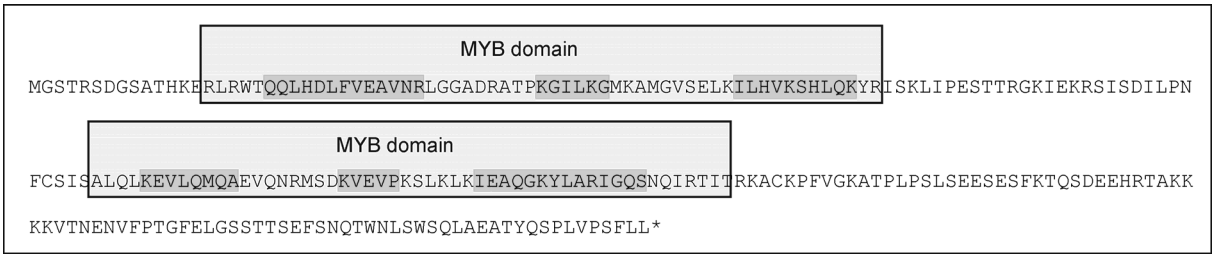

Figure III_2: Amino acid sequence of MtMyb1.
The sequence contains two N-terminal MYB domains (light grey boxes, predicted with Pfam, Punta *et al*. 2012), ranging from position 15 to 69 and from position 100 to 151, respectively. Both domains exhibit the typical repeat of three α-helices (marked in dark grey, predicted with NetSurfP, Petersen *et al*. 2009). *: stop codon.

Similar to *MtMyb1*, *MtBcp1* is also specifically activated in mycorrhizal roots (Supplemental Figure S_III_5). In general, blue copper proteins take part in redox processes where they transfer electrons from a donor to an acceptor via their active site containing a copper ion as a prosthetic group (de Rienzo *et al*. 2000). Figure III_3 shows the deduced amino acid sequence of the *MtBcp1* gene including the typical Cu binding site.

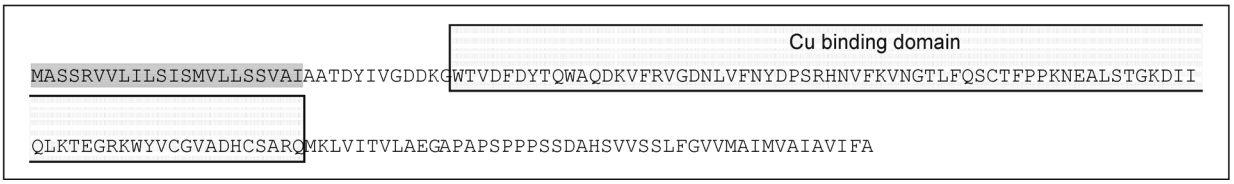

Figure III_3: Amino acid sequence of MtBcp1.
The sequence contains the characteristic Cu binding domain (light grey box, predicted with Pfam, Punta *et al*. 2012) and a signal peptide between position 1 and 22 (marked in dark grey, predicted with SignalP, Petersen *et al*. 2011), which probably directs the protein to the plasma membrane (Pumplin & Harrison 2009).

The expression of the annexin gene *MtAnn2* is restricted to seeds and roots, with strong activity in mycorrhizal roots as well as root nodules (Supplemental Figure S_III_6). Annexins are soluble cytosolic proteins which are capable of Ca^{2+}-dependent, reversible binding to membrane

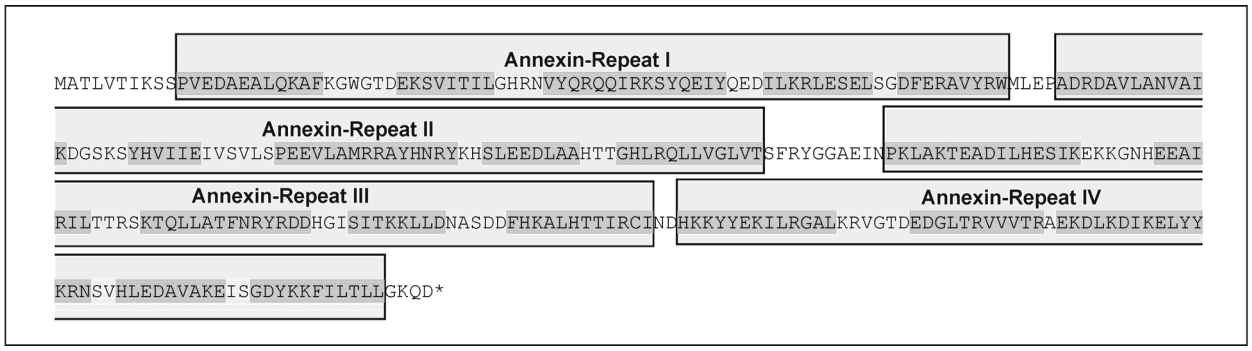

Figure III_4: Amino acid sequence of MtAnn2.
The sequence contains four typical annexin-repeats (light grey boxes, predicted with Pfam, Punta *et al*. 2012). Each repeat consists of approximately 70 amino acids, forming five short α-helices (marked in dark grey, predicted with NetSurfP, Petersen *et al*. 2009) which mediate Ca^{2+}-binding. *: stop codon.

phospholipids. The typical amino acid sequence contains up to four annexin repeats, consisting of five α-helices each (Figure III_4), which mediate Ca^{2+} and subsequent membrane-binding (Laohavisit & Davies 2011).

Assessing RNAi-knockdown-levels in transgenic hairy roots

RNAi constructs of *MtGRAS2, MtMyb1*, *MtAnn2* and *MtBcp1* as well as the control vectors obtained from the University of Minnesota were used for *Agrobacterium*-mediated induction of transgenic hairy roots on *Medicago truncatula* A17 seedlings. Different numbers of roots transformed with the respective constructs were obtained, depending on the efficiency of root transformation. Since all four candidate genes are strongly induced in *Medicago truncatula* roots during different stages of mycorrhization, analyses of expression levels and possible RNAi-effects were performed in mycorrhizal roots. Specifically, transgenic roots were harvested after five weeks of mycorrhization with *Glomus intraradices* and separated into two comparable samples, consisting of older and younger root parts. Whereas the first sample was used for RNA-isolation and RT-PCR measurements, the second part was used for phenotypical analyses. In total, 16 transgenic roots expressing one of the control constructs were obtained, in addition to 34 *MtAnn2*-RNAi roots, 17 *MtGRAS2*-RNAi roots and 21 *MtMyb1*-RNAi roots. For *MtBcp1*, two RNAi-constructs with slightly different target sequences were used for root transformation. Here, the target sequence of *MtBcp1*(a)-RNAi covered an additional 67 nucleotides upstream of the *MtBcp1*(b)_RNAi (Supplemental Figure S_III_1). In total, 31 transgenic roots were obtained for construct *MtBcp1*(a)-RNAi and 28 roots were obtained for construct *MtBcp1*(b)-RNAi.

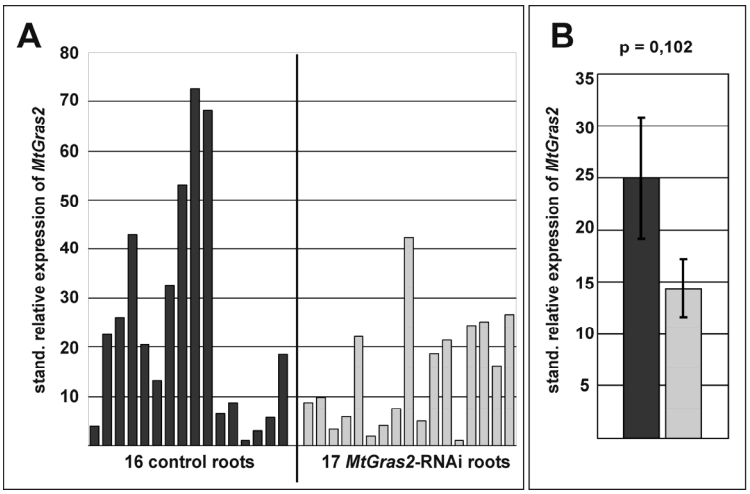

Figure III_5: Expression levels of *MtGRAS2* in *MtGRAS2*-RNAi roots.
Expression levels were quantified via real-time RT-PCR, normalized via the expression of *MtTefα* and standardized via the lowest value. **A**: Relative expression of *MtGRAS2* in 16 single control and 17 single RNAi roots. **B**: Mean relative expression of *MtGRAS2* in control roots in comparison to RNAi roots. Error bars represent standard errors. Abbreviations: p: p-value of Student's t-test; stand.: standardized.

In a first step, the knock-down level of the candidate genes in the RNAi roots was assessed via real-time RT-PCR. Care was taken to avoid a complete overlap of RNAi target sequences and RT-PCR amplificates (Supplemental Figure S_III_1) to rule out that expression of the transgene adulterated the results.

In general, expression levels of all four genes showed a high variation within the RNAi roots as well as the control roots (Figures III_5A – III_8A). This was probably caused by the poor quality of the available mycorrhiza inoculum, which resulted in a low overall rate of root mycorrhization with only 10 % –30 % root length colonization (RLC) in wt control roots (data not shown) and patchy

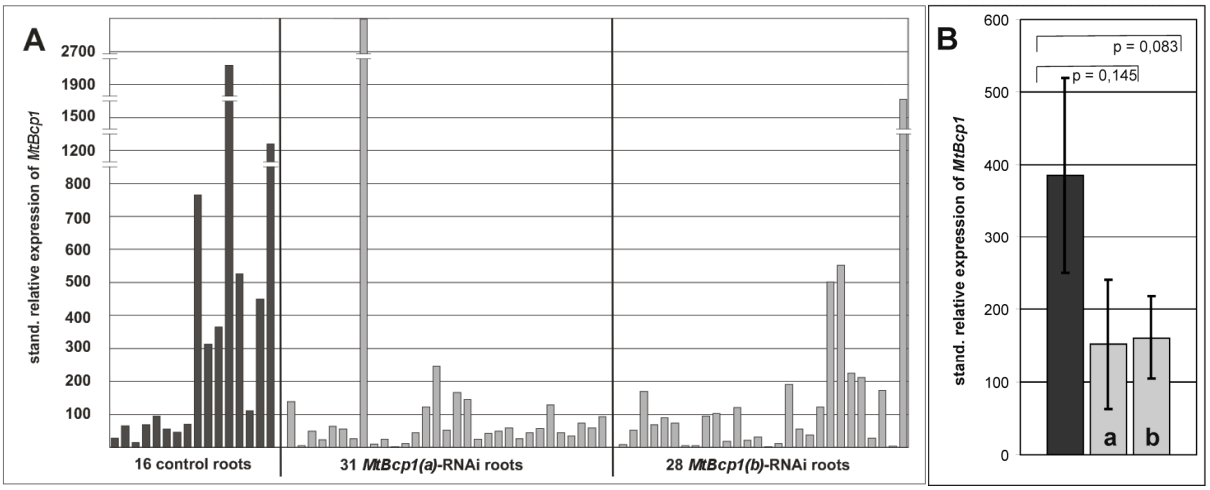

Figure III_6: Expression levels of *MtBcp1* in *MtBcp1*-RNAi roots.
RNAi roots were transformed with two different *MtBcp1*-RNAi-constructs (*MtBcp1*a and *MtBcp1*b). Expression levels were quantified via real-time RT-PCR, normalized via the expression of *MtTefα* and standardized via the lowest value. **A**: Relative expression levels of *MtBcp1* in 16 single control, 31 single *MtBcp1*(a)RNAi and 28 single *MtBcp1*(b)RNAi roots. **B**: Mean relative expression level of *MtBcp1* in control roots in comparison to RNAi roots transformed with construct a or b. Error bars represent standard errors. Abbreviations: p: p-value of Student's t-test; stand.: standardized.

distribution of mycorrhized areas in the samples. This was in particular obvious in the control samples, where single roots showed a very high or a very low expression of all four candidate genes, which was probably due to strong or weak mycorrhization of the respective samples. Nevertheless, this correlation was not very tight, since the genes investigated have different peaks of activity during mycorrhizal development. Based on the mean expression levels of the four candidate genes, transcription was reduced in the respective RNAi roots in comparison to the control roots in all cases (Figures III_5B – III_8B). This knock-down effect was comparatively weak and not significant in *MtGRAS2*-RNAi roots, where expression was reduced to 58% of the initial level (Figure III_5B). Also, both *MtBcp1*-RNAi constructs reduced the expression level of *MtBcp1* only weakly and not significantly to approximately 40% of the initial level (Figure III_6B). The *MtGRAS2*-RNAi roots and the *MtBcp1*-RNAi roots were therefore not analyzed further.

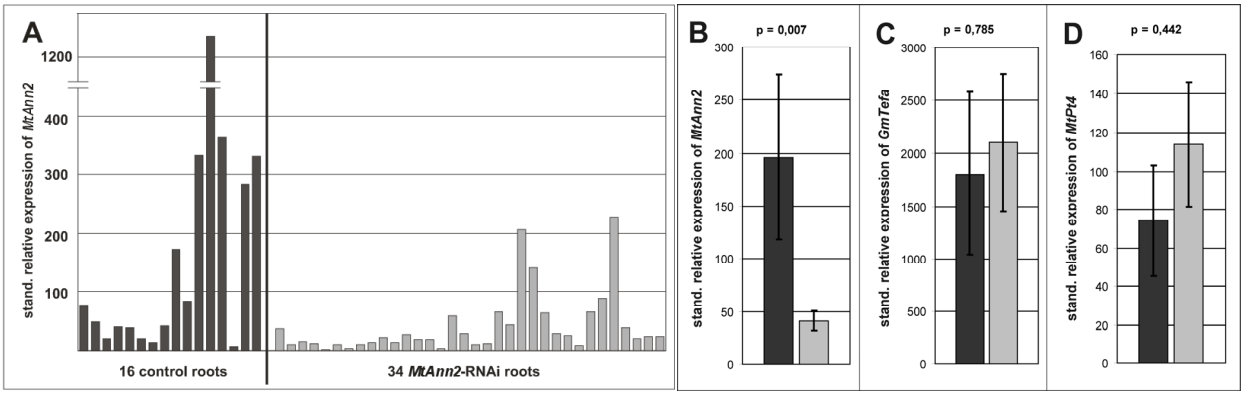

Figure III_7: Expression levels of *MtAnn2* and two mycorrhizal marker genes in *MtAnn2*-RNAi roots.
Expression levels were quantified via real-time RT-PCR, normalized via the expression of *MtTefα* and standardized via the lowest value. **A**: Relative expression levels of *MtAnn2* in 16 single control and 34 single RNAi roots. **B**: Mean relative expression level of *MtAnn2* in control roots in comparison to RNAi roots. **C**: Mean relative expression level of *GmTefα* in control roots in comparison to RNAi roots. **D**: Mean relative expression level of *MtPt4* in control roots in comparison to RNAi roots. Error bars represent standard errors. Abbreviations: p: p-value of Student's t-test; stand.: standardized.

In contrast to *MtGRAS2*- and *MtBcp1*-RNAi roots, significant knock-down effects were observed in *MtAnn2*- and *MtMyb1*-RNAi roots, where expression levels were reduced to 21% and 2 % of the transcription recorded in control roots (Figures III_7B, III_8B).

In a next step, expression of two mycorrhizal marker genes was measured in the *MtAnn2*-RNAi and the *MtMyb1*-RNAi roots. Whereas *GmTefα* is a fungal housekeeping gene which can be used to quantify the colonization of roots with mycorrhizal fungi, the expression of the plant phosphate

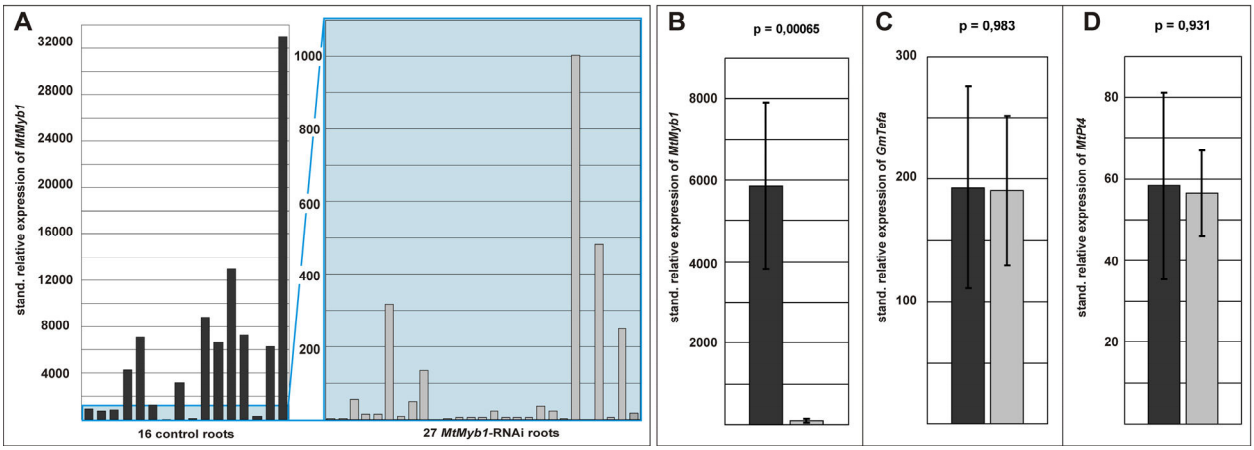

Figure III_8: Expression levels of *MtMyb1* and two mycorrhizal marker genes in *MtMyb1*-RNAi roots. Expression levels were quantified via real-time RT-PCR, normalized via the expression of *MtTefα* and standardized via the lowest value. **A**: Relative expression levels of *MtMyb1* in 16 single control and 27 single RNAi roots. Expression levels in RNAi roots were very low and are therefore displayed in a separate diagram. **B**: Mean relative expression level of *MtMyb1* in control roots in comparison to RNAi roots. **C**: Mean relative expression level of *GmTefα* in control roots in comparison to RNAi roots. **D**: Mean relative expression level of *MtPt4* in control roots in comparison to RNAi roots. Error bars represent standard errors. Abbreviations: p: p-value of Student's t-test; stand.: standardized.

transporter *MtPt4* is tightly correlated to arbuscule function and serves as a marker for the efficient nutrient transfer from the fungus to the plant (Harrison *et al.* 2002). Both marker genes showed no significant reduction of expression in the *MtAnn2-RNAi* roots (Figure III_7 C,D) and *MtMyb1-RNAi* roots (Figure III_8 C,D) in comparison to the control roots, respectively, indicating that despite the strong reduction of *MtAnn2* and *MtMyb1* expression levels, spread of fungal colonization as well as the function of the symbiosis was not markedly impaired in the RNAi roots.

Phenotypical analyses of mature AM structures in *MtAnn2*- and *MtMyb1*-RNAi roots

To gain additional information on the phenotype of mycorrhizal structures in *MtAnn2*-RNAi and *MtMyb1*-RNAi roots, the remaining half of the root was stained with Alexa488-WGA conjugate for all samples and some of the RNAi-samples. Since no differences were visible on first sight between control and RNAi-roots for both candidate genes, a detailed analysis considering overall root length colonization (RLC) as well as the developmental status of the colonized regions was performed. To this end, three developmental stages were defined, comprising areas where only extraradical hyphae were visible but the fungus had not penetrated the root, areas with intraradical hyphae but no arbuscule formation and finally areas with mature mycorrhiza displaying arbuscule and vesicle formation (Figure III_9 A). Here, *MtAnn2*-RNAi roots displayed a slight reduction in all measured parameters. Especially areas with extraradical hyphae and arbuscules were less abundant in RNAi

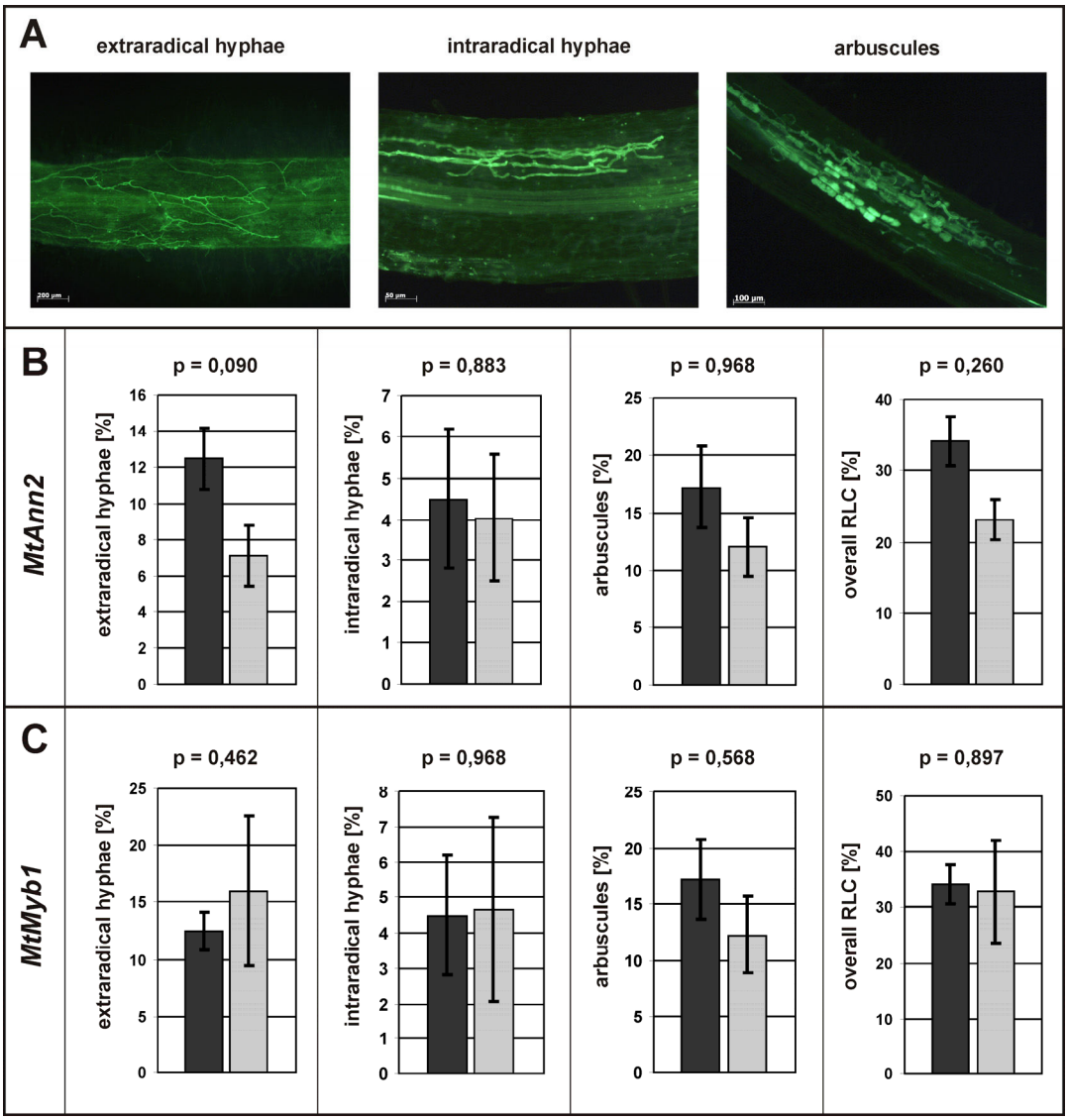

Figure III_9: Phenotype of mature mycorrhizal structures in *MtAnn2*-RNAi and *MtMyb1*-RNAi roots.

Roots were stained with Alexa488-WGA-conjugate and analyzed for the presence of fungal structures. **A**: Representative images of the three developmental stages that were distinguished during phenotyping of mycorrhizal roots: areas where only extraradical hyphae were present, areas with intraradical hyphae but no arbuscules, and areas with fully developed mycorrhiza including arbuscules and vesicles. The length of the respective areas was measured and results are shown as percentages of the overall root length. All colonized areas taken together give the overall root length colonization (RLC). **B**: Results for *MtAnn2*-RNAi roots based on 16 control roots (dark bars) and 21 *MtAnn2*-RNAi roots (light bars). **C**: Results for *MtMyb1*-RNAi roots based on 16 control roots (dark bars) and 3 *MtMyb1*-RNAi roots (light bars). Error bars represent standard errors. Abbreviations: p: p-value of Student's t-test.

roots than in control roots resulting in a reduced overall RLC from 34% in control roots to 23% in RNAi roots (Figure III_9 B). For *MtMyb1*-RNAi roots, the overall root length colonization was approximately the same for control and RNAi roots, but a slight shift in the distribution of developmental stages could be observed with a reduced share of areas which had progressed to

arbuscule formation and a slightly higher proportion of areas with only intraradical or extraradical hyphae (Figure III_9 C). Nevertheless, none of these effects was significant.

Phenotypical analyses of early infection events in *MtMyb1*-RNAi roots

To address the question, whether a reduced expression of *MtMyb* indeed leads to a delay in mycorrhizal development, we had a closer look at the phenotype of early infection units in *MtMyb1*-RNAi roots, since we supposed the effect to be more pronounced during initial phases of the symbiosis. To this end, transgenic roots were mycorrhized and analyzed already 7 dpi, when first infection units were present in the root system and arbuscule formation had started. Due to the fact that appressorium formation is a relatively rare event in the root system, it was not possible to perform the analysis with single transgenic roots like before. This time, all individual transgenic roots of one composite plant were pooled and treated as one sample. That way, 26 control root systems and 26 *MtMyb1*-RNAi root systems were analyzed. For each root system, the number of infection units was counted and separated into infection units which had already progressed to arbuscule formation and those which had not. Since the root systems differed in size and this correlates with the number of infection units, the fresh weight of each root system was determined and used for data normalization. No significant difference in fresh weight was detected between RNAi and control root systems (data not shown). In addition, the length of the infection units was measured, given by the spread of intraradical hyphae in the root cortex. Both the number of infection units with and without arbuscules as well as their length was slightly reduced in *MtMyb1*-RNAi roots (Figure III_10).

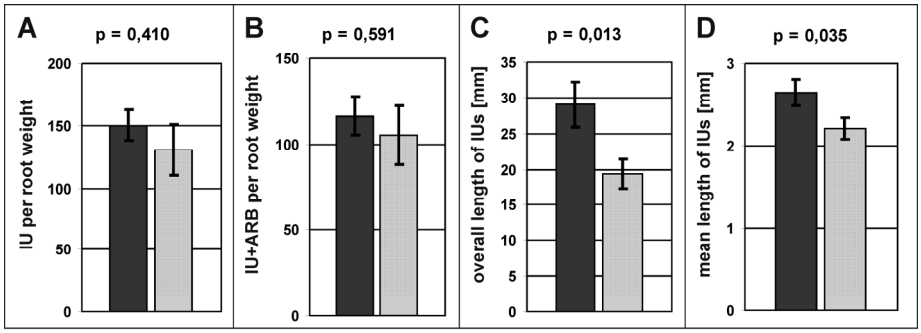

Figure III_10: Phenotype of early mycorrhizal infection units in *MtMyb1*-RNAi roots.
Number, length and developmental stage (presence of arbuscules) of infection units (IU) in 26 control root systems and 26 *MtMyb1*-RNAi root systems were analyzed. **A**: Number of infection units in control (dark bars) and RNAi root systems (light bars). To adjust for different sizes of the root systems, the number of infection units was correlated with the root fresh weight. **B**: Number of infection units containing arbuscules (+ARB) in control (dark bars) and RNAi root systems (light bars). To adjust for different sizes of the root systems, the number of infection units was correlated with the root fresh weight. **C**: Overall length of all infection units in control (dark bars) and RNAi root systems (light bars). **D**: Average length of single infection units in control (dark bars) and RNAi root systems (light bars). Error bars represent standard errors. Abbreviations: p: p-value of Student's t-test.

Whereas this effect was again not significant for the number of infection units (Figure III_10 A,B), a significant reduction of 35 % for the overall length of all infection units in a root system from 29 mm to 19 mm (Figure III_10 C) and of 17 % for the average length of single infection units from 2,65 mm to 2,21 mm (Figure III_10 D) was observed.

DISCUSSION

Four *Medicago truncatula* genes activated at different stages of mycorrhizal root colonization were selected for a functional analysis via RNAi, including the annexin gene *MtAnn2*, a gene encoding the blue copper protein *MtBcp1*, and the two transcription factor genes *MtMyb1* and *MtGRAS2*.

The *Medicago truncatula* GRAS transcription factor MtNsp1 was the first member of this gene family, for which direct DNA binding could be verified. MtNsp1 forms a complex with a second GRAS transcription factor called MtNsp2 and binds to promoter sequences of genes involved in early stages of the root nodule symbiosis, activating their transcription, with both DNA binding and protein-protein interaction depending on the LHR domains of the protein (Hirsch *et al*. 2009). The activation of MtNsp1 and MtNsp2 is triggered by the calcium-spiking induced upon perception of rhizobial Nod-factors (Hirsch *et al*. 2009). Whereas both *MtNsp1* and *MtNsp2* mutants are defective in the root nodule symbiosis (Smit *et al*. 2005, Kalo *et al*. 2005), only *MtNsp2* mutants are also partially impaired in the formation of the mycorrhizal symbiosis (Maillet *et al*. 2011). Since MtNsp2 is not capable of direct DNA binding (Hirsch *et al*. 2009), these data suggest that another GRAS transcription factor interacting with MtNsp1 during early mycorrhizal signaling might exist. MtGRAS2 seemed a possible candidate, since the respective gene showed an induced expression in roots inoculated for 6 hours with the supernatant from germinated spores of *Glomus intraradices* (N. Hohnjec, LUH, unpublished data) and thus probably reacts to diffusible signal molecules produced by the fungus at this developmental stage. Since expression of the gene was not influenced by Myc-LCO application (Czaja *et al*. 2012), it may represent the reaction to another yet unidentified signal molecule. The activation of the gene seems to be a transient event, since the gene was not among those induced in mature mycorrhizal roots or early infection stages (Hogekamp *et al*. 2011). This is validated by the *in silico* expression profile obtained from the *Medicago truncatula* GeneExpressionAtlas (Benedito *et al*. 2008) showing only slight differences in expression levels between mycorrhizal and non-mycorrhizal roots (Supplemental Figure S_III_3). Unfortunately, the knockdown effect achieved by the introduction of the RNAi-construct was too weak to allow an analysis of gene function in the AM symbiosis.

The same was true for the two RNAi-constructs directed against the gene *MtBcp1*. Often, blue copper proteins are not amenable for a functional analysis, since several isofunctional proteins exist, which can participate as electron shuttles in the same biological process (de Rienzo *et al*. 2000 and reverences therein). This might also be the case for the blue copper proteins involved in processes

related to the AM symbiosis. While it became apparent in the first comprehensive transcriptional analyses of AM roots that several blue copper protein genes are among those specifically upregulated during the symbiotic interaction in *Medicago truncatula* (Journet *et al*. 2002, Wulf *et al*. 2003, Küster *et al*. 2004, Hohnjec *et al*. 2005), much confusion was generated by the use of different identifiers and a detailed overview of those proteins was only recently published by Parádi *et al*. (2010). It turned out that three AM-related blue copper proteins had been identified so far, named MtBcp1, MtBcp2 and MtBcp3, and that four more exist (Parádi *et al*. 2010). The most extensively characterized protein is MtBcp1, where promoter-GUS-fusions revealed expression in arbusculated and surrounding cells (Hohnjec *et al*. 2005) and subcellular localization experiments showed that MtBcp1 is directed to the periarbuscular membrane surrounding the arbuscule-trunk (Pumplin & Harrison, 2009). Paradi *et al*. (2010) found that the respective gene locus actually consists of two highly similar isogenes, showing nearly identical patterns of activation in a mycorrhizal time course, although one isogene is considerably weaker expressed than the other (Parádi *et al*. 2010). Due to sequence inconsistencies between EST and genomic sequences, the target sequences of the two *MtBcp1*-RNAi constructs do not match 100% to either of the two orfs, which might contribute to the weak RNAi-effect we observed in our analysis.

In contrast to the first two genes, an RNAi-mediated knockdown of gene expression could be achieved for *MtAnn2*. Expression levels of the gene were significantly reduced to 21% of the gene expression in roots transformed with the control vector. Plant annexins have been shown to be involved in a brought range of cellular processes, ranging from redox reactions, ion homoeostasis and transport to the linkage of membranes, interactions with components of the cytoskeleton and exocytosis (Talukdar *et al*. 2009). The capability of Ca^{2+}-dependent membrane binding renders them important mediators between signaling processes and reorganization of cell architecture. Besides *MtAnn2*, a second annexin gene of *Medicago truncatula* has been investigated in detail so far. *MtAnn1* shares 75% sequence identity with *MtAnn2* (Talukdar *et al*. 2009) and seems to be involved in early infection events during root nodule symbiosis, since it is strongly induced in root cells upon perception of rhizobial Nod-factors and in the pre-infection zone of root nodules (de Carvalho-Niebel *et al*. 1998). Since MtAnn1 changes its localization from the cytoplasm to the nuclear periphery in root cells in response to the presence of symbiotic bacteria (de Carvalho-Niebel *et al*. 2002), a role in the induction of symbiotic calcium spiking has been proposed for this protein

(Talukdar *et al*. 2009). In contrast, *MtAnn2* is expressed in the vasculature of root nodules (Manthey *et al*. 2004) and in arbusculated cells during AM symbiosis (Manthey *et al*. 2004, Results – Chapter II). The *in silico* expression profile from the *Medicago* GeneExpression Atlas (Supplemental Figure S_III_5) shows an additional activity in seeds. At first sight, the arbuscule-specific expression seemed to make a connection of protein function to early calcium spiking unlikely. Still, recent investigations on calcium-signaling during root endosymbioses beyond the pre-infection stage provide new hints, since they revealed that calcium-spiking can also be observed during transcellular cortical infection with fungal hyphae or infection threads containing rhizobial bacteria (Sieberer *et al*. 2012). The detailed analysis also showed that two distinct calcium signals exist, with low spiking frequency in cells preparing for infection (indicated by pre-penetration-apparatus or pre-infection-thread formation) and high spiking frequency in cells which were actually invaded. Although inner cortical cells prone to arbuscule formation were not investigated, it seems feasible that the observed pattern of calcium signaling is also present in these cells. Evidence exists that MtAnn2 is localized in lipid drafts of the plasma membrane (Lefebvre *et al*. 2007) and in addition, a MtAnn2-GFP-fusion protein was found to be localized in the PAM of arbusculated cells (Wiese, 2009). In this regard, an activation of MtAnn2 via calcium spiking, leading to a specific localization in the PAM might be a link to endocytotic processes and rearrangements of the cytoskeleton allowing the development of the complex arbuscule surface.

The results obtained from the phenotypical analysis of *MtAnn2*-RNAi roots support the hypothesis that MtAnn2 might be needed for the extensive invagination of the plasma membrane in arbusculated cells, since they revealed a slightly reduced abundance of arbuscules in roots with reduced *MtAnn2* expression, although this effect was not significant. If MtAnn2 links calcium spiking to the actual colonization of inner cortical cells, a reduced protein level in these cells may prevent the formation of an arbuscule from the start. This is in line with the fact that no cells with arbuscules arrested at later stages of their development were found in the RNAi-roots. Nevertheless, this remains highly speculative, since the observed effect was very weak, probably because the reduction of the transcript level was not strong enough to generate a clear phenotype in all cells of the inner cortex. Alternative explanations include posttranslational regulatory mechanisms that balance the protein level irrespective of an reduced transcript level, or the existence of proteins with a redundant function that compensate for the knockdown of MtAnn2. A second gene encoding an annexin (*Mt*GeneChip identifier Mtr.16710.1.S1_at) was found to be induced in roots colonized

with *Glomus intraradices* or *Glomus mossae* (Results – Chapter II) and recently shown to be at least expressed at moderate levels in arbusculated cells (Hogekamp *et al*. 2012). Therefore this annexin gene likely fulfils a similar function as *MtAnn2*.

In contrast to annexins, blue copper proteins and GRAS transcription factors, the role of MYB type transcription factors during the development of root endosymbioses in legumes has not been investigated so far. Only one *Medicago truncatula* MYB gene designated *MtMyb1* was found to be induced during fungal colonization (Liu *et al*. 2003) and is preferentially expressed in arbusculated cells, although transcripts can also be found in the surrounding cortical cells (Results – Chapter II). Of the four RNAi-constructs, the one targeted against transcripts of *MtMyb1* displayed the strongest effect, with transcript levels reduced to 2% of that in control roots, representing nearly a complete knock-down. Also, this was the only RNAi-construct displaying a clearly impaired AM phenotype. First hints for a delayed development of symbiotic structures were observed in mature mycorrhizal roots, where a knock-down of the gene resulted in a slightly reduced number of arbuscules, although the overall root length colonization was not affected. When early infection processes were investigated, a significant reduction of infection unit length was observed, validating a delayed development of the symbiosis. While *MtMyb1* is most strongly expressed in arbusculated cells, a gene induction could not be observed during appressorium formation and the first colonization of the outer cortical cells (Results – Chapter II). Nevertheless, the phenotypical differences were most pronounced during the early infection events. In contrast to results on infection-related genes like *MtMSBP1* (Kuhn *et al*. 2009) or *MtVapyrin* (Pumplin *et al*. 2010), the phenotypical analyses of *MtMyb1* did not indicate that fungal penetration might be blocked or impeded in RNAi roots. Therefore, a possible explanation for the retarded spread of the microsymbiont in the cortex could be a negative feedback of disturbed arbuscule formation on fungal performance in the root. The transcription factor MtMyb1 might be involved in the activation of genes specifically needed during arbuscule formation. A knock-down of *MtMyb1* would result in a hindered activation of the respective genes which in turn leads to the observed reduction in arbuscule formation. Consequently, the propagation of the microsymbiont in the root is retarded, which might be due to a reduced nutrient uptake or to a flaw in synchronisation of the symbiotic development between the two partners. The fact that the observed effect was very weak, although the transcription level was strongly reduced, might be a hint that the participation of MtMyb1 is not essential and the

transcription factor merely acts as a modulator of gene transcription. Alternatively, the activity of the protein might be regulated posttranscriptionally, since protein studies were not performed here. Further investigations using plants with a complete knock-out of MtMyb1 and further functional analyses of the protein would be necessary to address these questions.

GENERAL DISCUSSION

The identification of large sets of genes activated in plant roots during interactions with AM fungi (Liu *et al*. 2003, Wulf *et al.* 2003, Frenzel *et al*. 2005, Hohnjec *et al*. 2005, Hohnjec *et al*. 2006, Küster *et al*. 2007b), the finding that Ca^{+}-signalling is involved in the perception and recognition of the microsymbiont via a common symbiotic pathway (Kistner *et al*. 2005, Kosuta *et al*. 2008, Oldroyd and Downie 2009), and the characterization of fungal Myc-factors (Maillet *et al*. 2011) were important hallmarks towards an understanding of the processes controlling mycorrhizal symbioses at the molecular level.

While it has been speculated for a long time that the different developmental stages of AM interactions are accompanied by the activation of distinct parts of the symbiotic program in the host, analyses of gene activity during defined stages were hampered by the asynchronous development of this mutualistic association. Two recently published investigations underlined the importance of a differentiation between different cell types and developmental steps when processes governing root endosymbioses are regarded. First, Rival *et al*. (2012) could show the specific activity of two genes important for symbiotic signalling in epidermal and cortical cells of *Medicago truncatula* during the establishment of the root nodule symbiosis. Similar results were obtained for *MtVapyrin*, which was shown to be significantly induced in isolated root hairs in comparison to the remaining root during infection of the root with rhizobia (Murray *et al*. 2011). Comparable analyses of gene activity patterns in mycorrhizal roots were so far restricted to investigations of single genes and their function. The technology of laser microdissection offered the possibility to obtain large quantities of defined cell types for downstream 'omics analyses and can thus be regarded as a valuable tool to achieve a precise temporal and spatial resolution of gene activity also during AM symbioses. Although several pioneering experiments existed for the use of laser microdissection in the analysis of gene expression in mycorrhizal roots at the start of this PhD thesis (Balestrini *et al*. 2007, Guether *et al*. 2009, Gomez *et al*. 2009), most of them focused on the analysis of a single group of genes or a single cell-type. The work presented here is the first which used laser microdissection for a genome-

wide inventory of gene expression patterns covering all four main developmental stages of the mycorrhizal symbiosis.

In the following, the key results obtained with this new method are recapitulatory discussed with regard to their reliability and their limitations in addition to the progress they provide in the understanding of AM associations. Results obtained via RNAi experiments in this study are compared to those from the transcriptome analysis and the information obtained on the transcriptional control of distinct symbiotic stages is summarized.

Laser microdissection: different approaches and their suitability for harvesting specific cell-types from arbuscular mycorrhizal roots

In spite of the elegant way to obtain defined cell pools that is offered by laser-microdissection, the preparation of samples and the RNA degradation that might occur along the way is an important issue, when cell-type specific transcriptomes are investigated. The reliability of the results strongly depends on an application of suitable protocols. We made use of a method involving fixation of roots with Farmer's fixative (3:1 ethanol:acetic acid) and subsequent embedding in Steedman's wax (Steedman 1957), which was developed for plant tissues by Kerk *et al*. (2003) and was already successfully applied to mycorrhizal roots of *Medicago truncatula* (Gomez *et al*. 2009). The protocol offers two advantages. First, it has often been reported that the use of precipitative fixatives like ethanol or acetone is preferable to the use of cross-linking fixatives such as aldehydes or formalin (Nelson *et al*. 2006 and references therein, Day *et al*. 2007), since cross-linking fixatives significantly reduce the extractability of macromolecules (Schutze *et al*. 1998). Second, the low melting temperature of the Steedman's wax is thought to prevent damage from the sample during infiltration. In pilot experiments, this method was compared to a microwave-protocol involving the embedding in classical paraffin-wax and the use of an extremely reduced preparation time (Inada and Wildermuth 2005). It turned out that in spite of the reduced exposition time, the high temperatures applied during infiltration of the root samples with classical paraffin-wax in the microwave protocol significantly enhanced RNA degradation in the root samples. In contrast, the use of the low-melting Steedman`s wax reduced RNA degradation to a tolerable level (Supplemental Figure S1), thereby validating the results obtained by Kerk *et al*. (2003) and Gomez *et al*. (2009).

An alternative to the embedding in paraffin is the use of cryosections, like it was applied in the approach of Gaude *et al*. (2012), who investigated gene expression in arbusculated and the

surrounding cortical cells of *Medicago truncatula* via GeneChip hybridizations. The availability of a similar dataset obtained with another preparation method offers the unique possibility to compare both methods. Although cryosectioning usually leads to a better quality of extracted RNA, samples may get impaired during freezing (Kerk *et al*. 2003). This is especially the case for delicate tissues like the thin roots of *Medicago truncatula* (usually several hundred µm in diameter, compare figures I_3, II-1), containing large vacuoles in the cortical cells and with lignification of cell walls limited to the central cylinder. The fact that Gaude *et al*. (2012) used 35 µm sections probably mirrors these issues and might entail further problems. Due to the growth pattern of the fungus inside the root, with arbuscules being present in all three dimensions surrounding the central cylinder, a prerequisite for the successful harvest of clean cell pools of arbusculated and non-arbusculated cells is the preparation of thin sections only comprising a single cell layer, which is 10-12 µm for longitudinal sections. Furthermore, if roots are not treated with a fixative prior to sectioning, this may cause cross-contaminations from the cytoplasm of cells opened during sectioning.

When ratios of gene expression between arbusculated and surrounding cortical cells are regarded, it becomes obvious that those measured in our wax-embedded samples are considerably higher than those measured in the cryosectioned samples. Whereas logFC (log fold change) ratios for the 100 genes most strongly induced in ARB ranged between 5,79 and 9,77 in our data, they range between 2,69 and 6,08 for data obtained from cryosections (Supplemental Table S_II_8). Although Gaude *et al*. (2012) did not distinguish between induced and specifically expressed genes, a detection of cell-specific expression patterns would probably be difficult here. On the other hand, the expression of 12 genes from the set of 62 genes, which we analyzed via RT-PCR before (Hogekamp *et al*. 2011), was below the detection threshold in CMR and ARB cells in our GeneChip experiment, indicating that RNA degradation led to a loss of less abundant transcripts with our method. At least two of these genes were detected by Gaude *et al*. (2012), which is in line with the fact that the use of cryosections prevents RNA degradation more efficiently. Therefore, results obtained with the two methods complement each other.

In general, the loss of transcripts for a limited set of genes seems tolerable, if the remaining results are reliable and accurate, as it was demonstrated in this work via comparison to expression data obtained by classical methods.

Marker genes facilitate the evaluation of cell-specific transcriptome profiles

The aspects discussed above illustrate that cell-specific marker genes are important in the analysis of data obtained from laser microdissected cells, to validate purity of the harvested cell pools and specificity of the gene expression patterns observed. Marker genes can also be utilized for the determination of detection thresholds in GeneChip experiments, as it was presented in this work, thereby enhancing the informative value of the data. While with *MtPt4* an ideal marker specifically expressed in arbusculated cells exists, things were more complicated with regard to a separation of epidermal and cortical cells. It would have been desirable to have an epidermal marker gene as well, to validate successful separation of EPI and CMR cell pools. An expansin gene with an *Arabidopsis* homologue shown to be specifically expressed in epidermal cells that was already used for the validation of successful root hair separation in *Medicago* (Murray *et al*. 2011) seemed an ideal candidate. Although this gene was successfully used for a real-time RT-PCR based validation of specific cell harvest of cortical and epidermal cells treated with diffusible signal molecules (Hürter 2011), it was among those with signals below detection level on GeneChips. A possible explanation may be that it is preferentially expressed in younger roots of *Medicago truncatula*, since it was also not detectable via RT-PCR in our samples.

Campos-Soriani *et al*. (2011) reported the differential expression of calcium-dependent protein kinases in laser microdissected epidermal and cortical cells of AM roots from rice, but did not use epidermal or cortical marker genes either. Due to this, a comparable validation for EPI and CMR cell pools like for ARB and CMR was not possible. With regard to gene expression influenced by mycorrhizal colonization this is of minor importance, since nearly no gene with a specific expression or induction in EPI were among those, for which a correlation to mycorrhizal symbiosis was postulated in this study. Nevertheless, it would be advantageous to identify further marker genes in the future, which are strongly and constitutively expressed in the respective cell types.

Sequential reprogramming of root cells during different stages of AM development

The hypothesis that distinct parts of the symbiotic program activated in AM roots control the different developmental stages of the symbiotic interaction was validated in this work via the use of laser microdissected cell pools from *Medicago truncatula*. Seven groups of genes were identified by a comparative analysis of the two datasets obtained from cells of mature mycorrhizal roots and roots harbouring first infection sites (Figure 8), relating to the four main developmental steps of AM

interactions: pre-contact phase (stage I), initial infection (stage II), intraradical growth of fungal hyphae (stage III), and arbuscule formation (stage IV). In the first stage, a subset of genes expressed in appressorial and non-appressorial areas of the root and additionally activated by Myc-factors was identified (Figure 8, Group A), and upon infection this group is complemented with a subset of genes specifically activated in appressorial areas (Figure 8, Group B). Whereas approximately one half of these genes is only active in the early stages, the other half remains active during stage III and IV, controling either general root colonization or arbuscule formation. They are supported by two further sets of genes, which are specifically activated during those last two stages (Figure 8, Group C+D). Furthermore, a set of genes was detected which undergo a root-internal shift of expression towards a preferential activity in arbusculated cells (Figure 8, Group E). In addition, evidence was provided that during initial infection and arbuscule formation, subsets of plant genes are downregulated to allow fungal colonization (Figure 8, Group F and G). Interestingly and in contrast to the other three stages, genes exclusively controlling the spread of intraradical hyphae (stage III) were not identified, indicating that the plant preferentially governs primary infection of the root and arbuscule formation, although mechanisms restricting the general colonization to certain parts of the host root exist. This was shown recently in an investigation of Lauressergues *et al.* (2012), who identified a miRNA, targeting the mRNA of the symbiotic GRAS transcription factor MtNSP2, and averting its activity in the root elongation zone, which normally doesn't get colonized by the fungus. Nevertheless, it seems that spread of fungal hyphae does not require much participation on the plant site, whereas infection and arbuscule formation represent concerted actions of both symbiotic partners. This is also mirrored in the identification of genes which are active during initial infection and preferentially expressed in arbusculated cells later on.

The knowledge on the specific place and time point of gene activation in the seven groups defined here, should allow a more accurate prediction of gene function. In the last part of this work, four *Medicago truncatula* genes were investigated for their functional role via an RNAi-mediated knockdown. The selected candidate genes were activated at different steps of the symbiotic development, with *MtGRAS2* being active in the pre-contact phase, *MtBcp1* being activated during initial infection and later on in arbusculated and the surrounding cortical cells, *MtMyb1* being preferentially expressed in arbusculated cells and *MtAnn2* specifically activated in arbusculated cells. We thus expected to find different phenotypes of fungal root colonization in the transgenic roots

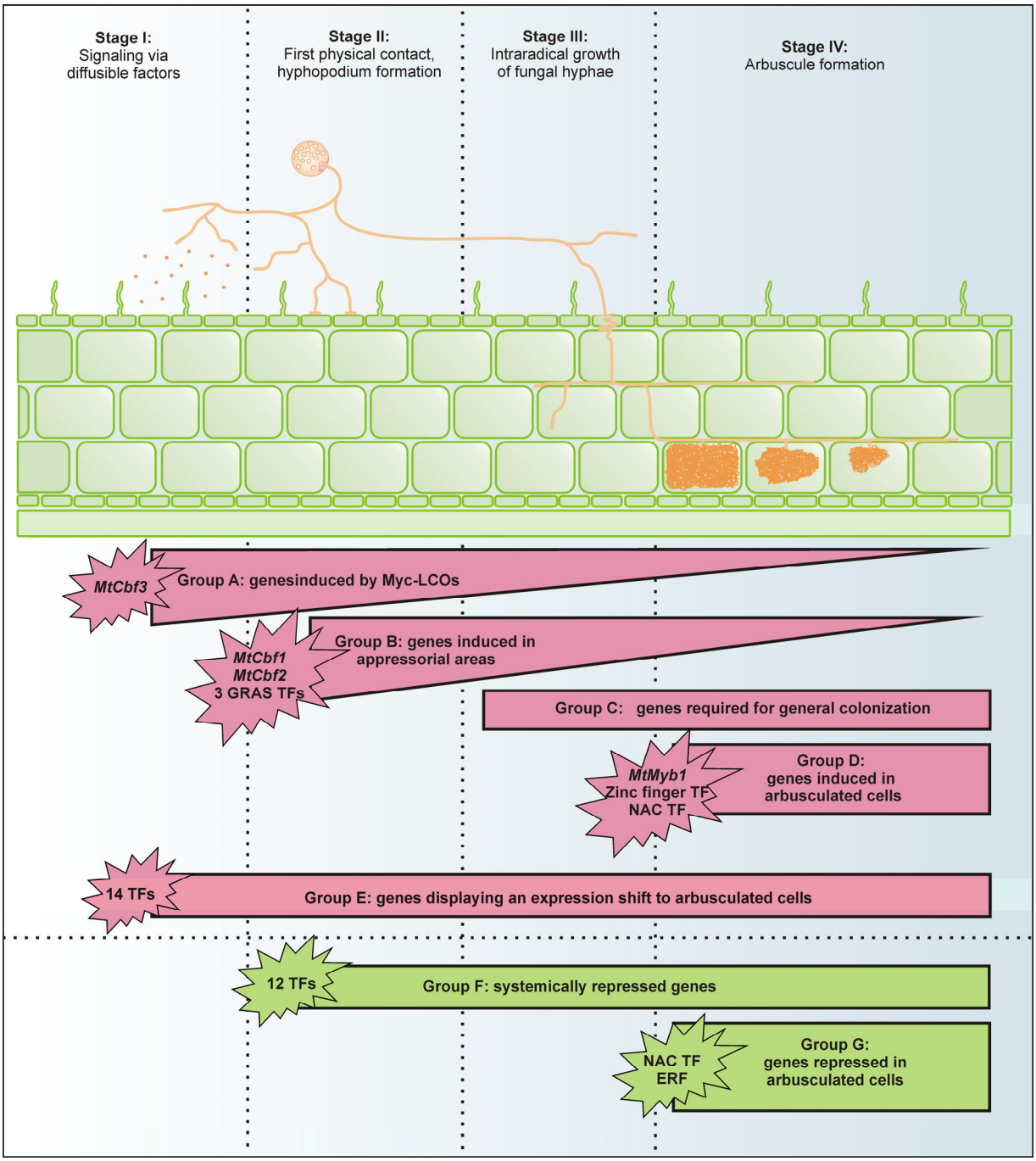

Figure 8: Schematic overview of sequential gene activation during the AM symbiosis.
Genes were classified into seven groups according to their expression pattern in the five cell-types obtained via laser-microdissection in this work and correlated to the main developmental stages (I-IV) of AM symbioses. **Group A**: genes activated in appressorial and non-appressorial areas and additionally by Myc-LCOs (Czaja *et al.* 2012), with continued expression in subsequent stages for some of the genes. **Group B**: genes induced in appressorial areas in comparison to non-appressorial areas, with continued expression in subsequent stages for some of the genes. **Group C**: genes activated in roots colonized by intraradical hyphae and arbusculated cells alike, thus being related to general root colonization. **Group D**: genes preferentially or specifically expressed in arbusculated cells. **Group E**: genes with unaltered expression on the level of whole roots, but induced in arbusculated cells, thus probably undergoing a shift of expression towards this cell-type. **Group F**: genes induced in non-appressorial areas in comparison to appressorial areas with low expression levels in mature mycorrhizal roots, thus repressed throughout all root cells in response to colonization by AM fungi. **Group G**: genes with reduced expression in arbusculated cells. Selected transcriptional regulator genes, displaying specific activation patterns in the five cell types studied in this work, are shown for the four stages. Abbreviations: LCOs: lipo-chitooligosaccharides, Cbf: CAAT-box binding transcription factor, ERF: ethylen-responsive transcription factor, TF: transcription factor

expressing the different RNAi-constructs. However, due to insufficient RNAi-mediated knock-down effects, a functional analysis was restricted to *MtAnn2* and *MtMyb1*, thus to the two genes activated during arbuscule development. Here, significant alterations of fungal root colonization was only observed in *MtMyb1*-RNAi roots. It is encouraging that the results obtained for *MtAnn2* and *MtMyb1* conform to their cellular expression patterns. While the slight reduction in fungal colonization observed in *MtAnn2*-RNAi roots was restricted to arbuscule development, the knockdown of *MtMyb1* obviously led to a slower propagation of the whole infection area, which correlates with its expression in both arbusculated and surrounding cortical cells and might be explained by a negative feedback of impaired arbuscule formation on the spread of the colonized area.

Apart from *MtMyb1* being activated at stage IV and the two CAAT-box transcription factor genes *MtCbf1* and *MtCbf2* showing activation at stage II, many other transcription factor genes were identified in the seven groups defined here, providing an insight into the pattern of transcriptional control during the different developmental stages (Supplemental Table S_II_7). In Figure 8, the most prominent candidates, displaying clear expression patterns in all relevant datasets are shown. This includes the CAAT-box transcription factor gene *MtCbf3*, which is obviously already involved in molecular control of pre-infection processes (Czaja *et al*. 2012). In addition to *MtCbf1* and *MtCbf2*, three GRAS transcription factors are strongly activated at stage II and maintain their activity in the subsequent steps. The next set of transcriptional regulators is activated as soon as arbuscule formation commences. Whereas *MtMyb1* along with a zinc finger and a NAC transcription factor belongs to the group of genes exclusively expressed during arbuscule formation in mature mycorrhizal roots, a large set of transcription factors was induced in arbuscules and also expressed in appressorial and non-appressorial areas, probably controling the expression shift we observed, which is not shown in detail here. The downregulation of genes observed during infection and arbuscule formation may similarly depend on the deactivation of certain transcription factors. In line with this, several TF genes were downregulated in appressorial areas and two additional genes showed a reduced expression in arbusculated cells. These transcription factors also represent potential targets for fungal effector molecules, like it was shown for a *Medicago truncatula* ethylene-responsive transcription factor controlling defence gene expression, which can be averted by a secreted *Glomus intraradices* effector (Kloppholz *et al*. 2011).

Future directions

The combination of cell-specific expression data derived from mature mycorrhizal roots with cell-specific gene expression profiles from early infection events significantly enlarged the informative value of the transcriptome study reported here. Further insights were gained via the comparison to GeneChip results from whole mycorrhizal roots (Hogekamp *et al*. 2011) and roots treated with Myc-LCOs (Czaja *et al*. 2012). While a gene expression atlas for different tissues of *Medicago truncatula* has already been established and allows cross-comparisons between experiments conducted by different groups (Benedito *et al*. 2008), an extension of these expression profiles to the cellular level, as developed for rice (Jiao *et al*. 2009), would be a valuable tool for the *Medicago* community as well.

In addition, an inventory of gene expression in different cell types of *Medicago truncatula* roots under non-symbiotic conditions, as well as in additional cell types from mycorrhizal roots (e.g. vascular tissue), would be a useful complement to the data presented here. With respect to our expression data, it would be interesting to validate the hypothesis, that genes we were not able to detect in our cell pools are expressed in other cell types. Moreover, the method of laser microdissection can be further exploited to discern between different stages of arbuscule formation. Since laser microdissection is principally capable to deliver sub-cellular resolution, this method could be applied to elucidate the protein composition of the peri-arbuscular membrane, which was recently shown to diverge between the arbuscule stem and the arbuscule branches (Pumplin and Harrison 2009).

In future experiments, the comprehensive use of laser microdissection on root nodule tissues would lead to an improved understanding of the processes that are common to both interactions, in particular for the group of genes we found to be activated in appressorial regions and arbusculated cells, thus probably being involved in cellular infection processes in general. Resolution on a cellular level would also give novel insights into commonalities between biological processes, which are not correlated on first sight. An example for this are the parallels found between root nodule and root nematode gall cells (Damiani *et al*. 2012).

The identification of distinct activation patterns of transcriptional regulator genes such as *MtCbf1* and *MtCbf2*, together with the first functional analysis of *MtMyb1* gives an impression of the regulatory network that governs distinct steps of the symbiotic program. First results on the interaction of transcription factors and probable *cis*-regulatory elements in the promoters of common symbiosis genes that are targeted by certain transcription factors are already available, but focused

mainly on the root nodule symbiosis (Adriankaja *et al*. 2007, Hirsch *et al*. 2009). The identification of groups of genes activated simultaneously at defined stages of the AM symbiosis could facilitate similar approaches in the investigation of this interaction by narrowing down the range of possible targets mediating the reprogramming of AM roots for an accomodation of benefical fungi.

REFERENCES

A

Akiyama K, Matsuzaki K, Hayashi H. 2005. Plant sesquiterpenes induce hyphal branching in arbuscular mycorrhizal fungi. Nature 435(7043):824-7.

Amiour N, Recorbet G, Robert F, Gianinazzi S, Dumas-Gaudot E. 2006. Mutations in DMI3 and SUNN modify the appressorium-responsive root proteome in arbuscular mycorrhiza. Mol Plant Microbe Interact 19(9):988-97.

Amor BB, Shaw SL, Oldroyd GE, Maillet F, Penmetsa RV, Cook D, Long SR, Denarie J, Gough C. 2003. The NFP locus of Medicago truncatula controls an early step of Nod factor signal transduction upstream of a rapid calcium flux and root hair deformation. Plant J 34(4):495-506.

Andriankaja A, Boisson-Dernier A, Frances L, Sauviac L, Jauneau A, Barker DG, de Carvalho-Niebel F. 2007. AP2-ERF transcription factors mediate Nod factor dependent Mt ENOD11 activation in root hairs via a novel cis-regulatory motif. Plant Cell 19(9):2866-85.

Ané JM, Levy J, Thoquet P, Kulikova O, de Billy F, Penmetsa V, Kim DJ, Debelle F, Rosenberg C, Cook DR, Bisseling T, Huguet T, Denarie J. 2002. Genetic and cytogenetic mapping of DMI1, DMI2, and DMI3 genes of Medicago truncatula involved in Nod factor transduction, nodulation, and mycorrhization. Mol Plant Microbe Interact 15(11):1108-18.

Ané JM, Kiss GB, Riely BK, Penmetsa RV, Oldroyd GE, Ayax C, Levy J, Debelle F, Baek JM, Kalo P, Rosenberg C, Roe BA, Long SR, Denarie J, Cook DR. 2004. Medicago truncatula DMI1 required for bacterial and fungal symbioses in legumes. Science 303(5662):1364-7.

Ané JM, Zhu H, Frugoli J. 2008. Recent Advances in Medicago truncatula Genomics. Int J Plant Genomics 2008:256597.

Arnon DI and HoaglandDR. 1940. Crop production in artificial culture solution and in soil
With reference to factors influencing yields and absorption of inorganic nutrients. Soil Sci. 50: 463-483.

Arlorio M, Ludwig A, Boller T, Bonfante P. 1992. Inhibition of fungal growth by plant chitinases and ß-1,3-glucanases. Protoplasma 171:34-43.

Arrighi JF, Barre A, Ben Amor B, Bersoult A, Soriano LC, Mirabella R, de Carvalho-Niebel F, Journet EP, Gherardi M, Huguet T, Geurts R, Denarie J, Rouge P, Gough C. 2006. The Medicago truncatula lysin motif-receptor-like kinase gene family includes NFP and new nodule-expressed genes. Plant Physiol 142(1):265-79.

Asano T, Masumura T, Kusano H, Kikuchi S, Kurita A, Shimada H, Kadowaki K. 2002. Construction of a specialized cDNA library from plant cells isolated by laser capture microdissection: toward comprehensive analysis of the genes expressed in the rice phloem. Plant J 32(3):401-8.

Atkinson EM, Palcic MM, Hindsgaul O, Long SR. 1994. Biosynthesis of Rhizobium meliloti lipooligosaccharide Nod factors: NodA is required for an N-acyltransferase activity. Proc Natl Acad Sci U S A 91(18):8418-22.

B

Baev N, Schultze M, Barlier I, Ha DC, Virelizier H, Kondorosi E, Kondorosi A. 1992. Rhizobium nodM and nodN genes are common nod genes: nodM encodes functions for efficiency of nod signal production and bacteroid maturation. J Bacteriol 174(23):7555-65.

Baier MC, Keck M, Godde V, Niehaus K, Küster H, Hohnjec N. 2010. Knockdown of the symbiotic sucrose synthase MtSucS1 affects arbuscule maturation and maintenance in mycorrhizal roots of Medicago truncatula. Plant Physiol 152(2):1000-14.

Balestrini R, Lanfranco L. 2006. Fungal and plant gene expression in arbuscular mycorrhizal symbiosis. Mycorrhiza 16(8):509-24.

Balestrini R, Gomez-Ariza J, Lanfranco L, Bonfante P. 2007. Laser microdissection reveals that transcripts for five plant and one fungal phosphate transporter genes are contemporaneously present in arbusculated cells. Mol Plant Microbe Interact 20(9):1055-62.

Barker DG, Bianchi S, Blondon F, Dattée Y, Duc G, Essad S, Flament P, Gallusci P, Génier G, Guy P, Muel X, Tourneur J, Dénarié J, Huguet T. 1990. Medicago truncatula, a model plant for studying the molecular genetics of the Rhizobium-legume symbiosis. Plant Mol. Biol. Rep. 8:40-49.

Bayrhuber H, Kull U. 1989. Linder Biologie. Schroedel Schulbuchverlag.

Bekel T, Henckel K, Küster H, Meyer F, Mittard Runte V, Neuweger H, Paarmann D, Rupp O, Zakrzewski M, Puhler A, Stoye J, Goesmann A. 2009. The Sequence Analysis and Management System -SAMS-2.0: data management and sequence analysis adapted to changing requirements from traditional sanger sequencing to ultrafast sequencing technologies. J Biotechnol 140(1-2):3-12.

Benedito VA, Torres-Jerez I, Murray JD, Andriankaja A, Allen S, Kakar K, Wandrey M, Verdier J, Zuber H, Ott T, Moreau S, Niebel A, Frickey T, Weiller G, He J, Dai X, Zhao PX, Tang Y, Udvardi MK. 2008. A gene expression atlas of the model legume Medicago truncatula. Plant J 55(3):504-13.

Benedito VA, Li H, Dai X, Wandrey M, He J, Kaundal R, Torres-Jerez I, Gomez SK, Harrison MJ, Tang Y, Zhao PX, Udvardi MK. 2010. Genomic inventory and transcriptional analysis of Medicago truncatula transporters. Plant Physiol 152(3):1716-30.

Besserer A, Puech-Pages V, Kiefer P, Gomez-Roldan V, Jauneau A, Roy S, Portais JC, Roux C, Becard G, Sejalon-Delmas N. 2006. Strigolactones stimulate arbuscular mycorrhizal fungi by activating mitochondria. PLoS Biol 4(7):e226.

Boisson-Dernier A, Chabaud M, Garcia F, Becard G, Rosenberg C, Barker DG. 2001. Agrobacterium rhizogenes-transformed roots of Medicago truncatula for the study of nitrogen-fixing and endomycorrhizal symbiotic associations. Mol Plant Microbe Interact 14(6):695-700.

Bonanomi A, Wiemken A, Boller T, Salzer P. 2001. Local Induction of a Mycorrhiza-Specific Class III Chitinase Gene in Cortical Root Cells of Medicago truncatula Containing Developing or Mature Arbuscules. Plant Biol. 3:194-200.

Bonfante P, Genre A. 2010. Mechanisms underlying beneficial plant-fungus interactions in mycorrhizal symbiosis. Nat Commun 1:48.

Bonfante P, Requena N. 2011. Dating in the dark: how roots respond to fungal signals to establish arbuscular mycorrhizal symbiosis. Curr Opin Plant Biol 14(4):451-7.

Brechenmacher L, Weidmann S, van Tuinen D, Chatagnier O, Gianinazzi S, Franken P, Gianinazzi-Pearson V. 2004. Expression profiling of up-regulated plant and fungal genes in early and late stages of Medicago truncatula-Glomus mosseae interactions. Mycorrhiza 14(4):253-62.

Brewin NJ. 1991. Development of the legume root nodule. Annu Rev Cell Biol 7:191-226.

Broekaert WF, Terras FR, Cammue BP, Osborn RW. 1995. Plant defensins: novel antimicrobial peptides as components of the host defense system. Plant Physiol 108(4):1353-8.

Bucher M. 2007. Functional biology of plant phosphate uptake at root and mycorrhiza interfaces. New Phytol. 173:11-26.

Buee M, Rossignol M, Jauneau A, Ranjeva R, Becard G. 2000. The pre-symbiotic growth of arbuscular mycorrhizal fungi is induced by a branching factor partially purified from plant root exudates. Mol Plant Microbe Interact 13(6):693-8.

Burleigh SH, Kristensen BK, Bechmann IE. 2003. A plasma membrane zinc transporter from Medicago truncatula is up-regulated in roots by Zn fertilization, yet down-regulated by arbuscular mycorrhizal colonization. Plant Mol Biol 52(5):1077-88.

C

Campos-Soriano L, Gomez-Ariza J, Bonfante P, San Segundo B. 2011. A rice calcium-dependent protein kinase is expressed in cortical root cells during the presymbiotic phase of the arbuscular mycorrhizal symbiosis. BMC Plant Biol 11:90.

Cannon SB, May GD, Jackson SA. 2009. Three sequenced legume genomes and many crop species: rich opportunities for translational genomics. Plant Physiol 151(3):970-7.

Casson S, Spencer M, Walker K, Lindsey K. 2005. Laser capture microdissection for the analysis of gene expression during embryogenesis of Arabidopsis. Plant J 42(1):111-23.

Chandran D, Inada N, Wildermuth MC. 2009. Laser microdissection of plant-fungus interaction sites and isolation of RNA for downstream expression profiling. Methods Mol Biol 712:241-62.

Chiou TJ, Liu H, Harrison MJ. 2001. The spatial expression patterns of a phosphate transporter (MtPT1) from Medicago truncatula indicate a role in phosphate transport at the root/soil interface. Plant J 25(3):281-93.

Clark RB, Zeto SK. 2000. Mineral acquisition by arbuscular mycorrhizal plants. Journal of Plant Nutrition 23:867-902.

Combier JP, Frugier F, de Billy F, Boualem A, El-Yahyaoui F, Moreau S, Vernie T, Ott T, Gamas P, Crespi M, Niebel A. 2006. MtHAP2-1 is a key transcriptional regulator of symbiotic nodule development regulated by microRNA169 in Medicago truncatula. Genes Dev 20(22):3084-8.

Combier JP, de Billy F, Gamas P, Niebel A, Rivas S. 2008. Trans-regulation of the expression of the transcription factor MtHAP2-1 by a uORF controls root nodule development. Genes Dev 22(11):1549-59.

Cook DR. 1999. Medicago truncatula - a model in the making! Curr Opin Plant Biol 2(4):301-4.

Cren M, Kondorosi A, Kondorosi E. 1995. NolR controls expression of the Rhizobium meliloti nodulation genes involved in the core Nod factor synthesis. Mol Microbiol 15(4):733-47.

Cullimore JV, Bennet MJ. 1992. Nitrogen assimilation in the legume root nodule; current status of the molecular biology of plant enzymes. Canadian Journal of Microbiology 38:461-466

Czaja LF, Hogekamp C, Lamm P, Maillet F, Martinez EA, Samain E, Denarie J, Kuster H, Hohnjec N. 2012. Transcriptional responses toward diffusible signals from symbiotic microbes reveal MtNFP- and MtDMI3-dependent reprogramming of host gene expression by arbuscular mycorrhizal fungal lipochitooligosaccharides. Plant Physiol 159(4):1671-85.

Czihak G, Langer H, Ziegler H (Hrsg.) 1990. Biologie – Ein Lehrbuch. Springer Verlag.

D

D'Haeze W, Holsters M. 2002. Nod factor structures, responses, and perception during initiation of nodule development. Glycobiology 12(6):79R-105R.

Damiani I, Baldacci-Cresp F, Hopkins J, Andrio E, Balzergue S, Lecomte P, Puppo A, Abad P, Favery B, Herouart D. 2012. Plant genes involved in harbouring symbiotic rhizobia or pathogenic nematodes. New Phytol 194(2):511-22.

Davies FT, Potter JR, Linderman RG. 1993. Drought Resistance of Mycorrhizal Pepper Plants Independent of Leaf P-Concentration - Response in Gas-Exchange and Water Relations. Physiologia Plantarum 87(1):45-53.

Day RC, Grossniklaus U, Macknight RC. 2005. Be more specific! Laser-assisted microdissection of plant cells. Trends Plant Sci 10(8):397-406.

Day RC, McNoe LA, Macknight RC. 2007. Transcript analysis of laser microdissected plant cells. Physiologia Plantarum 129:267-282

De Bary, A. 1879. Die Erscheinung der Symbiose. Privately printed in Strasburg.

De Carvalho Niebel F, Lescure N, Cullimore JV, Gamas P. 1998. The Medicago truncatula Mtann1 gene encoding an annexin is induced by Nod factors and during the symbiotic interaction with Rhizobium meliloti. Molecular Plant-Microbe Interactactions 11, 504–513

De Carvalho-Niebel F, Timmers AC, Chabaud M, Defaux-Petras A, Barker DG. 2002. The Nod factor-elicited annexin MtAnn1 is preferentially localised at the nuclear periphery in symbiotically activated root tissues of Medicago truncatula. Plant J 32(3):343-52.

Deguchi Y, Banba M, Shimoda Y, Chechetka SA, Suzuri R, Okusako Y, Ooki Y, Toyokura K, Suzuki A, Uchiumi T, Higashi S, Abe M, Kouchi H, Izui K, Hata S. 2007. Transcriptome profiling of Lotus japonicus roots during arbuscular mycorrhiza development and comparison with that of nodulation. DNA Res 14(3):117-33.

Demont N, Debelle F, Aurelle H, Denarie J, Prome JC. 1993. Role of the Rhizobium meliloti nodF and nodE genes in the biosynthesis of lipo-oligosaccharidic nodulation factors. J Biol Chem 268(27):20134-42.

Denarie J, Debelle F, Prome JC. 1996. Rhizobium lipo-chitooligosaccharide nodulation factors: signaling molecules mediating recognition and morphogenesis. Annu Rev Biochem 65:503-35.

De Rienzo F, Gabdoulline RR, Menziani MC, Wade RC. 2000. Blue copper proteins: a comparative analysis of their molecular interaction properties. Protein Sci 9(8):1439-54.

Doll J, Hause B, Demchenko K, Pawlowski K, Krajinski F. 2003. A member of the germin-like protein family is a highly conserved mycorrhiza-specific induced gene. Plant Cell Physiol 44(11):1208-14.

Douds DD, Pfeffer PE, Shachar-Hill Y. 2000. Carbon partioning, cost and metabolism of Arbuscular Mycorrhizae. In DD Douds, Y Kapulnik (eds) Arbuscular Mycorrhizas Physiology and Function. Kluwer Academic Publishers, Dordrecht, The Netherlands, pp107-130

Drissner D, Kunze G, Callewaert N, Gehrig P, Tamasloukht M, Boller T, Felix G, Amrhein N, Bucher M. 2007. Lyso-phosphatidylcholine is a signal in the arbuscular mycorrhizal symbiosis. Science 318(5848):265-8.

Dubos C, Stracke R, Grotewold E, Weisshaar B, Martin C, Lepiniec L. 2010. MYB transcription factors in Arabidopsis. Trends Plant Sci 15(10):573-81.

E

Emmert-Buck MR, Bonner RF, Smith PD, Chuaqui RF, Zhuang Z, Goldstein SR, Weiss RA, Liotta LA. 1996. Laser capture microdissection. Science 274(5289):998-1001.

Endre G, Kereszt A, Kevei Z, Mihacea S, Kalo P, Kiss GB. 2002. A receptor kinase gene regulating symbiotic nodule development. Nature 417(6892):962-6.

Ercolin F, Reinhardt D. 2011. Successful joint ventures of plants: arbuscular mycorrhiza and beyond. Trends Plant Sci 16(7):356-62.

F

Fend F, Specht K, Kremer M, Quintanilla-Martinez L. 2002. Laser capture microdissection in pathology. Methods Enzymol 356:196-206.

Fiorilli V, Catoni M, Miozzi L, Novero M, Accotto GP, Lanfranco L. 2009. Global and cell-type gene expression profiles in tomato plants colonized by an arbuscular mycorrhizal fungus. New Phytol 184(4):975-87.

Floss DS, Schliemann W, Schmidt J, Strack D, Walter MH. 2008a. RNA interference-mediated repression of MtCCD1 in mycorrhizal roots of Medicago truncatula causes accumulation of C27 apocarotenoids, shedding light on the functional role of CCD1. Plant Physiol 148(3):1267-82.

Floss DS, Hause B, Lange PR, Kuster H, Strack D, Walter MH. 2008b. Knock-down of the MEP pathway isogene 1-deoxy-D-xylulose 5-phosphate synthase 2 inhibits formation of arbuscular mycorrhiza-induced apocarotenoids, and abolishes normal expression of mycorrhiza-specific plant marker genes. Plant J 56(1):86-100.

Fournier J, Timmers AC, Sieberer BJ, Jauneau A, Chabaud M, Barker DG. 2008. Mechanism of infection thread elongation in root hairs of Medicago truncatula and dynamic interplay with associated rhizobial colonization. Plant Physiol 148(4):1985-95.

Frank AB. 1885. Ueber die auf Wurzelsymbiose beruhende Ernährung gewisser Bäume durch unterirdische Pilze. Berichte der Deutschen Botanischen Gesellschaft 3: 128-145

Frenzel A, Manthey K, Perlick AM, Meyer F, Puhler A, Kuster H, Krajinski F. 2005. Combined transcriptome profiling reveals a novel family of arbuscular mycorrhizal-specific Medicago truncatula lectin genes. Mol Plant Microbe Interact 18(8):771-82.

Frugier F, Poirier S, Satiat-Jeunemaitre B, Kondorosi A, Crespi M. 2000. A Kruppel-like zinc finger protein is involved in nitrogen-fixing root nodule organogenesis. Genes Dev 14(4):475-82.

Fusaro AF, Matthew L, Smith NA, Curtin SJ, Dedic-Hagan J, Ellacott GA, Watson JM, Wang MB, Brosnan C, Carroll BJ, Waterhouse PM. 2006. RNA interference-inducing hairpin RNAs in plants act through the viral defence pathway. EMBO Rep 7(11):1168-75.

G

Galibert F, Finan TM, Long SR, Puhler A, Abola P, Ampe F, Barloy-Hubler F, Barnett MJ, Becker A, Boistard P, Bothe G, Boutry M, Bowser L, Buhrmester J, Cadieu E, Capela D, Chain P, Cowie A, Davis RW, Dreano S, Federspiel NA, Fisher RF, Gloux S, Godrie T, Goffeau A, Golding B, Gouzy J, Gurjal M, Hernandez-Lucas I, Hong A, Huizar L, Hyman RW, Jones T, Kahn D, Kahn ML, Kalman S, Keating DH, Kiss E, Komp C, Lelaure V, Masuy D, Palm C, Peck MC, Pohl TM, Portetelle D, Purnelle B, Ramsperger U, Surzycki R, Thebault P, Vandenbol M, Vorholter FJ, Weidner S, Wells DH, Wong K, Yeh KC, Batut J. 2001. The composite genome of the legume symbiont Sinorhizobium meliloti. Science 293(5530):668-72.

Gaude N, Bortfeld S, Duensing N, Lohse M, Krajinski F. 2012. Arbuscule-containing and non-colonized cortical cells of mycorrhizal roots undergo extensive and specific reprogramming during arbuscular mycorrhizal development. Plant J 69(3):510-28.

Geisler M, Murphy AS. 2006. The ABC of auxin transport: the role of p-glycoproteins in plant development. FEBS Lett 580(4):1094-102.

Genre A, Chabaud M, Timmers T, Bonfante P, Barker DG. 2005. Arbuscular mycorrhizal fungi elicit a novel intracellular apparatus in Medicago truncatula root epidermal cells before infection. Plant Cell 17(12):3489-99.

Genre A, Chabaud M, Faccio A, Barker DG, Bonfante P. 2008. Prepenetration apparatus assembly precedes and predicts the colonization patterns of arbuscular mycorrhizal fungi within the root cortex of both Medicago truncatula and Daucus carota. Plant Cell 20(5):1407-20.

Genre A, Ivanov S, Fendrych M, Faccio A, Zarsky V, Bisseling T, Bonfante P. 2011. Multiple exocytotic markers accumulate at the sites of perifungal membrane biogenesis in arbuscular mycorrhizas. Plant Cell Physiol 53(1):244-55.

George E, Marschner H, Jakobsen I. 1995. Role of Arbuscular Mycorrhizal Fungi in Uptake of Phosphorus and Nitrogen from Soil. Critical Reviews in Biotechnology 15(3-4):257-270.

Geurts R, Lillo A, Bisseling T. 2012. Exploiting an ancient signalling machinery to enjoy a nitrogen fixing symbiosis. Curr Opin Plant Biol 15(4):438-43.

Gianinazzi-Pearson V, Dumas-Gaudot E, Golotte A, Tahiri-Alaouf A, Gianinazzi S. 1996. Cellular and molecular defence-related root responses to invasion by arbuscular mycorrhizal fungi. New Phytol. 133:45-57.

Gillespie JW, Ahram M, Best CJ, Swalwell JI, Krizman DB, Petricoin EF, Liotta LA, Emmert-Buck MR. 2001. The role of tissue microdissection in cancer research. Cancer J 7(1):32-9.

Gomez SK, Javot H, Deewatthanawong P, Torres-Jerez I, Tang Y, Blancaflor EB, Udvardi MK, Harrison MJ. 2009. Medicago truncatula and Glomus intraradices gene expression in cortical cells harboring arbuscules in the arbuscular mycorrhizal symbiosis. BMC Plant Biol 9:10.

Gonzalez-Chavez Mdel C, Ortega-Larrocea Mdel P, Carrillo-Gonzalez R, Lopez-Meyer M, Xoconostle-Cazares B, Gomez SK, Harrison MJ, Figueroa-Lopez AM, Maldonado-Mendoza IE. 2009. Arsenate induces the expression of fungal genes involved in As transport in arbuscular mycorrhiza. Fungal Biol 115(12):1197-209.

Gough C, Cullimore J. 2011. Lipo-chitooligosaccharide signaling in endosymbiotic plant-microbe interactions. Mol Plant Microbe Interact 24(8):867-78.

Govindarajulu M, Pfeffer PE, Jin H, Abubaker J, Douds DD, Allen JW, Bucking H, Lammers PJ, Shachar-Hill Y. 2005. Nitrogen transfer in the arbuscular mycorrhizal symbiosis. Nature 435(7043):819-23.

Grunwald U, Nyamsuren O, Tamasloukht M, Lapopin L, Becker A, Mann P, Gianinazzi-Pearson V, Krajinski F, Franken P. 2004. Identification of mycorrhiza-regulated genes with arbuscule development-related expression profile. Plant Mol Biol 55(4):553-66.

Guether M, Balestrini R, Hannah M, He J, Udvardi MK, Bonfante P. 2009. Genome-wide reprogramming of regulatory networks, transport, cell wall and membrane biogenesis during arbuscular mycorrhizal symbiosis in Lotus japonicus. New Phytol 182(1):200-12.

Gutjahr C, Casieri L, Paszkowski U. 2009. Glomus intraradices induces changes in root system architecture of rice independently of common symbiosis signaling. New Phytol 182(4):829-37.

H

Hacquard S, Delaruelle C, Legue V, Tisserant E, Kohler A, Frey P, Martin F, Duplessis S. 2010. Laser capture microdissection of uredinia formed by Melampsora larici-populina revealed a transcriptional switch between biotrophy and sporulation. Mol Plant Microbe Interact 23(10):1275-86.

Hammond SM, Caudy AA, Hannon GJ. 2001. Post-transcriptional gene silencing by double-stranded RNA. Nat Rev Genet 2(2):110-9.

Handberg K, DStougaard J. 1992. Lotus japonicus, an autogamous, diploid legume species for classical and molecular genetics. Plant J. 2:487-496.

Haney CH, Long SR. 2010. Plant flotillins are required for infection by nitrogen-fixing bacteria. Proc Natl Acad Sci U S A 107(1):478-83.

Hannon GJ. 2002. RNA interference. Nature 418(6894):244-51.

Harrison MJ, Dixon RA. 1993. Isoflavonoid accumulation and expression of defense gene transcripts during the establishment of vesicular-arbuscular mycorrhizal associations in roots of Medicago truncatula. Molecular Plant Microbe Interactions 6:643-654.

Harrison MJ. 1996. A sugar transporter from Medicago truncatula: altered expression pattern in roots during vesicular-arbuscular (VA) mycorrhizal associations. Plant J 9(4):491-503.

Harrison MJ. 1999. Molecular and Cellular Aspects of the Arbuscular Mycorrhizal Symbiosis. Annu Rev Plant Physiol Plant Mol Biol 50:361-389.

Harrison MJ, Dewbre GR, Liu J. 2002. A phosphate transporter from Medicago truncatula involved in the acquisition of phosphate released by arbuscular mycorrhizal fungi. Plant Cell 14(10):2413-29.

Harrison MJ. 2005. Signaling in the arbuscular mycorrhizal symbiosis. Annu Rev Microbiol 59:19-42.

He J, Benedito VA, Wang M, Murray JD, Zhao PX, Tang Y, Udvardi MK. 2009. The Medicago truncatula gene expression atlas web server. BMC Bioinformatics 10:441.

Helber N, Requena N. 2008. Expression of the fluorescence markers DsRed and GFP fused to a nuclear localization signal in the arbuscular mycorrhizal fungus Glomus intraradices. New Phytol 177(2):537-48.

Helber N, Wippel K, Sauer N, Schaarschmidt S, Hause B, Requena N. 2011. A versatile monosaccharide transporter that operates in the arbuscular mycorrhizal fungus Glomus sp is crucial for the symbiotic relationship with plants. Plant Cell 23(10):3812-23.

Helliwell C, Waterhouse P. 2003. Constructs and methods for high-throughput gene silencing in plants. Methods 30(4):289-95.

Henckel K, Runte KJ, Bekel T, Dondrup M, Jakobi T, Küster H, Goesmann A. 2009. TRUNCATULIX - a data warehouse for the legume community. BMC Plant Biol 9:19.

Henckel K, Küster H, Stutz LJ, Goesmann A. 2010. MediPlEx - a tool to combine in silico & experimental gene expression profiles of the model legume Medicago truncatula. BMC Res Notes 3:262.

Hijikata N, Murase M, Tani C, Ohtomo R, Osaki M, Ezawa T. 2010. Polyphosphate has a central role in the rapid and massive accumulation of phosphorus in extraradical mycelium of an arbuscular mycorrhizal fungus. New Phytol 186(2):285-9.

Hirsch S, Kim J, Munoz A, Heckmann AB, Downie JA, Oldroyd GE. 2009. GRAS proteins form a DNA binding complex to induce gene expression during nodulation signaling in Medicago truncatula. Plant Cell 21(2):545-57.

Hogekamp C, Arndt D, Pereira PA, Becker JD, Hohnjec N, Kuster H. 2011. Laser microdissection unravels cell-type-specific transcription in arbuscular mycorrhizal roots, including CAAT-box transcription factor gene expression correlating with fungal contact and spread. Plant Physiol 157(4):2023-43.

Hohnjec N, Becker JD, Puhler A, Perlick AM, Küster H. 1999. Genomic organization and expression properties of the MtSucS1 gene, which encodes a nodule-enhanced sucrose synthase in the model legume Medicago truncatula. Mol Gen Genet 261(3):514-22.

Hohnjec N, Perlick AM, Puhler A, Küster H. 2003. The Medicago truncatula sucrose synthase gene MtSucS1 is activated both in the infected region of root nodules and in the cortex of roots colonized by arbuscular mycorrhizal fungi. Mol Plant Microbe Interact 16(10):903-15.

Hohnjec N, Vieweg MF, Puhler A, Becker A, Küster H. 2005. Overlaps in the transcriptional profiles of Medicago truncatula roots inoculated with two different Glomus fungi provide insights into the genetic program activated during arbuscular mycorrhiza. Plant Physiol 137(4):1283-301.

Hohnjec N, Henckel K, Bekel T, Gouzy J, Dondrup M, Goesmann A, Küster H. 2006. Transcriptional snapshots provide insights into the molecular basis of arbuscular mycorrhiza in the model legume Medicago truncatula. Funct. Plant Biol. 33:737-748.

Horvath B, Yeun LH, Domonkos A, Halasz G, Gobbato E, Ayaydin F, Miro K, Hirsch S, Sun J, Tadege M, Ratet P, Mysore KS, Ane JM, Oldroyd GE, Kalo P. 2011. Medicago truncatula IPD3 is a member of the common symbiotic signaling pathway required for rhizobial and mycorrhizal symbioses. Mol Plant Microbe Interact 24(11):1345-58.

Hürter AL. 2011. Zellspezifische Analyse symbiose-induzierter Medicago truncatula Gene durch Lasermikrodissektion. Leibniz Universität Hannover

Humphreys CP, Franks PJ, Rees M, Bidartondo MI, Leake JR, Beerling DJ. 2010. Mutualistic mycorrhiza-like symbiosis in the most ancient group of land plants. Nat Commun 1:103.

I

Inada N, Wildermuth MC. 2005. Novel tissue preparation method and cell-specific marker for laser microdissection of Arabidopsis mature leaf. Planta 221(1):9-16.

Ithal N, Mitchum MG. 2011. Laser capture microdissection of nematode feeding cells. Methods Mol Biol 712:227-40.

Ivanov S, Fedorova EE, Limpens E, De Mita S, Genre A, Bonfante P, Bisseling T. 2012. Rhizobium-legume symbiosis shares an exocytotic pathway required for arbuscule formation. Proc Natl Acad Sci U S A 109(21):8316-21.

Ivashikina N, Deeken R, Ache P, Kranz E, Pommerrenig B, Sauer N, Hedrich R. 2003. Isolation of AtSUC2 promoter-GFP-marked companion cells for patch-clamp studies and expression profiling. Plant J 36(6):931-45.

J

Javot H, Penmetsa RV, Terzaghi N, Cook DR, Harrison MJ. 2007. A Medicago truncatula phosphate transporter indispensable for the arbuscular mycorrhizal symbiosis. Proc Natl Acad Sci U S A 104(5):1720-5.

Jiang K, Zhang S, Lee S, Tsai G, Kim K, Huang H, Chilcott C, Zhu T, Feldman LJ. 2006. Transcription profile analyses identify genes and pathways central to root cap functions in maize. Plant Mol Biol 60(3):343-63.

Jiao Y, Tausta SL, Gandotra N, Sun N, Liu T, Clay NK, Ceserani T, Chen M, Ma L, Holford M, Zhang HY, Zhao H, Deng XW, Nelson T. 2009. A transcriptome atlas of rice cell types uncovers cellular, functional and developmental hierarchies. Nat Genet 41(2):258-63.

Journet EP, van Tuinen D, Gouzy J, Crespeau H, Carreau V, Farmer MJ, Niebel A, Schiex T, Jaillon O, Chatagnier O, Godiard L, Micheli F, Kahn D, Gianinazzi-Pearson V, Gamas P. 2002. Exploring root symbiotic programs in the model legume Medicago truncatula using EST analysis. Nucleic Acids Res 30(24):5579-92.

K

Kalo P, Gleason C, Edwards A, Marsh J, Mitra RM, Hirsch S, Jakab J, Sims S, Long SR, Rogers J, Kiss GB, Downie JA, Oldroyd GE. 2005. Nodulation signaling in legumes requires NSP2, a member of the GRAS family of transcriptional regulators. Science 308(5729):1786-9.

Kerk NM, Ceserani T, Tausta SL, Sussex IM, Nelson TM. 2003. Laser capture microdissection of cells from plant tissues. Plant Physiol 132(1):27-35.

Kistner C, Winzer T, Pitzschke A, Mulder L, Sato S, Kaneko T, Tabata S, Sandal N, Stougaard J, Webb KJ, Szczyglowski K, Parniske M. 2005. Seven Lotus japonicus genes required for transcriptional reprogramming of the root during fungal and bacterial symbiosis. Plant Cell 17(8):2217-29.

Klink VP, Hosseini P, Matsye PD, Alkharouf NW, Matthews BF. 2010. Syncytium gene expression in Glycine max([PI 88788]) roots undergoing a resistant reaction to the parasitic nematode Heterodera glycines. Plant Physiol Biochem 48(2-3):176-93.

Kloppholz S, Kuhn H, Requena N. 2011. A Secreted Fungal Effector of Glomus intraradices Promotes Symbiotic Biotrophy. Curr Biol 21(14):1204-9.

Kosuta S, Chabaud M, Lougnon G, Gough C, Denarie J, Barker DG, Becard G. 2003. A diffusible factor from arbuscular mycorrhizal fungi induces symbiosis-specific MtENOD11 expression in roots of Medicago truncatula. Plant Physiol 131(3):952-62.

Kosuta S, Hazledine S, Sun J, Miwa H, Morris RJ, Downie JA, Oldroyd GE. 2008. Differential and chaotic calcium signatures in the symbiosis signaling pathway of legumes. Proc Natl Acad Sci U S A. 105(28):9823-8.

Krajinski F, Biela A, Schubert D, Gianinazzi-Pearson V, Kaldenhoff R, Franken P. 2000. Arbuscular mycorrhiza development regulates the mRNA abundance of Mtaqp1 encoding a mercury-insensitive aquaporin of Medicago truncatula. Planta 211(1):85-90.

Krajinski F, Hause B, Gianinazzi-Pearson V, Franken P. 2002. Mtha1, a plasma membrane H+-ATPase gene from Medicago truncatula, shows arbuscule-specific induced expression in mycorrhizal tissue. Plant Biol. 4:754-761.

Kuhn H, Küster H, Requena N. 2010. Membrane steroid-binding protein 1 induced by a diffusible fungal signal is critical for mycorrhization in Medicago truncatula. New Phytol 185(3):716-33.

Küster H, Hohnjec N, Krajinski F, El YF, Manthey K, Gouzy J, Dondrup M, Meyer F, Kalinowski J, Brechenmacher L, van Tuinen D, Gianinazzi-Pearson V, Puhler A, Gamas P, Becker A. 2004. Construction and validation of cDNA-based Mt6k-RIT macro- and microarrays to explore root endosymbioses in the model legume Medicago truncatula. J Biotechnol 108(2):95-113.

Küster H, Becker A, Firnhaber C, Hohnjec N, Manthey K, Perlick AM, Bekel T, Dondrup M, Henckel K, Goesmann A, Meyer F, Wipf D, Requena N, Hildebrandt U, Hampp R, Nehls U, Krajinski F, Franken P, Puhler A. 2007a. Development of bioinformatic tools to support EST-sequencing, in silico- and microarray-based transcriptome profiling in mycorrhizal symbioses. Phytochemistry 68(1):19-32.

Küster H, Vieweg MF, Manthey K, Baier MC, Hohnjec N, Perlick AM. 2007b. Identification and expression regulation of symbiotically activated legume genes. Phytochemistry 68(1):8-18.

L

Laohavisit A, Davies JM. 2011. Annexins. New Phytol 189(1):40-53.

Lauressergues D, Delaux PM, Formey D, Lelandais-Briere C, Fort S, Cottaz S, Becard G, Niebel A, Roux C, Combier JP. 2012. The microRNA miR171h modulates arbuscular mycorrhizal colonization of Medicago truncatula by targeting NSP2. Plant J.

Lee JM, Roche JR, Donaghy DJ, Thrush A, Sathish P. 2010. Validation of reference genes for quantitative RT-PCR studies of gene expression in perennial ryegrass (Lolium perenne L.). BMC Mol Biol 11:8.

Lefebvre B, Furt F, Hartmann MA, Michaelson LV, Carde JP, Sargueil-Boiron F, Rossignol M, Napier JA, Cullimore J, Bessoule JJ, Mongrand S. 2007. Characterization of lipid rafts from Medicago truncatula root plasma membranes: a proteomic study reveals the presence of a raft-associated redox system. Plant Physiol 144(1):402-18.

Lerouge P, Roche P, Faucher C, Maillet F, Truchet G, Prome JC, Denarie J. 1990. Symbiotic host-specificity of Rhizobium meliloti is determined by a sulphated and acylated glucosamine oligosaccharide signal. Nature 344(6268):781-4.

Lévy J, Bres C, Geurts R, Chalhoub B, Kulikova O, Duc G, Journet EP, Ane JM, Lauber E, Bisseling T, Denarie J, Rosenberg C, Debelle F. 2004. A putative Ca2+ and calmodulin-dependent protein kinase required for bacterial and fungal symbioses. Science 303(5662):1361-4.

Libault M, Joshi T, Benedito VA, Xu D, Udvardi MK, Stacey G. 2009. Legume transcription factor genes: what makes legumes so special? Plant Physiol 151(3):991-1001.

Limpens E, Ramos J, Franken C, Raz V, Compaan B, Franssen H, Bisseling T, Geurts R. 2004. RNA interference in Agrobacterium rhizogenes-transformed roots of Arabidopsis and Medicago truncatula. J Exp Bot 55(399):983-92.

Liu H, Trieu AT, Blaylock LA, Harrison MJ. 1998. Cloning and characterization of two phosphate transporters from Medicago truncatula roots: regulation in response to phosphate and to colonization by arbuscular mycorrhizal (AM) fungi. Mol Plant Microbe Interact 11(1):14-22.

Liu J, Blaylock L, Endre G, Cho J, Town C, VandenBosch K, Harrison MJ. 2003. Transcript profiling coupled with spatial expression analyses reveals genes involved in distinct developmental stages of an arbuscular mycorrhizal symbiosis. Plant Cell 15:2106-2123.

Lohar DP, Sharopova N, Endre G, Penuela S, Samac D, Town C, Silverstein KA, VandenBosch KA. 2006. Transcript analysis of early nodulation events in Medicago truncatula. Plant Physiol 140(1):221-34.

Lopez-Millan AF, Ellis DR, Grusak MA. 2004. Identification and characterization of several new members of the ZIP family of metal ion transporters in Medicago truncatula. Plant Mol Biol 54(4):583-96.

Ludwig-Muller J, Guther M. 2007. Auxins as signals in arbuscular mycorrhiza formation. Plant Signal Behav 2(3):194-6.

M

Maier W, Peipp H, Schmidt J, Wray V, Strack D. 1995. Levels of a terpenoid glycoside (blumenin) and cell wall-bound phenolics in some cereal mycorrhizas. Plant Physiol 109(2):465-70.

Maillet F, Poinsot V, Andre O, Puech-Pages V, Haouy A, Gueunier M, Cromer L, Giraudet D, Formey D, Niebel A, Martinez EA, Driguez H, Becard G, Denarie J. 2011. Fungal lipochitooligosaccharide symbiotic signals in arbuscular mycorrhiza. Nature 469(7328):58-63.

Maity SN, de Crombrugghe B. 1998. Role of the CCAAT-binding protein CBF/NF-Y in transcription. Trends Biochem Sci 23(5):174-8.

Manthey K, Krajinski F, Hohnjec N, Firnhaber C, Puhler A, Perlick AM, Küster H. 2004. Transcriptome profiling in root nodules and arbuscular mycorrhiza identifies a collection of novel genes induced during Medicago truncatula root endosymbioses. Mol Plant Microbe Interact 17(10):1063-77.

Mantovani R. 1998. A survey of 178 NF-Y binding CCAAT boxes. Nucleic Acids Res 26(5):1135-43.

Markmann K, Parniske M. 2009. Evolution of root endosymbiosis with bacteria: How novel are nodules? Trends Plant Sci 14(2):77-86.

Martin F, Gianinazzi-Pearson V, Hijri M, Lammers P, Requena N, Sanders IR, Shachar-Hill Y, Shapiro H, Tuskan GA, Young JP. 2008. The long hard road to a completed Glomus intraradices genome. New Phytol 180(4):747-50.

Matas AJ, Agusti J, Tadeo FR, Talon M, Rose JK. 2010. Tissue-specific transcriptome profiling of the citrus fruit epidermis and subepidermis using laser capture microdissection. J Exp Bot 61(12):3321-30.

Matusova R, Rani K, Verstappen FW, Franssen MC, Beale MH, Bouwmeester HJ. 2005. The strigolactone germination stimulants of the plant-parasitic Striga and Orobanche spp. are derived from the carotenoid pathway. Plant Physiol 139(2):920-34.

McGonigle T, Miller M, Evans D, Fairchild D, Swan J. 1990. A new method which gives an objective measure of colonization of roots by vesicular-arbuscular mycorrhizal fungi. New Phytol. 115:495-501.

Middleton PH, Jakab J, Penmetsa RV, Starker CG, Doll J, Kalo P, Prabhu R, Marsh JF, Mitra RM, Kereszt A, Dudas B, VandenBosch K, Long SR, Cook DR, Kiss GB, Oldroyd GE. 2007. An ERF transcription factor in Medicago truncatula that is essential for Nod factor signal transduction. Plant Cell 19(4):1221-34.

Mrosk C, Forner S, Hause G, Küster H, Kopka J, Hause B. 2009. Composite Medicago truncatula plants harbouring Agrobacterium rhizogenes-transformed roots reveal normal mycorrhization by Glomus intraradices. J Exp Bot 60(13):3797-807.

Murray JD. 2011. Invasion by invitation: rhizobial infection in legumes. Mol Plant Microbe Interact 24(6):631-9.

Murray JD, Muni RR, Torres-Jerez I, Tang Y, Allen S, Andriankaja M, Li G, Laxmi A, Cheng X, Wen J, Vaughan D, Schultze M, Sun J, Charpentier M, Oldroyd G, Tadege M, Ratet P, Mysore KS, Chen R, Udvardi MK. 2011. Vapyrin, a gene essential for intracellular progression of arbuscular mycorrhizal symbiosis, is also essential for infection by rhizobia in the nodule symbiosis of Medicago truncatula. Plant J 65(2):244-52.

N

Nagahashi G, Douds DD. 1997. Appressorium formation by AM fungi on isolated cell walls of carrot roots. New Phytologist 136(2):299-304.

Nakazono M, Qiu F, Borsuk LA, Schnable PS. 2003. Laser-capture microdissection, a tool for the global analysis of gene expression in specific plant cell types: identification of genes expressed differentially in epidermal cells or vascular tissues of maize. Plant Cell 15(3):583-96.

Navazio L, Moscatiello R, Genre A, Novero M, Baldan B, Bonfante P, Mariani P. 2007. A diffusible signal from arbuscular mycorrhizal fungi elicits a transient cytosolic calcium elevation in host plant cells. Plant Physiol 144(2):673-81.

Nehls U, Grunze N, Willmann M, Reich M, Küster H. 2007. Sugar for my honey: carbohydrate partitioning in ectomycorrhizal symbiosis. Phytochemistry 68(1):82-91.

Nelson T, Tausta SL, Gandotra N, Liu T. 2006. Laser microdissection of plant tissue: what you see is what you get. Annu Rev Plant Biol 57:181-201.

Nultsch W. 2001. Allgemeine Botanik. Georg Thieme Verlag.

O

Oldroyd GE, Harrison MJ, Udvardi M. 2005. Peace talks and trade deals. Keys to long-term harmony in legume-microbe symbioses. Plant Physiol 137(4):1205-10.

Oldroyd GE, Downie JA. 2008. Coordinating nodule morphogenesis with rhizobial infection in legumes. Annu Rev Plant Biol 59:519-46.

Oldroyd GE, Harrison MJ, Paszkowski U. 2009. Reprogramming plant cells for endosymbiosis. Science 324(5928):753-4.

Oldroyd GE, Murray JD, Poole PS, Downie JA. 2011. The rules of engagement in the legume-rhizobial symbiosis. Annu Rev Genet. 45: 119-44

Oliveros, J.C. 2007. VENNY. An interactive tool for comparing lists with Venn Diagrams.

Op den Camp R, Streng A, De Mita S, Cao Q, Polone E, Liu W, Ammiraju JS, Kudrna D, Wing R, Untergasser A, Bisseling T, Geurts R. 2011. LysM-type mycorrhizal receptor recruited for rhizobium symbiosis in nonlegume Parasponia. Science 331(6019):909-12.

Ortu G, Balestrini R, Pereira PA, Becker JD, Kuster H, Bonfante P. 2012. Plant genes related to gibberellin biosynthesis and signaling are differentially regulated during the early stages of AM fungal interactions. Mol Plant 5(4):951-4.

P

Paradi I, van Tuinen D, Morandi D, Ochatt S, Robert F, Jacas L, Dumas-Gaudot E. 2010. Transcription of two blue copper-binding protein isogenes is highly correlated with arbuscular mycorrhizal development in Medicago truncatula. Mol Plant Microbe Interact 23(9):1175-83.

Parniske M. 2000. Intracellular accommodation of microbes by plants: a common developmental program for symbiosis and disease? Curr Opin Plant Biol 3(4):320-8.

Parniske M. 2008. Arbuscular mycorrhiza: the mother of plant root endosymbioses. Nat Rev Microbiol 6(10):763-75.

Paszkowski U, Kroken S, Roux C, Briggs SP. 2002. Rice phosphate transporters include an evolutionarily divergent gene specifically activated in arbuscular mycorrhizal symbiosis. Proc Natl Acad Sci U S A 99(20):13324-9.

Paszkowski U. 2006. Mutualism and parasitism: the yin and yang of plant symbioses. Curr Opin Plant Biol 9(4):364-70.

Paulsen IT, Skurray RA. 1994. The POT family of transport proteins. Trends Biochem Sci 19(10):404.

Penmetsa RV, Cook DR. 1997. A Legume Ethylene-Insensitive Mutant Hyperinfected by its Rhizobial Symbiont. Science 275(5299):527-30.

Pirozynski KA, Malloch DW. 1975. The origin of land plants: a matter of mycotrophism. Biosystems 6(3):153-64.

Petersen B, Petersen TN, Andersen P, Nielsen M, Lundegaard C. 2009. A generic method for assignment of reliability scores applied to solvent accessibility predictions. BMC Structural Biology

Plett JM, Kemppainen M, Kale SD, Kohler A, Legue V, Brun A, Tyler BM, Pardo AG, Martin F. 2011. A Secreted Effector Protein of Laccaria bicolor Is Required for Symbiosis Development. Curr Biol 21(14):1197-203.

Portillo M, Lindsey K, Casson S, Garcia-Casado G, Solano R, Fenoll C, Escobar C. 2009. Isolation of RNA from laser-capture-microdissected giant cells at early differentiation stages suitable for differential transcriptome analysis. Mol Plant Pathol 10(4):523-35.

Prouse MB, Campbell MM. 2011. The interaction between MYB proteins and their target DNA binding sites. Biochim Biophys Acta 1819(1):67-77.

Pumplin N, Harrison MJ. 2009. Live-cell imaging reveals periarbuscular membrane domains and organelle location in Medicago truncatula roots during arbuscular mycorrhizal symbiosis. Plant Physiol 151(2):809-19.

Pumplin N, Mondo SJ, Topp S, Starker CG, Gantt JS, Harrison MJ. 2010. Medicago truncatula Vapyrin is a novel protein required for arbuscular mycorrhizal symbiosis. Plant J 61(3):482-94.

Punta M, Coggill PC, Eberhardt RY, Mistry J, Tate J, Boursnell C, Pang N, Forslund K, Ceric G, Clements J, Heger A, Holm L, Sonnhammer EL, Eddy SR, Bateman A, Finn RD. 2012. The Pfam protein families database. Nucleic Acids Res 40(Database issue):D290-301.

Pysh LD, Wysocka-Diller JW, Camilleri C, Bouchez D, Benfey PN. 1999. The GRAS gene family in Arabidopsis: sequence characterization and basic expression analysis of the SCARECROW-LIKE genes. Plant J 18(1):111-9.

Q

Quackenbush J, Cho J, Lee D, Liang F, Holt I, Karamycheva S, Parvizi B, Pertea G, Sultana R, White J. 2001. The TIGR Gene Indices: analysis of gene transcript sequences in highly sampled eukaryotic species. Nucleic Acids Res 29(1):159-64.

Quandt HJ, Pühler A, Broer I. 1993. Transgenic root nodules of Vicia hirsuta: a fast and efficient system for the study of gene expression in indeterminate-type nodules. Mol.Plant Microbe Interact. 6, 699-706.

R

Radutoiu S, Madsen LH, Madsen EB, Felle HH, Umehara Y, Gronlund M, Sato S, Nakamura Y, Tabata S, Sandal N, Stougaard J. 2003. Plant recognition of symbiotic bacteria requires two LysM receptor-like kinases. Nature 425(6958):585-92.

Ramsay K, Wang Z, Jones MG. 2004. Using laser capture microdissection to study gene expression in early stages of giant cells induced by root-knot nematodes. Mol Plant Pathol 5(6):587-92.

Rausch C, Daram P, Brunner S, Jansa J, Laloi M, Leggewie G, Amrhein N, Bucher M. 2001. A phosphate transporter expressed in arbuscule-containing cells in potato. Nature 414(6862):462-70.

Redecker D, Kodner R, Graham LE. 2000. Glomalean fungi from the Ordovician. Science 289(5486):1920-1.

Requena N, Breuninger M, Franken P, Ocon A. 2003. Symbiotic status, phosphate, and sucrose regulate the expression of two plasma membrane H+-ATPase genes from the mycorrhizal fungus Glomus mosseae. Plant Physiol 132(3):1540-9.

Rival P, de Billy F, Bono JJ, Gough C, Rosenberg C, Bensmihen S. 2012. Epidermal and cortical roles of NFP and DMI3 in coordinating early steps of nodulation in Medicago truncatula. Development 139(18):3383-91.

Roche P, Maillet F, Plazanet C, Debelle F, Ferro M, Truchet G, Prome JC, Denarie J. 1996. The common nodABC genes of Rhizobium meliloti are host-range determinants. Proc Natl Acad Sci U S A 93(26):15305-10.

Rose R. 2008. Medicago truncatula as a model for understanding plant interactions with other organisms, plant development and stress biology: past, present and future. Funct. Plant Biol. 35:253-264.

Rozen S, Skaletsky H. 2000. Primer3 on the WWW for general users and for biologist programmers. Methods Mol Biol 132:365-86.

S

Salzer P, Bonanomi A, Beyer K, Vogeli-Lange R, Aeschbacher RA, Lange J, Wiemken A, Kim D, Cook DR, Boller T. 2000. Differential expression of eight chitinase genes in Medicago truncatula roots during mycorrhiza formation, nodulation, and pathogen infection. Mol Plant Microbe Interact 13(7):763-77.

Sanders IR, Croll D. 2010. Arbuscular mycorrhiza: the challenge to understand the genetics of the fungal partner. Annu Rev Genet 44:271-92.

Sagan M, Morandi D, Tarenghi E, Duc G. 1995. Selection of nodulation and mycorhizal mutants in the model plant Medicago truncatula Gaertn after gamma rays mutagenesis.Plant Science 111**:** 63-71.

Schaarschmidt S, González M, Roitsch T, Strack D, Sonnewald U, Hause B. 2007. Regulation of arbuscular mycorrhization by carbon. The symbiotic interaction cannot be improved by increased carbon availability accomplished by root-specifically enhanced invertase activity. Plant Physiol. 143:1827-1840.

Schaarschmidt S, Hause B. 2008. Apoplastic invertases: Multi-faced players in the arbuscular mycorrhization. Plant Signal Behav 3(5):317-9.

Schütze K, Becker B, Bernsen M, Björnsen T, Broksch D, Bush C, Clement-Sengewald A. 2003. Tissue microdissection, laser pressure catapulting. In Bowtell D, Sambrook J, eds. DNA Microarrays: A Molecular Cloning Manual. Cold Spring Harbor, NY, Cold Spring Harbor Laboratory Press, 331–356

Schutze K, Lahr G. 1998. Identification of expressed genes by laser-mediated manipulation of single cells. Nat Biotechnol 16(8):737-42.

Schüssler A, Schwarzott D, Walker C. 2001. A new fungal phylum, the Glomeromycota: phylogeny and evolution. Mycol. Res. 105:1413-1421.

Siciliano V, Genre A, Balestrini R, Cappellazzo G, deWit PJ, Bonfante P. 2007. Transcriptome analysis of arbuscular mycorrhizal roots during development of the prepenetration apparatus. Plant Physiol 144(3):1455-66.

Sieberer BJ, Chabaud M, Fournier J, Timmers AC, Barker DG. 2012. A switch in Ca^{2+} spiking signature is concomitant with endosymbiotic microbe entry into cortical root cells of Medicago truncatula. Plant J 69(5):822-30.

Singh LP, Gill SS, Tuteja N. 2011. Unraveling the role of fungal symbionts in plant abiotic stress tolerance. Plant Signal Behav 6(2):175-91.

Smit P, Raedts J, Portyanko V, Debelle F, Gough C, Bisseling T, Geurts R. 2005. NSP1 of the GRAS protein family is essential for rhizobial Nod factor-induced transcription. Science 308(5729):1789-91.

Smith SE, Smith FA, Jakobsen I. 2003. Mycorrhizal fungi can dominate phosphate supply to plants irrespective of growth responses. Plant Physiol 133(1):16-20.

Smith SE, Read DJ. 2008. Mycorrhizal symbioses. Third edition. Academic Press, London, Cambridge.

Steedman HF. 1957. Polyester wax; a new ribboning embedding medium for histology. Nature 179(4574):1345.

Stekel DJ, Git Y, Falciani F. 2000. The comparison of gene expression from multiple cDNA libraries. Genome Res 10(12):2055-61.

Stockinger H, Walker C, Schüssler A. 2009. 'Glomus intraradices DAOM197198', a model fungus in arbuscular mycorrhiza research, is not Glomus intraradices. New Phytol. 183(1):212-23.

Strack D, Fester T, Hause B, Walter MH. 2001. Die arbuskuläre Mykorrhiza. Biologie in unserer Zeit 31(5):286-295

Stracke S, Kistner C, Yoshida S, Mulder L, Sato S, Kaneko T, Tabata S, Sandal N, Stougaard J, Szczyglowski K, Parniske M. 2002. A plant receptor-like kinase required for both bacterial and fungal symbiosis. Nature 417(6892):959-62.

T

Tadege M, Wen J, He J, Tu H, Kwak Y, Eschstruth A, Cayrel A, Endre G, Zhao PX, Chabaud M, Ratet P, Mysore KS. 2008. Large-scale insertional mutagenesis using the Tnt1 retrotransposon in the model legume Medicago truncatula. Plant J 54(2):335-47.

Takeda N, Haage K, Sato S, Tabata S, Parniske M. 2011. Activation of a Lotus japonicus subtilase gene during arbuscular mycorrhiza is dependent on the common symbiosis genes and two cis-active promoter regions. Mol Plant Microbe Interact 24(6):662-70.

Talukdar T, Gorecka KM, de Carvalho-Niebel F, Downie JA, Cullimore J, Pikula S. 2009. Annexins - calcium- and membrane-binding proteins in the plant kingdom: potential role in nodulation and mycorrhization in Medicago truncatula. Acta Biochim Pol 56(2):199-210.

Tamasloukht M, Sejalon-Delmas N, Kluever A, Jauneau A, Roux C, Becard G, Franken P. 2003. Root factors induce mitochondrial-related gene expression and fungal respiration during the developmental switch from asymbiosis to presymbiosis in the arbuscular mycorrhizal fungus Gigaspora rosea. Plant Physiol 131(3):1468-78.

Tang W, Coughlan S, Crane E, Beatty M, Duvick J. 2006. The application of laser microdissection to in planta gene expression profiling of the maize anthracnose stalk rot fungus Colletotrichum graminicola. Mol Plant Microbe Interact 19(11):1240-50.

Tauris B, Borg S, Gregersen PL, Holm PB. 2009. A roadmap for zinc trafficking in the developing barley grain based on laser capture microdissection and gene expression profiling. J Exp Bot 60(4):1333-47.

Taylor TN, Remy W, Hass H, Kerp H. 1995. Fossil arbuscular mycorrhizae from the Early Devonian. Mycologia 87(4): 560-573

Thevissen K, Terras FR, Broekaert WF. 1999. Permeabilization of fungal membranes by plant defensins inhibits fungal growth. Appl Environ Microbiol 65(12):5451-8.

Thevissen K, Osborn RW, Acland DP, Broekaert WF. 2000. Specific binding sites for an antifungal plant defensin from Dahlia (Dahlia merckii) on fungal cells are required for antifungal activity. Mol Plant Microbe Interact 13(1):54-61.

Thomma BP, Cammue BP, Thevissen K. 2002. Plant defensins. Planta 216(2):193-202.

Timmers AC, Auriac MC, Truchet G. 1999. Refined analysis of early symbiotic steps of the Rhizobium-Medicago interaction in relationship with microtubular cytoskeleton rearrangements. Development 126(16):3617-28.

Tisserant E, Kohler A, Dozolme-Seddas P, Balestrini R, Benabdellah K, Colard A, Croll D, Da Silva C, Gomez SK, Koul R, Ferrol N, Fiorilli V, Formey D, Franken P, Helber N, Hijri M, Lanfranco L, Lindquist E, Liu Y, Malbreil M, Morin E, Poulain J, Shapiro H, van Tuinen D, Waschke A, Azcon-Aguilar C, Becard G, Bonfante P, Harrison MJ, Kuster H, Lammers P, Paszkowski U, Requena N, Rensing SA, Roux C, Sanders IR, Shachar-Hill Y, Tuskan G, Young JP, Gianinazzi-Pearson V, Martin F. 2011. The transcriptome of the arbuscular mycorrhizal fungus Glomus intraradices (DAOM 197198) reveals functional tradeoffs in an obligate symbiont. New Phytol 193(3):755-69.

U

Uehlein N, Fileschi K, Eckert M, Bienert GP, Bertl A, Kaldenhoff R. 2007. Arbuscular mycorrhizal symbiosis and plant aquaporin expression. Phytochemistry 68(1):122-9.

Usadel B, Nagel A, Thimm O, Redestig H, Blaesing OE, Palacios-Rojas N, Selbig J, Hannemann J, Piques MC, Steinhauser D, Scheible WR, Gibon Y, Morcuende R, Weicht D, Meyer S, Stitt M. 2005. Extension of the visualization tool MapMan to allow statistical analysis of arrays, display of corresponding genes, and comparison with known responses. Plant Physiol 138(3):1195-204.

V

Van Wees SC, Van der Ent S, Pieterse CM. 2008. Plant immune responses triggered by beneficial microbes. Curr Opin Plant Biol 11(4):443-8.

Venkateshwaran M, Cosme A, Han L, Banba M, Satyshur KA, Schleiff E, Parniske M, Imaizumi-Anraku H, Ane JM. 2012. The recent evolution of a symbiotic ion channel in the legume family altered ion conductance and improved functionality in calcium signaling. Plant Cell 24(6):2528-45.

Verma DP, Hong Z. 1996. Biogenesis of the peribacteroid membrane in root nodules. Trends Microbiol 4(9):364-8.

Vierheilig H, Coughlan AP, Wyss U, Piche Y. 1998. Ink and vinegar, a simple staining technique for arbuscular-mycorrhizal fungi. Appl Environ Microbiol 64(12):5004-7.

Vieweg MF, Fruhling M, Quandt HJ, Heim U, Baumlein H, Puhler A, Küster H, Andreas MP. 2004. The promoter of the Vicia faba L. leghemoglobin gene VfLb29 is specifically activated in the infected cells of root nodules and in the arbuscule-containing cells of mycorrhizal roots from different legume and nonlegume plants. Mol Plant Microbe Interact 17(1):62-9.

W

Walter MH, Hans J, Strack D. 2002. Two distantly related genes encoding 1-deoxy-d-xylulose 5-phosphate synthases: differential regulation in shoots and apocarotenoid-accumulating mycorrhizal roots. Plant J 31(3):243-54.

Weidmann S, Sanchez L, Descombin J, Chatagnier O, Gianinazzi S, Gianinazzi-Pearson V. 2004. Fungal elicitation of signal transduction-related plant genes precedes mycorrhiza establishment and requires the dmi3 gene in Medicago truncatula. Mol Plant Microbe Interact 17(12):1385-93.

Wesley SV, Helliwell CA, Smith NA, Wang MB, Rouse DT, Liu Q, Gooding PS, Singh SP, Abbott D, Stoutjesdijk PA, Robinson SP, Gleave AP, Green AG, Waterhouse PM. 2001. Construct design for efficient, effective and high-throughput gene silencing in plants. Plant J 27(6):581-90.

Wiese M. 2007. Analyse von Fusionen des Medicago truncatula Annexingens MtAnn2 mit dem GFP-Reportergen zur subzellulären Lokalisation in Wurzelgeweben & Promotor-GUS-Fusion des Promotors pMtAnn2 zur Analyse der Promotoraktivität. Universität Bielefeld

Wulf A, Manthey K, Doll J, Perlick AM, Linke B, Bekel T, Meyer F, Franken P, Küster H, Krajinski F. 2003. Transcriptional changes in response to arbuscular mycorrhiza development in the model plant Medicago truncatula. Mol Plant Microbe Interact 16(4):306-14.

Y

Young ND, Udvardi M. 2009. Translating Medicago truncatula genomics to crop legumes. Curr Opin Plant Biol 12(2):193-201.

Young ND, Debelle F, Oldroyd GE, Geurts R, Cannon SB, Udvardi MK, Benedito VA, Mayer KF, Gouzy J, Schoof H, Van de Peer Y, Proost S, Cook DR, Meyers BC, Spannagl M, Cheung F, De Mita S, Krishnakumar V, Gundlach H, Zhou S, Mudge J, Bharti AK, Murray JD, Naoumkina MA, Rosen B, Silverstein KA, Tang H, Rombauts S, Zhao PX, Zhou P, Barbe V, Bardou P, Bechner M, Bellec A, Berger A, Berges H, Bidwell S, Bisseling T, Choisne N, Couloux A, Denny R, Deshpande S, Dai X, Doyle JJ, Dudez AM, Farmer AD, Fouteau S, Franken C, Gibelin C, Gish J, Goldstein S, Gonzalez AJ, Green PJ, Hallab A, Hartog M, Hua A, Humphray SJ, Jeong DH, Jing Y, Jocker A, Kenton SM, Kim DJ, Klee K, Lai H, Lang C, Lin S, Macmil SL, Magdelenat G, Matthews L, McCorrison J, Monaghan EL, Mun JH, Najar FZ, Nicholson C, Noirot C, O'Bleness M, Paule CR, Poulain J, Prion F, Qin B, Qu C, Retzel EF, Riddle C, Sallet E, Samain S, Samson N, Sanders I, Saurat O, Scarpelli C, Schiex T, Segurens B, Severin AJ, Sherrier DJ, Shi R, Sims S, Singer SR, Sinharoy S, Sterck L, Viollet A, Wang BB, Wang K, Wang M, Wang X, Warfsmann J, Weissenbach J, White DD, White JD, Wiley GB, Wincker P, Xing Y, Yang L, Yao Z, Ying F, Zhai J, Zhou L, Zuber A, Denarie J, Dixon RA, May GD, Schwartz DC, Rogers J, Quetier F, Town CD, Roe BA. 2011. The Medicago genome provides insight into the evolution of rhizobial symbioses. Nature 480(7378):520-4.

Z

Zhang Q, Blaylock LA, Harrison MJ. 2010. Two Medicago truncatula half-ABC transporters are essential for arbuscule development in arbuscular mycorrhizal symbiosis. Plant Cell 22(5):1483-97.

ABBREVIATIONS

µg	microgram
µl	microliter
µm	micrometer
AM	arbuscular mycorrhiza
AMF	arbuscular mycorrhizal fungi
APP	appressorial areas
ARB	cortical cells containing arbuscules
aRNA	amplified RNA
BLAST	basic local alignement search tool
bp	basepairs
CBF	CAAT-box binding transcription factor
CCR	cortical cells from non-colonized control roots
cDNA	copy DNA
CMR	cortical cells from mycorrhizal roots
CSP	common symbiotic pathway
cv.	cultivar
DCL	Dicer-like
DFCI	Dana Farber Cancer Institute
DNA	deoxyribonucleic acid
dpi	days post inoculation
EPI	epidermal cells from mycorrhizal roots
ERF	ethylene-responsive transcription factor
EST	expressed sequence tag
et al.	et alii
FDR	false discovery rate
GEA	GeneExpressionAtlas
GFP	green fluorescent protein
GO	Gene Ontology
GUS	beta-glucuronidase
*gus*Aint	*gus*A gene containing an intron
hpRNA	hairpin RNA
IR	infrared
IVT	in vitro transcription
KOG	EuKaryotic Orthologous Group
LAM	Laser-assisted microdissection
LCM	Laser capture microdissection
LCO	lipo-chitooligosaccharide
LEM	Laser excision microdissection
LMPC	Laser microdissection and pressure catapulting
min	minutes

ml	milliliter
mM	millimolar
mRNA	messenger RNA
NAP	non-appressorial controls
ng	nanogram
PAM	peri-arbuscular membrane
PBM	peri-bacteroid membrane
PBS	Phosphate Buffered Saline
PCR	polymerase chain reaction
pHG8	pHellsgate8
PIT	pre-infection-thread
PPA	pre-penetration apparatus
RISC	RNA induced silencing complex
RLC	root length colonization
RMA	Robust Multichip Average
RNA	ribonucleic acid
RNAi	RNA-interference
RNS	root nodule symbioses
RT-PCR	reverse transcription polymerase chain reaction
siRNAs	small interfering RNAs
SSH	Suppressive subtractive hybridization
SYM	symbiotic
TFs	transcription factors
UTR	untranslated region
UV	ultraviolet
WGA	wheat germ agglutinin

LIST OF FIGURES

LIST OF TABLES

SUPPLEMENT

Supplemental Figures – Chapter I

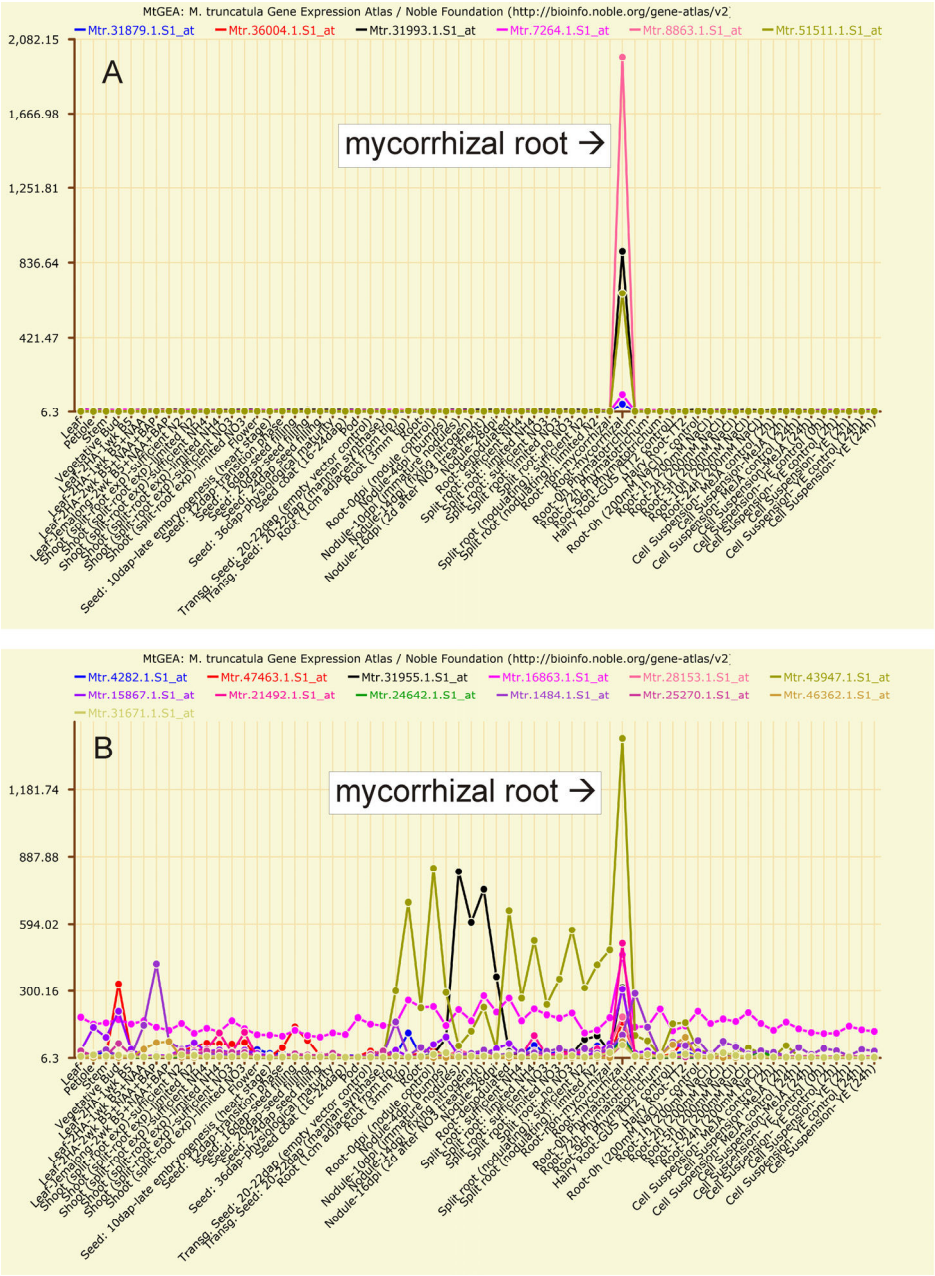

Supplemental Figure S_I_1: Identification of AM-specific and AM-enhanced transcription factor genes. The expression of the 20 genes encoding transcriptional regulators (including 2 genes from *Glomus intraradices*) was analysed in the *Medicago* Gene Expression Atlas (He *et al*. 2009). While six genes were specifically expressed in AM tissues (A), 13 were activated stronger in mycorrhizal vs non-mycorrhizal roots (B). In some cases, marked expression in additional symbiotic or non-symbiotic conditions was evident for the genes displayed in (B).

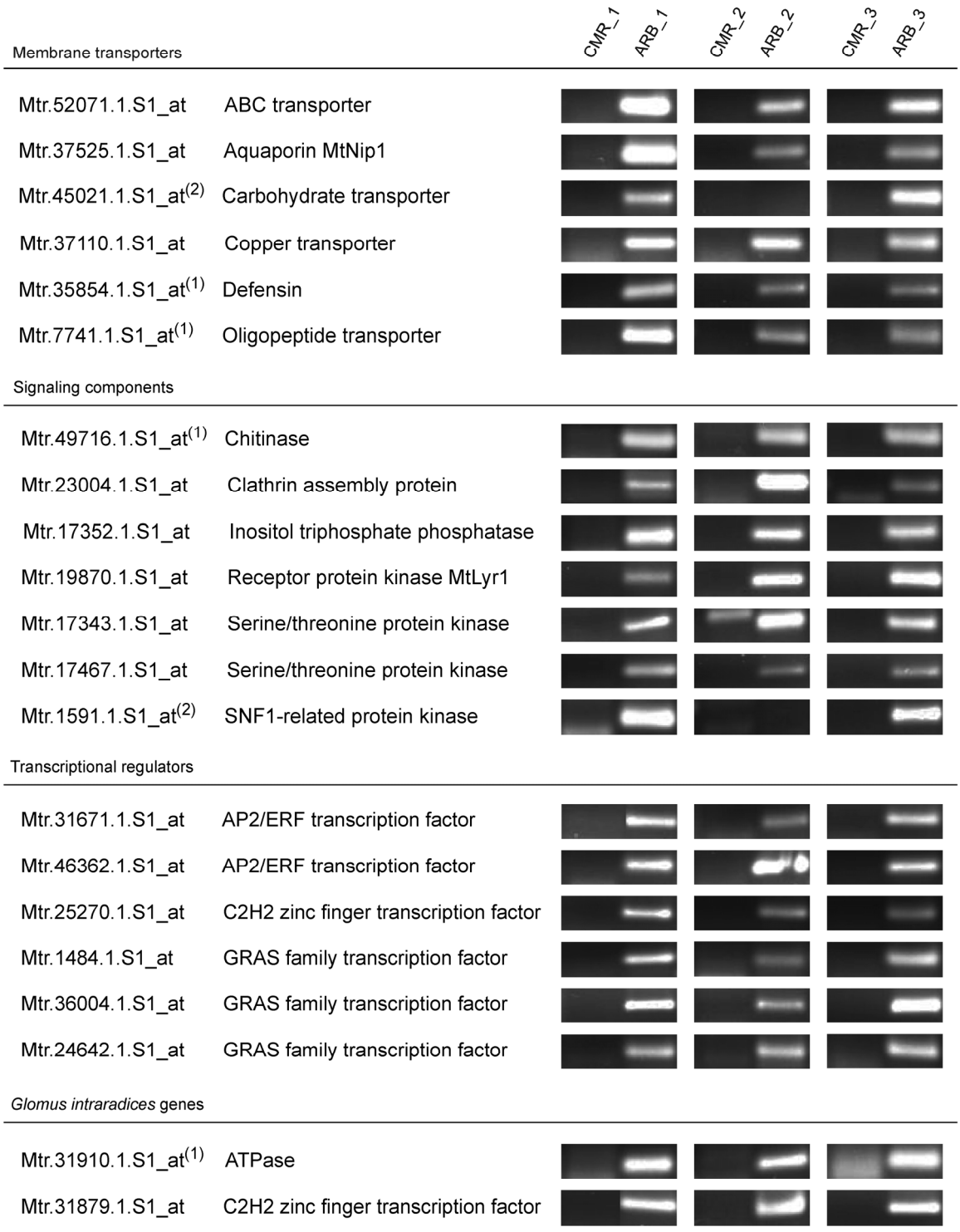

Supplemental Figure S_I_2: Genes exclusively expressed in arbuscule-containing cells.
Gel-electrophoresis of the final real-time RT-PCR amplification products representing those genes classified as arbuscule-specific in Figure I_5. Gene expression was measured in three biological replicates of two different cell-types: cortical cells from mycorrhized roots (CMR), and arbuscule-containing cells (ARB). All amplified fragments had the correct sizes. For Mtr.17343.1.S1_at, Mtr.1591.1.S1_at, and Mtr.31910.1.S1_at, an unspecific amplification product is visible in CMR_2, CMR_1, and CMR_3, respectively, which had a different size and melting temperature than the specific product. Footnotes are as indicated in Figure I_5.

```
MtCbf1  ATGAGACAAGCAGGTGCATATTCAGGTATACTAAATGGTGGCATAGGAAG   50
        ||||||||||||||||||||||||||||| ||||||||||||||||||
MtCbf2  ATGAGACAAGCAGGTGCATATTCAGGTATAGTAAATGGTGGCATAGGAAG   50

MtCbf1  AACAGGTCCACATTCATTACCATTAGCAAGAATAAAGAAGATAATGAAGA  100
        ||||||||||||||||||||||||||||||||||||||||||||||||||
MtCbf2  AACAGGTCCACATTCATTACCATTAGCAAGAATAAAGAAGATAATGAAGA  100

MtCbf1  ATTCTAGTGAAGACGTGAAAATGATATCAGGTGTAGCTCCAATTGTTTTC  150
        |||||||||||||||||||||||||||||| || ||||||||||||||||
MtCbf2  ATTCTAGTGAAGACGTGAAAATGATATCAGGGGTTGCTCCAATTGTTTTC  150

MtCbf1  TCAAAAGCTTGTGAACTTTTCATTGAAGAACTTACAAGAAGGTCTTGGAT  200
        ||||||||||||||||||||||||||||||||||||||||||||||||||
MtCbf2  TCAAAAGCTTGTGAACTTTTCATTGAAGAACTTACAAGAAGGTCTTGGAT  200

MtCbf1  TATGGCTATTGATGCTAAAAGAAGAACTTTGAATAAAGAAGATGTTGCTT  250
        ||||||||||||||||||||||||||||||||||||||||||||||||||
MtCbf2  TATGGCTATTGATGCTAAAAGAAGAACTTTGAATAAAGAAGATGTTGCTT  250

MtCbf1  CTGCTGTTATAGCTACTGATATTTTTGATTTTTTGATCACTTTGGTTTCT  300
        ||||||||||||||||||||||||||||||||||||||||||||||||||
MtCbf2  CTGCTGTTATAGCTACTGATATTTTTGATTTTTTGATCACTTTGGTTTCT  300

MtCbf1  AATTCTGATTC---CACTGATGATACCACTGTCATGCAAATGGAAACTAT  347
        ||||||||||||    |||||||  |||||| ||||||||||||||| |||
MtCbf2  AATTCTGATTCTAGTACTGATGCCACCACTCTCATGCAAATGGAAAGTAT  350

MtCbf1  GAATTCTTCTTAA                                      360

MtCbf2  ATGA                                               354
```

Supplemental Figure S_I_3: Alignment of the coding sequences of the two CAAT-box binding transcription factor genes *MtCbf1* and *MtCbf2*.
Identical nucleotides are marked by asterisks. The start and stop codons are depicted in bold type.

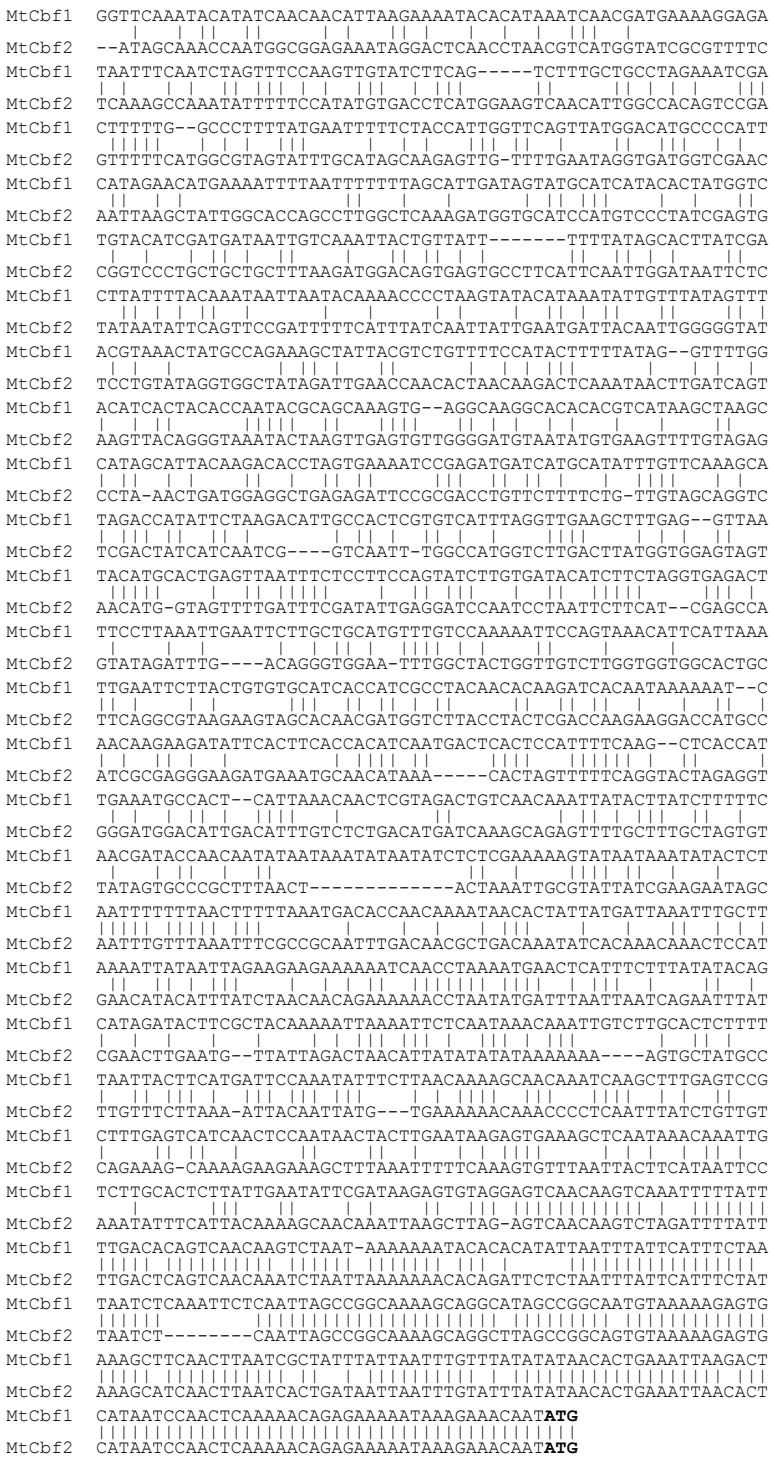

Supplemental Figure S_I_4: Alignment of promoter sequences of the two CAAT-box binding transcription factor genes *MtCbf1* and *MtCbf2*.

Sequences shown represent the regions from -1513 to +3 for *MtCbf1* and from -1486 to +3 for *MtCbf*2. Identical nucleotides are marked by asterisks. The start codon is depicted in bold type.

Supplemental Tables – Chapter I

All supplemental Tables can be found on the data CD enclosed in this work.

Supplemental Table S_I_1

Gene expression in *Medicago truncatula* roots in response to *Glomus intraradices* colonization (28 dpi, at 20 µM phosphate), *Glomus mosseae* colonization (28 dpi, at 20 µM phosphate), and a 28 day treatment with 2 mM phosphate. Roots grown for 28 days in the presence of 20 µM phosphate were used as common controls.

Supplemental Table S_I_2

Medicago truncatula genes co-activated in response to *Glomus intraradices* and *Glomus mosseae* colonization. The individual sheets contain selected subsets of genes, as explained in the Supplemental file.

Supplemental Table S_I_3

AM-activated *Medicago truncatula* genes encoding membrane transporters.

Supplemental Table S_I_4

AM-activated *Medicago truncatula* genes encoding signaling-related proteins.

Supplemental Table S_I_5

Real time RT-PCR primers used in this study and size of predicted PCR-products.

Supplemental Tables – Chapter II

All supplemental Tables can be found on the data CD enclosed in this work.

Supplemental Table S_II_1a

Complete dataset obtained from cell-types of mature mycorrhizal roots (ARB, CMR, EPI).

Supplemental Table S_II_1b

Complete dataset obtained from cell-types of roots harbouring first infection units (APP, NAP).

Supplemental Table S_II_2

Expressed genes in the three cell-types from mature mycorrhizal roots (ARB, CMR, EPI).

Supplemental Table S_II_3

Expression types in the samples APP and NAP. KOG classifications and comparisons to the AM core set are included.

Supplemental Table S_II_4

Fungal genes.

Supplemental Table S_II_5

Expression types in the samples ARB, CMR and EPI. KOG classifications and comparisons to the AM core set are included.

Supplemental Table S_II_6

Seven groups of genes as defined in Figure II_11.

Supplemental Table S_II_7

Overview of transcription factor genes.

Supplemental Table S_II_8

Comparison of the 100 genes most strongly induced in ARB to the results of Gaude *et al*. (2012).

Supplemental Figures – Chapter III

MtBcp1

ATGGCTTCTTCTCGTGTAGTTTTGATCCTTTCCATTTCCATGGTTTTACTTTCATCAGTTGCAATTGCTGCAACTGATTATATTGTTGGTGAT
GACAAGGGTTGGACCGTTGATTTTGATTACACTCAATGGGCTCAAGACAAAGTTTTTCGTGTTGGAGACAACCTAGTTTTCAACTATGACCCT
TCAAGGCACAATGTTTTTAAAGTGAATGGCACACTCTTCCAGAGCTGCACTTTTCCACCAAAAAACGAAGCACTTTCTACCGGAAAGGATATC
ATTCAACTAAAAACTGAAGGAAGAAAGTGGTATGTTTGTGGAGTTGCTGATCACTGTTCGGCTCGTCAAATGAAGTTGGTCATCACTGTTCTA
GCCGAAGGTGCACCTGCTCCTTCTCCACCACCTTCTTCTGATGCTCACTCTGTTGTTTCATCTCTGTTTGGAGTTGTCATGGCAATCATGGTT
GCAATTGCAGTCATCTTTGCA**TGA**GACACTTACGAAGCTTTATATTGTTATTAATACAACTATTTGTGTTAATCTTTCCATCATTGGCAATAT
ATATTGCTATATTTGTTTGAATTTTTTGAATTATATGATTATTTATGTTAATTAATGTCATTGTAATTTGATCCTCAATTTTATATCTTGTTA
TGTTTTGGTTTGTTCTCGAGTTTCCTTCAAATCAGATTGTAACTCTCCCATTCATTAAGAATTTGTTATTAAAAGTGTTAGCTTACTTCTTAT

MtAnn2

ATGGCTACTCTTGTTACAATAAAATCATCTCCTGTGGAAGATGCTGAGGCTCTCCAAAAGGCCTTTAAAGGATGGGGGACTGATGAGAAGAG
TGTTATCACAATATTAGGTCATAGAAATGTTTATCAGAGACAACAAATCAGAAAATCTTATCAGGAAATTTACCAAGAGGATATCCTCAAAC
GCCTTGAATCTGAACTCTCTGGTGACTTTGAGAGAGCTGTGTACCGTTGGATGCTGGAACCTGCGGATCGCGATGCTGTTTTGGCCAATGTA
GCCATCAAGGATGGAAGCAAAAGTTACCATGTGATTATTGAAATTGTTTCTGTTCTTTCACCTGAAGAAGTGTTGGCAATGAGACGTGCTTA
TCATAACCGTTACAAGCATTCTTTAGAAGAAGATTTAGCTGCTCATACCACCGGTCATCTTCGCCAGCTGTTGGTTGGATTGGTGACCTCGT
TTAGATATGGCGGTGCTGAGATAAATCCGAAATTGGCAAAAACTGAAGCTGACATTCTTCATGAATCAATCAAAGAGAAAAAAGGAAATCAT
GAAGAAGCCATTAGAATCCTTACTACAAGGAGCAAGACTCAGCTTTTGGCAACTTTCAACCGCTACAGAGATGACCATGGCATTTCCATAAC
TAAGAAACTGTTGGATAATGCATCTGATGATTTTCACAAGGCATTGCACACTACGATTCGATGCATCAATGACCATAAGAAGTACTATGAAA
AGATTCTACGCGGTGCGTTGAAAAGGGTTGGAACCGATGAGGATGGACTGACTCGTGTGGTCGTGACAAGAGCCGAGAAAGATCTGAAGGAC
ATCAAAGAGCTGTATTATAAGAGAAACAGTGTTCACCTTGAGGATGCAGTGGCAAAGGAAATTTCAGGAGACTACAAGAAGTTCATCCTTAC
CTTGTTGGGGAAGCAAGAT**TGA**

MtMyb1

GGTACGCAGGGGGACCTCTTTCAGACCCCAAGAGTTCAGTT**ATG**GGTTCCACTCGCTCAGATGGCTCTGCCACACACAAAGAACGCTTAAGA
TGGACACAACAACTCCATGATCTCTTTGTGGAGGCTGTAAATAGGCTTGGGGGTGCAGATAGGGCAACACCAAAAGGTATATTGAAAGGAAT
GAAGGCTATGGGAGTTTCAGAATTGAAAATATTACACGTCAAAAGCCACTTGCAGAAATACAGGATCTCCAAATTGATTCCAGAATCCACCA
CAAGAGGAAAAATTGAGAAGAGAAGCATATCAGATATACTGCCAAATTTCTGTTCTATATCTGCTCTTCAGCTAAAGGAAGTCCTTCAAATG
CAGGCAGAGGTGCAAAACCGCATGAGTGATAAAGTTGAGGTTCCAAAAAGCTTGAAGCTGAAGATTGAAGCACAAGGAAAGTATCTAGCCAG
AATTGGACAAAGTAATCAAATCAGAACAATTACAAGAAAAGCTTGCAAGCCTTTTGTTGGTAAAGCAACCCCTTTGCCCTCTCTTTCCGAGG
AATCTGAATCCTTTAAAACACAATCCGACGAAGAACATCGAACAGCGAAAAAGAAAAAGGTCACAAATGAGAATGTTTTTCCTACAGGTTTT
GAACTGGGATCATCCACTACCTCGGAATTCAGCAACCAAACCTGGAACCTTTCTTGGAGTCAGCTGGCTGAAGCAACCTACCAATCACCTTT
GGTGCCTAGTTTCTTATTA**TAG**

MtGras2

AATTTTCCTGAGGCTGATGCTTGATTTCTGATTCGCCAGGTCGATTATTACGATCTCTTCTCGCATAAGACATCTTATTCATCATCGTAGT**A**
TGGACTCGCAGCAGCTTTATAGTTACAGTATGAGTAATGCAGGATTACCTTACATGTCATCTTTTCCATCACTGCCAAATGGTTTGCTTGGA
TCCTTGAAAGTTGGCTTTGGAAACTCACCCGATTCACCGTTTTCCTCTCATTTTGATTCCGATACTCTTTCTGCATTTAGTGACAGCCACGA
GCAACACAACTCAGGAGAAATTCTCTCTGGTATAAGCCCTTCGTGTAACTCATCACTTGAAACCAATCATTATACGCAAAGATCATTCTCTT
CGATCAACAGTCTCAAAGACAGTTTGCAACTATATTCTGCTAGAAATTCTTTTCTACCAAGTAACCAGAAAATCAGACACGCCTTGTTGGAA
CTAGAAACTGCTCTGATGGCCCCCGATGATAACGAAGTTACCACATCTAATTCTTCATTGGGTGAGAGCATCAAGGAAACAGCATCCGGCCC
GAGATATAGATCATGGAGTAATGAGCACCAAGGGTCACAATATATTCAAAGTCAACCGTCACATGTTACCAGCAGTAGCAGGCAATCAAATG
AAGCAGTGCATGTAGAGAAACGACGTAAGTTGGAAGAGGATTCATCTCTACAAGGGTTTCCATCGGGCGATTTGAAGCAATTACTGATTGCA
TGTGCCAAAGCCATGGCTGAAAATAACACAGAACTTTTTGACCGATTGATAGAAACGGCTAGAAATGCCGTGTCTATCAATGGGGAGCCAAT
CCAGAGGCTCGGTGCTTATATGGTAGAAGGTCTTGTTGCAAGGACAGAAGCGTCAGGGAATAGTATCTATCATGCCCTTAAGTGCAGAGAGC
CTGAAGGTGAAGAATTACTCACTTACATGCAACTGCTTTTCGAAATCTGTCCCTACTTAAAATTTGGTTACATGGCTGCCAATGGAGCCATT
GCCGAAGCTTGCAGGAATGAGGATCACATACACATCAT
AGACTTCCAAATTGCTCAAGGAACTCAATGGATGACACTTCTTCAAGCTCTTGCCGCGAGACCTGGTGGGGCACCCCACGTGCGGATCACAG
GAATCGACGATCCAGTCTCTAAATATGCCCGTGGCAAGGGACTCGAAGTAGTTGGAGAGAGATTGTCCTTGATGTCTAAGAAATTCGGCATA
CCGGTTGAGTTTCATGGGATTCCTGTTTTCGGTCCAGATGTGACAAGGGACATGCTTGATATCAGACACGGAGAAGCTTTGGCGGTGAATTT
TCCACTGCAGCTCCATCACACAGCTGATGAGAGTGTTGATGTGAATAATCCAAGGGATGGACTTTTGAGATTGGTGAAGTCTCTCTCTCCTA
AAGTGGTCACCCTTGTGGAGCAAGAATCAAACACAAACACAACACCTTTCTTCAACAGGTTCATAGAAACTCTAGACTACTACTTGGCAATC
TTCGAGTCCATCGATGTCACCCTCTCAAGAAATAGCAAGGAGAGGATTAATGTGGAGCAACATTGTTTGGCCCGGGATATCGTCAATGTCAT
TGCGTGTGAAGGAAAAGAAAGGGTCGAGCGACACGAACTGTTTGGTAAGTGGAAGTCTAGGTTGACAATGGCCGGATTTCGTCAATGTCCTT
TGAGTTCTTATGTGAATTCTGTTATAAGAAGCCTTCTGAGATGCTATTCAGAGCACTATACACTAGTTGAGAAAGATGGGGCAATGCTCTTA
GGGTGGAAGAGCAGAAATTTGATATCTGCTTCAGCTTGGCAT**TGA**

Supplemental Figure S_III_1: Target sequences and RT-PCR amliplificate sequences.
For each of the four candidate genes, the coding sequence is displayed. Start- and Stop-codons are printed in bold. If target sequences or RT-PCR amplificates cover the 5' or 3' prime regions, those are shown, too. Target sequences are highlighted in red and for *MtBcp1* the target sequence of *MtBcp1*(b)-RNAi is underlined to distinguish between MtBcp1(a) and MtBcp1(b). Sequences of RT-PCR-amplificates are highlighted in blue, while primer annealing sites are underlined.

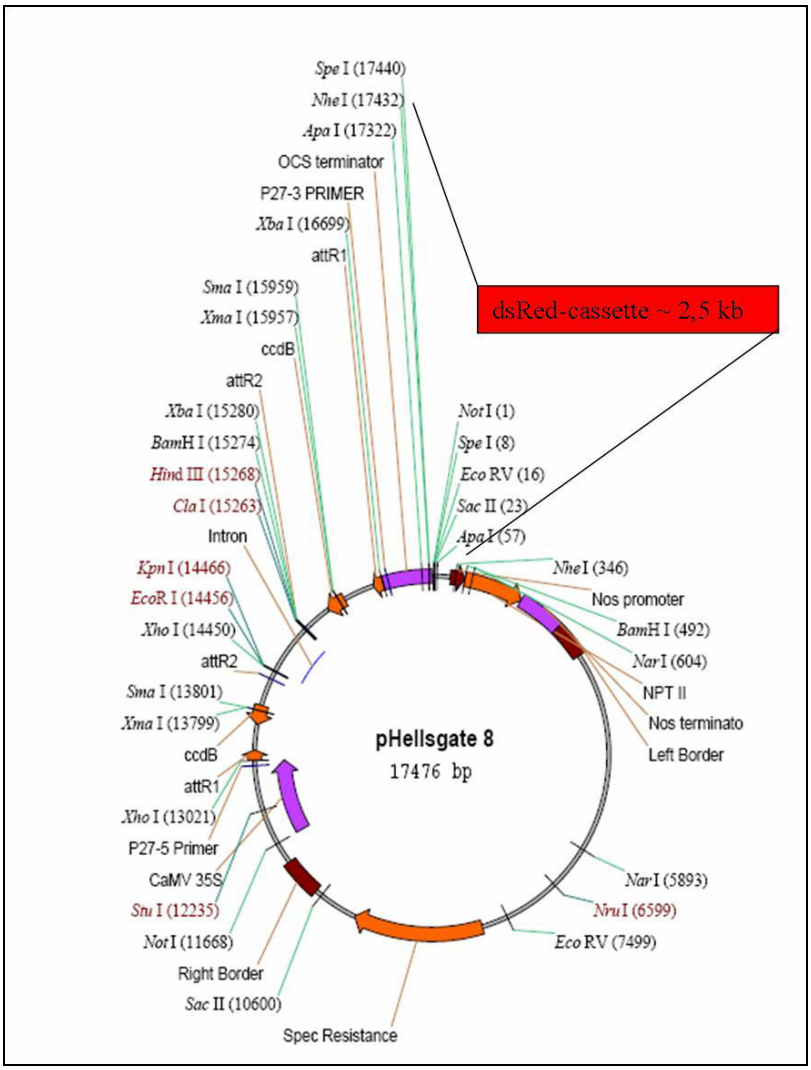

Supplemental Figure S_III_2: Schematic overview of the binary vector pHellsgate (pHG8).
The diagram shows restriction sites, primer binding sites and gene cassettes. ORFs and primer binding sites are marked in orange, promoters and terminators in pink. The region between left and right border (brown) contains the RNAi-cassette consisting of the CaMV 35S promoter, two reverse complementary *ccdB*-genes flanked by the attR-sites used for recombination, the central intron and the OCS terminator, as well as the NPTII-cassette mediating Kanamycin-resistance in plants. The dsRed-cassette (red) was inserted between the other two cassettes using the *Nhe*I restriction sites.

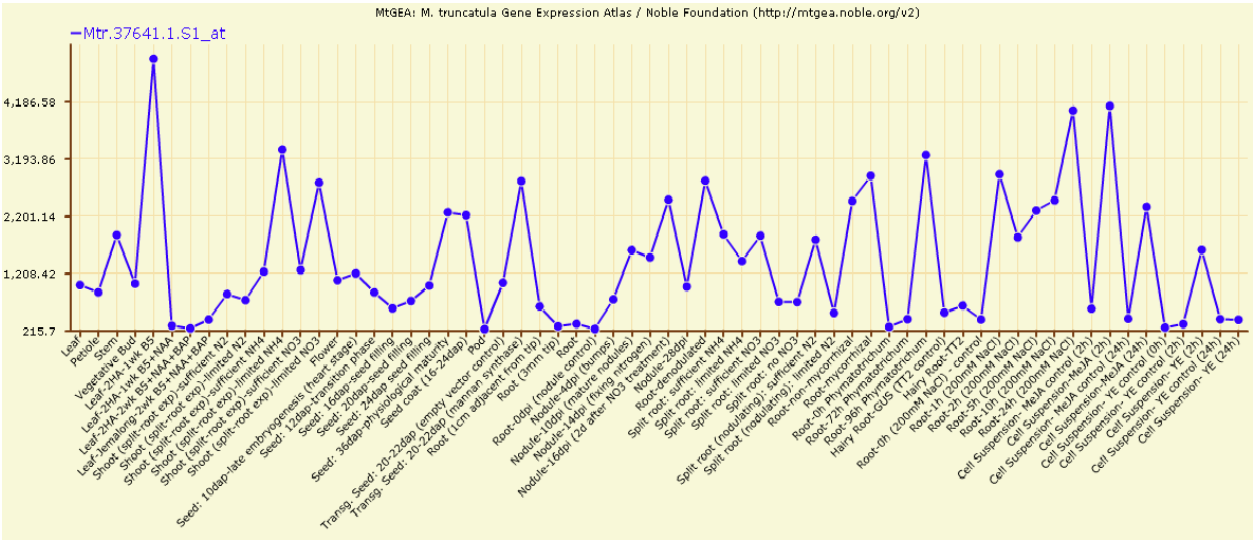

Supplemental Figure S_III_3: *In silico* gene expression profile of *MtGRAS2*.
The expression profile was generated via the *Medicago truncatula* GeneExpressionAtlas (Benedito *et al*. 2008). Only slight differences between expression levels of the transcription factor gene in mycorrhizal and non-mycorrhizal roots are visible. The gene is also expressed in leafs, shoots and seeds.

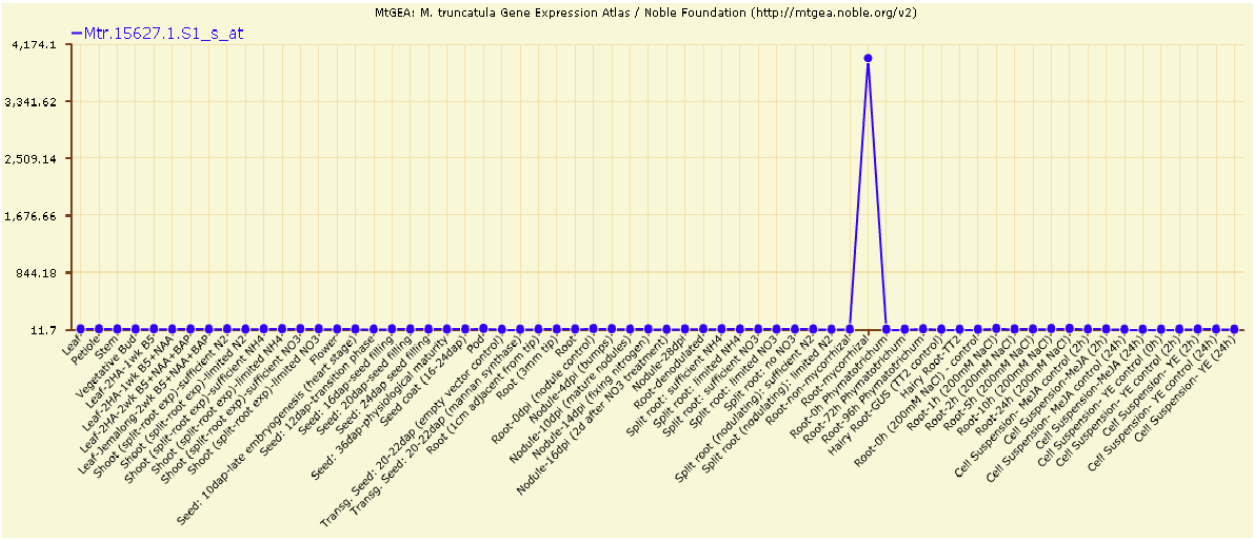

Supplemental Figure S_III_4: *In silico* gene expression profile of *MtBcp1*.
The expression profile was generated via the *Medicago truncatula* GeneExpressionAtlas (Benedito *et al*. 2008). The gene is exclusively expressed in mycorrhizal roots.

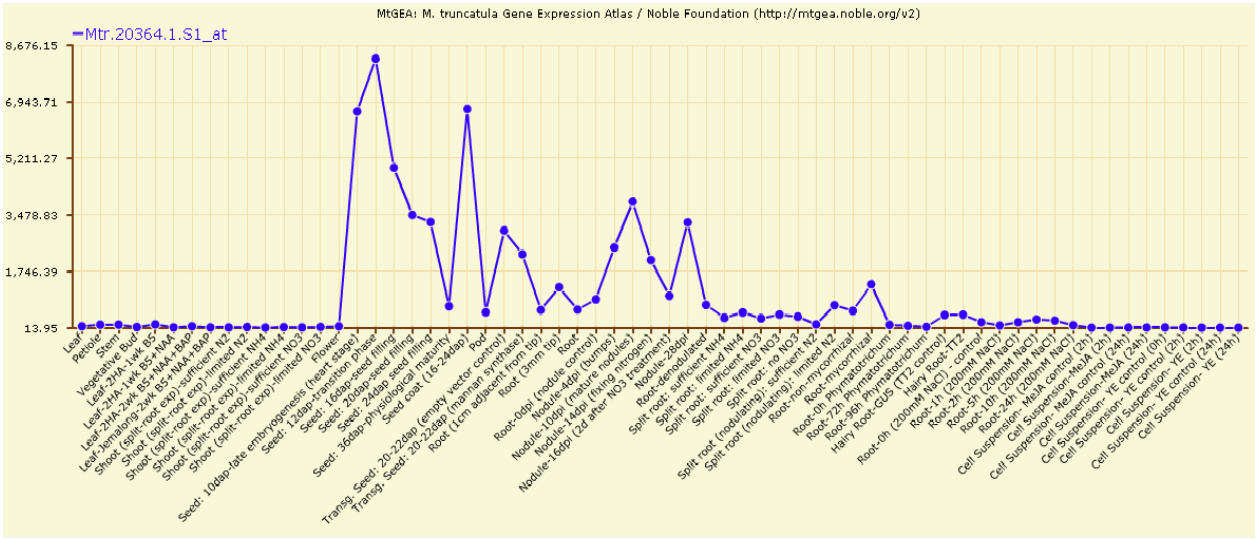

Supplemental Figure S_III_5: *In silico* gene expression profile of *MtAnn2*.
The expression profile was generated via the *Medicago truncatula* GeneExpressionAtlas (Benedito *et al*. 2008). *MtAnn2* is expressed in seeds and roots and induced during root nodule and mycorrhizal symbioses.

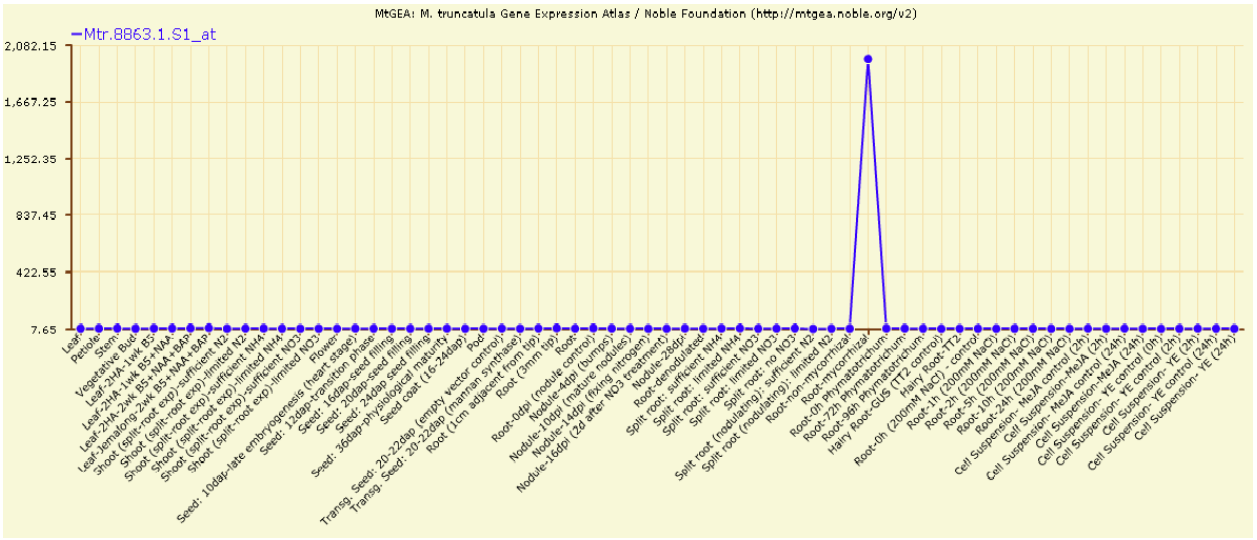

Supplemental Figure S_III_6: *In silico* gene expression profile of *MtMyb1*.
The expression profile was generated via the *Medicago truncatula* GeneExpressionAtlas (Benedito *et al*. 2008). The gene is exclusively expressed in mycorrhizal roots.

Supplemental Tables

Supplemental Table S_III_1: RNAi-fusions used for the induction of transgenic roots on *Medicago truncatula*.

Name	Target gene	Length of target sequence [bp]
pHG8::1641-RNAi	MtAnn2	383
pHG8::1976-RNAi (a)	MtBcp1	358
pHG8::2500-RNAi (b)	MtBcp1	291
pHG8::1855-RNAi	MtMyb1	519
pHG8::2582-RNAi	MtGras	390

Supplemental Table S_III_2: Primers used for sequencing and real-time RT-PCR.
*(Helliwell & Waterhouse, 2003)

A: Primers used for sequencing	
p27-3	GAGCTACACATGCTCAG*
p27-5	GGGATGACGCACAATCC*
pHG8-ocs	CCCCAAATGAAGTGCAGGTC
pHG8-dsRed-ATG	TGATGACGTTCTTGGAGGAG
B: Primers used for real-time RT-PCR	
MtTefa_for	ACTGTGCAGTAGTACTTGGTG
MtTefa_rev	AAGCTAGGAGGTATTGACAAG
MtAnn2_for	GCAAAAGTTACCATGTGATTA
MtAnn2_rev	CTTCTTCATGATTTCCTTTTT
MtBcp1_for	CATCTTTGCATGAGAGACTTA
MtBcp1_rev	AATGAATGGGAGAGTTACAAT
MtMyb_for	TACTGCCAAATTTCTGTTCTA
MtMyb_rev	GGATTGTGTTTTAAAGGATTC
MtGras_for	ATTATTACGATCTCTTCTCGC
MtGras_rev	AGTTACACGAAGGGCTTATAC
MtPt4_for	TTCACATCTTCTCAGTTCTTG
MtPt4_rev	AATTTGATAGGATTCTTTTGC
GmTefα_for	TTGACAAACGTACAATAGAGAA
GmTefα_rev	GCAGCAATAATTAAAATAGCA

Supplemental Figure – General Discussion

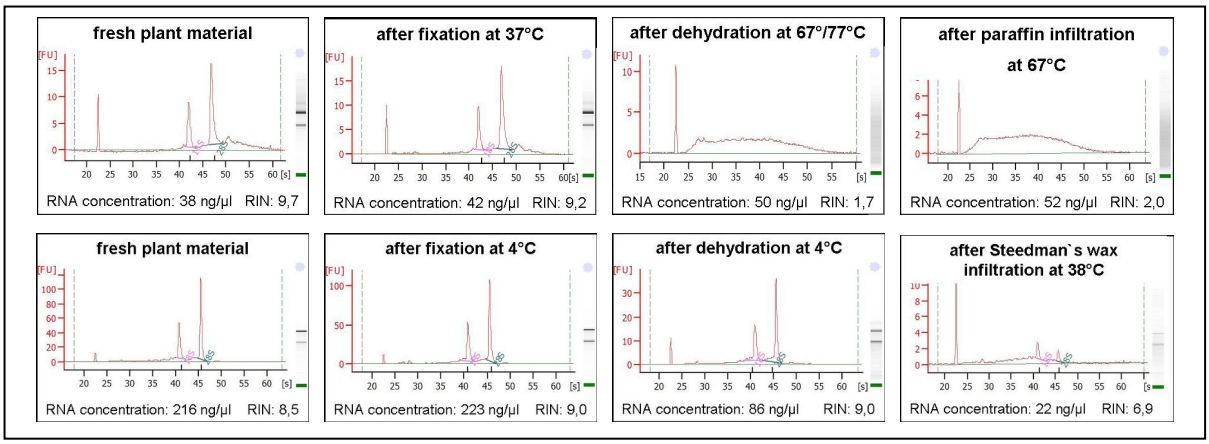

Supplemental Figure S1: Quality of RNA isolated from whole roots during embedding procedure as assessed by a Bioanalyzer run. Bioanalyzer run was performed using the RNA 6000 Pico Kit. The upper row shows the development of RNA degradation during the microwave-assisted embedding with normal Paraffin, the lower row shows the development for Steedman`s wax embedding. RNA-concentrations differ due to different amounts of root material, but RNA degradation is more severe during the Paraffin embedding as can be deduced from RIN numbers and the detection of ribosomal RNA peaks.

CURRICULUM VITAE

Name: **Claudia Hogekamp**

Date of birth: 1st June 1982
Place of birth: Emmerich
Nationality: German

Schooling

08/1988 - 06/1992	primary school at the "Karl-Leisner-Grundschule" in Kleve, Germany
08/1992 - 06/2001	secondary school at the "Johanna-Sebus-Gymnasium" in Kleve, Germany

Studies

10/2001–03/2008	studies of biology at the University of Bielefeld, Germany
03/2008	diploma at the University of Bielefeld, Germany title of diploma thesis: "Transkriptionelle Veränderungen in *Medicago truncatula* Wurzeln als Reaktion auf Signalmoleküle des Mikrosymbionten *Sinorhizobium meliloti*"

Graduation

since 05/2008	graduate studies at the University of Bielefeld, Germany (until 04/2009) and the Leibniz Universität Hannover, Germany (since 04/2009) topic of thesis: Sequential reprogramming of *Medicago truncatula* root cells during the accommodation of symbiotic arbuscular mycorrhizal fungi

SCIENTIFIC PUBLICATIONS

Hogekamp C, Arndt D, Pereira PA, Becker JD, Hohnjec N, Küster H. 2011. Laser microdissection unravels cell-type-specific transcription in arbuscular mycorrhizal roots, including CAAT-box transcription factor gene expression correlating with fungal contact and spread. Plant Physiol 157(4):2023-43.

Czaja LF, Hogekamp C, Lamm P, Maillet F, Martinez EA, Samain E, Denarie J, Küster H, Hohnjec N. 2012. Transcriptional responses toward diffusible signals from symbiotic microbes reveal MtNFP- and MtDMI3-dependent reprogramming of host gene expression by arbuscular mycorrhizal fungal lipochitooligosaccharides. Plant Physiol 159(4):1671-85.

Hogekamp C and Küster H. 2013. A roadmap of cell-type specific gene expression during sequential stages of the arbuscular mycorrhizal symbiosis. Submitted to BMC Genomics

Poster presentations

07/2009: Model Legume Congress 2009, Asilomar, USA

09/2010: Symposium “Genetics of Plant Mineral Nutrition”, Hannover, Germany

ACKNOWLEDGEMENTS

I would like to thank…

…my supervisor Prof. Helge Küster for giving me the possibility to carry out my PhD-thesis in his group and for providing me with an interesting and challenging project. I am very grateful for his professional guidance and steady support during the past years and his ability to motivate me, whenever I felt like giving up.

…Dr. Natalija Hohnjec for her scientific and personal support throughout the last years, which was very valuable for me - and for a wonderful roadtrip to the Grand Canyon and back.

…Dr. Karen Gomez and Prof. Maria Harrison (Boyce Thompson Institute for Plant Research, Tower Road, Ithaca, USA) for sharing the embedding-protocol and for helpful discussions on laser-microdissection.

…Dr. Jörg Becker and Patrica Pereira for the Medicago GeneChip hybridizations.

…Dr. Colby G. Starker (Department of Plant Biology, University of Minnesota) for providing the RNAi-constructs.

…all current and former members of the Plantgenomics working group, the Institute of Biophysics and the ISR for a wonderful working atmosphere. Especially, I want to thank Lisa Czaja for her friendship in the last years and for sharing all the bad and good times, making the former easier and the latter even more enjoyable.

…the “Werkstatt”-staff for excellent technical support and never ceasing supply of “brain food”.

…my parents and Tim for their continued love and support.

Erklärung zur Dissertation

gemäß §6(1) der Promotionsordnung der Naturwissenschaftlichen Fakultät der Gottfried Wilhelm Leibniz Universität Hannover für die Promotion zum Dr. rer. nat.

Hierdurch erkläre ich, dass ich meine Dissertation mit dem Titel

"Sequential reprogramming of *Medicago truncatula* root cells during the accommodation of symbiotic arbuscular mycorrhizal fungi"

selbständig verfasst und die benutzten Hilfsmittel und Quellen sowie gegebenenfalls die zu Hilfeleistungen herangezogenen Institutionen vollständig angegeben habe.

Die Dissertation wurde nicht schon als Masterarbeit, Diplomarbeit oder andere Prüfungsarbeit verwendet.